The binding behavior of fluorinated π-receptors with anions and other aromatics

Hai Yi

The binding behavior of fluorinated π-receptors with anions and other aromatics

Von der Fakultät für Mathematik, Informatik und Naturwissenschaften
der RWTH Aachen University zur Erlangung des akademischen Grades
eines Doktors der Naturwissenschaften genehmigte Dissertation

vorgelegt von

Master of Science

Hai Yi

aus He'nan, China

Berichter: Universitätsprofessor Dr. Markus Albrecht
Universitätsprofessor Dr. Dieter Enders

Tag der mündlichen Prüfung: 14. 09. 2015

Contents

Introduction

Introduction of anion-π interactions

In 2002, an unprecedented and counterintuitive concept, namely "anion-π interactions", was described by Pere M. Deyà and Antonio Frontera etc.. With quantum chemistry calculation of the interactions between anions (H^-, F^-, Cl^-, Br^-, CN^-, NO_3^-, CO_3^{2-}) and hexafluorobenzene, as well as exploring existing crystallographic structures in the Cambridge Structural Database (CSD), "anion-π interactions" were confirmed that "They Do Exist".[1]

Nearly simultaneously (also in 2002), Mark Mascal and Alan Armstrong etc. showed that several anions could be close to the aryl centriod of 1,3,5-triazine or trifluoro-1,3,5-triazine, which was supported by an *ab initio* study of the interaction between 1,3,5-triazine and the fluoride, chloride and azide anions at the MP2 level of theory.[2]

Two years later, Patrick Gamez and Jan Reedijk etc. and Franc Meyer etc. separately observed anion-π interactions between anions and electron-deficient arenes in crystal structures (Scheme 1).[3-4] These were pioneering studies in the field that human intentionally investigate anion-π interactions experimentally, although this kind of interactions which had never been focused on before was already found in the CSD for a long time.

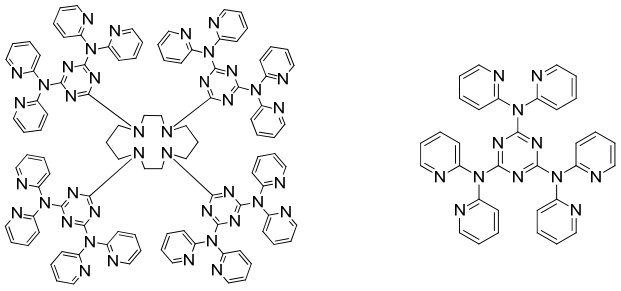

1 **2**

Scheme 1. The first two receptors used for the experimental research of anion-π interactions by Patrick Gamez and Jan Reedijk etc. (**1**) and Franc Meyer etc. (**2**).

It is not surprising that anion-π interactions did not attract human's attention until 21st century, for it is a kind of attractive effect arising between anions and aromatic rings that are surrounded by electron-clouds. This is unimaginable especially relative to "cation-π interactions" existing between cations and arenes. In fact, with the deepgoing theoretical study of aromatic cyclic-compounds by quantum chemistry calculation, the function of the permanent quadrupole moments (Q_{zz}) of benzene and hexafluorobenzene rationalized the counterintuitive phenomenon.[5-6] Definitely, anion-π interactions are regarded as favorable non-covalent attractions between an anion and an electron-deficient aromatic system, which is generally dominated by electrostatics and anion-induced polarization as well as dispersion.[7-8] The topological analysis of the electron density showed that, for anion-π interactions, the magnitude of the arene Q_{zz} has an obvious correlation with the electrostatic contribution to anion-π interactions, specifically, the larger positive Q_{zz} lead to more favorable attraction. Additionally, the anion-induced polarization correlates with the arene's polarizability ($\alpha_{//}$) and has a significant

contribution to the anion-π interactions existing in high $\alpha_{//}$ aromatic systems.[9-10] For the aromatic ring with a high positive Q_{zz}, the electrostatic effect plays a pivotal role in anion-π interactions and the polarization makes a dominant role in the low positive Q_{zz} aromatic ring system.[9]

Typically, anion-π interaction have been investigated in terms of supramolecular chemistry defined as the "chemistry of the intermolecular bond" by Jean-Marie Lehn etc.[11] According to theoretical investigation, the bond energies of anion-π interactions are in the range 20-70 kJ/mol,[2, 12] which is weaker than that of the hydrogen-bond (energy: 12-120 kJ/mol),[13] close to cation-π interactions energies (5-80 kJ/mol)[14] and stronger than the energies of π-π stacking (2-10 kJ/mol).[15] Moreover, some thorough research of the Protein Database (PDB) pointed out that only a small number of examples in regard to anion-π interaction were found.[16] Nevertheless, these results prove anion-π interaction play an important role to protein structures and the activities.

The latest research advances of anion-π interactions

In recent years, a growing number of investigations on anion-π interaction are in process and resulted in dramatic results both in theoretical and experimental fields. In this part, a brief review of the literature relating to the research of anion-π interaction published after 2011 was attempted displaying the latest advances in the fresh scientific realm. Firstly, several new results of theoretical research were selected, due to the particularity of study. Then, development of experimental research for anion-π interactions was focused on and summarized with five areas emphasized by favorable non-covalent contacts between electron-deficient aromatic systems and anions: (a) anion transport; (b) molecular assembly; (c) anion sensors; (d) catalysis with anion-π interactions; (e) anion-π interactions in metal-complexes. Because of the significant role of anion-π interaction in biochemistry, increased number of research results about interactions between anions and aromatic ring moieties in proteins were reported during last several years, which are discussed in the third part followed by the quick glance over other advances for anion-π interactions in the last part of this introduction.

(1) Selected results of theoretical research

A theoretical NMR study of anion-π or cation-π interactions between 1,3,5-trifluorobenzene (TFB) and ions revealed the reverse direction changes of NMR spectra parameters (δ^H, δ^F, $^1J_{C\text{-}H}$, $^1J_{C\text{-}F}$, $^1J_{C\text{-}C}$). When anion-π interaction was induced between TFB and halide anions (F^-, Cl^-, Br^-), the coupling constants $^1J_{C\text{-}H}$ and $^1J_{C\text{-}F}$ decrease while $^1J_{C\text{-}C}$ increase. For chemical shifts, both δ^H and δ^F decreased due to the enhancement of shielding effects. Moreover, the bond length ($d_{C\text{-}C}$, $d_{C\text{-}H}$, $d_{C\text{-}F}$) also be influenced by the ion above the plane of TFB. The anions increased the $d_{C\text{-}F}$ and decreased the $d_{C\text{-}C}$ and $d_{C\text{-}H}$, while cation-π interaction led to the reverse changes.[17]

Checking the X-ray structures showing anion-π interactions existing in CSD, the examples in which the anion is located exactly above the center of the ring are few compared to cation-π interactions. A. Frontera etc. revealed, in the anion-π complex of hexafluorobenzene and chloride, the migration of anion from the center above the ring in either x or y direction did not cause a significant interaction energy loss (≤7 %), which explained the fact that the anion could be located at any position over the ring.[18]

Anion-π interaction is up to now considered to be a favorable contact between anion and electron-deficient arene. However, a kind of attractive effect between fluoride and electron-rich aromatic hydrocarbons, namely orbital effect-induced anomalous anion-π interactions, was reported. With calculations of the adsorption of fluoride to aromatic condensed rings with different sizes at the MP2/6-31+G (d, p) and ωB97X-D/6-31+G (d, p) levels of theory, the orbital effect-induced anomalous anion-π interactions was found between F^- and large π hydrocarbon rings ($C_{14}H_{10}$, $C_{18}H_{12}$, $C_{24}H_{12}$, $C_{40}H_{16}$, $C_{50}H_{18}$, $C_{66}H_{22}$), while for the smaller rings, ex. C_6H_6 and $C_{10}H_8$ rings, unfavorable anion-π interactions displayed, which showed the favorable anion-π interactions between F^- and electron-rich aromatic rings enhance with increasing number of π electrons and the size of π rings. The energy decomposition analysis explained the phenomena, as the negative charge of fluoride delocalization to the unoccupied π* orbitals of large π rings, the orbital effect-induced anomalous anion-π interactions generated.[19]

(2) Selected results of experimental research

Anion-π interaction, a non-covalent attractive effect, has aroused large research enthusiasm and already gained numerous exiting results in recent years both theoretically and experimentally. Like other non-covalent bonding contacts including hydrogen-bonds, π-π stacking, CH-π and cation-π interactions, anion-π interactions have been explored as a supramolecular tool in biochemistry, design of crystal structures, environmental applications and organic synthesis etc..

(a) Anion transport with anion-π interaction

A new series of selective transporters, namely "two-wall" aryl-extended calix[4]pyrroles **3** (Scheme 2), were synthesized and the properties of transporters in binding various anions (F^-, Cl^-, Br^-, I^-, Ac^-, NO_3^-, ClO_4^-) were studied. Due to the presence of two substituents connecting to the α,α-isomers liking "two-wall", appropriate anion could be bound between the two π-acid moieties and carried through lipophilic membranes. Among them, the most active ion transporters, **3c** and **3e**, showed a distinct selectivity for the transport of nitrate over other anions tested.[20]

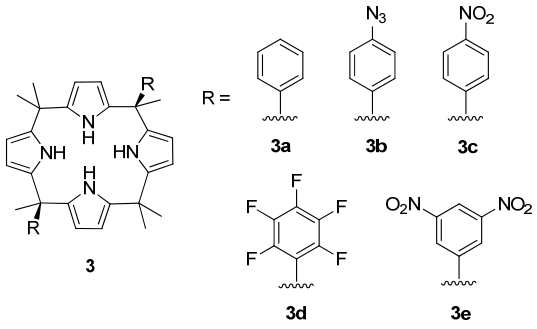

Scheme 2. The structures of α,α-isomers of "two-wall" aryl-extended calix[4]pyrroles **3**.

(b) Anion-directed molecular self-assembly

D-X Wang's group achieves impressive results involving research of spuramolecular assemblies for the past few years. They designed and synthesized some "V-shape" π-receptors based on oxacalix[2]arene[2]triazene framework (Scheme 3). Each of the π-acidic molecules possesses two electron-deficient triazene rings arranging into a "V-shape" cavity and could tune the size of the cavity thereby "swallowing" different anions.

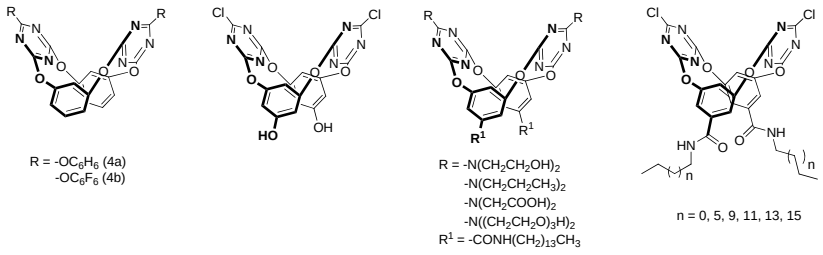

4 **5** **6** **7**

Scheme 3. Some "V-shape" molecules used for the research of molecular self-assembly.

The crystal of pure molecule **4a** obtained through evaporation of the solution of dichloromethane and hexane, formed a cyclic hexamer structure with lone-pair electron-π and hydrogen bond in the solid state (Figure 1, a). The co-crystal with chloride and water molecules with **4a** self-assembled into a rectangular supramolecular cage instead of the foregoing hexamer (Figure 1, b). Because of the presence of chloride, anion-π interaction along with lone-pair electron-π interactions, hydrogen bonds and π-π stacking induced the formation of the rectangular cage structures.[21]

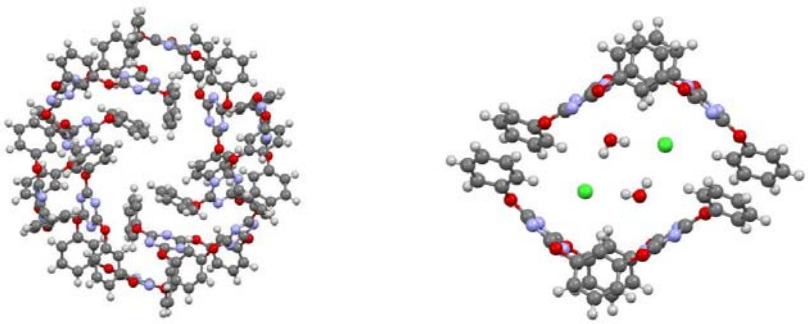

(a) (b)

Figure 1. Crystal structures of the hexamer of **4a** (a) and the rectangular cage of **4a** (b).

The design that a hydroxyl group was introduced on each of the phenyl rings of the macrocyclic structure rendered the tetraoxacalix[2]arene[2]triazine **5** as an unique donor-acceptor functional building block. As found in the X-ray structure with Cl^-, cooperative non-covalent bonds guided the host-guest system to be an infinite self-assembly motif. Specifically, Cl^- positioned above the triazine ring with the distance of 3.42 Å to the plane and connected to hydroxyl with hydrogen bond ($Cl^-\cdots H$ = 2.21 Å). Besides, the intermolecular lone-pair electron-π interaction emerged between one oxygen of the hydroxyl group and the triazine plane of another molecule nearby with the distance of 3.31 Å.[22]

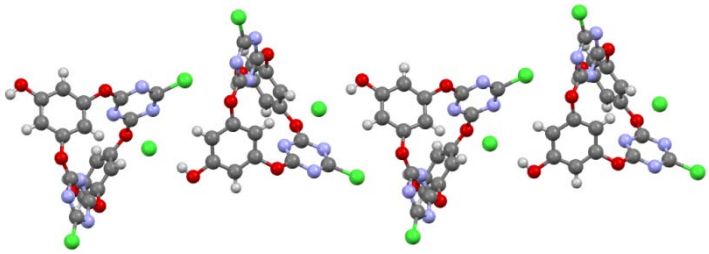

Figure 2. Infinite self-assembly of the tetraoxacalix[2]arene[2]triazine **5**.

Different from the structures **4** or **5**, substituted oxacalix[2]arene[2]triazine **6** or **7** are amphiphilic molecules which bear hydrophobic groups on the one terminal of the "V-shape" structures. Analysis of the structural properties of **6** or **7** indicated that, the lipophilic port containing electron-deficient arenes could self-tune to bind different anions. Both of the two amphiphilic molecules could self-assemble into size-regulated vesicles separately in water or a mixture of THF and water by the influence of anions. For amphiphile **6**, the size of vesicular entities were responsive to anions and followed the selectivity in the order NO_3^- > Cl^- >Br^- >ClO_4^-. Similarly, divers anions were also able to affect the size of self-assembled vesicles of **7**, following the order of NO_3^- > Cl^- >Br^- >BF_4^- >SCN^- >ClO_4^- >F^-.[23]

Normally, because of the complicacy of π-aromatic structures including electronegative atoms with lone-pair electrons, π-bond and active hydrogen atoms, the examples that supramolecular self-assembly induced only by anion-π interaction are rare. Commonly, the process of molecular self-assembly is promoted by synergistic effect of several non-covalent bonds, ex. anion/cation-π interaction, lone-pair electron-π interaction, π-π stacking and hydrogen bonds. Moreover, cations interacting with the π-systems always can boost the acidity of the arenes and even turn the electron-deficient arenes into π^+-acid, which are more attractive to anions.

Two terpyridine derivatives **8a** and **8b** (Figure 6) were synthesized as π-receptors which could produce complex salts, namely $[PTPH_3]^{3+}(X)_3^{3-}$, with HBr or $HClO_4$ respectively (X = Br or ClO_4). The aggregation of the complexes in solid state displayed the cooperation of the aforementioned non-covalent bonds for the realization of supramolecular self-assembly.[24]

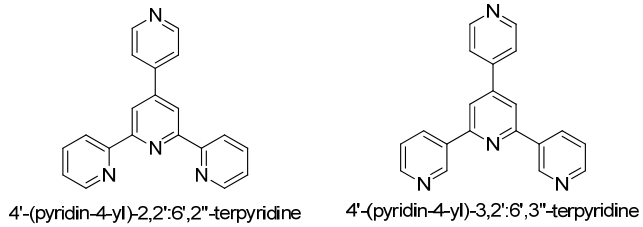

8a **8b**

Scheme 4. The structures of π-receptors **8a** and **8b**.

Similarly, each of the bis-*N*-imidazolylpyrimidine salts **9-11** consists of one doubly protonated *bimipyr* molecule, which modify the tricyclic π-receptor to a stronger acceptor (Scheme 5). In the X-ray crystal structures of the five salts, hydrogen bonds, anion-π interactions and π-π stacking all play significant roles in the construction of three-dimensional supramolecular frameworks.[25]

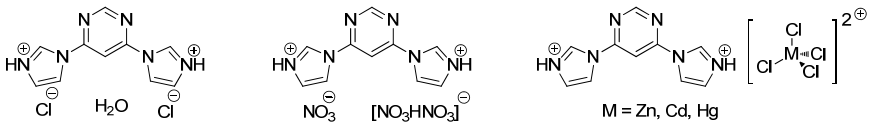

9 **10** **11**

Scheme 5. The structures of the tricyclic complexes **9**, **10** and **11**.

(c) Anion sensors based on anion-π interaction

Profits from the attractive property of electron-deficient π-receptors to anions, it is realized that π-acids are able to be designed as anion sensors. UV-Vis spectra and fluorescence spectra are the

efficient tools in respect to the test of selectivity between the sensor and anions. In recent years, an increasing number of π-receptors involving anion sensing were synthesized and this field is becoming a promising research area.

A fluorinated heteroarene **12** was obtained in 19% yield through a one-pot, solid-state reaction under an argon atmosphere. This molecule bearing an imidazo[4,5-b]phenazine moiety and a tetrafluorophenyl group, due to the existence of string intramolecular hydrogen bonds, adopt a plane structure, which was characterized by X-ray single-crystal diffraction. The two electron-deficient rings in the molecule rendered the flat π-acid as a multi-response anion sensor. Through colorimetric and fluorescent responses, the fluorinated heteroarene can selectively detect F^- over Cl^-, Br^-, I^-, NO_3^-, HSO_4^-, ClO_4^- and BF_4^-.[26]

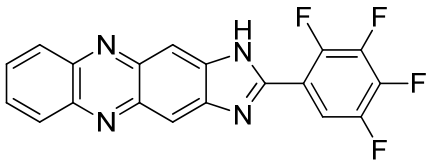

12

2-(2,6-Diisopropylphenyl)benzo[1',10']phenanthrolino[3',2':1,2]imidazo[4,5-*b*]phenazine-1,3,6(2*H*)-trione **13**, which can selectively detect CN^- and F^- with multiple responses including fluorescent, colorimetric and near-infrared absorption signaling among a total of twelve anions (BF_4^-, PF_6^-,Cl^-, F^-, SO_4^{2-}, NO_3^-, I^-, $H_2PO_4^-$, ClO_4^-, Ac^-, Br^- and CN^-). Moreover, Cu^{2+} or Fe^{3+} can reverse the sensing ability with CN^- and F^-, that is, when Cu^{2+} or Fe^{3+} added into the mixture of sensor **13** and CN^- or F^-, the UV-Vis spectra curves tend to recover the free state without anion.[27]

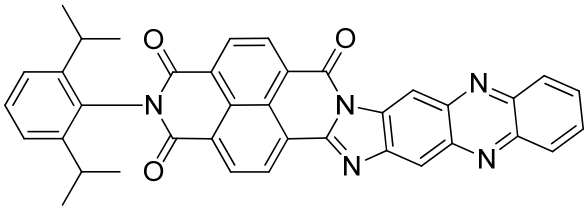

13

Bis(phenylcarbamoyl)-functionalized tetraoxacalix[2]arene[2]triazine **14** bearing a "V-shape" cavity where an anion could be bound. Among several tested anions ($H_2PO_4^-$, Cl^-, Br^-, NO_3^-, HSO_4^-, SCN^-, BF_4^-, and PF_6^-), only $H_2PO_4^-$ led to a quench of the original fluorescence emission (310 nm for **14a**, 308 nm for **14b**) and an increased emission at 420 nm and 412 nm respectively for **14a** and **14b**.[28]

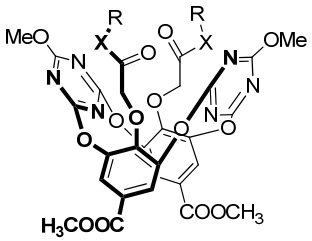

XR = OEt (a)
NHPh (b)

14

Under visible light, the complex of calix[4]pyrrole derivatives **15** and fluorides dissolved in chloroform was colorless, while the solution turned to dark red in acetonitrile, instead of chloroform. Further, it showed that **15** could detect F^- among various anions (F^-, Cl^-, Br^-, I^-, $H_2PO_4^-$, HSO_4^-, ClO_4^-, CH_3COO^-, NO_3^-, CN^- and PF_6^-) *via* UV-Vis spectral test. Only fluoride decreased the free **15** absorption band at 316 nm and induced two new absorption bands at 337 nm and 515 nm. HOMO-LUMO energy level determination indicated that charge transferred from the fluoride to the ethene bonds during the complex formation; Besides, ^1H NMR spectra also showed that the NH did not shift after the F^- was added, which proved no hydrogen bonds were formed between fluoride and NH. Thus, molecule **15** is a colorimetric sensor for fluoride.[29]

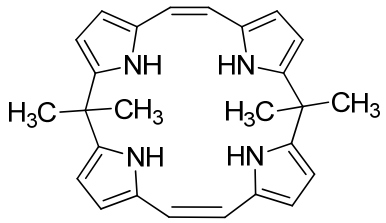

15

(d) Anion-π catalyst

Catalysis with anion-π interaction is a new research subject about which only one catalyst with anion-π interaction was reported up to now, to the best of our knowledge. Matile and co-workers designed and synthesized naphthalenediimide (NDI) core catalyst **16a** and **16b** with π-acidic surface (Scheme 6) which catalyzed the Kemp elimination of 5-nitrobenzisooxazole (5NBZ). They declared that introduction of electron-withdrawing groups on the π-acidic surface could tune the catalytic activity and π-π stacking was less important for anion-π catalysis.[30]

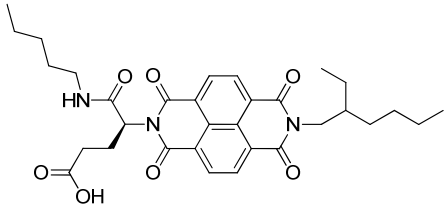

16a

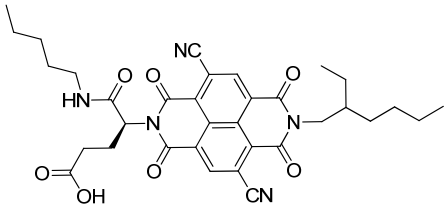

16b

Scheme 6. The structures of two NDI-core anion-π catalysts. The catalytic activity of **16b** is higher than that of **16a** because of the presence of cyanogroups.[30]

Although the examples on anion-π catalysis are rare, it is a newborn study area which will attract more enthusiasm in future.[30]

(e) Anion-π interactions in metal-complexes

Metal coordination always can strongly increase the π-acidity of the electron-deficient aromatic rings. Therefore the adhibition of metal-complexes with aromatic rings is a sensible strategy to construct anion-π receptors. These years, numerous metal assisted π-receptors were synthesized and used for novel crystals or materials involving anion-π interactions (Scheme 7).[31]

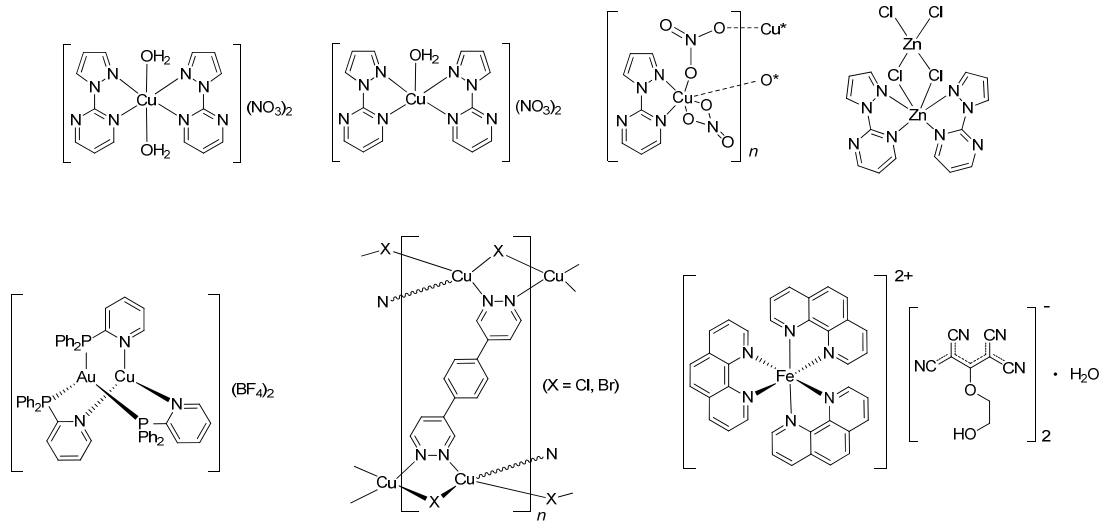

Scheme 7. Several examples of metal-complexes which self-assemble induced by anion-π interactions in the solid state.

(3) Study of anion-π interaction in protein chemistry

Up to now, investigation of anion-π interaction related to protein chemistry mainly base on the searching for anion-π pairs in the Protein Data Bank, as well as theoretical quantum chemistry calculations. For theoretical research, *ab initio* calculations and Density Functional Theory (DFT) are the efficient tools to simulate the position of an anion to the π-ring and calculate the energy of anion-π pairs in proteins.[32] In terms of search results in PDB, anion-π pairs were proved not only to exist, but probably to influence the activities of certain enzymes.[33-39]

(4) Other advances for the research of anion-π interaction during recent years

It is obvious that the investigation of the newfound interaction between anions and π-rings have already obtained huge achievements during the last few years in the aforementioned subjects. Besides, some dramatic research results were also gained in other areas in regard to anion-π interaction.

Prof. D-X Wang and Prof. M-X Wang's group designed and synthesized the "V-shape" π-receptors bearing azacrowns *via* one-pot reactions (Scheme 8). These receptors could efficiently recognize different anions and metal ions. With fluorescence titration method, it was found both **17a** and **17b** could bind anions (F^-, CN^-, CH_3O^-) and the range of binding constants calculated were from 1.11×10^3 to 6.59×10^3 M^{-1}. Moreover, the receptor **17b** could recognize both alkali metals and transition and heavy metals tested, while **17a** could only complex with transition and heavy metals. In addition, the receptors **17a** and **17b** were able to bind metal ions and anions simultaneously by coordination bonds in the azacrown motives and anion-π interaction in the π-rings. Thus, it demonstrated that the receptors of anion-π interaction can be used for the recognition of ion pairs.[40]

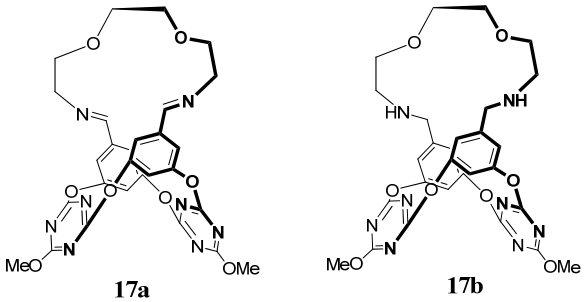

17a **17b**

Scheme 8. Ion pair receptors **17a** and **17b**.

Taking advantage of both cation-π and anion-π interations in one receptor **18**, namely hemicryptophane, selected zwitterions could be recognized in a competitive aqueous medium and DFT optimized structure of complex of **18** with each zwitterion showed the zwitterion was displaced along the C_3 axis of the receptor with the $-NH_3^+$ ion approached to the three methoxylated phenyls and the anion (COO^- or SO_3^-) terminal directed to the tri-carbonylated phenyl. The range of association constants between zwitterions and receptor **18**, which was determined by ^{1}H NMR-titration experiments of NH in **18,** was from 1.5×10^4 to 5.0×10^5 M^{-1}.[41]

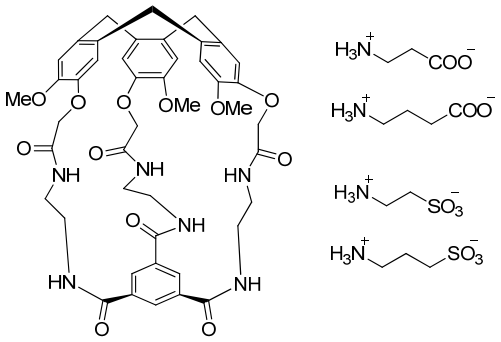

18 zwitterions

Not only organic π aromatic systems, but inorganic rings with more or less aromatic character also displayed favorable effects with different anions by means of the Bader's theory of "atoms-in-molecules" and the SAPT method (Scheme 9). The range of the interaction energies at the RI-MP2/aug-cc-Pvdz level of theory with the BSSE corrections was from -2.5 to -34.4 kcal/mol. In addition, the experimental example of anion-π interaction between the inorganic ring and anion was found by the CSD searching work, which regarded to the interaction of chloride with a 1,4,2,3,5,6-dioxatetraborinane-2,3,5,6-tetrol ring.[42]

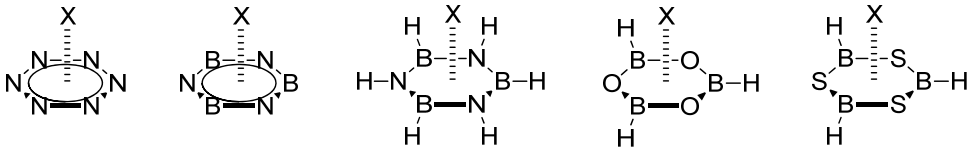

$X = F^-, Cl^-, Br^-, NO_3^-, BF_4^-$

Scheme 9. Several six-membered inorganic rings showed anion-π interaction with anions by theoretical *ab initio* study.

Fruitful achievements are precious gifts to men who are struggling and talented. Prof. Albrecht's group have already obtained huge success concerned to the study of anion-π interaction since 2008.[43] Thorough research work based on petafluorophenyl group designed in π-receptors systematically discovered dramatic results related to the novel favorable effect between the electron-deficient arene and anions.[44] Numerous π-receptors were obtained by Prof. Albrecht's group during the last several years, because design and synthesis of new anion receptors is one of the main targets in the investigation of anion-π interaction. For extending the range of research area and making the fundamental of anion-π interaction more unambiguous, series of new anion receptors, which contained petafluorophenyl groups or perfluorinated arene moieties as well as 3,5-bis(trifluoromethyl)phenyl groups, were synthesized and studied both in the solid state and in solution. Thereinto, the CF_3-receptors are the firstly mentioned and investigated to the best of our knowledge.

Chapter 1 Motivation

Prof. Albrecht's group has accumulated prominent progress and gathered luxuriant experience involving the research of anion-π interaction focused on pentafluorophenyl-based anion receptors. Abundant host-guest complexes of positively charged C_6F_5-receptors with different anions were obtained and analyzed with X-ray single crystal diffraction in the solid state, previously. To shed light on the status of different anion-π systems in solution, some new C_6F_5-type receptors were synthesized and tested with $^1H/^{19}F$ NMR-titration experiments as a part of this work.

Developing new series of π-receptors is one of the most challenging missions in the investigation of anion-π interaction. It is well known that the trifluoromethyl group is a key structural block in many biological and pharmaceutical compounds, because of its strong electronegativity and the mimic effect.[45] While, to the best of our knowledge, there is still no trifluoromethylated aromatics as hosts using anion-π interaction, despite the potential interests of this kind of electron-deficient arenes in supramolecuar chemistry and biological properties. Owing to the strong electronegativity of the trifluoromethyl group, the aromatic compounds bearing CF_3 may display favorable effect with anions. Trifluoromethylated aromatic rings could probably be the candidates of receptors for anion-π interaction. The most attractive is, that these trifluoromethylated π-receptors could play significant role in the biological field.

Therefore, a series of commercially available CF_3-containing compounds (3,5-bis(trifluoromethyl)benzyl bromide **19**, 3,5-bis(trifluoromethyl)benzyl chloride **20**, 3,5-bis(trifluoromethyl)benzyl amine **21**, 3,5-bis(trifluoromethyl)benzoyl chloride **22** or 3,5-bis(trifluoromethyl)benzamide **23**) were introduced as building blocks to construct novel CF_3 π-receptors, which is the original part of the research work (Scheme 10).

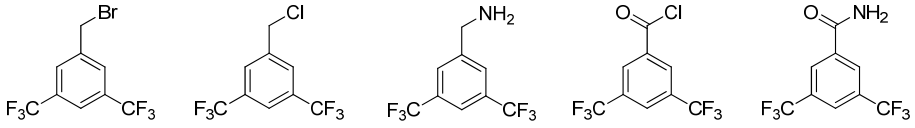

19 **20** **21** **22** **23**

Scheme 10. Some trifluoromethylated compounds which were used to synthesize π-receptors for anions in this work.

It is reasonable to consider perfluorinated aromatic compounds as potential anion-π receptors, due to their electron-deficient property. However, there is rare experimental work about perfluorinated arenes as anion-π repcetors reported in spite of the fact that abundant theoretical calculations announced about this item. Thus, perfluoro-1,1′-biphenyl **24** and perfluoronaphthalene **25** and their derivatives were introduced into our investigation field and were found as new receptors of anion-π interaction experimentally.

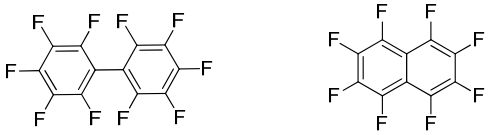

24 **25**

Chapter 2 The interaction of perfluoro-1,1′-biphenyl or perfluoronaphthalene with anions and their derivatives as π-receptors for anions

2.1 Introduction

A computational study of interaction of anions with perfluoro-aromatic compounds reported by Ibon Alkorta etc. revealed that a favorable effect may be induced between perfluoronaphthalene **25** and anions with the corrected interaction energies of -17.31, -16.70, -16.51 kcal/mol for the complexes with Cl^-, Br^- and CN^-, respectively. The anions were located over the C(4a)-C(8a) bond with distances from 3.056 to 2.988 Å relevant to the center of the C(4a)-C(8a) bond.[46] This computational work proved that it is possible to design π-receptors with perfluoro-aromatic compounds on theory. Moreover, these aromatic compounds are widely used in the areas of materials science, environmental science, crystal engineering, fuel cells and supramolecular chemistry,[47] which enables the perfluoro-aromatic compounds to be promising π-receptors for anions in the future.

However, until now these compounds have not been systematically used in the studies of anion-π interactions. Thus, we study two of these perfluoro-arenes: perfluoronaphthalene **25** and perfluoro-1,1′-biphenyl **24** as π-receptors for anions in solution. In addition, their DABCO bromide salts (**26** and **27**) were synthesized for co-crystal investigation (Scheme 11).

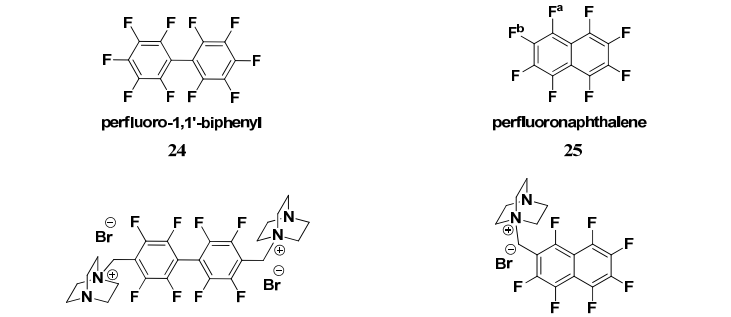

Scheme 11. Perfluorinated aromatic receptors compounds (**24** and **25**) and their derivatives (**26** and **27**) studied in this part.

2.2 The anion binding behavior of the perfluoro-1,1′-biphenyl and perfluoronaphthalene in solution

The status of the electron-deficient arenes **24** and **25** binding anions was investigated in $CDCl_3$ at room temperature ^{19}F NMR-titrations with various anions as their tertabutyammonium (TBA) salts (TBA·Cl, TBA·Br, TBA·F, TBA·I, TBA·NO_3 and TBA·BF_4). Similar spectra are observed in all ^{19}F NMR-titrations for both **24** and **25** (Figure 3 and 4).

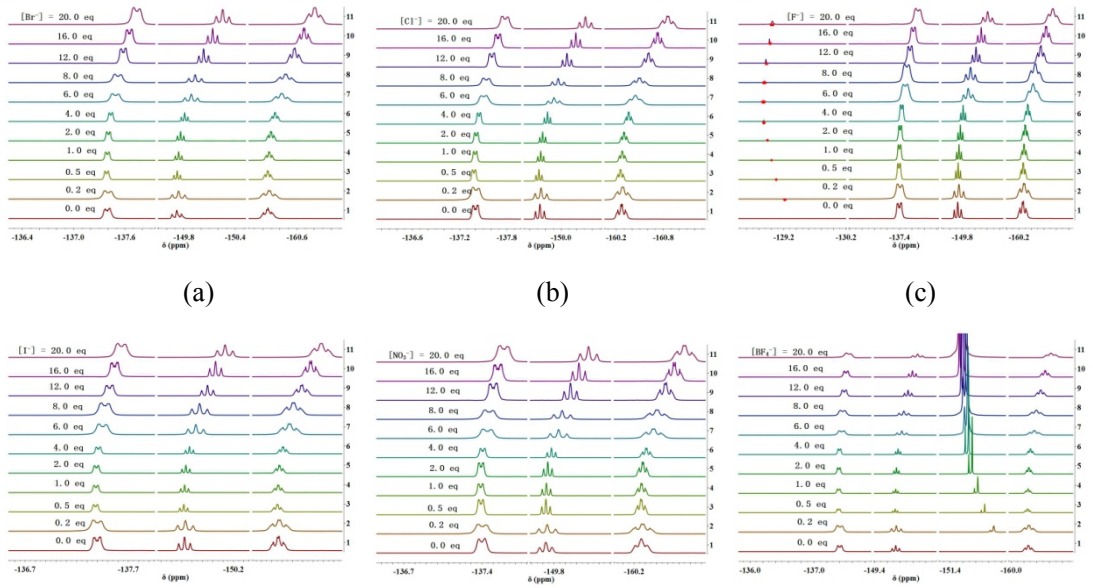

(a) (b) (c)

(d) (e) (f)

Figure 3. ^{19}F NMR-titrations of perfluoro-1,1′-biphenyl **24** with the TBA salts in $CDCl_3$. (298 K)

As shown in Figure 3, the ^{19}F NMR spectra revealed high-field shifting of all fluorine peaks of **24**. Specifically, halide anions induced a little larger high-field shifting of ^{19}F NMR signals than nitrate or tetrafluoroborate did (Table 1). The changes of ^{19}F NMR chemical shift values decreased in the order of $Cl^- > Br^- > I^-$ (Table 1 Entry 1-2, 4), which is probably because of their different volumes, dispersion, polarization and electrostatic properties. Due to the strongest basicity of F^-, when the quantities of F^- were no more than 6.0 equivalents, F^- tended to associate with protons in solution or generated Meisenheimer-type complexes with **24**, whichever situation resulted in the de-shielding effect leading to the down-field shifting of F^- NMR signal (from -129.076 to -128.874 ppm) and no obvious chemical shift change in the ^{19}F NMR spectra of **24** (Figure 3, c). Then excess F^- added to 20.0 equivalents practically interacted with π-bond and the signals of F^- peaks shifted high-field from -128.874 ppm to -129.020 ppm (Figure 3, c). As to NO_3^- and BF_4^-, the tiny changes of ^{19}F NMR chemical shifts revealed less interaction with the perfluorinated arene **24** (Table 1, Entry 5-6). With the addition of TBA·BF_4, a down-field shifting of the BF_4^- resonance was observed, which revealed the fluoride resonance of the tetrafluoroborated anion was also dependent on the ratio between the electron-deficient aromatic compound and the anions (Figure 3, f).

Table 1. The changes of ^{19}F NMR chemical shifts of perfluoro-1,1′-biphenyl **24** *

Entry	anion	$\Delta\delta(^{19}F_{ortho})$ / ppm	$\Delta\delta\ (^{19}F_{meta})$ / ppm	$\Delta\delta\ (^{19}F_{para})$ / ppm
1	Cl^-	0.38	0.59	0.58
2	Br^-	0.35	0.55	0.53
3	F^-	0.29	0.49	0.48
4	I^-	0.23	0.42	0.39
5	NO_3^-	0.19	0.39	0.38
6	BF_4^-	0.14	0.35	0.34

"*" The values were calculated by ^{19}F NMR-titration experiments.

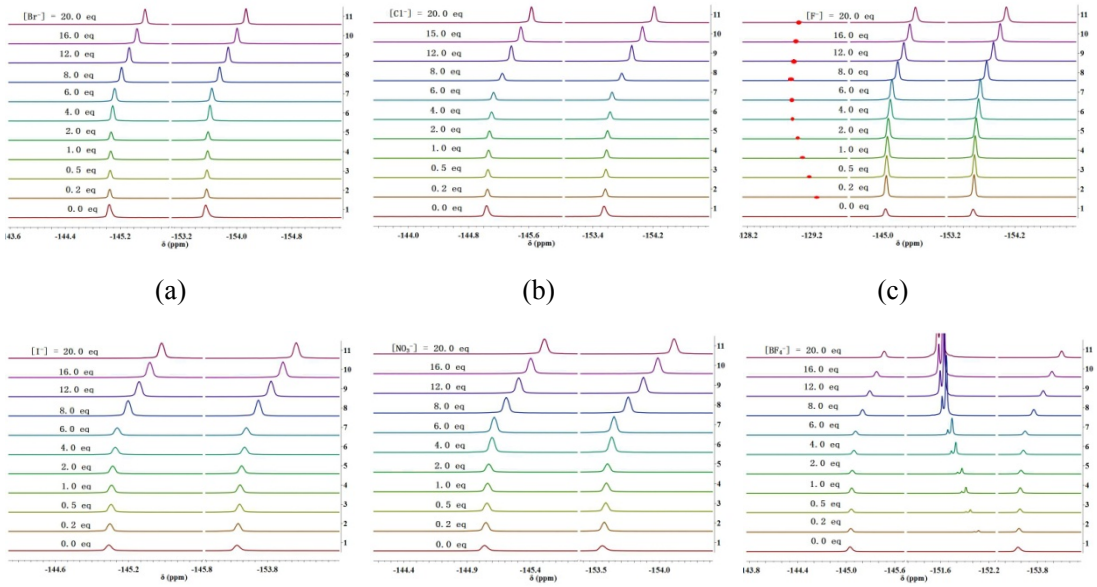

(a) (b) (c)

(d) (e) (f)

Figure 4. ^{19}F NMR-titrations of perfluoronaphthalene **25** with the TBA salts in $CDCl_3$. (298 K)

For the situation between perfluoronaphthalene **25** and anions, the ^{19}F NMR spectra displayed all fluorine signals of **25** moved to high-field (Figure 4). Cl^- or Br^- always led to the largest chemical shift changes to F^a (α-F) and F^b (β-F) (Table 2, Entry 1-2). NO_3^- caused larger shift change than F^- or I^-, which is different from perfluoro-1,1′-biphenyl **24**. BF_4^- made the middle shift change to F^b and the minimum to F^a (Table 2, Entry 4). For all of the different kinds of anions, F^a underwent smaller chemical shift changes than F^b.

Table 2. The changes of ^{19}F chemical shifts of perfluoronaphthalene **25** *

Entry	anion	$\Delta\delta(^{19}F^b)$ / ppm	$\Delta\delta(^{19}F^a)$ / ppm
1	Cl^-	0.667	0.596
2	Br^-	0.588	0.522
3	NO_3^-	0.566	0.473
4	BF_4^-	0.539	0.422
5	F^-	0.514	0.462
6	I^-	0.485	0.431

"*" The values were calculated by ^{19}F NMR titration experiments.

In conclusion, the ^{19}F NMR signals of both the perfluorinated electron-deficient aromatics revealed some high-field shifting with TBA salts added and a more or less linear relation between the addition of anions and ^{19}F NMR peak shifting revealed an interaction taking place between the perfluoroaryl unit and anions, although it cannot be assigned to a specific binding.

2.3 The synthesis and crystal structure of the perfluoro-1,1′-biphenyl or perfluoronaphthalene derivatives

In order to investigate the anion-π interaction of receptors containing perfluoro-1,1′-biphenyl or perfluoronaphthalene unit in the solid state, the bromide salts **26** and **27** were prepared (Scheme 12). The cationic DABCO methylene unit was introduced as a corresponding cationic substituent according to our previous research on pentafluorophenyl receptors.[48]

Complex **26** or **27** were synthesized *via* a similar substitution reaction route from the starting compounds **24** or **25**, respectively. The perfluorinated parent compounds were methylated twice (for **26**) or once (for **27**) with methyl lithium at low temperature. Then the methylated derivative **28** or **30** was brominated by NBS to afford bromomethyl derivative **29** or **31**, which produced the bromide salts **26** or **27** by nucleophilic substitution reaction with DABCO, respectively.

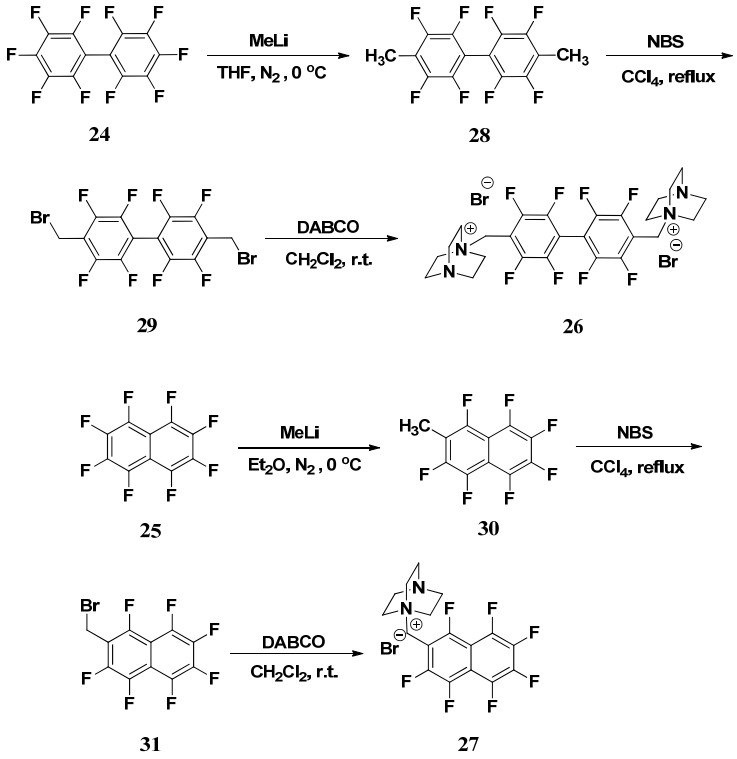

Scheme 12. Synthesis of complexes **26** and **27**.

The dicationic derivative **26** was crystallized by diffusing Et_2O into the methanol solution of **26**. The salt crystallized in the chiral space group *C*2 with half a molecule in the asymmetric unit. The two DABCO methylene substituents were anti-orientated related to the perfluorobiphenyl unit and the biphenyl moiety had a torsional angle (49.4°) between the planes of two fluorinated aromatic rings. The bromide anions are slightly disordered (92:8) above two rings and are directed to the α-hydrogen atoms of the corresponding DABCO parts. As shown in Figure 5 (a), the bromide anion was not located above the centroid of the aromatic ring, due to the torsion of the biphenyl units. Instead, it was fixed at the rim of the perfluorophenyl unit with distances of 3.62, 3.64, 3.90 and 3.92 Å to the neighboring CF carbon atoms. Meanwhile, the distances from the bromide anion to the centroid of the adjacent ring were 3.66 Å. It indicated that a favorable η^4-type anion-π interaction was generated between the bromide anion and the perfluorophenyl ring. Besides, each

bromide orientated towards hydrogen atoms of the DABCO and methylene moieties in another nearby molecule by Br···H interactions with distances of 2.75 to 2.77 Å, respectively (Figure 5, b).

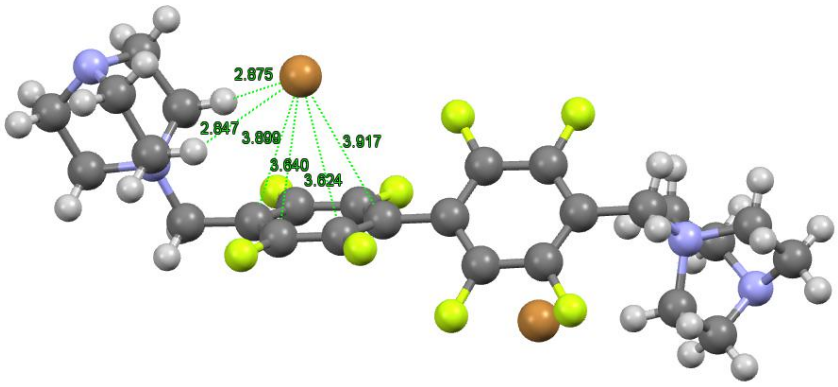

(a)

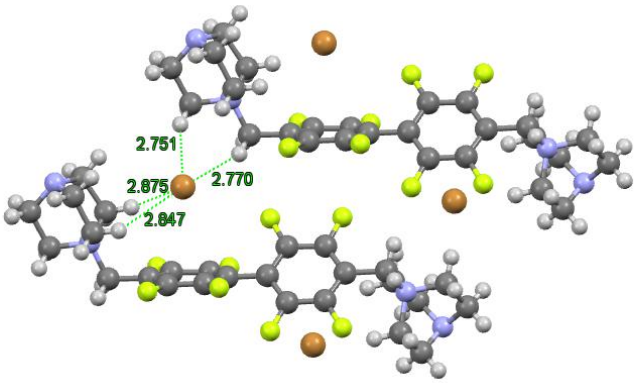

(b)

Figure 5. X-ray crystal structure of bisbromide salt **26** showing η^4-type anion-π interaction (a) and intermolecular Br···H interactions (b). The bromide anions are disordered. (black: C, gray: H, yellow-green: F, blue: N, brown: Br)

Crystals of complex **27** were obtained from methanol by slow evaporation as methanol solvate. The salt crystallized in the space group *pbca* with a methanol molecule co-crystallized (Figure 6, a). The bromide anion was also not located above the centroid of the perfluoronaphthyl ring but is fixed close to the α and β carbon atoms of the ring system bearing DABCO methylene unit conforming η^4-type anion-π interaction with distances of 3.57, 3.64, 3.74 and 3.87 Å. In addition, the anion contacted with the α-hydrogen atoms of the corresponding DABCO unit and the methanol nearby with Br···H interactions.

Meanwhile, the crystal structure demonstrated a multi intra-/intermolecular interaction motif (Figure 6, b). The anion was encompassed with Br···H interactions by four DABCO methylene units forming a cavity as well as interacting with the perfluoronaphthyl ring by means of anion-π interaction. Moreover, the two perfluoronaphthyl rings adopted a parallel orientation with π-π stacking interactions ($centriod_{C(4a\text{-}8a)}$···$centroid_{C(4a\text{-}8a)}$ = 3.66 Å).

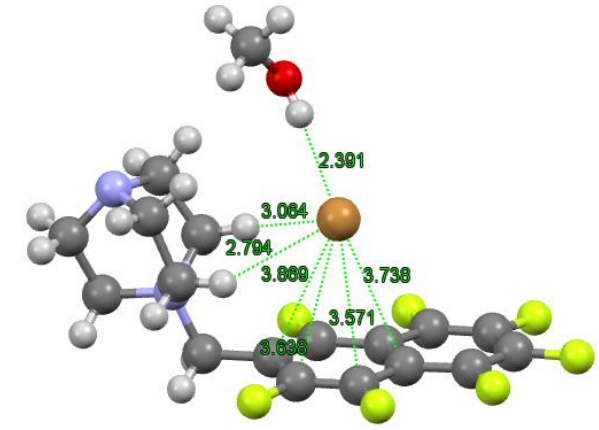

(a)

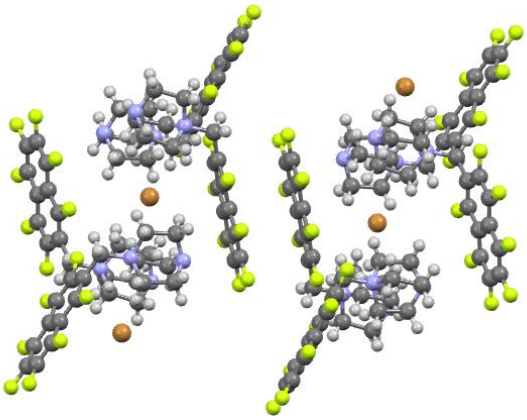

(b)

Figure 6. X-ray crystal structure of **27** showing η^4-type anion-π interaction (a) and multi intra-/intermolecular interaction (b, some bromides and methanol molecules were omitted for clarity). (black: C, gray: H, yellow-green: F, blue: N, brown: Br, red: O)

2.4 Conclusion

This work focused on the study of perfluorinated biphenyl or naphthyl units as π-receptors for anions. Solution studies demonstrated the ^{19}F NMR peaks of the fluorinated aromatics **24** and **25** shifted upon the addition of TBA salt with various anions, which may be induced by anion-π interaction due to the electron-deficient nature of the aromatic ring systems, although the underlying interactions are not specific. Crystal structure analyses of the two bromide salt derivatives **26** and **27** obviously revealed the favorable effect between bromide anion and the electron-deficient rings. Due to the substituent of the DABCO methylene unit as well as the torsion of the biphenyl units, the anion was not located on the top of the center of the aromatic unit, thus η^4-type anion-π interaction were taken place in both perfluorinated aromatic systems.

Chapter 3 The investigation of trifluoromethylated aromatic compounds as π-receptors for anions

3.1 Introduction

According to previous investigations, the trifluoromethyl group (CF_3) is a highly electronegative group[49] and always results in dramatic modification of the physical, chemical and biological properties of the organic molecules bearing this group.[50] Therefore, both the synthesis and the practical investigation of trifluoromethylated compounds have drawn much attention to this functionality.[51] For example, several kinds of drugs containing CF_3 groups have been used in clinic.[52] Recently, trifluoromethylated organic compounds are also investigated as catalysts for asymmetric reactions[53].

It is well known that anion-π interaction is a kind of electrostatic effect combined with polarization and London dispersion interactions, resulting in attraction between anions and electron-deficient arenes. The study of anion-π interaction has afforded numerous achievements in both theoretical and experimental research methodologies in the last several years.[54] The electron-withdrawing groups connecting to an aromatic ring reduce the density of the π-cloud of the arene, so that a positive permanent quadrupole moment (Q_{zz}) is induced consequently, which generates a weak attraction to anions above the electron-deficient aromatic ring. Thus, electron-withdrawing groups or electronegative atoms of the aromatics play a significant role in the generation of anion-π interactions.

However, the trifluoromethyl group, despite the extremely strong electronegativity and the important role in medicinal chemistry or organic synthesis, has not been used in the study of anion-π interactions.

Until now, a large number of electron-deficient aromatic rings containing fluorine, chlorine, bromine, nitryl or cyan etc. have been reported as π-receptors for anions.[55] Which is different from the aforementioned electron-withdrawing groups, the steric configurational tetrahedron of CF_3 group probably allows various interactions between anions and trifluoromethylated aromatic rings.

Our group cooperated with Prof. Raabe and selected several trifluoromethylated aromatic compounds (**28**-**32**) for calculating the anion binding behavior of them on theory. Both of the permanent quadrupole moments (Q_{zz}) and the polarizabilities ($\alpha_{\parallel}$) of the neutral charged aromatic compounds increase along with the added degrees of trifluoromethylation (Scheme 13). The selected anions (F^-, Cl^- and Br^-) showed different behavior to the CF_3-arenes. Specifically, both F^- and Cl^- produce Meisenheimer-type σ-complexes or induce hydrogen bonding interactions with these CF_3-arenes; in contrast, anion-π complexes are generated from the interaction between bromide anion and the trifluoromethylated compounds (**30**, **31** or **32**).[56]

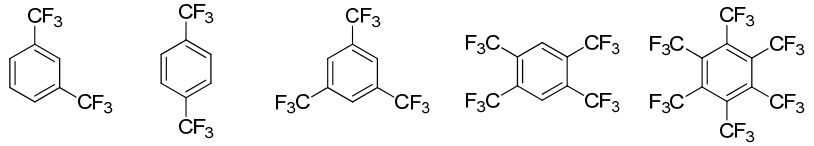

28
Qzz = -1.77 B
α_{II} = 90.44 a.u.

29
Qzz = +0.31 B
α_{II} = 90.65 a.u.

30
Qzz = +3.15 B
α_{II} = 103.03 a.u.

31
Qzz = +5.35 B
α_{II} = 118.28 a.u.
(MP2/6-311++G**)
Qzz = +5.49 B
α_{II} = 120.66 a.u.
(MP2/6-31+G*)

32
Qzz = +5.56 B
(MP2/6-311++G**)
Qzz = +5.50 B
(MP2/6-31+G*)

Scheme 13. The permanent quadrupole moments (Q_{zz}) and the polarizabilities ($\alpha_{//}$) of the selected trifluoromethylated aromatic compounds.

3.2 The synthesis and crystal structures of trifluoromethylated aromatic complexes

The quantum chemical calculations abovementioned indicate the theoretical feasibility to design novel π-receptors for anions with electron-deficient aromatic compounds bearing CF_3 groups. In order to test the results of the computational chemistry, some charged CF_3-complexes were prepared from commercially available materials, namely 3,5-bis(trifluoromethyl)benzyl bromide (**19**) or chloride (**20**). Then their crystals were cultivated and studied by X-ray single crystal diffraction thereby understanding the interactions between anions and CF_3-arenes experimentally.

(a) The synthesis of CF_3-substituted-aryl compounds

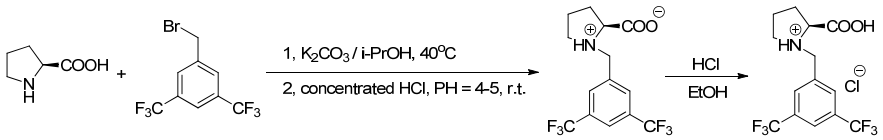

33 **19** **34** **35**

Scheme 14. The preparation of L-proline derivative **34** and its HCl adduct **35**.

According to the synthesis of the pentafluorophenylated counterpart,[57] trifluoromethylated L-proline derivative **34** was obtained by nucleophilic substitution reaction of 3,5-bis(trifluoromethyl)benzyl bromide **19** with L-proline **33**. The acidification of **34** by ethanol solution of HCl at room temperature afforded the co-crystal of chloride salt **35** (Scheme 14).

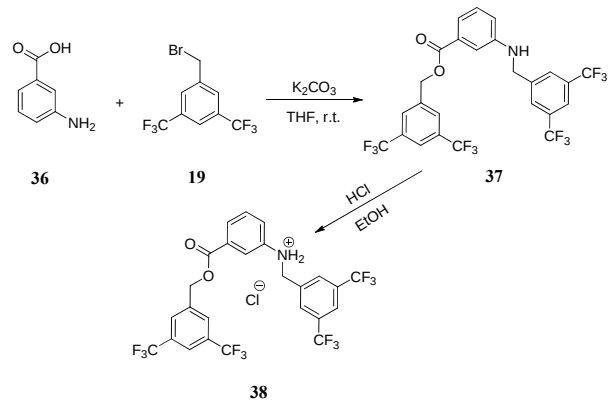

36 **19** **37** **38**

Scheme 15. The synthesis of compound **37** and its chloride complex **38**.

Double bis(trifluoromethyl)benzylation of 3-aminobenzoic acid **36** at room temperature produced ester **37** bearing two electron-deficient arenes at both terminals. With the similar method aforementioned, complex **38** was obtained as crystals from ethanol (Scheme 15).

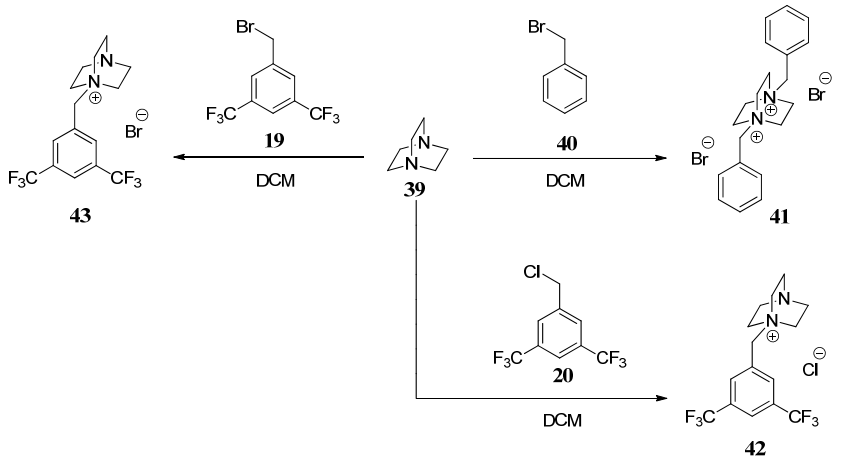

Scheme 16. The preparation of DABCO substituted complexes **41**-**43**.

In previous structure determinations of the pentafluorophenyl systems, diazabicyclo[2.2.2]octane (DABCO) has been a sufficient substituent to fix anions on top of the aromatic rings through CH···anion interactions. Therefore, for obtaining the CF_3-substituted research objects and their crystals, derivatives **42** and **43** were prepared from DABCO and trifluoromethylated benzyl bromide or chloride. In addition, non-fluorinated salt **41** was synthesized as a comparison compound (Scheme 16).

(b) The crystal structures of CF_3-substituted-aryl compounds

The synthesized derivatives **35**, **38**, **41**-**43** and commercially available 3,5-bis(trifluoromethyl)benzamide **44** were selected for structral research (Scheme 17).

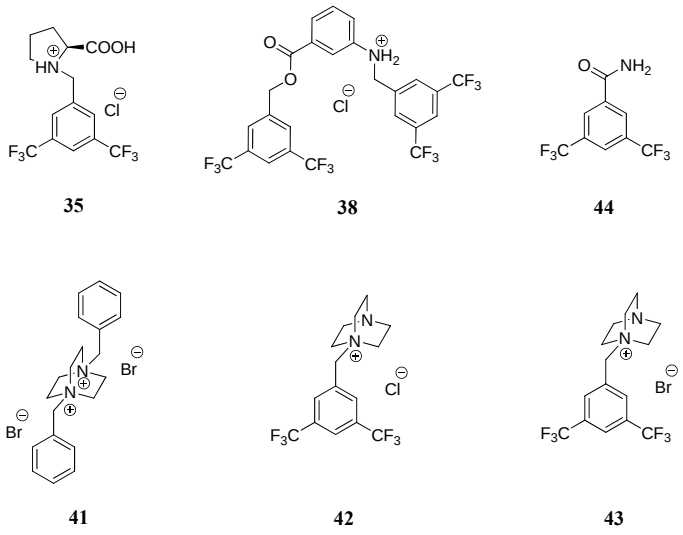

Scheme 17. Compounds prepared for structure research.

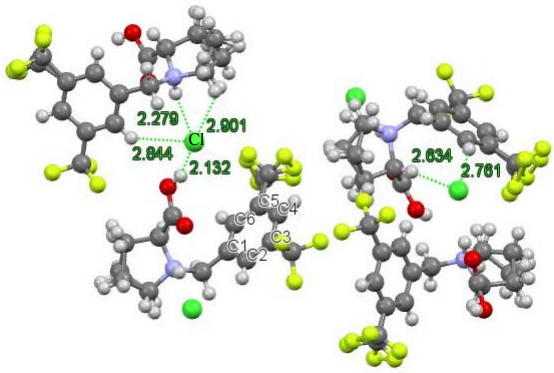

Figure 7. The crystal structure of **35**. Some fluorine atoms and the L-proline moieties are disordered. (black: C, gray: H, yellow-green: F, blue: N, green: Cl, red: O)

The chloride salt **35** was crystallized in the space group $P2_12_12_1$. For each 3,5-bis(trifluoromethyl)benzylated L-prolin cation, there are two chloride anions adjacent to it, as shown in Figure 7. One of the chloride anions approaches to the rim of the CF_3-ring and the other one is fixed above the aromatic ring (C1-C6) by hydrogen bonds and other CH···Cl interactions. The shortest distance from Cl^- to the carbon atoms of the ring (C1-C6) is 5.116 Å which is far beyond the Van der Waals radii of carbon atom and chloride anion.[18] It demonstrates that the hydrogen bonding interactions are the most prominent effects between the chloride anion and the organic cations in the solid state.

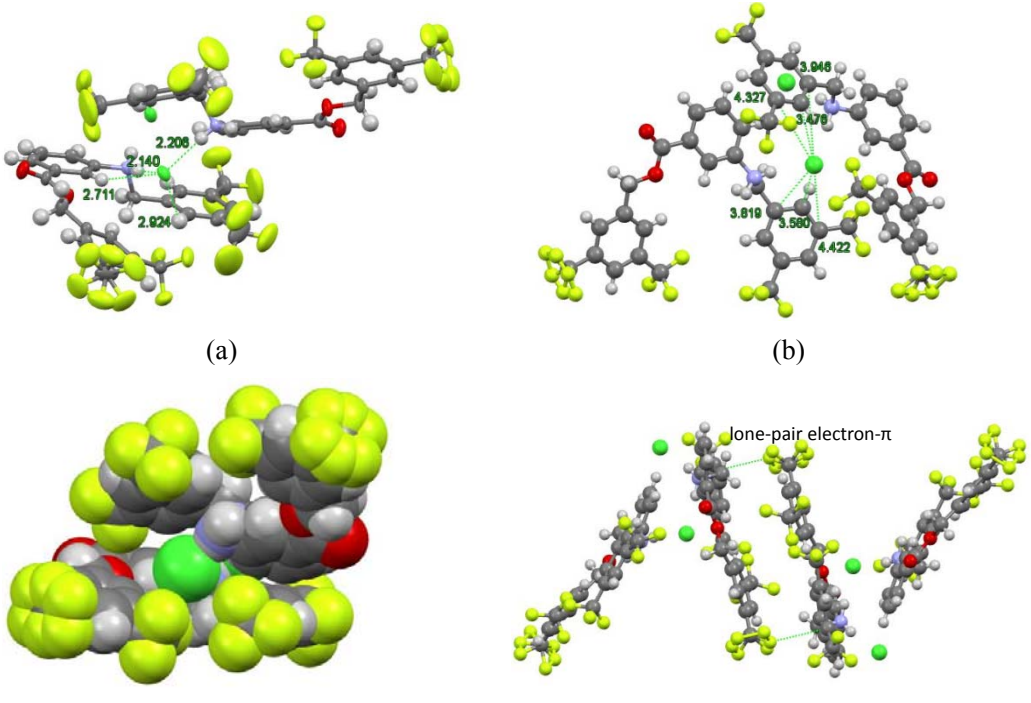

(a) (b)

(c) (d)

Figure 8. The structure of **38** in crystals. (a) The chloride anion fixed by NH···Cl and CH···Cl interactions; (b) The distances between Cl^- and the carbon atoms of the CF_3-rings nearby; (c) Fixation of chloride in the cleft of the organic cation; (d) The parallel and "zigzag" arrangement of the structure of **38** in crystals. Some fluorine atoms are disordered. (black: C, gray: H, yellow-green: F, blue: N, green: Cl, red: O)

The crystal structure of chloride salt **38** is shown in Figure 8. Even though three electron-deficient arenes exist in the molecule, none of the chloride located on the top of π-rings. The dominant interaction is hydrogen bonding between chloride and the two ammonium cations with NH···Cl = 2.14 and 2.21 Å (Figur 8, a). The closest distance of chloride to a CF_3-ring carbon atom is 3.48 Å, while it is not classical anion-π interaction due to the large shift of Cl^- relative to the ring (Figure 8, b). Cooperative effect of NH···Cl and CH···Cl interactions fix the chloride in the cleft of the organic cation (Figure 8, c). Additionally, the framework of complex **38** arrange to a parallel or "zigzag" conformation in the crystal (space group $P2_1C$) with H···Cl and lone pair electron-π interactions as linkages (Figure 8, d).

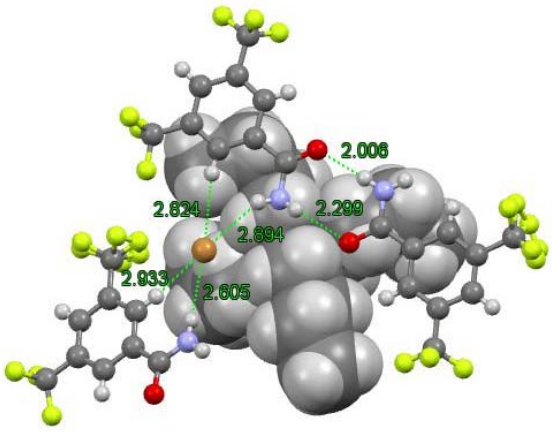

Figure 9. The crystal structure of the 2:1 adduct of **44** with TBA·Br (Bu_4N^+ is shown as the space filling model). Some fluorine atoms are disordered. (black: C, gray: H, yellow-green: F, blue: N, brown: Br, red: O)

Compound **44** is a neutral trifluoromethylated receptor in the tested series. Correspondingly, the complex of pentafluorobenzamide with Br^- shows the bromide is fixed on top of the aromatic unit by the cooperation of anion-π and hydrogen bonding interactions.[58] However, in the 2:1 co-crystal (space group *P*mc2) of 3,5-bis(trifluoromethyl)benzamide with Br^-, the anion-π interaction cannot be observed. Instead, major interactions are hydrogen bonding of the anion with NH- and CH- moieties (NH···Cl = 2.89, 2.61 Å, CH···Cl = 2.82, 2.93 Å). In addition, between the two acylamino groups head to head, the hydrogen bonds participate in organizing an intermolecular 8-member ring (Figure 9).

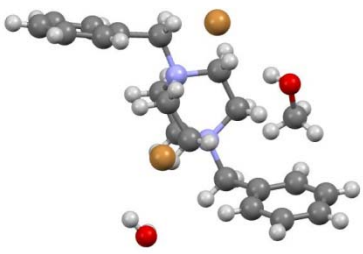

Figure 10. The crystal structure of non-fluorinated derivative **41**. (black: C, gray: H, blue: N, brown: Br, red: O)

The double benzyl substituted complex **41** does not possess the electron-deficient aromatic ring and no anion-π interaction can be found in the solid state. The two Br^- are located far away from

the aromatic units showing CH···Br short contacts with the DABCO and the methylene units. A water and a methanol co-crystallized in the structure and the latter was fixed in the cavity of the DABCO with one benzyl unit in the opposite direction which the oxygen atom of methanol points to (Figure 10).

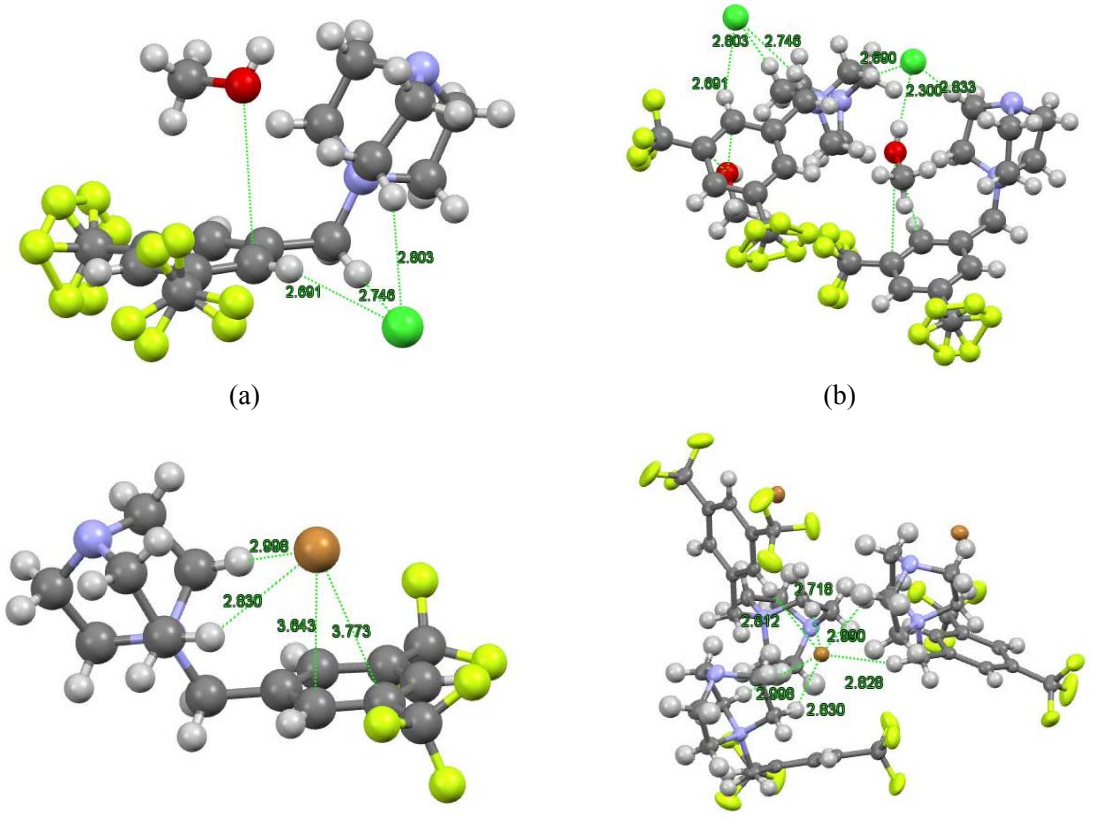

(a) (b)

(c) (d)

Figure 11. The structures of trifluorormethylated derivatives **42** and **43** in crystals. Some fluorine atoms are disordered. (black: C, gray: H, yellow-green: F, blue: N, green: Cl, brown: Br, red: O)

Compounds **42** and **43** are two electron-deficient aromatic substituted derivatives with chloride and bromide anions, respectively. The crystal structure analyses of **42** and **43** somewhat support the results calculated by computational chemistry for **28**-**32**. For the chloride anion complex **42**, a side-on binding of the chloride has been found as prediction. The Cl^- interacts with the aryl unit only by CH_{aryl}···Cl bond (2.69 Å), additionally with DABCO and methylene units by CH···Cl short contacts as well as hydrogen bonding interaction with the methanol co-crystallized over the top of the electron-deficient aromatic ring (Figure 11, b). Differently from the status of the methanol co-crystallized in **41**, the oxygen of the methanol in **42** points to the plane of the 3,5-bis(trifluorormethyl)phenyl unit, which reveals lone-pair electron-π interaction between oxygen and the electron-deficient ring (Figure 10, a).

In terms of the bromide derivative **43**, probably because of the higher polarization of Br^- than that of Cl^-, it reveals more obviously favorable interaction between the anion and the π-system. As shown in Figure 11 (c), the bromide locates above the π-ring by the additional fixation by hydrogen bonds with two DABCO hydrogen atoms (H···Br = 2.83, 3.00 Å). However, the anion is not on top of the center of the π-ring but shifting over its rim which can be described as η^2-type

anion-π interaction showing distances C···Br = 3.64 and 3.77 Å somewhat longer than Van der Waals distances. Additionally, the bromide interacts to other two neighboring organic cations with hydrogen bonding (CH_{aryl}···Br = 2.81 Å) and short contacts ($CH_{methylene}$···Br = 2.83 Å, CH_{DABCO}···Br = 2.72 and 2.99 Å) (Figure 11, d).

3.3 Conclusion

In this part, we introduced CF_3-substituted arenes into the research of anion-π interactions, which is a pioneering work of supramolecular chemistry. Firstly, we calculated the binding behavior of several selected trifluoromethylated aromatics (**28**-**32**) with fluoride, chloride or bromide anion. Only Meisenheimer-type σ-complexes or hydrogen bonding interactions were produced between π-system and F^- or Cl^-. Interestingly, although Br^- interacted with CF_3 aromatics **28** or **29** separately by forming σ-complex or hydrogen bonds, anion-π interactions were induced between bromide and **30**, **31** or **32**, separately. It indicated CF_3-substituted electron-deficient aromatics could be properly designed as π-receptors for anions. Then experimental research focused on the 3,5-bis(trifluoromethyl)phenylated aromatic compounds, due to their commercially available advantages. Five CF_3 π-receptors (**35**, **38**, **42**, **43** and **44**) and one non-fluorinated comparison compound **41** were prepared and the crystal investigation results coincide to the conclusion of the computational chemistry, which demonstrates that in the solid state, Cl^- always interacts to the hydrogen atoms of the 3,5-bis(trifluoromethyl)phenyl units and Br^- enables this kind of CF_3 aromatics to be π-receptors by anion-π interactions.

Chapter 4 Study of anion-π interactions by NMR in solution: pentafluorophenyl or 3,5-bis(trifluoromethyl)phenyl derivatives as π-receptors for anions

4.1 Introduction

Different from the study of anion-π interactions in the solid state which has provided numerous results proving the attraction of the electron-deficient aromatics to anions, the investigation of this weak effect in solution is still an open question, mainly due to the solvation of anions as well as the competition of other non-covalent interactions. The issue which methodology can be used as a sufficient tool to detect or calculate anion-π interaction is ambiguous until now. Although previously some research work already studied the anion binding behavior of π-receptors with UV-Vis spectra, fluorescence spectra or NMR spectra, the results are not always satisfactory.[26, 29, 41, 59]

Because of the attraction, it is not surprising that in solution, the position of anions or the binding affinities of π-receptors with anions could be influenced by the properties of electron-deficient hosts, ex. the Q_{zz} and London dispersion as well as the polarizability of anions. Obviously, the quantity of the electron-deficient units of the π-receptors also effects the binding situation of the host-guest systems. An *ab initio* study on anion-π, anion-π_2 and anion-π_3 complexes revealed the additivity of anion-π interactions, that is, the increase of binding energies depending on the addition of the electron-deficient units in the receptors.[54]

Besides, pentafluorophenyl derivatives have already been reported as ideal π-receptors for anions in crystals by our group, anion-π interaction was recently found existing between bromide anion and trifluoromethylated aromatic cation in the crystal structure of complex **43** as abovementioned. In this chapter, a series of derivatives bearing pentafluorophenyl or 1,3-bis(trifluoromethyl)phenyl groups were synthesized and studied as π-receptors for anions in solution by NMR spectroscopy.

4.2 The preparation of C_6F_5/CF_3 π-receptors for solution studies

To minimize the competitive non-covalent effects which may cover the anion-π interactions in solution, structurally simple compounds with mono-, di- or tetra- electron-deficient aromatic units were separately prepared. As NH is able to direct the location of the anion to the aromatics,[60] amino, acylamino or imide unit was introduced into the prepared π-receptor.

Nucleophilic substitution reaction is the dominant strategy to synthesize pentafluorophenyl derivatives **46**-**50** (Scheme 18). From commercially available materials, these receptors were obtained at room temperature with moderate to good yields. The structures of **46** and **47** are both secondary amines without carbonyl group. As exception, compound **46** contains two pentafluorophenyl groups while a phenyl ring is found in **47** instead of one C_6F_5. Compound **48** is an imide with the *N*,*N*-bis(pentafluorobenzoyl) unit, so that there is only one residual hydrogen atom in the structure. Derivatives **49**, **50** and **51** are amides with one carbonyl and at least one pentafluorophenyl on different positions.

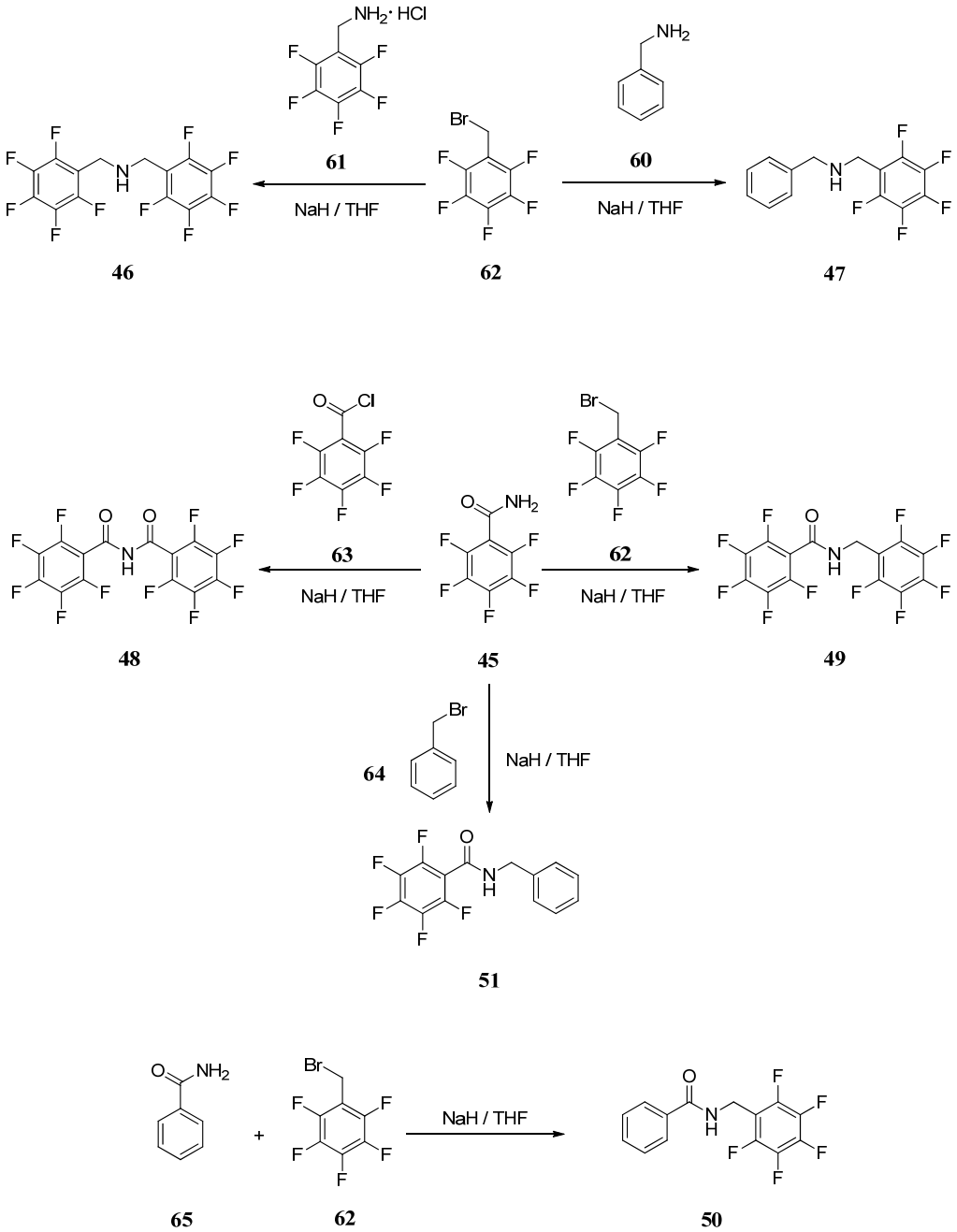

Scheme 18. The preparation of the pentafluorophenylated compounds.

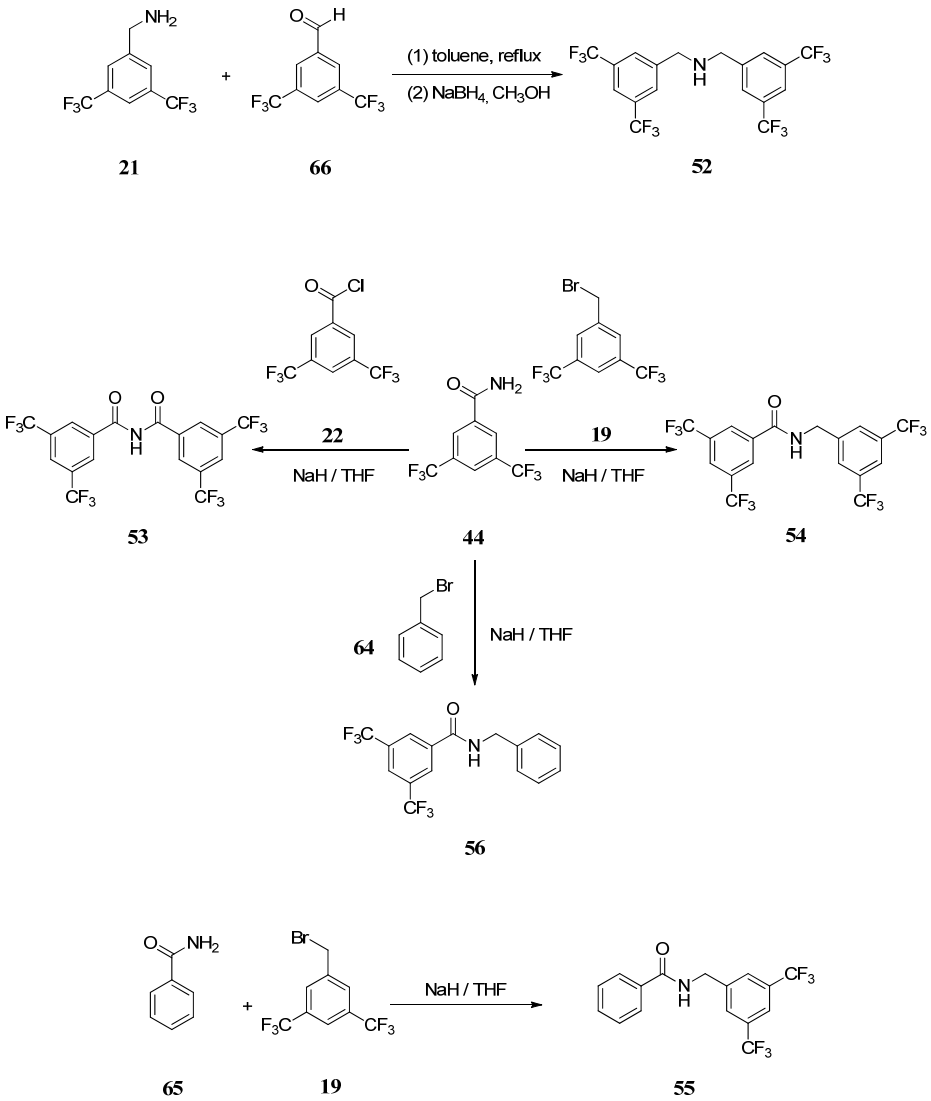

Scheme 19. The preparation of the trifluoromethylated compounds.

The synthetic methods for compounds **53-56** were similar to that of pentafluorophenylated derivatives (Scheme 19). However, for preparation of amine **52**, the nucleophilic substitution reaction was not sufficient. Instead, according to literature,[61] the symmetric amine **52** was obtained by reduction of the imine which was produced *via* condensation reaction of 3,5-bis(trifluoromethyl)phenylated amine **21** and aldehyde **66**.

In addition, some electron-deficient tetra-aromatics **57-59** and **69-70** were produced from 2,4,6-trichloro-1,3,5-triazine **67** or benzene-1,3,5-tricarbonyl trichloride **68** reacting with 3 equiv. fluorinated aromatic materials. Therefore, each of the prepared electron-deficient multi-aromatic compounds contains three fluorinated electron-deficient moieties as well as an electron-deficient aromatic core (Scheme 20).

For comparison of additive effect induced by the addition of aromatic units, the two commercially available and structurally simple compounds **44** and **45** were also studied by NMR spectroscopy as π-receptors for anions.

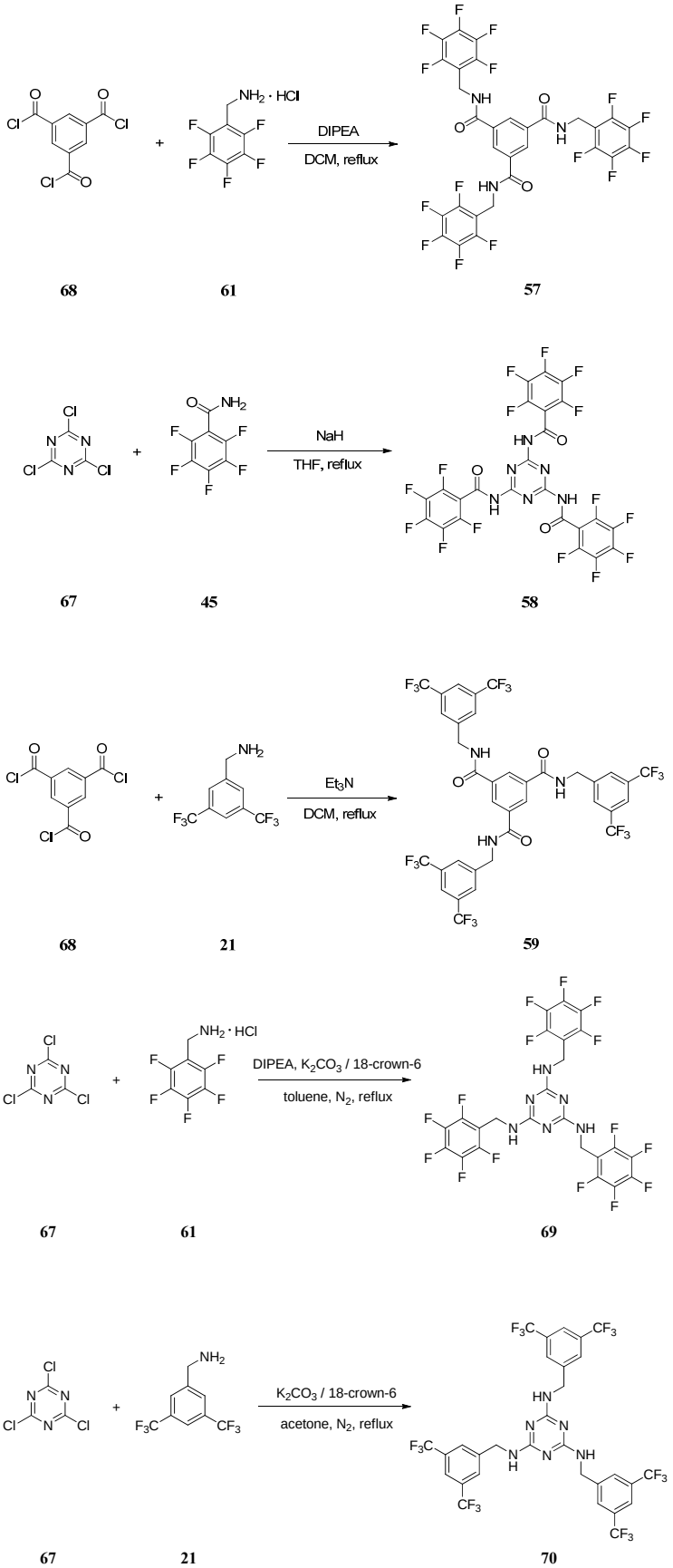

Scheme 20. The preparation of electron-deficient tetra-aromatic compounds.

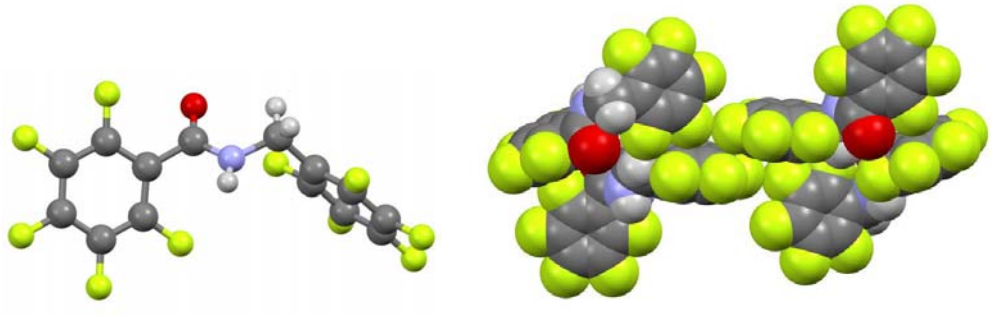

(a) (b)

Figure 12. (a) The crystal structure of compound **49**. (b) Spacefill mode showing part of the crystal lattice of **49**. (black: C, gray: H, yellow-green: F, blue: N, red: O)

Compound **49** was crystallized from MeOH/Et_2O in the space group $P2_1/c$. As shown in Figure 12, the amide group and the carbon atom of the methylene unit are in the same plane which forms interplanar angles of 46.64° and 80.56° respectively with the planes of two pentafluorophenyl rings. T-shaped CF-π interaction can be observed in the crystal lattice (Figure 12, b). In addition, the oxygen atom of the carbonyl interacts with the NH of the neighboring molecule with intermolecular hydrogen binding effect (CO···HN = 2.84 Å).

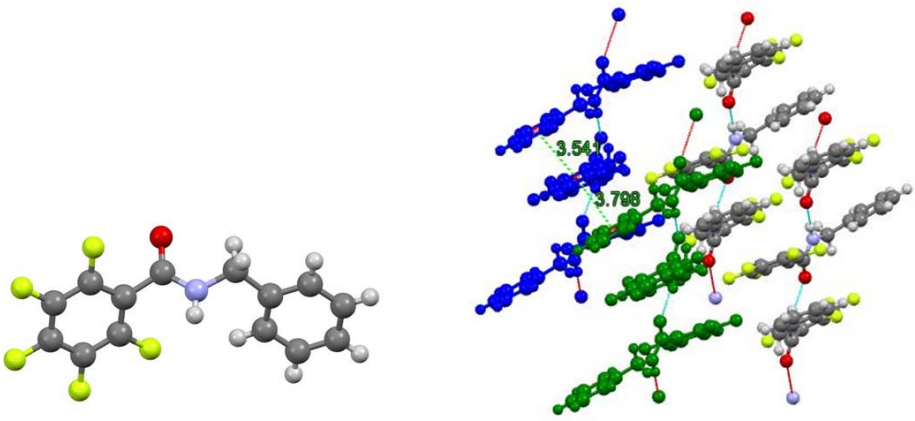

(a) (b)

Figure 13. (a) The crystal structure of compound **51**. (b) Molecule chains showing amide-to-amide hydrogen bonds and π-π stacking interactions in the crystal of **51**. (black: C, gray: H, yellow-green: F, blue: N, red: O)

The crystal of compound **51** was obtained from MeOH/Et_2O in the space group $P2_1/c$ and its structure is shown in Figure 13 (a). The plane of the amide with the carbon atom of methylene forms interplanar angles of 56.75° and 55.95° respectively with the planes of pentafluorophenyl and the phenyl rings. The amide NH forms a hydrogen bond to a neighboring amide carbonyl with a NH···OC distance of 2.88 Å, resulting in an amide-to-amide hydrogen bonded polymer. The polymer is further supported by π-π stacking between pentafluorophenyl and phenyl units with center to center distances of 3.54 and 3.80 Å for the intra- and inter-hydrogen-bonding-chain interactions, respectively.

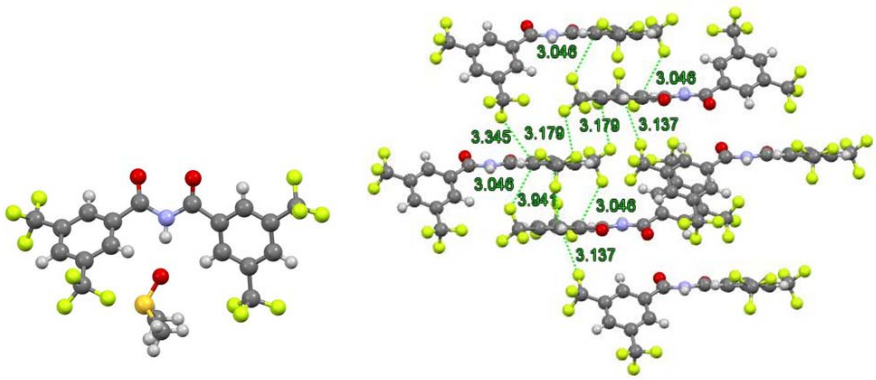

(a) (b)

Figure 14. (a) The crystal structure of molecule **53** showing a DMSO co-crystallizes by hydrogen binding with NH. (b) Part of the crystal lattice of **53** showing the CF-π interaction which results in the intermolecular parallel orientation between the 3,5-bis(trifluoromethyl)phenyl rings. The co-crystallized DMSO molecules are omitted for clarity. (black: C, gray: H, yellow-green: F, blue: N, red: O)

The crystal of compound **53** was cultivated from DMSO/Et_2O with a solvent molecule co-crystallized. The single molecule of **53** adopts a conformation with a planar C(=O)-NH-C(=O) unit, whereas the aromatic rings are tilted towards this plane with interplanar angles of 7.95° and 46.94°, respectively (Figure 14, a). Besides the hydrogen binding effect between the oxygen atom of DMSO and the NH unit, CF-π interaction can be observed in the crystal lattice with a (C)F···C distances from 3.05 to 3.35 Å and induce a parallel arrangement of CF_3 aromatic rings.

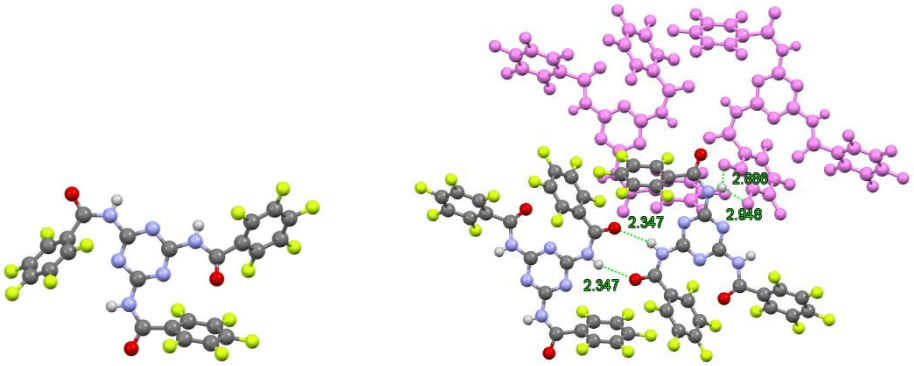

(a) (b)

Figure 15. (a) The crystal structure of compound **58**. (b) Part of the crystal lattice of **58** showing non-classical CF···HN and C=O···HN hydrogen bonding. (black: C, gray: H, yellow-green: F, blue: N, red: O)

Compound **58** was crystallized from MeOH/Et_2O in the space group *P*-1. The single molecule of **58** is shown in Figure 15 (a) and possesses a plane of the triazine ring which forms interplanar angles of 56.37°, 64.64° and 68.25° with each plane of the pentafluorophenyl ring. One of the oxygen atoms of the carbonyl groups points to the pentafluorophenyl ring and causes lone-pair electron-π interaction with distances from 3.05 to 3.49 Å. The C=O···HN hydrogen bonding (2.35 Å) results in a dimer which is displayed in Figure 15 (b) and long contacts of 2.89 and 2.95 Å between CF and the NH unit of the neighboring molecule were also observed.

4.3 The binding behavior of the fluorinated π-receptors for anions in solution

4.3.1 The stoichiometry of the electron-deficient tetra-aromatic receptors with halide anions

Three fluorinated derivatives **57**, **58** and **59** bearing four aromatic rings were prepared and investigated in this part. The chloride, bromide or iodide anion was introduced to investigate the complexation with these receptors in solution.

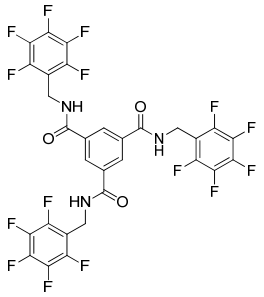

57

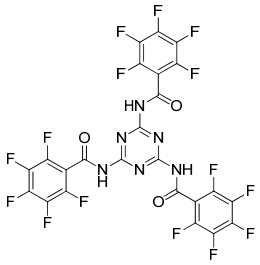

58

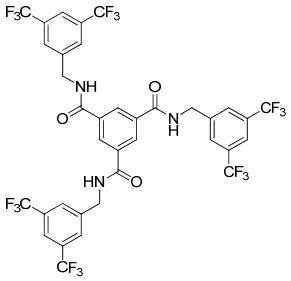

59

Job-plots are used to calculate the ratio of host to guest in the complex. This work used Job-plots by $^{1}H/^{19}F$ NMR chemical shifts as data to reveal the stoichiometry of the electron-deficient multi-aromatic receptors to halide anions (Cl^-, Br^-, I^-).

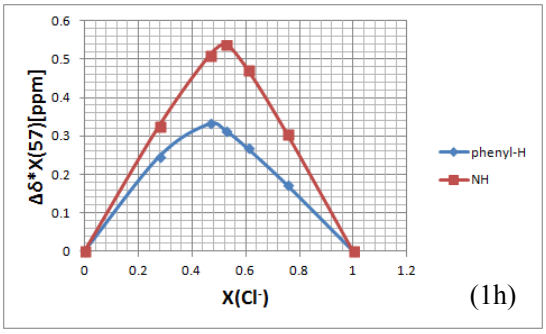

(1h)

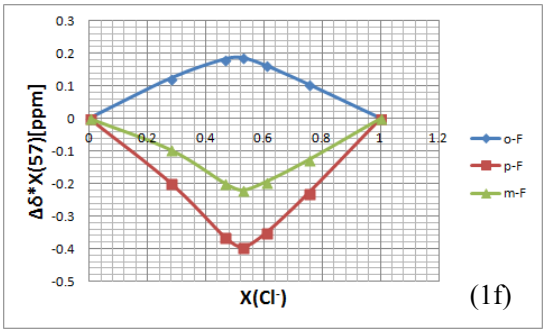

(1f)

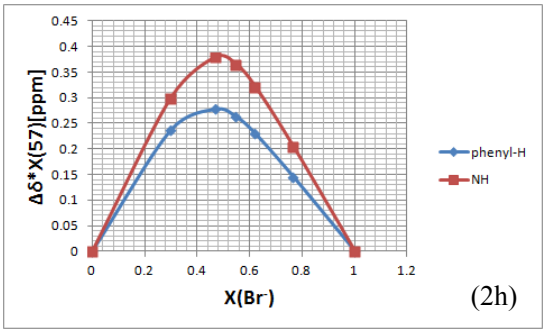

(2h)

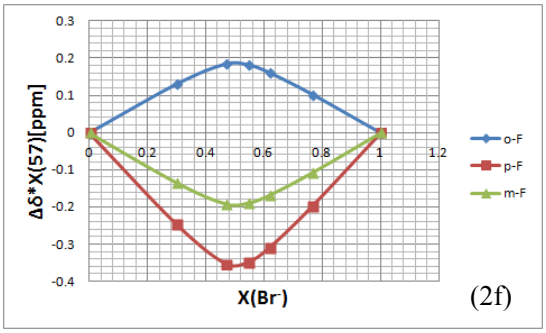

(2f)

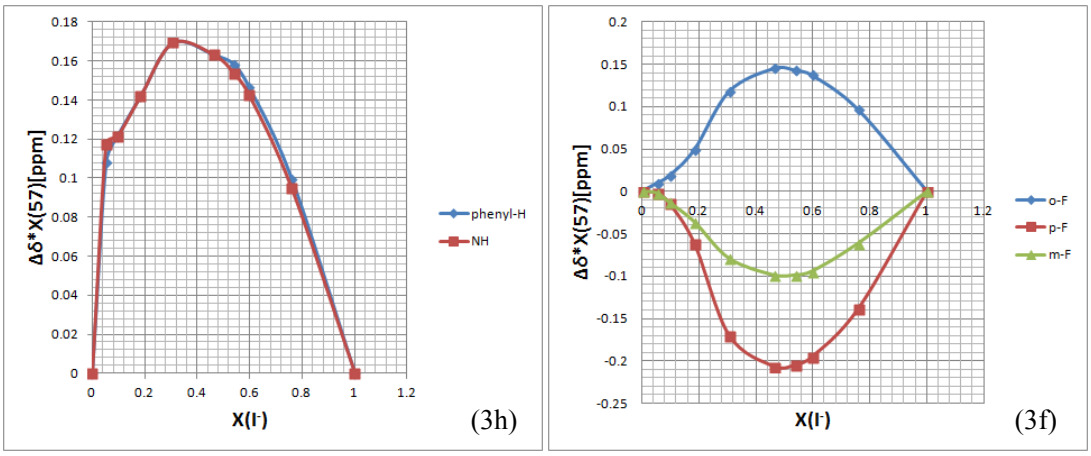

Figure 16. Job-Plots of receptor **57** with Cl^- (1h, 1f), Br^- (2h, 2f) and I^- (3h, 3f). The data calculated were obtained from $^1H/^{19}F$ NMR spectra in acetone-d_6 at room temperature.

As shown in Figure 16, Job-Plots determined either with Cl^- or Br^- formed a 1:1 complex with receptor **57**. However, the stiochiometry of iodide anion with compound **57** is ambiguous. Specifically, checking from phenyl-H or NH of the electron-deficient core, the stiochiometry is 2:1 (host:guest). Differently, the fluorine Job-Plots revealed a 1:1 complex of compound **57** with the iodide anion.

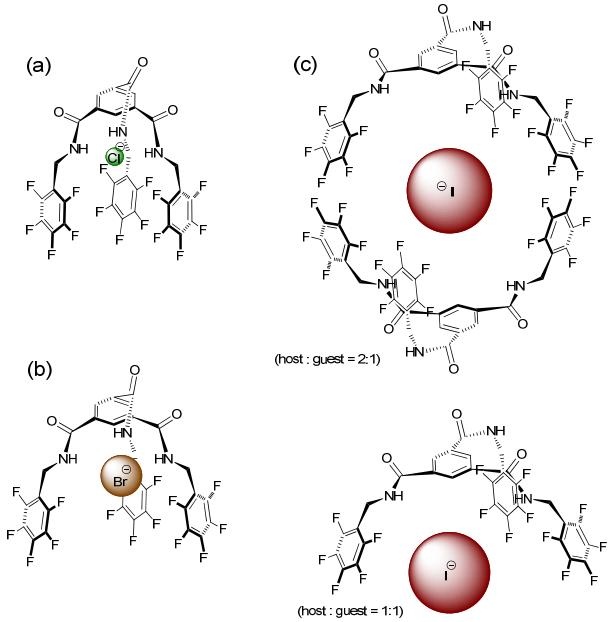

Scheme 17. Possible complexation modes of compound **57** with halide anions (Cl^-, Br^-, I^-) in acetone-d_6 at room temperature.

Since either Cl^- or Br^- has a smaller Van der Waals volume than I^-, the anion may be packed in one receptor's cavity and fixed by hydrogen bonds with NH of the same receptor (Scheme 17, a and b). Due to the large Van der Waals volume as well as the easier polarization, one I^- could interact with two receptors simultaneously determined by ^1H NMR Job-Plots or form a 1:1 complex with the receptor revealed by ^{19}F NMR Job-Plots (Scheme 17, c).

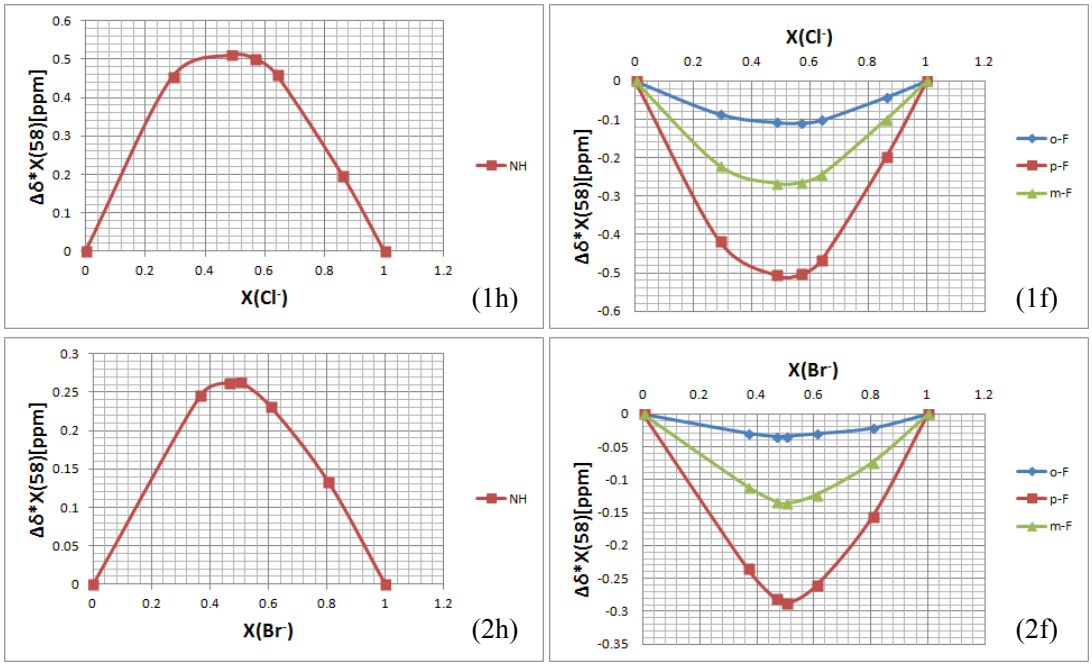

Figure 18. Job-plots of receptor **58** with Cl^- (1h, 1f), Br^- (2h, 2f). The data calculated were obtained from $^1H/^{19}F$ NMR spectra in acetone-d_6 at room temperature.

Stiochiometry clearly shows a 1:1 binding ratio of compound **58** with Cl^- or Br^- (Figure 18). But there is no special ratio for the binding between **58** and iodide anion. Probably because of the short length of the pentafluorobenzamide unit, the structure of **58** could not form a cavity of correct size to hold an iodide anion (Apendix, Figure S13).

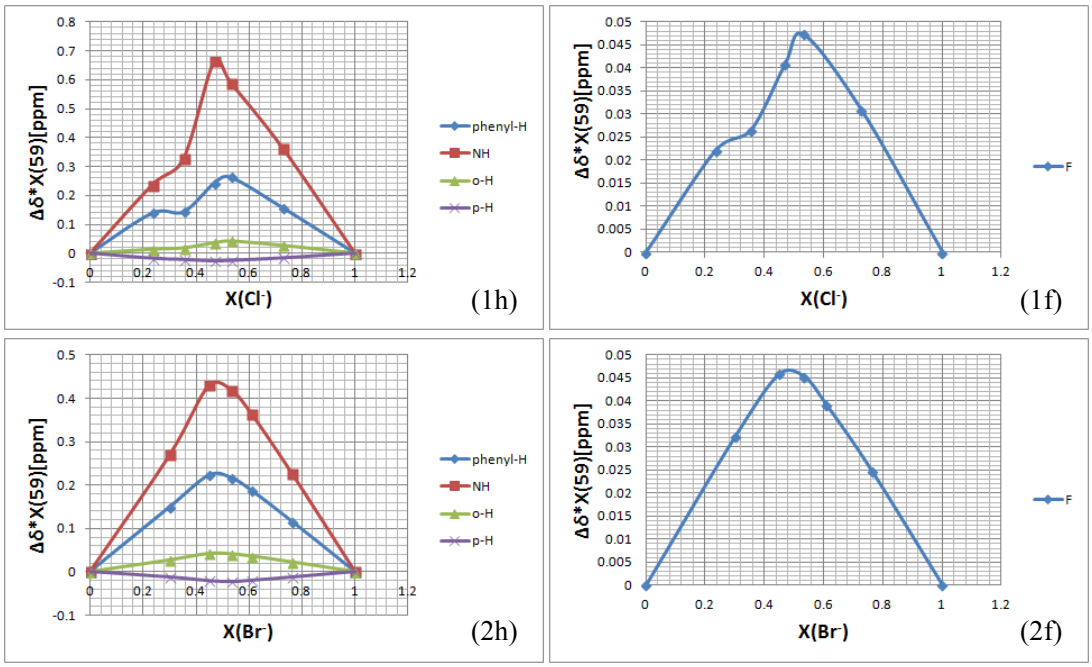

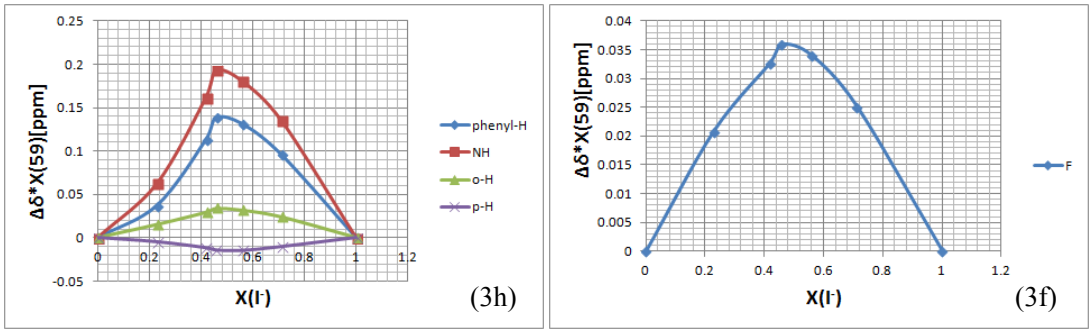

Figure 19. Job-plots of receptor **59** with Cl^- (1h, 1f), Br^- (2h, 2f) and I^- (3h, 3f). The data calculated were obtained from $^1H/^{19}F$ NMR spectra in acetone-d_6 at room temperature.

The CF_3 π-receptor **59** associates with halide anions (Cl^-, Br^-, I^-) by 1:1 binding ratio (Figure 19). It is notable that only with 3,5-bis(trifluoromethyl)benzyl instead of pentafluorobenzyl group, the I^- could be able to bind with the host **59** by 1:1 ratio.

4.3.2 The binding behavior of C_6F_5-receptors with anions in solution

The binding behavior of a series of C_6F_5 π-receptors with various anions (Cl^-, Br^-, I^-, NO_3^-) were investigated and the corresponding binding constants (K_a) and Gibbs free energies (ΔG) were calculated with $^1H/^{19}F$ NMR-titration experiments. The anions were introduced into the solution as tetrabutylammonium (TBA) salts and deuterated chloroform or acetone was used as solvent according to the different solubility of receptors. Consequentely, each C_6F_5-receptor showed the similar binding behavior to these different anions (see Appendix 1) and selected $^1H/^{19}F$ NMR-titration curves are displayed in this part as representative examples.

(a) The interactions between C_6F_5-receptors and chloride anions in solution

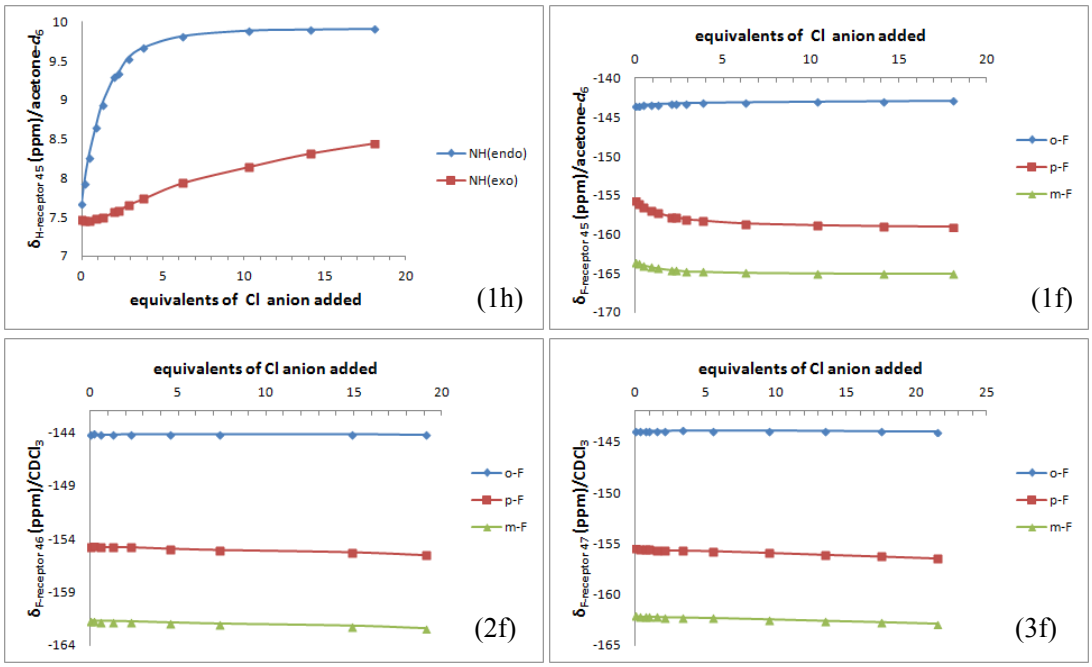

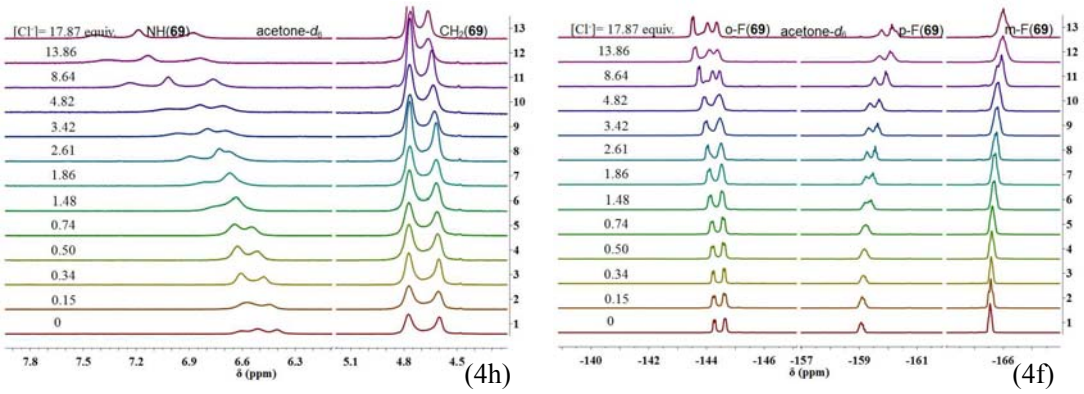

Figure 20. $^{1}H/^{19}F$ NMR chemical shifts of selected C_6F_5 receptors (**45**, **46**, **47** and **69**) with the addition of TBA·Cl in $CDCl_3$ or acetone-d_6. (298 K)

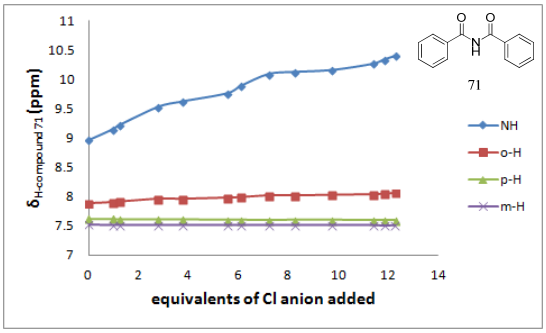

Figure 21. ^{1}H NMR chemical shifts of compound **71** with the addition of TBA·Cl in $CDCl_3$. (298 K)

The $^{1}H/^{19}F$ NMR-titration curves show the related chemical shifting of C_6F_5 receptors (**45**, **46**, **47** and **69**) with the chloride anion added (Figure 20). The NH^{exo} of receptor **45** displays a linear relation with the addition of Cl^-, which cannot reveal any special non-covalent binding effect. The similar situations are also found in the compared system of compound **71** with Cl^- (Figure 21). In addition, the shifting of meta- or para-H in the phenyl group of **71** did not change with the addition of anions. Therefore, there is no obvious defined interaction between anions and the π-bond of **71**. However, the NH^{endo} of **45** binds Cl^- obviously with hydrogen bond and the titration curve demonstrates a kind of saturated state. Interestingly, in the receptor **46** or **47** without carbonyl in the structure, the peaks of ^{19}F NMR shift to high-field with increasing concentration of anions showing a linear relation (Figure 20, 2f and 3f). It should be caused by the effect of the π-bond with anions, due to the electron-deficient property of pentafluorobenzyl units. The peak splitting of the $^{1}H/^{19}F$ NMR peaks of derivative **69** without carbonyl demonstrate σ-complexes may be generated with the addition of chloride anions (Figure 20, 4h and 4f).

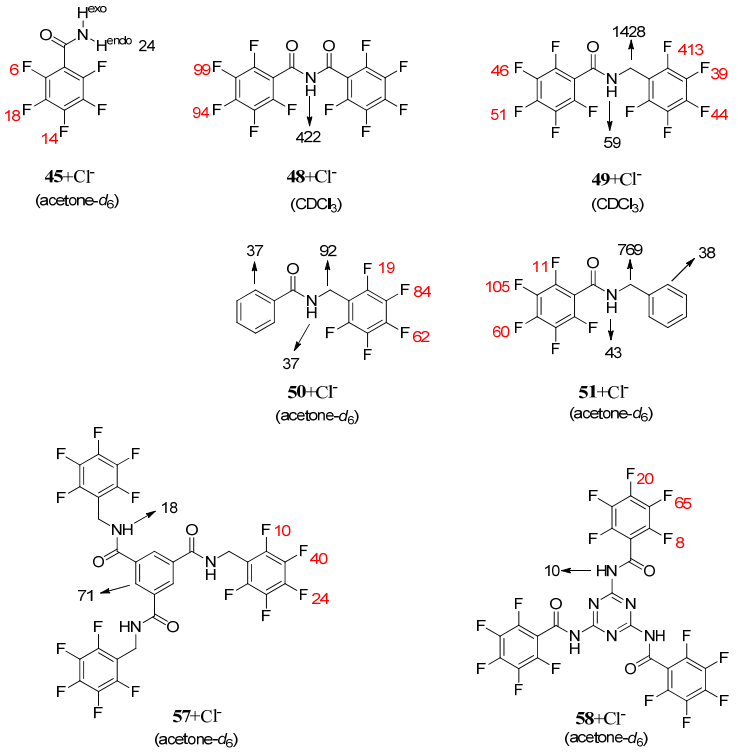

Scheme 21. Different binding constants (K_a: M^{-1}) for the complexes of C_6F_5 π-receptors with chloride anions. The binding constants were determined by $^1H/^{19}F$ NMR spectrometric analyses in $CDCl_3$ or acetone-d_6 at room temperature. Errors are estimated to be lower than 20%.

As shown in Scheme 21, the K_a of either NH or fluorine in **48** is largely increased than that in **45**. The pentafluorobenzamide **45** as π-receptor only displays affinity to chloride with the endo-hydrogen H^{endo} (K_a=24 M^{-1}) of the amide (Figure 20, 1h), as well as the effect between anions and pentafluorophenyl units. Especially, the meta- and para-fluorine demonstrate a larger influence than ortho-fluorine (meta-F: K_a=18 M^{-1}; para-F: K_a=14 M^{-1}; ortho-F: K_a=6 M^{-1}), which show much more obvious chemical shifts of meta- and para-F in NMR spectra (Figure 20, 1f). For imide derivative **48** bearing two pentafluorobenzoyl groups and only one active hydrogen atom, the binding constant K_a of NH increases to 422 M^{-1} and of meta- and para-fluorine rise above 90 M^{-1}. This may have two reasons: 1. the two pentafluorobenzoyl groups largely enhance the acidity of the NH, so that the association constant between hydrogen and Cl^- is increased; 2. the two electron-deficient aromatics (C_6F_5) afford more affinity to anions with anion-π interaction, which is the compensation to the hydrogen bonding. The increase of the K_a of fluorines in **48** reveals the interaction existing between chloride and C_6F_5 units. The absence of one carbonyl (for compound **49**) makes the decrease of K_a both in hydrogen and fluorines, except the large K_a of ortho-fluorine in pentafluorobenzyl moiety. The analogue **50** fixes the Cl^- with the NH and ortho-H of phenyl as well as the attraction of C_6F_5. As to derivative **51** with a benzyl unit substituting the H^{exo} of **45**, both the hydrogen bonding and interactions between anions and C_6F_5 were enhanced obviously. In addition, the Cl^- was fixed with NH and ortho-H of the benzyl unit.

The compound **57** could be recognized as the tri-substituted derivative of **50**. Although compound **57** contains four electron-deficient aromatics: one tri-carboxyphenyl unit and three pentafluorophenyl groups, the NH does not display stronger affinity to Cl^- but also weakens the interactions between anions and C_6F_5 units, which may be induced by the formation of NH···O=C

contact nearby. However, the $H_{(phenyl)}$ demonstrats stronger attraction to Cl^- which makes the K_a of $H_{(phenyl)}$ increase from 37 to 71 M^{-1}. Similarly, the receptor **58** bearing a triazene unit as a core also reveals a weaker attraction than that of **51**, for either NH or pentafluorophenyl unit.

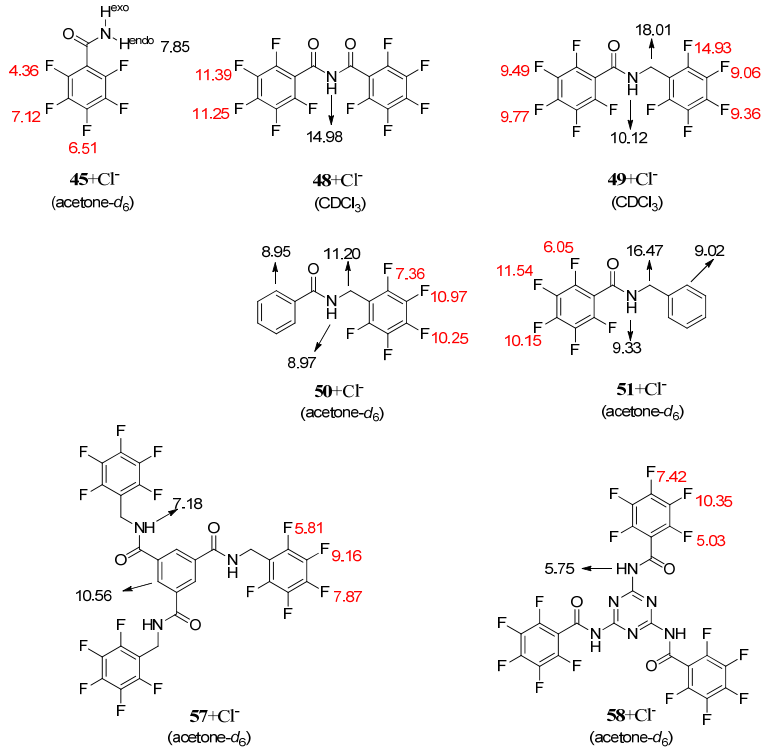

Scheme 22. Different Gibbs free energies (ΔG: kJ/mol) for the complexes of C_6F_5 π-receptors with chloride anions. The Gibbs free energies were determined by $^1H/^{19}F$ NMR spectrometric analyses in $CDCl_3$ or acetone-d_6 at room temperature.

Calculated Gibbs free energies with NH as standard (Scheme 22), the binding affinity (14.98 kJ/mol) of **48** is two times as that (7.85 kJ/mol) of **45**. When one carbonyl was absent, the Cl^- tends to contact with methylene rather than with NH in compound **49**. The different positions of C_6F_5 and carbonyl group make no obvious effect to the binding affinity of receptors with chloride anions (see compounds **50** and **51** in scheme 22). When the C_6F_5 unit in **49** is changed into C_6H_5 (structure **51)**, the affinity is decreased by about 1 kJ/mol for NH. Therefore, both the carbonyl and the C_6F_5 unit made an important influence to the attraction between receptors and anions.

(b) The interactions between C_6F_5-receptors and bromide anions in solution

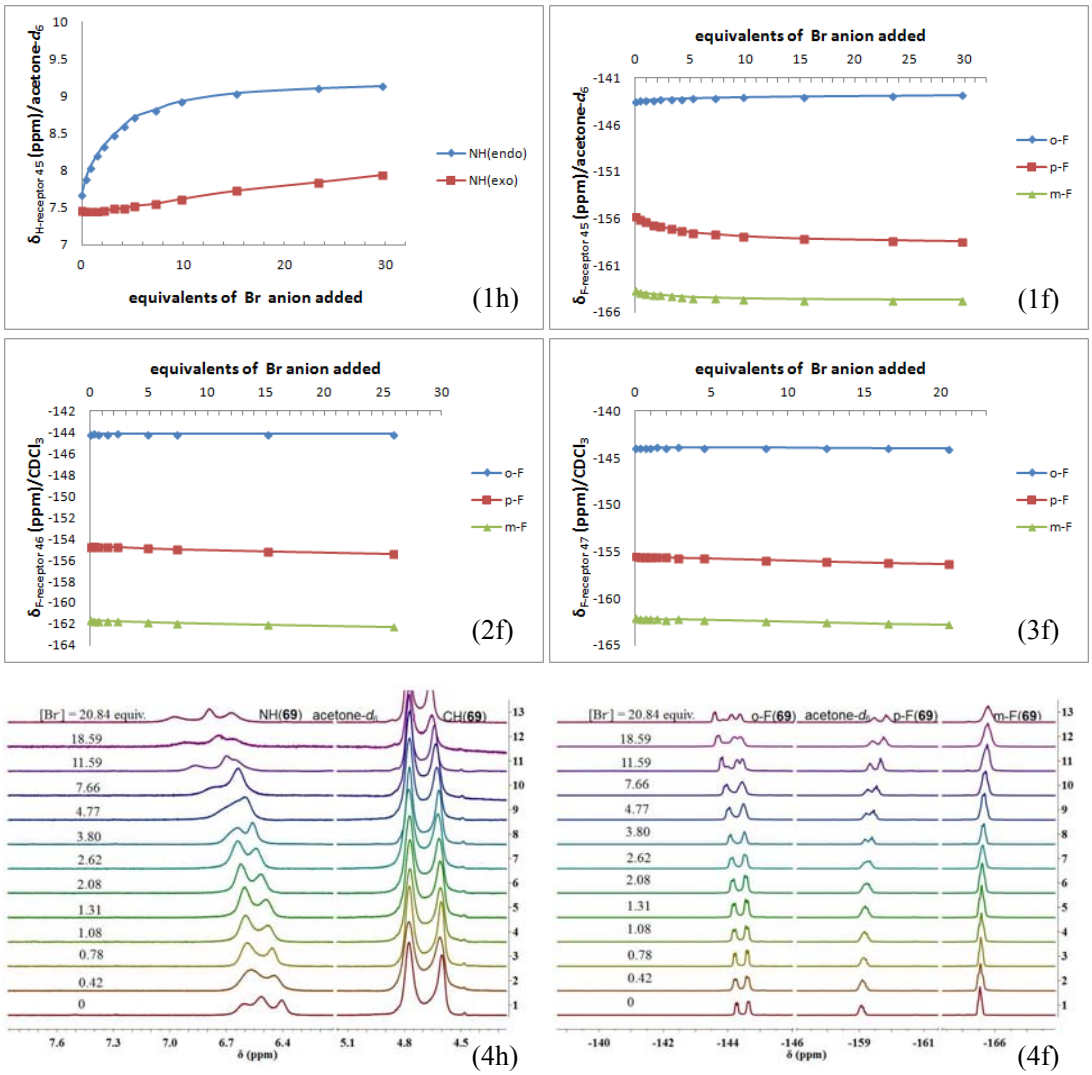

Figure 22. $^{1}H/^{19}F$ NMR chemical shifts of selected C_6F_5 receptors with the addition of TBA·Br in $CDCl_3$ or acetone-d_6. (298 K)

The chloride anion always contributes to lager down-field shifting of the NH in each of the receptors with **45** as an example than bromide (Figure 20 and 22). It reveals the higher affinity of Cl^- to NH, but the binding constants of NH with Cl^- in both **57** and **58** are still less than in the Br^- counterparts (Scheme 21 and 23), which indicats that anion-π interaction makes an important role in the anion binding behavior of π-receptors, because of the different polarization of anions.

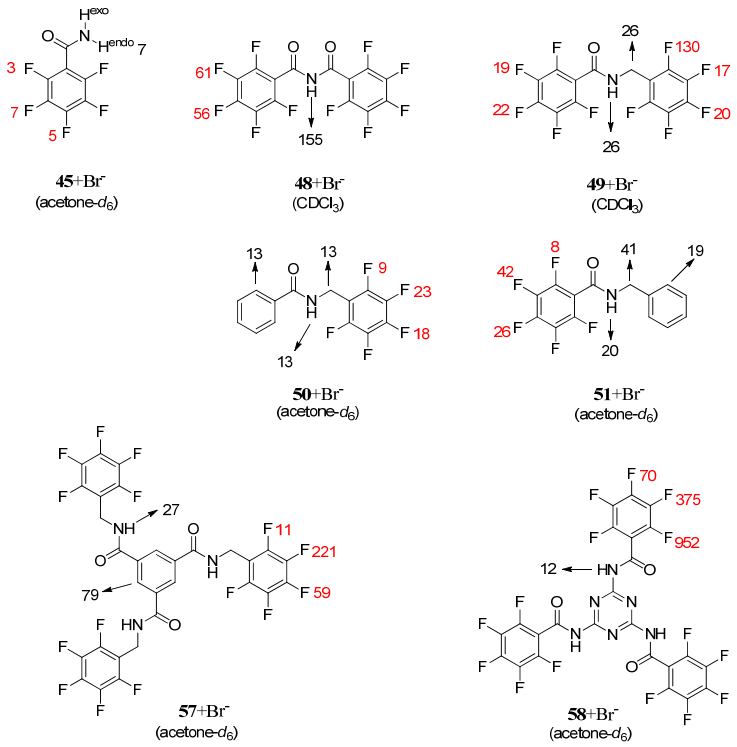

Scheme 23. Different binding constants (K_a: M^{-1}) for the complexes of C_6F_5 π-receptors with bromide anions. The binding constants were determined by $^1H/^{19}F$ NMR spectrometric analyses in $CDCl_3$ or acetone-d_6 at room temperature. Errors are estimated to be lower than 20%.

The bromide was also attracted by these receptors with hydrogen bonds as well as anion-π interactions in solution (Scheme 23). Nevertheless, the association constants of receptors **45** and di-cyclic derivatives **48-51**with Br^- are smaller than with Cl^-. The K_a of hydrogen binding in the Cl^- complexes is generally two or three times as large as K_a in the Br^- complexes, which may be due to the higher basicity of chloride as well as the larger Van der Waals volume of bromide.

On the other hand, in the complexes of tetra-cyclic receptors **57** and **58** with anions, the electron-deficient derivatives display favorable effects preferring Br^- over Cl^-. Due to the huger available spaces of tetra-cyclic compounds than those of di-cyclic receptors, the effect induced by basicity and Van der Waals volume of anions are covered by the polarization of anions. Therefore, the binding constants of pentafluorophenyl units with Br^- are obviously increased and even surpass the enhancement of hydrogen binding interactions.

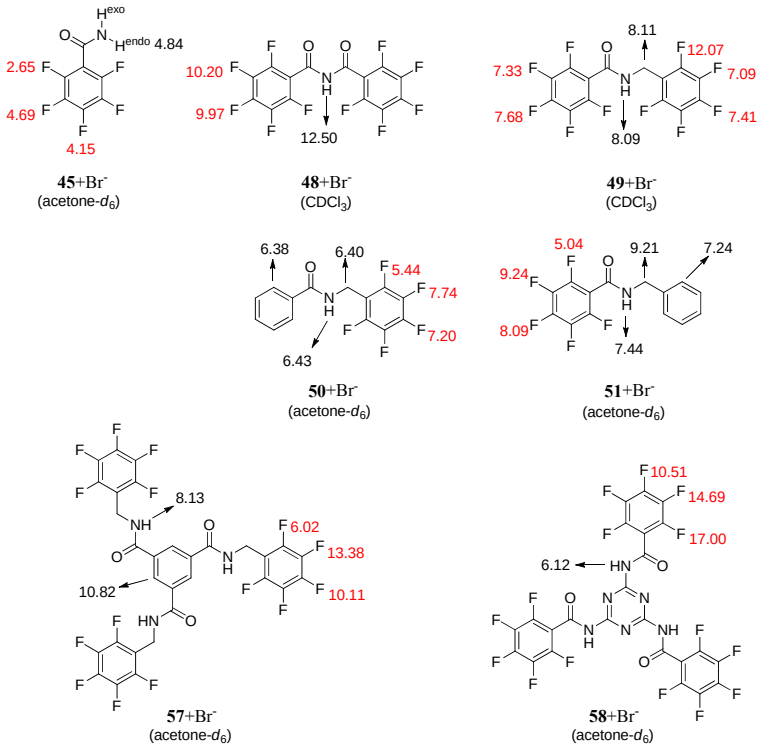

Scheme 24. Different Gibbs free energies (ΔG: kJ/mol) for the complexes of C_6F_5 π-receptors with bromide anions. The Gibbs free energies were determined by $^1H/^{19}F$ NMR spectrometric analyses in $CDCl_3$ or acetone-d_6 at room temperature.

Besides the hydrogen binding effect with NH and ortho-H of C_6H_5 moieties, the bromide shows affinity to $CH_{(methylene)}$ in receptors **49-51**with energies of 6.40-9.21 kJ/mol close to the hydrogen bond energy in the same host-guest system, respectively (Scheme 24).

The hydrogen binding energies of receptor **57** or **58** with Br^- are nearly equal to that with Cl^-, while the affinity between C_6F_5 and Br^- are evidently larger. Moreover, compared to K_a and ΔG of receptor **57** and **58** with Cl^- or Br^-, the bromide interacts more with C_6F_5 units than with the triazene core in **58** and the chloride prefers the tri-carboxyphenyl core in **57**.

(c) The interactions between C_6F_5-receptors and iodide anion in solution

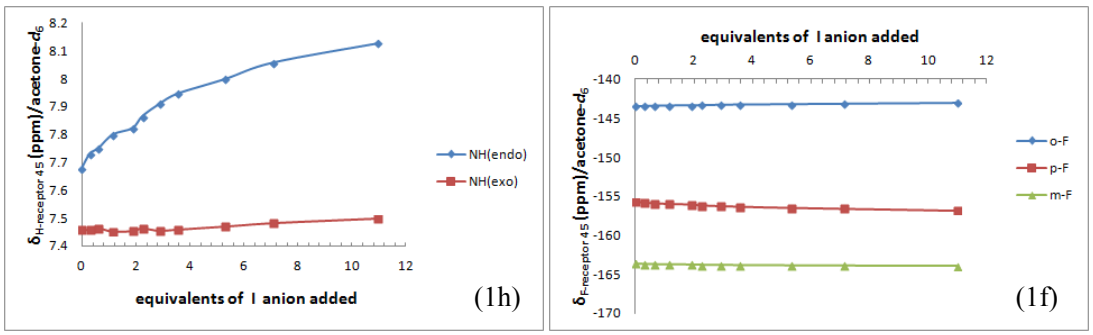

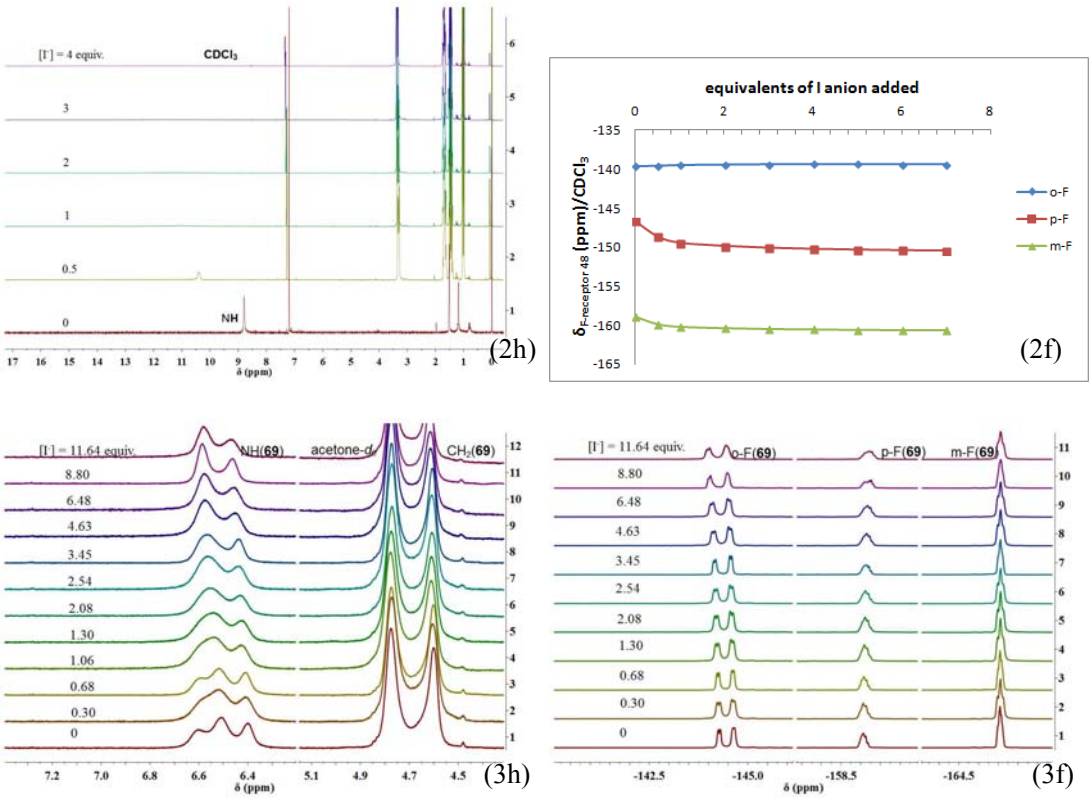

Figure 23. $^{1}H/^{19}F$ NMR chemical shifts of selected C_6F_5 receptors with the addition of TBA·I in $CDCl_3$ or acetone-d_6. (298 K)

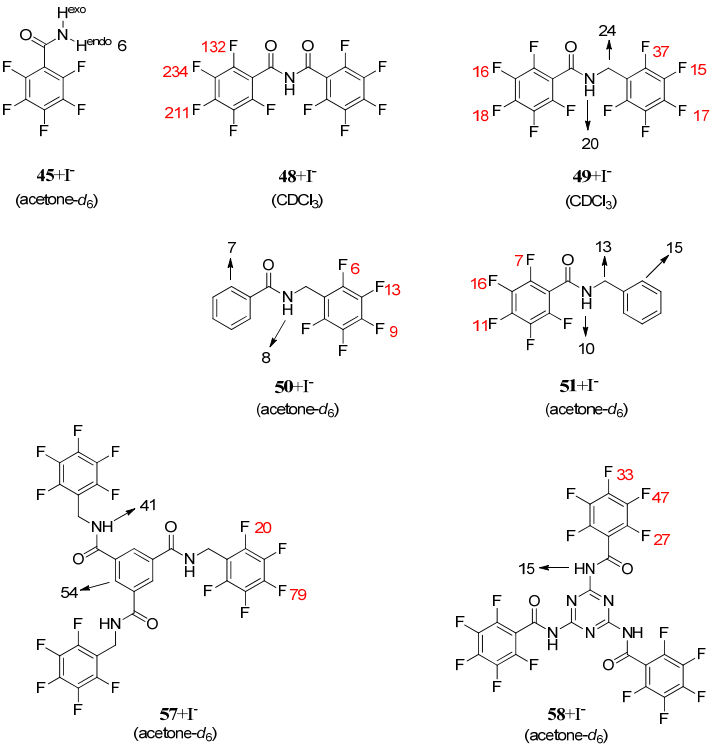

Scheme 25. Different binding constants (K_a: M^{-1}) for the complexes of C_6F_5 π-receptors with iodide anions. The binding constants were determined by $^{1}H/^{19}F$ NMR spectrometric analyses in $CDCl_3$ or acetone-d_6 at room temperature. Errors are estimated to be lower than 20%.

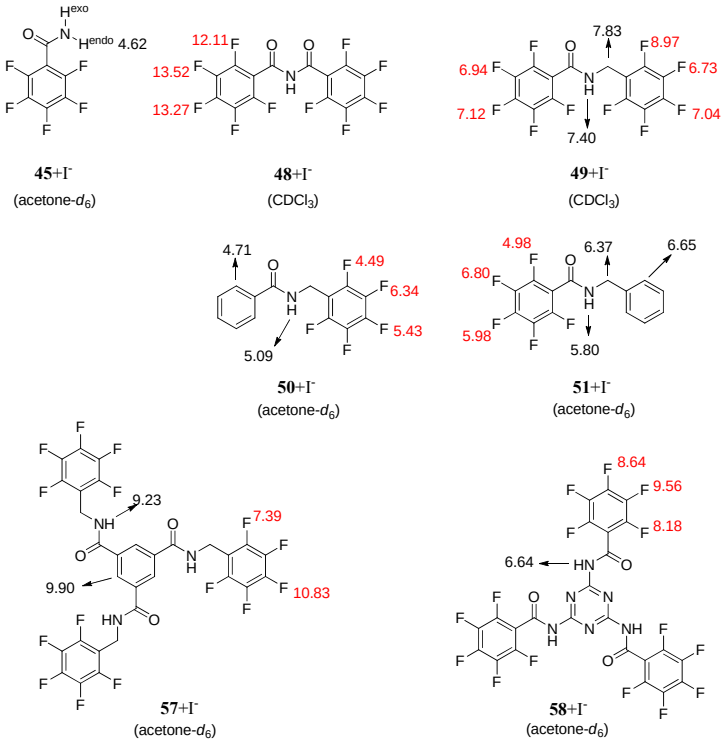

Scheme 26. Different Gibbs free energies (ΔG: kJ/mol) for the complexes of C_6F_5 π-receptors with iodide anions. The Gibbs free energies were determined by $^1H/^{19}F$ NMR spectrometric analyses in $CDCl_3$ or acetone-d_6 at room temperature.

Although the NH^{endo} shows weak affinity to iodide (K_a = 6 M^{-1}), the pentafluorophenyl unit in **45** does not reveal any obvious interaction with I^- and the chemical shifts of ^{19}F NMR peaks do not change obviously with the addition of iodide anions (Figure 23, 1f). In fact, the binding constants of fluorine with iodide in the receptors shown in scheme 25 are generally smaller than that with Cl^- or Br^-, except the case of compound **48** with I^-. With the addition of TBA·I, the peak of NH in **48** was reduced and vanished when the amount of I^- exceeded equal equivalents (Figure 23, 2h). However, the binding constants of pentafluorophenyl unit with I^- are extremely bigger even than with bromide or chloride anions. Instead one carbonyl of **48** with a methylene unit, the binding constants of ^{19}F decreased rapidly shown with **49**. Compound **57** with a tri-substitution of phenyl core attracts iodide anions much powerfully than mono-substituted **50** do, due to the presence of three amides as well as three pentafluorobenzyl units. Comparison with **51**, despite three pentafluorobenzamide groups and a triazene core inside, the compound **58** affords only a little more stabilization energy (6.64 kJ/mol vs. 5.80kJ/mol) to I^- with hydrogen bond and moderate increase of affinity with anion-π interactions (Scheme 26). Different from chloride or bromide anions, neither NH···I^- nor I^-···π interaction was induced between the iodide and compound **69** (Figure 23, 3h and 3f), even though several electron-deficient aromatics present in the structure, but the carbonyl groups are absent in contrast to compound **58**.

(d) The interactions between C_6F_5-receptors and nitrate anions in solution

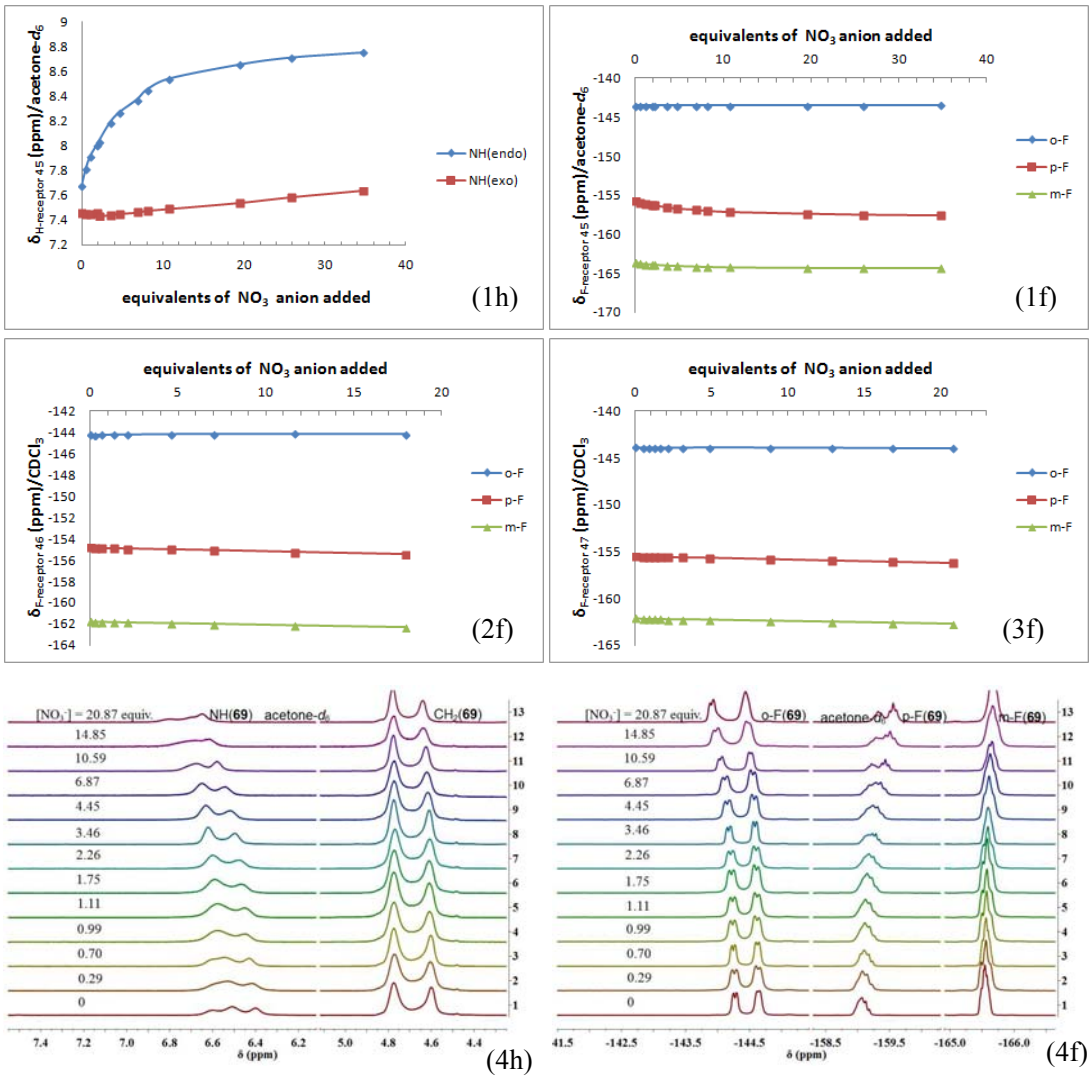

Figure 24. $^{1}H/^{19}F$ NMR chemical shifts of selected C_6F_5 receptors with the addition of TBA·NO_3 in $CDCl_3$ or acetone-d_6. (298 K)

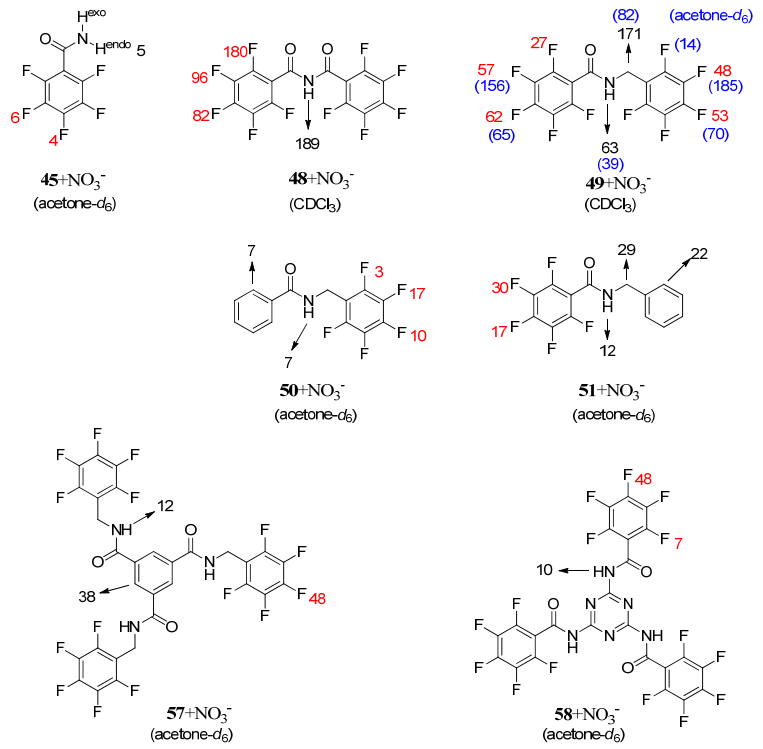

Scheme 27. Different binding constants (K_a: M^{-1}) for the complexes of C_6F_5 π-receptors with nitrate anions. The binding constants were determined by $^1H/^{19}F$ NMR spectrometric analyses in $CDCl_3$ or acetone-d_6 at room temperature. Errors are estimated to be lower than 20%.

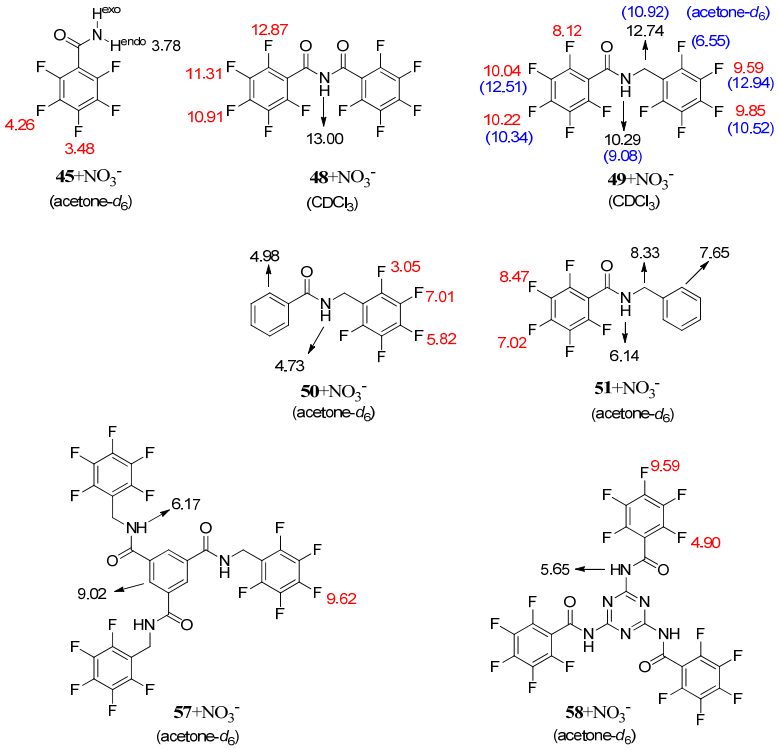

Scheme 28. Different Gibbs free energies (ΔG: kJ/mol) for the complexes of C_6F_5 π-receptors with nitrate anions. The Gibbs free energies were determined by $^1H/^{19}F$ NMR spectrometric analyses in $CDCl_3$ or acetone-d_6 at room temperature.

Nitrate anions interact with NH^{endo} of pentafluorobenzamide **45** by the weakest hydrogen bonding (K_a = 5 M^{-1}, ΔG = 3.78 kJ/mol) among the four kinds of anions (Cl^-, Br^-, I^- and NO_3^-) and the binding constants of fluorine in the complex of **45** with NO_3^- are close to the values with Br^-. In addition, the K_a of NH in complex of **48** with NO_3^- is definitely lower than with Cl^- (189 vs. 422 M^{-1}), but the K_a of fluorine are at the same degree of the value with Cl^-. Therefore, it is not reasonable to estimate the degree of $NO_3^-\cdots\pi$ interaction by the K_a of NH as standard. The effect of π-π stacking induced between the π-bond of NO_3 anions and the electron-deficient aromatic units may cover the attractive anion-π interaction.

The hydrogen binding of receptor **49** with nitrate anions is weakened when acetone-d_6 is used as solvent instead of $CDCl_3$, while the effects of anions with pentafluorophenyl units are enhanced. This result may attribute to the affinity between the oxygen atom of acetone and the hydrogen atom of receptor **49**, combined with the solvation of the nitrate anion.

4.3.3 The binding effect of CF_3-receptors for anions in solution

Trifluoromethylated aromatic compounds could be investigated as π-receptors for anions, due to the strong electronegativity of the CF_3 group which may hugely reduce the Q_{zz} of the aromatic unit in receptors.

Theoretical quantum chemistry calculation demonstrats in gas state, although fluoride or chloride anions prefer to form σ-complexes with the CF_3-compounds as abovementioned, the bromide anions are able to interact with these CF_3-receptors by anion-π interaction. Crystal structure research of 3,5-bis(trifluoromethyl)phenylated derivatives with chloride or bromide anions support these calculation results. For a clear explanation to the fact of CF_3 aromatics as π-receptors for anions, the solution study of the prepared 3,5-bis(trifluoromethyl)phenylated receptors with halide anions (Cl^-, Br^-, I^-) as well as NO_3^- was done using $^1H/^{19}F$ NMR-titration experiments.

(a) The interactions between CF_3-receptors and anions in $CDCl_3$

Compounds **21**, **44**, **52** and **54** were selected to study their binding behavior for anions in $CDCl_3$.

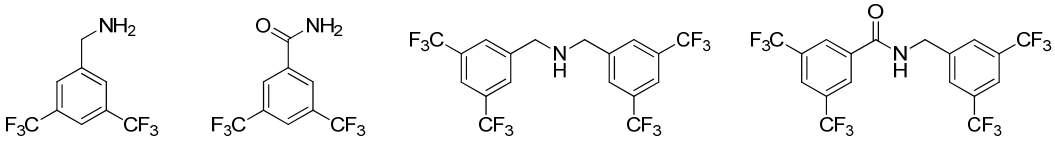

21 **44** **52** **54**

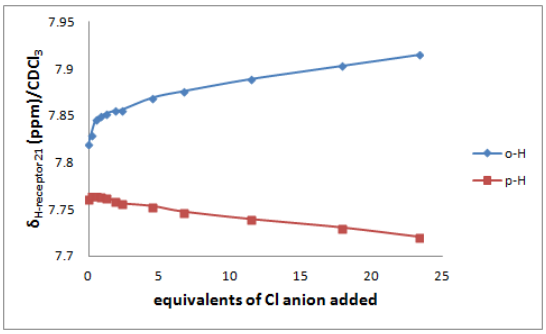

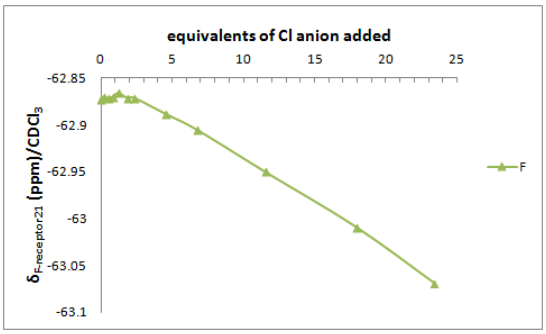

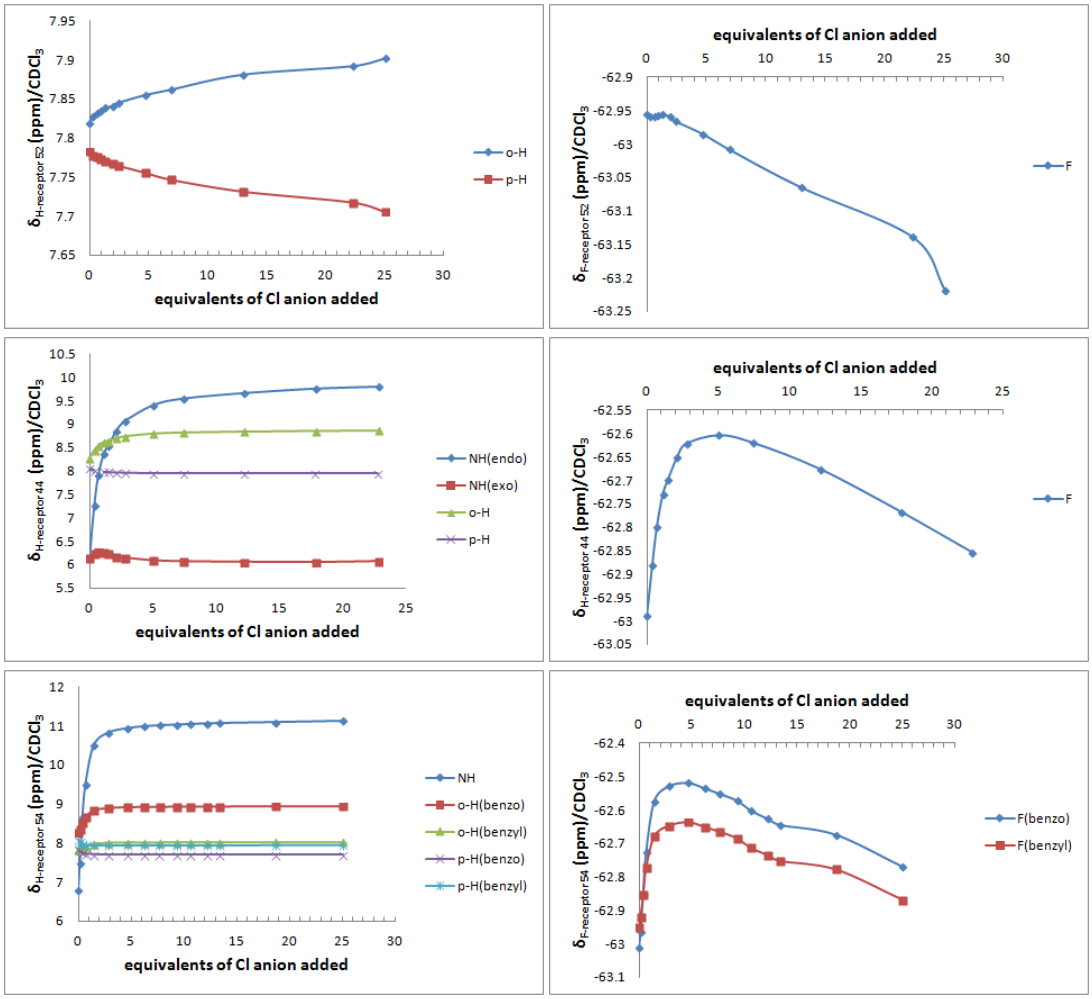

Figure 25. $^{1}H/^{19}F$ NMR chemical shifts of selected CF_3-receptor (**21**, **44**, **52** and **54**) with the addition of TBA·Cl in $CDCl_3$. (298 K)

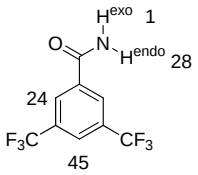

44+Cl^-
($CDCl_3$)

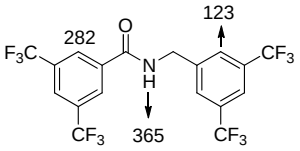

54+Cl^-
($CDCl_3$)

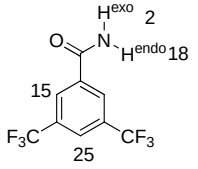

44+Br^-
($CDCl_3$)

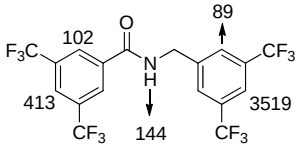

54+Br^-
($CDCl_3$)

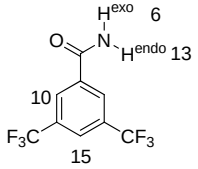

44+I^-
($CDCl_3$)

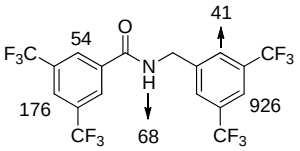

54+I^-
($CDCl_3$)

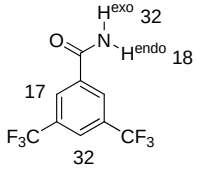

44+NO_3^-
($CDCl_3$)

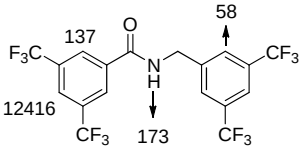

54+NO_3^-
($CDCl_3$)

Scheme 29. Different binding constants (K_a: M^{-1}) for the complexes of selected CF_3-receptors **44** and **54** with anions. The binding constants were determined by ^1H NMR spectrometric analyses in $CDCl_3$ at room temperature. Errors are estimated to be lower than 20%.

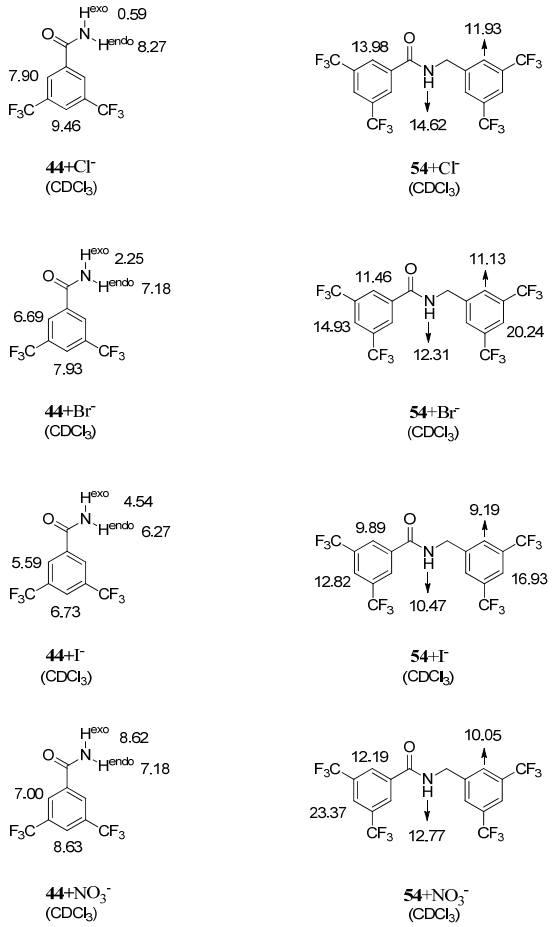

Scheme 30. Different Gibbs free energies (ΔG: kJ/mol) for the complexes of CF_3-receptors **44** and **54** with anions. The Gibbs free energies were determined by ^1H NMR spectrometric analyses in $CDCl_3$ at room temperature.

As representative examples, Figure 25 shows the selected results of $^1H/^{19}F$ NMR-titration experiments of amine (**21** and **52**) or amide (**44** and **54**) with Cl^- in $CDCl_3$ and others can be found in the Appendix 1 (1.2). The proton signals of NH in both amine derivatives are too weak to display their chemical shifts with the addition of anions. The chemical shifts of both the ortho-H and para-H in the aromatic rings of **21** or **52** show a more or less linear relation with the addition of anions. Specifically, the peaks of ortho-H shift to down-field while the para-H shows high-field shifting. There is no special binding effect existing between the protons of **21** or **52** and the anions in $CDCl_3$. However, the ^1H NMR-titration experiments for the amide derivative **44** or **54** reveals the binding effect for all protons in the structures with anions.

The ^{19}F NMR-titration experiments show some similar results for either amine or amide, with the down-field shiftings of ^{19}F NMR peaks initially and then high-field shiftings are revealed when the amount of anions exceeded 2 equivalents (for **21** or **52**) or 5 equivalents (for **44** or **54**). It is probably induced by the combined effects from the anion-π interaction to anion aggregation with the increased amount of anions.

The H^{endo} shows more affinity with halide anions than the H^{exo} and the binding constants of NH^{endo} of carbonyl groups as well as the hydrogen atoms of the aromatic rings in **44** or **54** with anions are enhanced in the order of $Cl^->Br^->I^-$, which shows an inverse order of the NH^{exo} with

halide anions (Scheme 29). The different Van der Waals volumes of halide anions may play a dominant role to this situation. Because of the large volume of nitrate anion, it induces higher binding constants to H^{exo} (32 M^{-1}) than to H^{endo} (18 M^{-1}). Despite that, the π-π effect between NO_3^- and the π-rings contribute to a favorable attraction of the electron-deficient aromatic rings with the nitrate anions. Replacing one hydrogen atom of the amide group in **44** by a 3,5-bis(trifluoromethyl)benzyl moiety, the binding affinities of all hydrogen atoms with anions are improved. Specifically, the ΔG of NH in compound **54** is nearly two times large as that of H^{endo} in **44** with respective anions (Scheme 30), which more or less proves the additivity of the CF_3 aromatic ring to the attraction between the π-receptors and anions, because as a linker between the NH and the CF_3-ring, the methylene unit without electron-withdrawing effect cannot enhance the acidity of the hydrogen atom of the NH unit.

(b) The interactions between CF_3-receptors and anions in acetone-d_6

Compounds **21**, **44**, **52**, **53**, **54**, **55**, **56** and **59** were selected to study their binding behavior for anions in acetone-d_6.

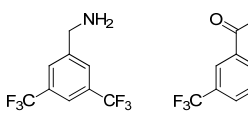

21

44

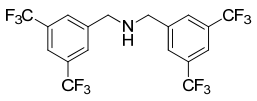

52

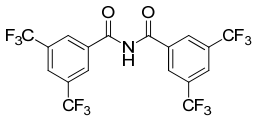

53

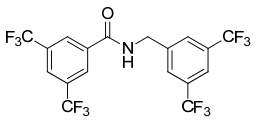

54

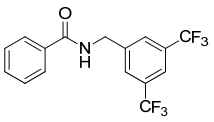

55

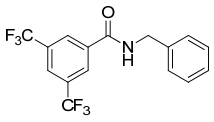

56

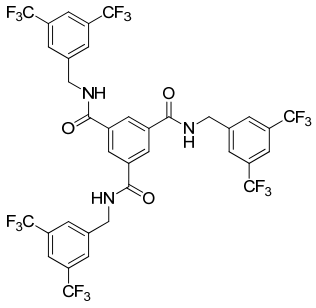

59

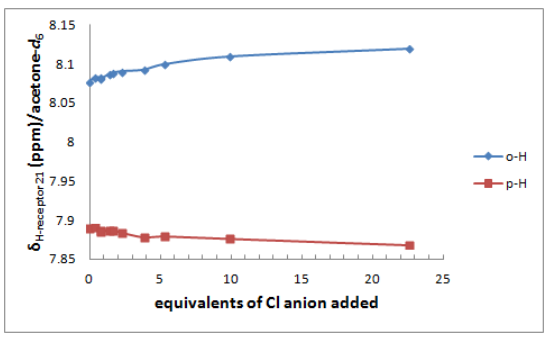

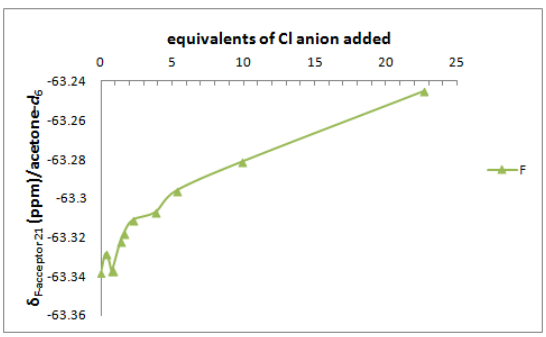

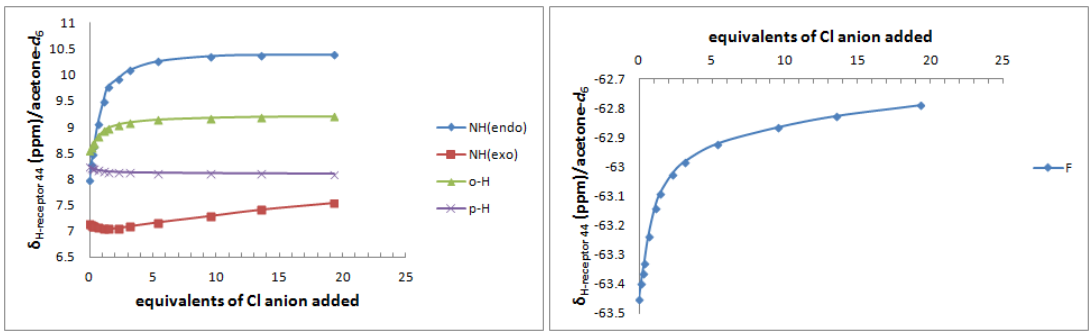

Figure 26. $^{1}H/^{19}F$ NMR chemical shifts of selected CF_3-receptors (**21** and **44**) with the addition of TBA·Cl in acetone-d_6. (298 K)

As a representative example, the results of $^{1}H/^{19}F$ NMR-titration experiments shown in Figure 26 reveal the amine derivative **21** does not interact with chloride anion with any special binding effect, on the contrary, the amide derivative **44** shows binding effects to Cl^- with both hydrogen binding and anion-π interaction. In fact, the selected amide derivatives (**44**, **53**, **54**, **55**, **56** and **59**) interact with chloride or bromide anions with obvious hydrogen binding or anion-π interaction, while only weak binding effect as well as somewhat linear relations of $^{1}H/^{19}F$ chemical shifts can be found with the addition of iodide or nitrate anions (see Appendix, Figure S9-S12). It seems the Van der Waals volumes of different anions influence the binding effect in a large degree, that is, the larger the volume of anions, the weaker binding effect of the host-guest system.

There is a remarkable feature when comparing the ^{19}F NMR-titration curves in the two different solvents ($CDCl_3$ and acetone-d_6), which is worth mentioning. In $CDCl_3$, the ^{19}F signals shift to down-field initially and then to high-field continually when the excessive amount of anions are added. However, the ^{19}F NMR chemical shifts keep the trend of down-field shifting with the addition of anions in acetone-d_6 and even some of them demonstrate the binding effect which is probably the anion-π interaction between the CF_3 aromatic rings and anions. In case this opinion could be able to be accepted, a verdict may be emerged: anion-π interaction could be induced much sufficiently in acetone than in chloroform. In fact, the anions can be much more easily solvated in acetone, while they tend to aggregate in chloroform. It probably results in the high-field shiftings of ^{19}F NMR signals when the amounts of anions are excessive and therefore the anion-π interaction will be covered in chloroform.

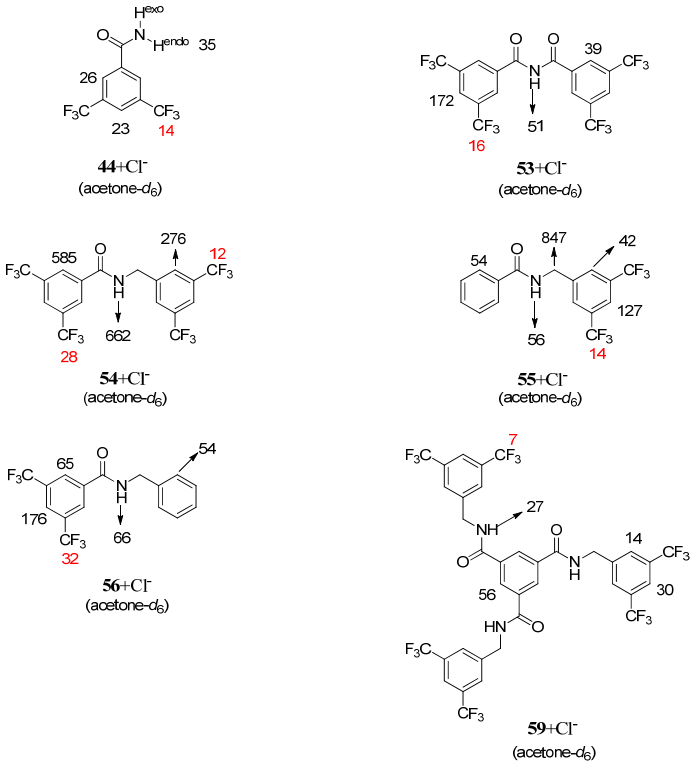

Scheme 31. Different binding constants (K_a: M^{-1}) for the complexes of selected CF_3-receptors with chloride anions. The binding constants were determined by $^1H/^{19}F$ NMR spectrometric analyses in acetone-d_6 at room temperature. Errors are estimated to be lower than 20%.

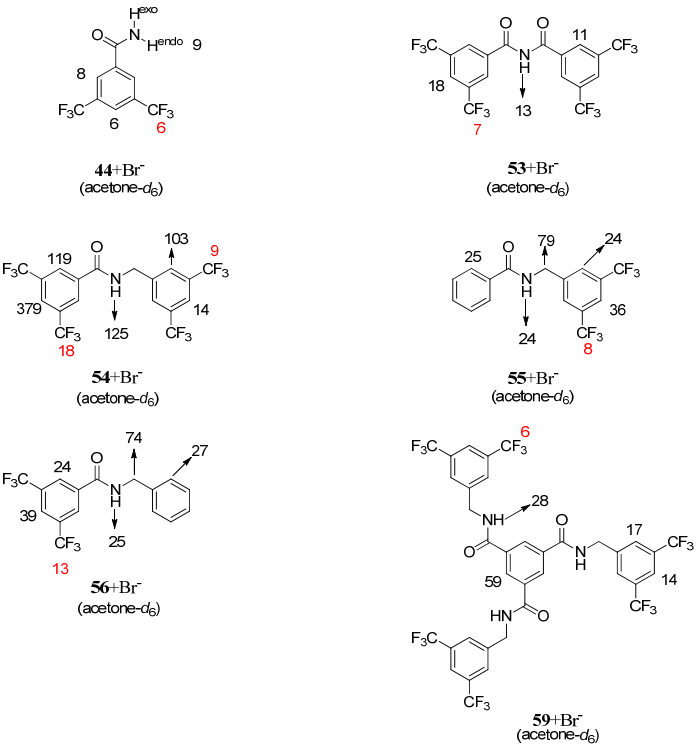

Scheme 32. Different binding constants (K_a: M^{-1}) for the complexes of selected CF_3-receptors with bromide anions. The binding constants were determined by $^1H/^{19}F$ NMR spectrometric analyses in acetone-d_6 at room temperature. Errors are estimated to be lower than 20%.

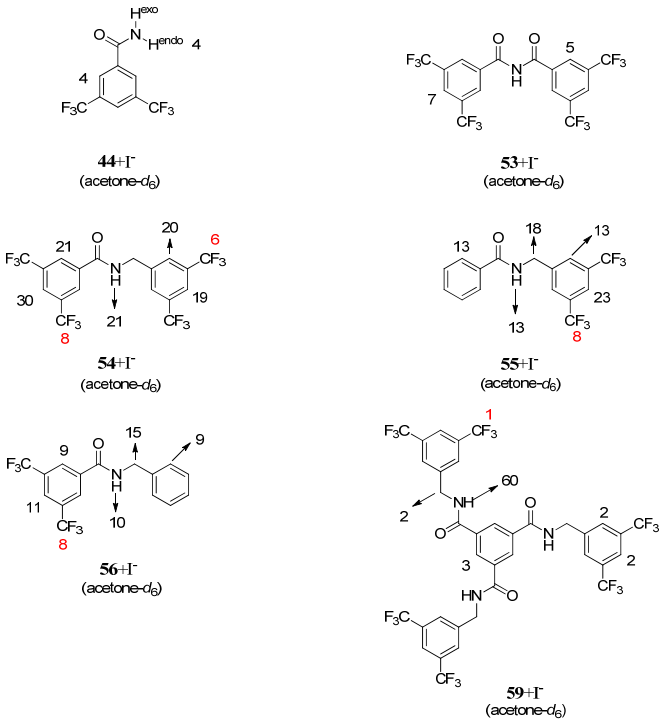

Scheme 33. Different binding constants (K_a: M^{-1}) for the complexes of selected CF_3-receptors with iodide anions. The binding constants were determined by $^1H/^{19}F$ NMR spectrometric analyses in acetone-d_6 at room temperature. Errors are estimated to be lower than 20%.

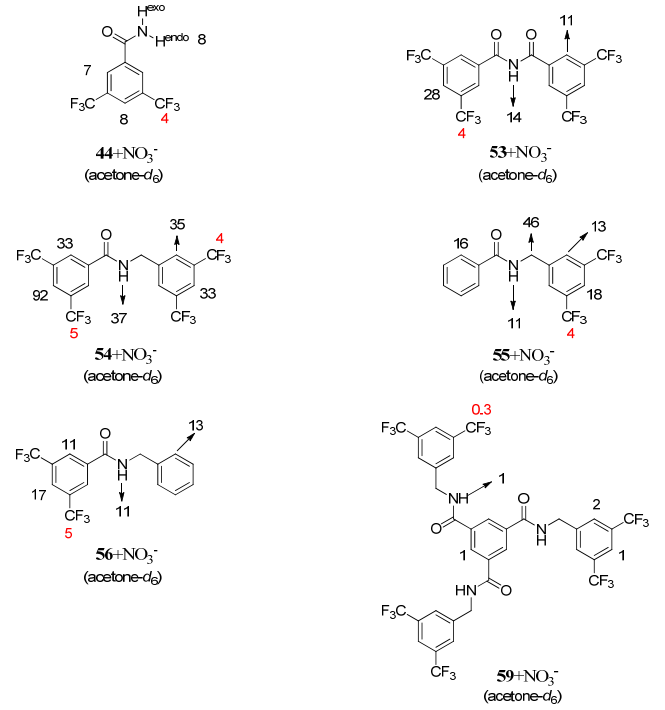

Scheme 34. Different binding constants (K_a: M^{-1}) for the complexes of selected CF_3-receptors with nitrate anions. The binding constants were determined by $^1H/^{19}F$ NMR spectrometric analyses in acetone-d_6 at room temperature. Errors are estimated to be lower than 20%.

As shown in Scheme 31-34, the binding constants of the amide derivatives (**44**, **53**, **54**, **55** and

56) except compound **59**, which are calculated by either ^{1}H or ^{19}F NMR spectrometric analyses, are increased with the order of $Cl^{-}>Br^{-}>I^{-}\approx NO_3^{-}$. Comparing the two receptors **53** and **54** with respective kinds of anions (Cl^{-} or Br^{-}), although the activity of NH in imide **53** is higher than in amide **54**, all the binding constants of hydrogen atoms with anions in **54** are obviously larger than in **53** and the K_a in **54** calculated by ^{19}F NMR spectra are also increased. Therefore, considering the interaction of amine derivatives **21** and **52** with anions, although the carbonyl group is necessary for the binding between the receptor and anions, more carbonyl groups are needless to enhance the binding effect between NH and anions. The corresponding K_a of compound **55** or **56** with anions show the position of the carbonyl is not influencing the binding behavior of the receptor to anions.

Different from anion-π interaction which could be induced much sufficiently in acetone than in chloroform as abovementioned, the hydrogen binding effect will be weakened in acetone comparing the corresponding K_a of receptor **44** in both kinds of solvent, especially with bromide, iodide or nitrate anion.

The triple-substituted derivative of benzene **59** compared with receptor **55**. The corresponding K_a of compound **59** with chloride and bromide anions are nearly equal, but the binding constants in the complexes of **55** with the two kinds of anions are about a factor 2 different. Possibly because of the huge cavity constructed by the four aromatic rings in **59**, the differences of the volumes between chloride and bromide anions can be offset. Moreover, the K_a of NH in **59** is decreased with Cl^{-}, the same with Br^{-} and increased with I^{-}, as well as no binding effect can be found between compound **59** and nitrate anions.

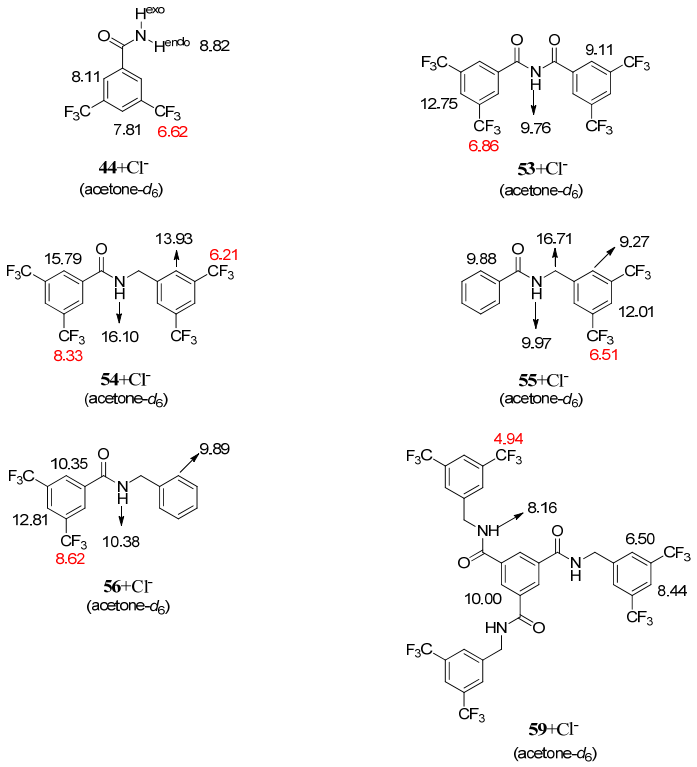

Scheme 35. Different Gibbs free energies (ΔG: kJ/mol) for the complexes of selected CF_3-receptors with chloride anions. The Gibbs free energies were determined by $^{1}H/^{19}F$ NMR spectrometric analyses in acetone-d_6 at room temperature.

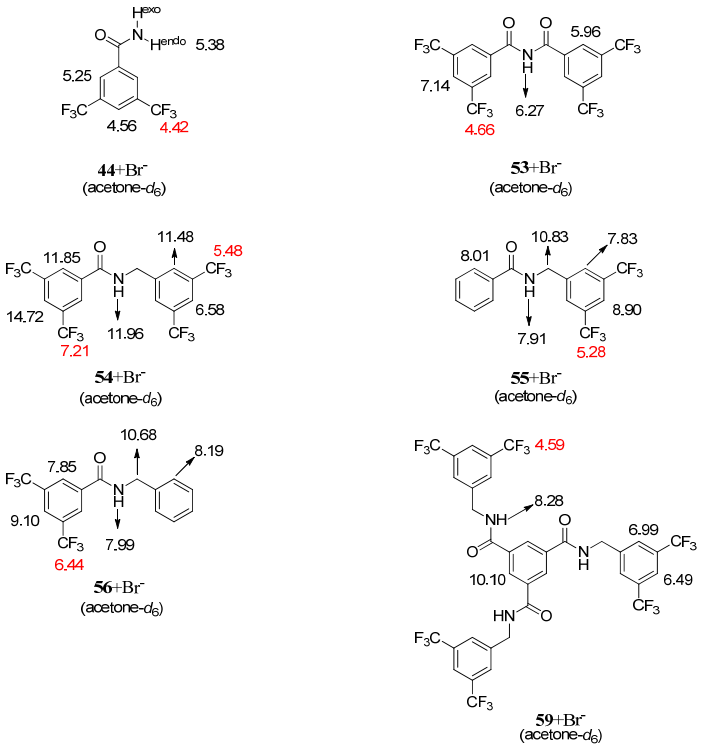

Scheme 36. Different Gibbs free energies (ΔG: kJ/mol) for the complexes of selected CF_3-receptors with bromide anions. The Gibbs free energies were determined by $^1H/^{19}F$ NMR spectrometric analyses in acetone-d_6 at room temperature.

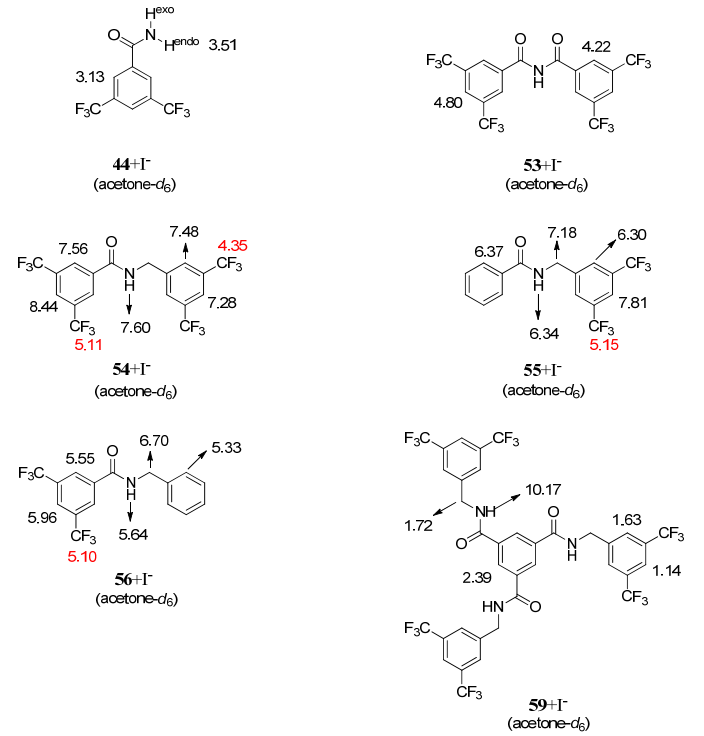

Scheme 37. Different Gibbs free energies (ΔG: kJ/mol) for the complexes of selected CF_3-receptors with iodide anions. The Gibbs free energies were determined by $^1H/^{19}F$ NMR spectrometric analyses in acetone-d_6 at room temperature.

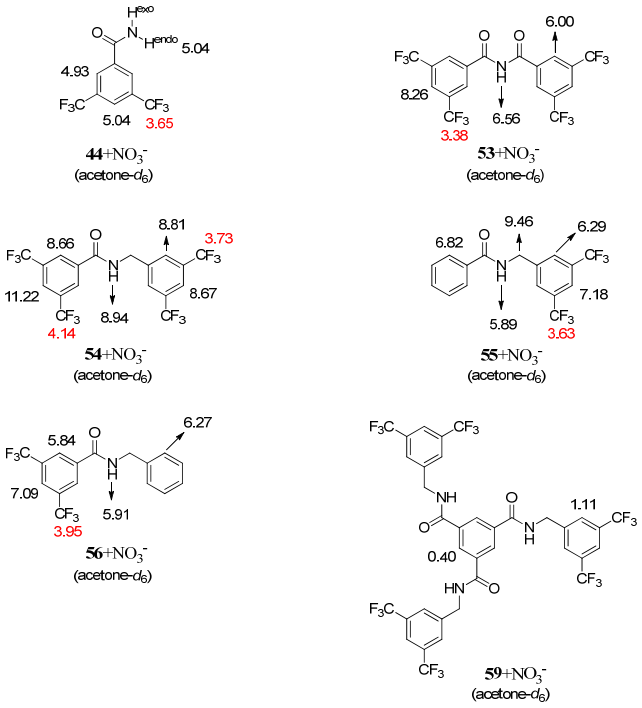

Scheme 38. Different Gibbs free energies (ΔG: kJ/mol) for the complexes of selected CF_3-receptors with nitrate anions. The Gibbs free energies were determined by $^1H/^{19}F$ NMR spectrometric analyses in acetone-d_6 at room temperature.

Compound **56** or **54** is the derivative of 3,5-bis(trifluoromethyl)benzamide **44** with one hydrogen atom of NH_2 substituted by a benzyl group or a 3,5-bis(trifluoromethyl)benzyl group, respectively. The binding affinities of the two derivatives with anions (Cl^-, Br^-, I^- and NO_3^-) are enhanced, especially for the CF_3-aromatic substituted derivative **54**, the K_a of NH with anions are approximate two times larger as that of **44** with respective anions. This reveals the additivity of the CF_3 aromatic ring as the π-receptor for anions.

4.4 Conclusion on the interactions between C_6F_5-/CF_3-receptors and anions in solution

Pentafluorophenylated derivatives could be studied as ideal π-receptors for anions in co-crystal structures. Systematic research of anion-π interactions with C_6F_5-receptors in the solid state led to numerous results until now. Trifluoromethylated aromatics, specifically 3,5-bis(trifluoromethyl)phenylated derivatives, are able to be introduced as novel π-receptors for anions in the solid state, which was found firstly by our group and has been already discussed in the aforementioned chapter. However, exploration of C_6F_5-/CF_3-compounds as π-receptors for anions in solution is still lacking. Therefore, in this section, several derivatives bearing pentafluorophenyl/3,5-bis(trifluoromethyl)phenyl groups were synthesized and then investigated as π-receptors with various anions in solution. $^1H/^{19}F$ NMR-titration experiments were adopted as the significant method with deuterated chloroform or acetone as solvent.

To each receptor (**45**, **48-51**) bearing one or two electron-deficient aromatic units, the affinity of NH to halide anions are reduced in the order of $Cl^- > Br^- > I^-$, which is responding to the alkalinity of anions. Chloride anion is the most attractive to the pentafluorophenyl units in these receptors, although bromide has a higher polarization than chloride. Probably owing to the stronger

hydrogen bonding between Cl^- and NH, it more efficiently fixes the Cl^- close to the top of C_6F_5. The iodide anion, which is the most polarizable halide anion, generally has the similar degree of K_a of fluorine as Br^-, but obviously smaller than Cl^-, except the receptor **48**. In the case of pentafluorobenzamide **45**, the iodide anions do not make any effect to the C_6F_5 unit, but chloride or bromide anions interact with this electron-deficient unit both in solid and in solution. Because of the π-π interaction which exists between the nitrate anion and the C_6F_5 unit, as well as the hydrogen bonding, it is complicated to identify anion-π interaction in $NO_3^-\cdots\pi$ complexes.

Electron-deficient tetra-aromatics **57** and **58** undergo specific binding with halide anions or nitrate anion, respectively. Both **57** and **58** interact with bromide anions by C_6F_5 units distinctively, which are displayed with the largest K_a of fluorine. In addition, the effect between electron-deficient tetra-aromatics and chloride or iodide anion are moderate and even nearly no interaction can be observed between NO_3^- and C_6F_5 units.

In terms of the binding behavior of CF_3-receptors, all the kinds of selected anions (Cl^-, Br^-, I^- and NO_3^-) are able to interact with them by anion-π interaction or the effect induced by the electron-deficient property of CF_3 rings. Moreover, this weak binding effect between the π-bond of electron-deficient aromatics and anions can be observed more distinctly in acetone than in chloroform.

It is mentionable that two significant features are revealed when comparing these $^1H/^{19}F$ NMR-titration spectra for both C_6F_5- and CF_3-receptors with diverse anions.

1. The ^{19}F NMR signals (ortho-, meta- and para-F) for C_6F_5 units, as well as of ^1H NMR signals (ortho- and para-H) for CF_3-aromatic units with the addition of anions, undergo opposite directions of high- or down-field shifting. It is probably induced by the uneven-distribution of the π-bond electrons generated by the attraction between the aromatic ring and anions and it is additionally influenced by the combined effects of hydrogen binding and anion-π interactions in CF_3-receptor-anion systems.

2. With the amine derivative receptors **46**, **47** and **69** (for C_6F_5-receptors) or **21** and **52** (for CF_3-receptors), which are without carbonyl group in their structures, the ^{19}F shifts or ^1H shifts of aromatic units change with the addition of anions with linear relations. It is not induced by the classical anion-π interactions, but it should be attributed by the effect between anions and fluorinated rings because of the electron-deficient property of the aromatics. Thus, two assumptions result: 1. Because of the more activity of hydrogen atoms of NH in amide or imide receptors than in amine receptors, much sufficient hydrogen binding is generated between anions and the receptors and the anions aggregate around the electron-deficient aromatic rings with a saturated mode which leads the $^1H/^{19}F$ NMR chemical shifts to steadily change when the amount of anions exceed at last. However, in the amine host-guest systems without hydrogen binding effect as sufficient as in amide systems, the anions surround the aromatic rings with an unsaturated mode and therefore the chemical shifts change continuously with the increase amount of anions. 2. The conjugation of the lone-pair electron of nitrogen atom with the carbonyl group in amide decrease the electronic repulsion between anions and amide moieties, so that the anions are much closer to aromatic rings and consequently a binding effect is induced. While, in amine receptors, the electronic repulsion prevents anions to approach the aromatic rings sufficiently.

This work is an attempt for exploring the interactions between C_6F_5-/CF_3-receptors and anions in solution. To achieve the fundamental revelation of anion-π interactions in solution, much additional theoretical and experimental research work is necessary in the future.

Chapter 5 L-Proline zwitterions bearing the C_6F_5/CF_3 electron-deficient aromatic ring as π-receptor for anions

5.1 Introduction

With the development of anion-π interactions, an increasing number of new electron-deficient aromatic rings have been found as receptors by theoretical studies. Some of them have already been used as building blocks to design receptors for anion-π interaction study.[55] While, to the best of our knowledge, all the π-receptors known until now are either cations or neutral molecules.

Zwitterions which offer both cation and anion moieties in one structure could afford adverse charges in different acid-base conditions. In the alkaline solution, zwitterions are able to display negative charge and become anions, which may induce anion-π interaction; on the contrary, zwitterions will turn into cations and provide positive charge, then anion-π interaction is vanished. Therefore, it is not unrealistic to control the existence of anion-π interaction induced by zwitterions in the variation of acid-base conditions (Scheme 39).

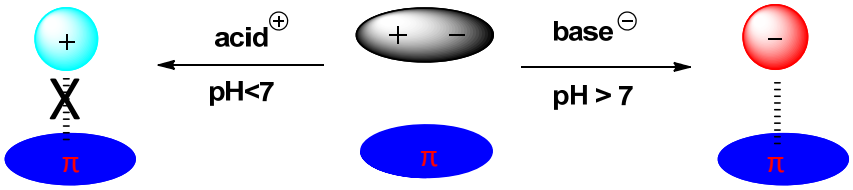

no anion-π interaction anion-π interaction

Scheme 39. Control the existence of anion-π interaction by acid-base adjustion.

L-proline, which is one of the structurally most simple amphoteric compounds, always plays a significant role in scientific research[62]. Therefore, it is reasonable to introduce L-proline into the π-receptor and assign it as a pivotal moiety of the zwitterion in this work.

5.2 The synthesis and crystal structure of the C_6F_5 zwitterion-receptor

Zwitterion-receptor **72** was synthesized according to a reference with potassium carbonate instead of potassium hydroxide as base (Scheme 40)[63]. Because of the presence of the pentafluorophenyl group and the carboxylate anion in the structure, X-ray crystal diffraction of the compound **72** displays that intermolecular anion-π interaction is induced (Figure 27, a). It is probably due to the longer distance between the carboxylate anion and the pentafluorophenyl in the one molecule, so that the intermolecular anion-π interaction is preferential (Figure 27, b). The carboxyl group is located at the rim of C_6F_5 unit of the neighboring zwitterion but not on top of the center, which reveals a η^2-type intermolecular anion-π interaction. In addition, the two oxygen atoms of the carboxyl are fixed by the NH of L-proline unit nearby with intermolecular hydrogen binding effect.

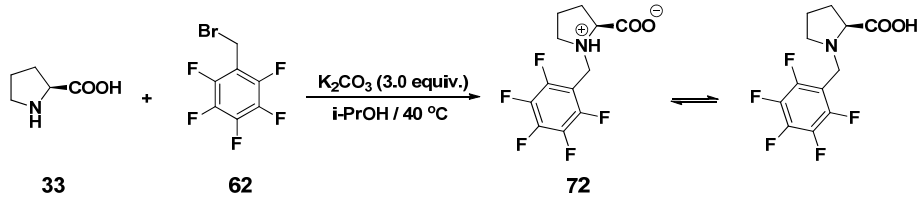

Scheme 40. Synthesis of zwitterion 7**2** which may transform into the neutral mode in solution.

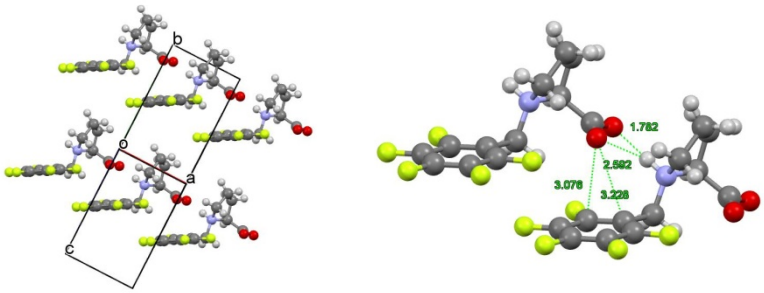

(a)

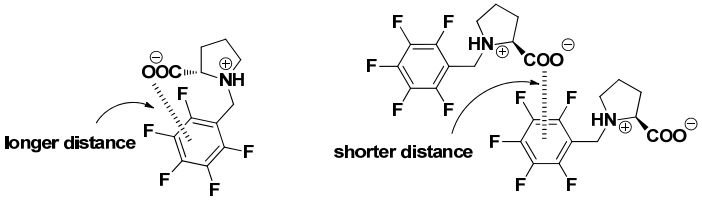

(b)

Figure 27. (a) X-ray crystal diffraction of the crystal structure of 7**2** showing intermolecular anion-π interaction (η^2: O···C = 3.076 Å, 3.228 Å; NH···O = 1.782 Å, 2.592 Å). (b) Comparison of intra- and intermolecular anion-π interaction in the structure of zwitterions **72**. (green: F, gray: H, black: C, red: O)

5.3 The adjustment of anion-π interactions existing in the C_6F_5 zwitterion in solution

Because of the similar structures of hexafluorobenzene and pentafluorophenyl unit, the C_6F_6 was firstly investigated as a reference compound. As hexafluorobenzene was calculated in large scope as a π-receptor for anions by theoretical research of anion-π interactions; however, there are only rare experimental results. In this work, initially, C_6F_6 was introduced as host and L-proline as guest. Moreover, tosylic acid (TsOH) or *N*,*N*-Diisopropylethylamine (DIPEA) was employed as acid or base, separately. Due to the solubility, deuterated DMSO or methanol was used as solvent in NMR-titration experiments. Consequently, treating with deuterated DMSO in the presence of DIPEA caused the ^{19}F peaks of C_6F_6 underwent slightly high-field shift, which demonstrated a large number of L-proline offered more carboxylate anions that made effect on the π-bond (Figure 28, c). On the other hand, the chemical shifts of ^{19}F did not suffer on influence either in deuterated methanol or in DMSO-d_6 with TsOH or not (Figure 28, a-b and e-f). Most noteworthy is that DIPEA or TsOH did not induce any obvious electronic effect on C_6F_6 according to ^{19}F NMR-titrations (Figure 29). Due to the similarity, it is reasonable to expand the results abovementioned from C_6F_6 to C_6F_5 moiety of the zwitterion **72**.

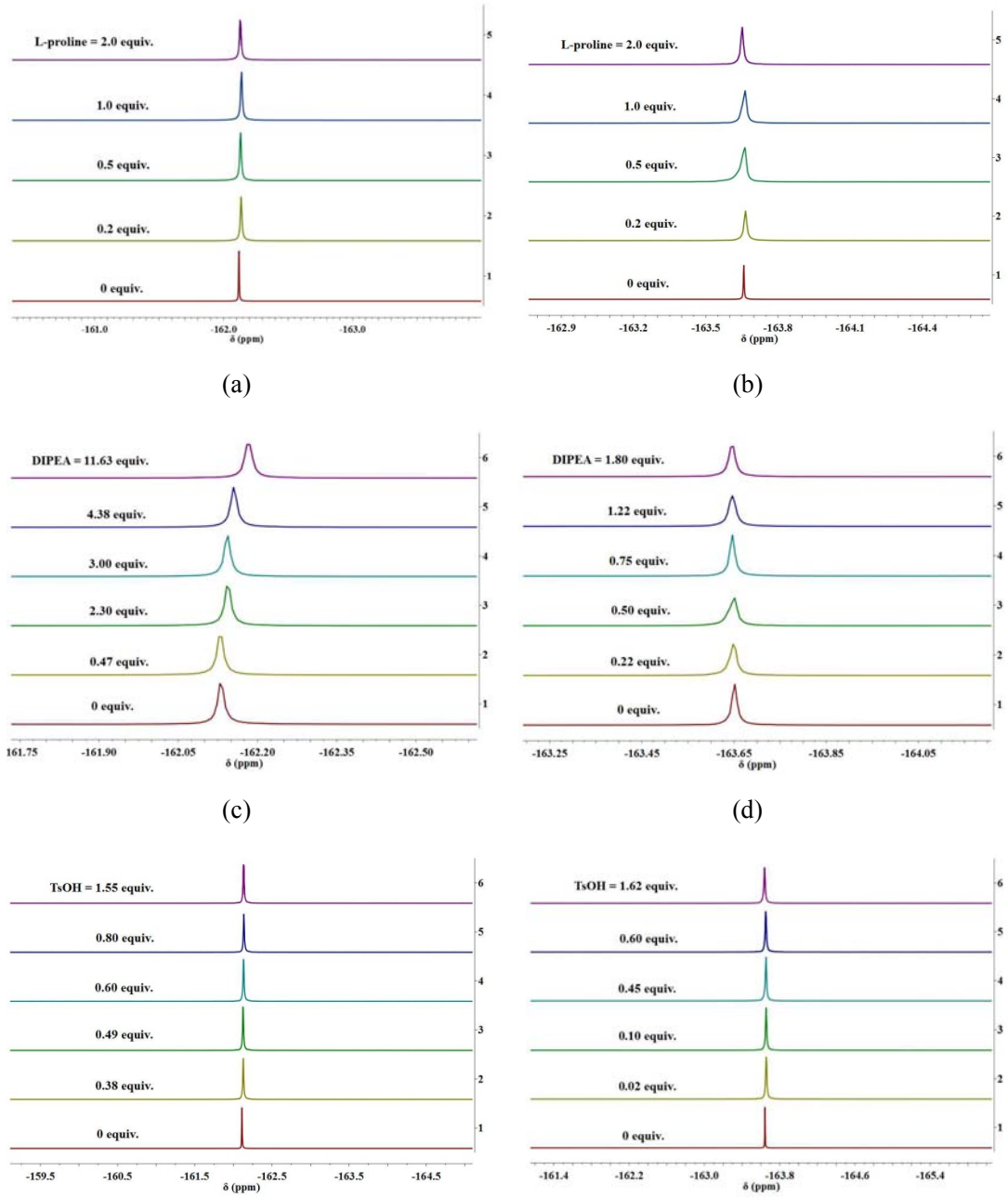

Figure 28. ^{19}F NMR titration of C_6F_6 with L-proline in different acid-base solution. (298 K)
(1) C_6F_6 (0.025 mmol, 0.003 mL, 1.0 equiv.) with increase equivalents of L-proline in DMSO-d_6 (a) and in methanol-d_4 (b).
(2) mixture of C_6F_6 (0.025 mmol, 0.003 mL, 1.0 equiv.) and L-proline (0,025 mmol, 0.003 g, 1.0 equiv.) with increase equivalents of DIPEA in DMSO-d_6 (c) and in methanol-d_4 (d).
(3) mixture of C_6F_6 (0.025 mmol, 0.003 mL, 1.0 equiv.) and L-proline (0,025 mmol, 0.003 g, 1.0 equiv.) with increase equivalents of TsOH in DMSO-d_6 (e) and in methanol-d_4 (f).

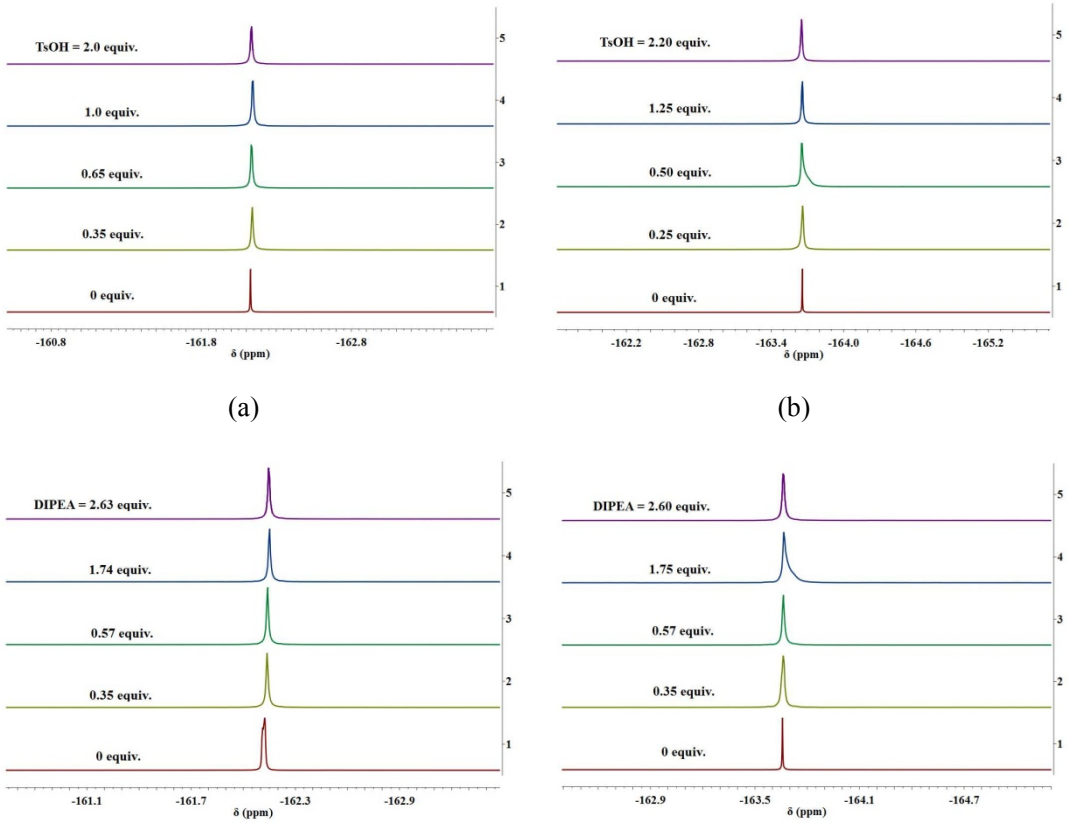

Figure 29. ^{19}F NMR titration of C_6F_6 with different equivalents of TsOH or DIPEA in DMSO-d_6 or in methanol-d_4. (298 K)
(1) C_6F_6 (0.025 mmol, 0.003 mL, 1.0 equiv.) with increase equivalents of TsOH in DMSO-d_6 (a) and in methanol-d_4 (b).
(2) C_6F_6 (0.025 mmol, 0.003 mL, 1.0 equiv.) with increase equivalents of DIPEA in DMSO-d_6 (c) and in methanol-d_4 (d).

Treating zwitterion 7**2** with the increasing amount of TsOH in deuterated solvent, all the fluorine peaks (ortho-, meta- and para-F) showed down-field shifting, which were much more obvious in DMSO-d_6, due to the alkaline solvent itself. Moreover, in both solutions, all the fluorine peaks did not change anymore when the amount of TsOH added exceeds 1.0 equivalent, which indicated the carboxylate moieties were all protonated. Consequently, intrinsic intermolecular anion-π interaction was weakened (Figure 30).

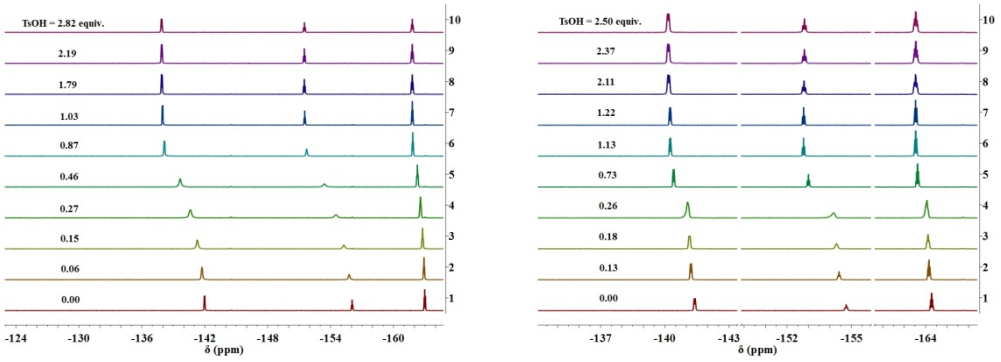

(a) (b)

Figure 30. The ^{19}F NMR-titration spectra of zwitterion 7**2** with TsOH in DMSO-d_6 (a) or in methanol-d_4 (b). (298 K)

On the contrary, DIPEA enhanced this weak effect between carboxylate anion and the neighbouring zwitterion and this phenomenon was expressed much distinct in methanol-d_4. All the fluorine peaks shifted to high-field and kept stable after the amount of DIPEA was added more than 1.0 equivalent in methanol-d_4. While, in DMSO-d_6, ^{19}F NMR peaks maintained high-field shifting with the addition of base, but the rate of change would be slow down after the base was added excessively (Figure 31).

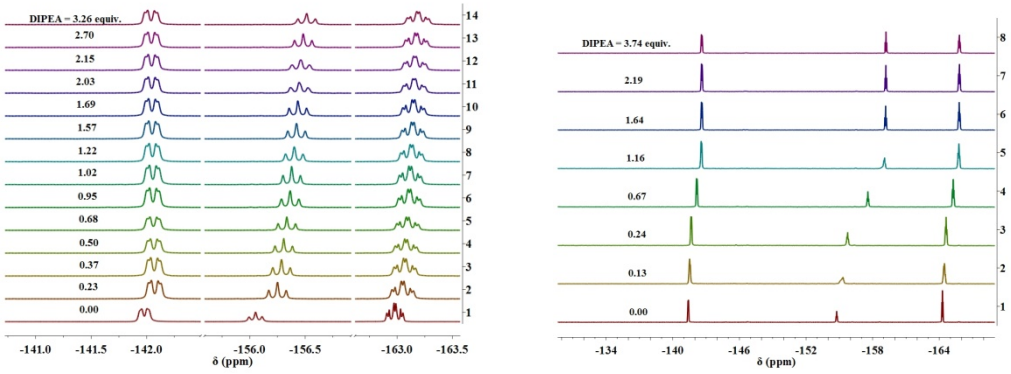

(a) (b)

Figure 31. The ^{19}F NMR-titration spectra of zwitterion 7**2** with DIPEA in DMSO-d_6 (a) or in methanol-d_4 (b). (298 K)

In short, once the acid or base was excess, no matter DMSO or methanol as solvent, the anion-π interaction will neither be weakened nor be enhanced anymore; thus, the probability of influence caused by solvent to anion-π interaction could be more or less excluded. Moreover, due to the large stereoscopic volumes of TsO^- anion and $DIPEAH^+$ cation, the big ions could contribute an ignorable influence to the π-bonds of pentafluorophenyl moieties, which was also proven by the aforementioned NMR experiments between C_6F_6 and TsOH or DIPEA. It may be that an equilibrium between zwitterion **72** and its neutral compound by the protonation and deprotonation of carboxylate moieties (Figure 32), as a result, the excess amount of DIPEA cause the carboxylates deprotonated completely and intermolecular anion-π interaction was intensified; on the contrary, excessive acid protonated carboxyl anions existing in zwitterions, so that it recedes this kind of originally weak interaction (Scheme 41).

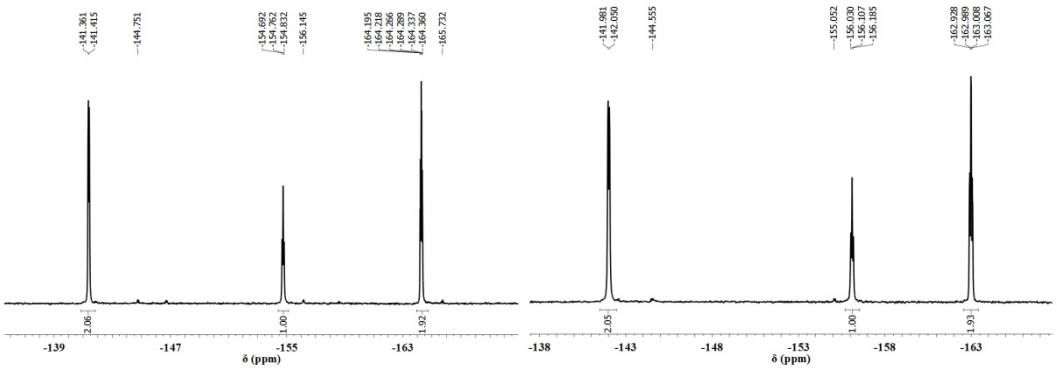

(a) (b)

Figure 32. ^{19}F NMR spectra of zwitterion **72** in methanol-d_4 (a) and in DMSO-d_6 (b) (298 K). The ^{19}F peaks in 144.751 ppm, 156.145 ppm, 165.732 ppm (a) and in 144.555 ppm, 155.052 ppm (b) demonstrate the equilibrium for the protonation and deprotonation of carboxylate moieties of zwitterion **72** and its neutral molecule in solution.

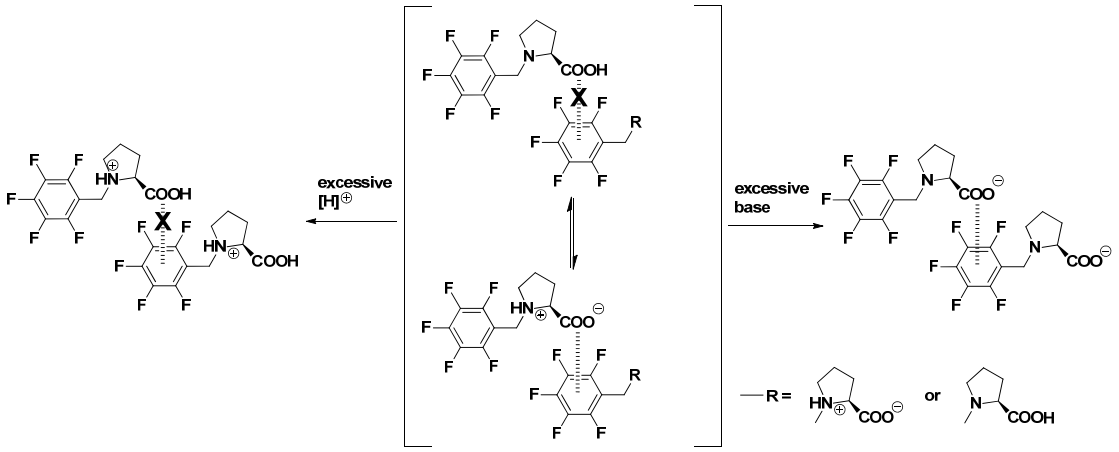

Scheme 41. Control anion-π interaction of zwitterions in solution with acid and base.

The reversibility of anion-π interaction produced by zwitterions, which is caused by different acid-base systems, could be observed both in deuterated methanol (Figure 33) and DMSO (Figure 34). In deuterated methanol for example, introducing some base firstly and then acid or the reverse sequence, the ^{19}F peaks can recover like a switch. Respectively, when TsOH was added firstly, the anion-π interaction was weakened and then excessive DIPEA enhanced the interaction and kept the intensive trend. At last, more TsOH was input to neutralize the previous DIPEA and the ^{19}F NMR signals went back to original (Figure 33, a). The relative phenomenon was contributed by the inverse order of acid-base added and consequently, the transition to the neutral situation occurred (Figure 33, b).

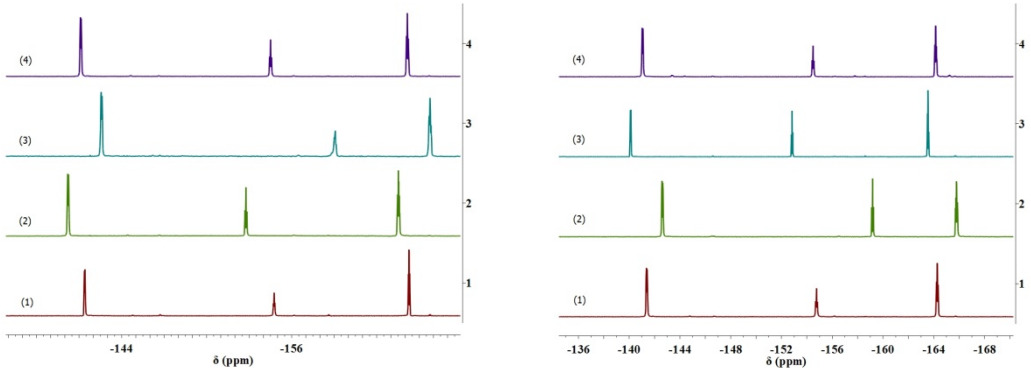

(a) (b)

Figure 33. The ^{19}F NMR-titration spectra of zwitterion 7**2** with TsOH or DIPEA in methanol-d_4. (298 K)

(a): 1) zwitterion 7**2** as the sample without acid or base; 2) 1.27 equiv. of TsOH was added; 3) 2.21 equiv. of DIPEA was added in sequence; 4) 1.12 equiv. of TsOH was input to neutralize excessive DIPEA.

(b): 1) zwitterion 7**2** as the sample without acid or base; 2) 2.09 equiv. of DIPEA was added; 3) 3.38 equiv. of TsOH was added in sequence; 4) 1.64 equiv. of DIPEA was input to neutralize excessive TsOH.

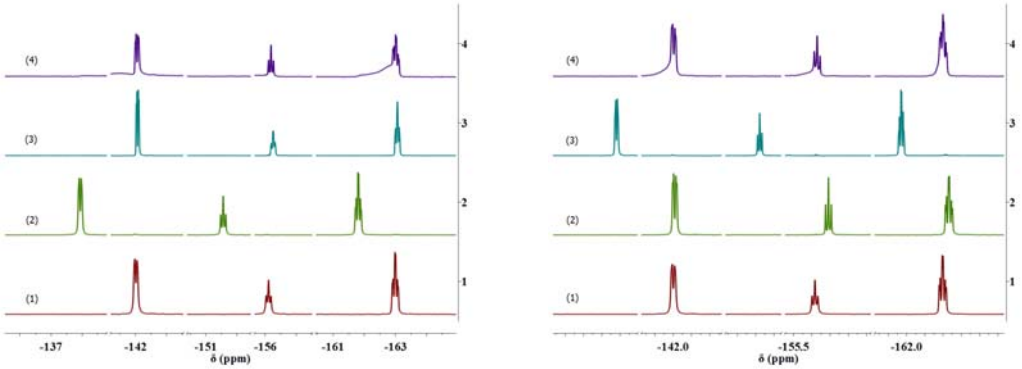

(a) (b)

Figure 34. The ^{19}F NMR titration of zwitterion 7**2** with TsOH or DIPEA in DMSO-d_6. (298 K)

(a): 1) zwitterion 7**2** as the sample without acid or base; (2) 1.07 equiv. of TsOH was added; (3) 1.77 equiv. of DIPEA was added in sequence; (4) 0.79 equiv. of TsOH was input to neutralize excessive DIPEA.

(b): (1) zwitterion 7**2** as the sample without acid or base; (2) 1.89 equiv. of DIPEA was added; (3) 3.04 equiv. of TsOH was added in sequence; (4) 1.32 equiv. of DIPEA was input to neutralize excessive TsOH.

5.4 The adjustment of anion-π interaction for the CF_3 zwitterion in solution

Our previous research showed that trifluoromethylated arenes could be designed into a kind of π-receptor for anions. For enhancing the zwitterions as π-receptors, analogous CF_3-zwitterion **34** was synthesized *via* the similar method as the synthesis of zwitterion 7**2**. According to NMR

experimental results, DIPEA caused the peaks of protons on the aromatic ring of **34** shifting to high-field and ^{19}F NMR signals showed down-field shifting. Excess DIPEA did not exert an influence to arenes any more, which indicated all zwitterion **34** were deprotonation and the enhancement of anion-π interaction occurred (Figure 35). Oppositely, the anion-π interaction was weakened when TsOH existed, due to a growing number of CF_3-zwitterion **34** acidized by the addition of strong acid (Figure 36). Besides, similar as displayed in zwitterion 7**2**, the reversibility of anion-π interaction is also observed for **34** when acid or base is introduced on sequences (Figure 37).

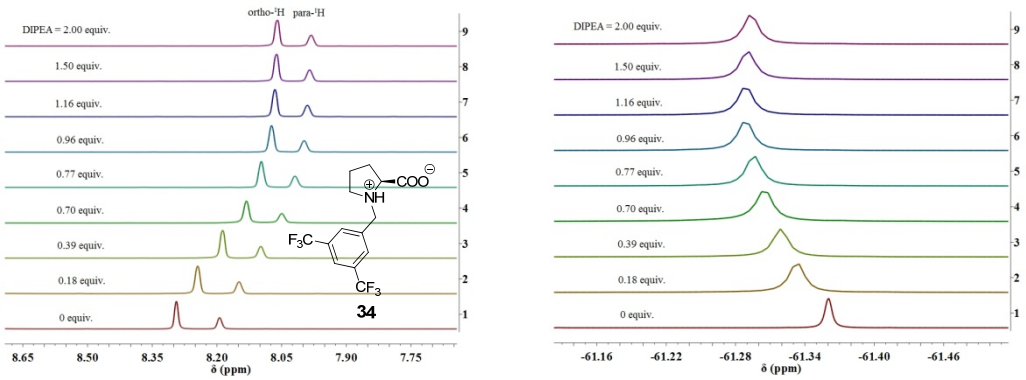

(a) (b)

Figure 35. The ^{1}H (a) and ^{19}F (b) NMR-titration spectra of zwitterion **34** with DIPEA in DMSO-d_6. (298 K)

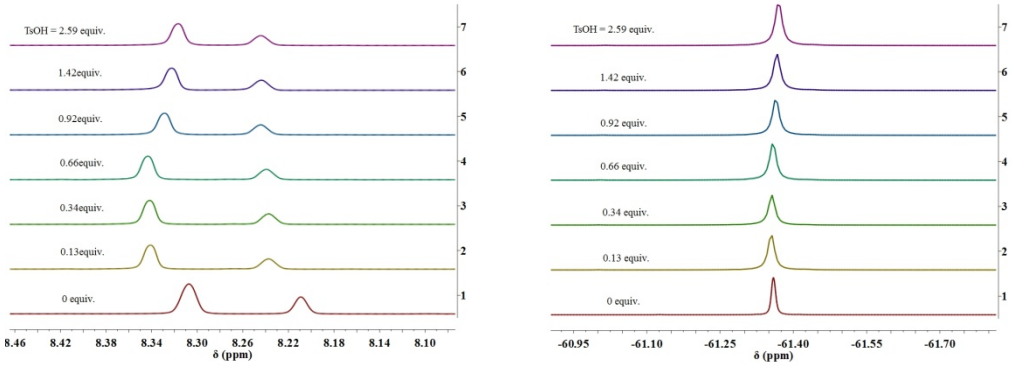

(a) (b)

Figure 36. The ^{1}H (a) and ^{19}F (b) NMR-titration spectra of zwitterion **34** with TsOH in DMSO-d_6. (298 K)

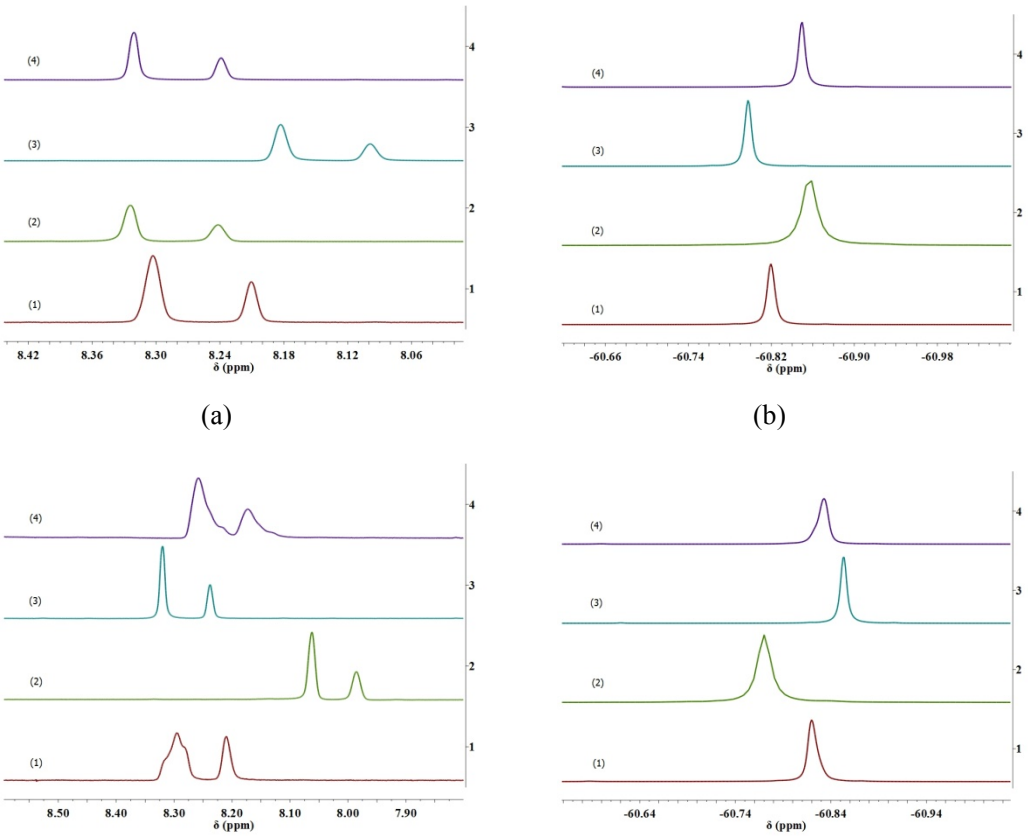

Figure 37. The ^{1}H (a, c) and ^{19}F (b, d) NMR-titration spectra of zwitterion **34** with TsOH or DIPEA in DMSO-d_6. (298 K)

For (a) and (b): (1) zwitterion **34** as the sample without acid or base; (2) 1.43 equiv. of TsOH was added; (3) 2.14 equiv. of DIPEA was added in sequence; (4) 1.38 equiv. of TsOH was input to neutralize excessive DIPEA.

For (c) and (d): (1) zwitterion **34** as the sample without acid or base; (2) 1.39 equiv. of DIPEA was added; (3) 2.88 equiv. of TsOH was added in sequence; (4) 1.98 equiv. of DIPEA was input to neutralize excessive TsOH.

5.5 Conclusion

Anion-π interaction is inside the range of attractive electrostatic effect relative to cation-π interaction. Although the research of anion-π interaction has gained large achievement during the last several decades, it is the first time to investigate zwitterions as host-guest systems in anion-π interaction. This preliminary work focused on the investigation of anion-π interaction both in crystal and in solution. Intermolecular anion-π interaction was found in X-ray crystal structure of zwitterion 7**2**. Moreover, for both C_6F_5- and CF_3-zwitterion, properly amount of acid or base could selectively control anion-π interaction to be weakened or enhanced, separately. Specifically the switch of anion-π interaction caused by zwitterion in various acid-base solutions may break the reaseach of anion-π interaction into new areas which are waiting for advances deeply in the future.

Chapter 6 The binding behavior of the indole derivatives containing C_6F_5/CF_3 electron-deficient aromatic units with anions

6.1 Introduction

Indole derivatives are important organic compounds which have been found in many natural products and pharmaceuticals (Scheme 42). For example, 5-HT, Melatonin, IAA, Trp and Hypaphorine etc. are isolated from animals or plants;[64] DMT and Indometacin etc. are synthesized to adjust human's physiological activities. Probably due to the high reactivity at position 3 of the indole molecule, 3-substituted indole compounds are the most widespread of all the indole derivatives.

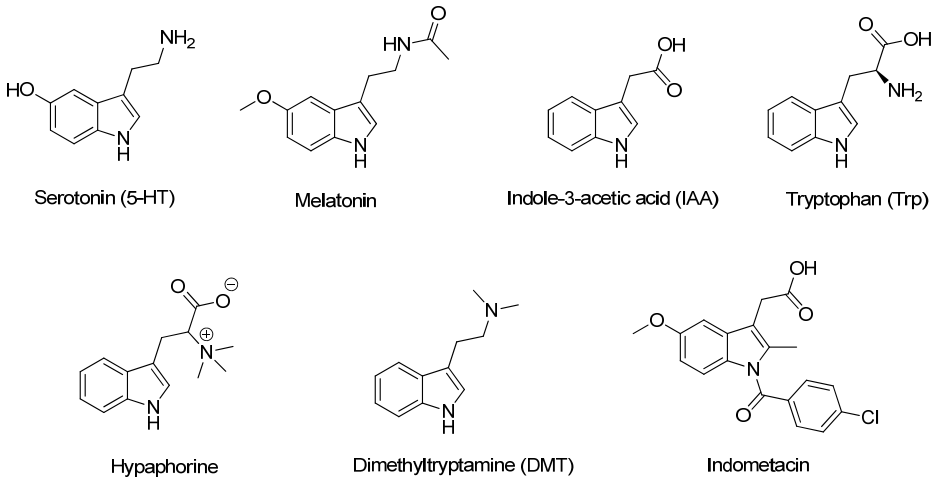

Scheme 42. Some natural products and pharmaceuticals containing indole structures.

Indole, as a good ion-pair receptor and the most general unit in the ion-π interactions existing in protein systems, has been investigated as one of the most attractive subjects in chemistry and biology for a long history.[65] Recently, the synthesis of new indole derivatives providing physiological activities[66] and the study of π-receptors based on indole structures for ions have been largely developed.[67] Previously, some C2- or C7-substituted indole derivatives were already synthesized and researched as π-receptors for anions in our group.[68] Especially, the pentafluorophenyl unit connecting to the C7 of the indole molecule could enhance the affinity of the indole derivative to chloride anion in solution, which is probably resulted by electron-withdrawing effect of C_6F_5 unit.[68b]

In this work, four C3-substituted and two C2-substituted indole derivatives bearing C_6F_5 or 3,5-bis(trifluoromethyl)benzyl unit were prepared (Scheme 43) and their binding activity with anions (Cl^-, Br^-, I^- and NO_3^-) was studied in solution.

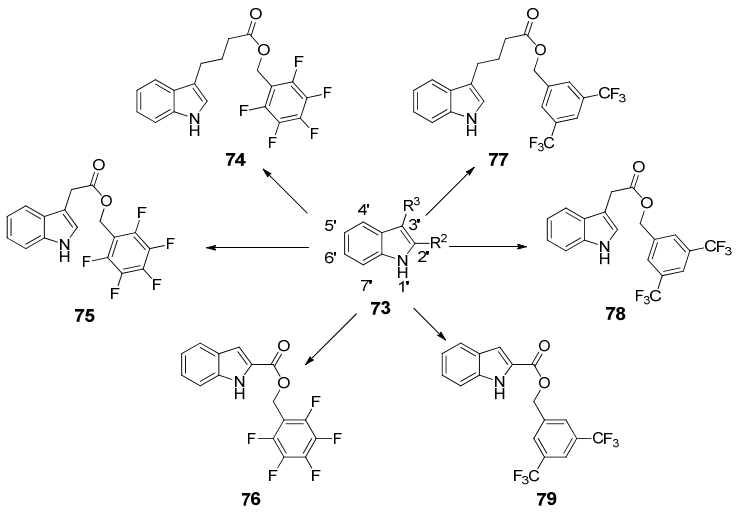

73a: R^2 = H, R^3 = $(CH_2)_3COOH$;

73b: R^2 = H, R^3 = CH_2COOH;

73c: R^2 = COOH, R^3 = H.

Scheme 43. The preparation of C2- or C3-substituted indole derivatives bearing fluorinated electron-deficient aromatic units.

The binding analysis of indole or its derivatives with anions in solution was performed by $^1H/^{19}F$ NMR-titration experiments. Comparison of the different binding constants of indole structures with anions could reveal the effect induced by the electron-deficient aromatics to the indole unit. Because there is one (for **75** or **78**) or three (for **74** or **77**) methylene units connecting the indole and electron-deficient aromatic ester moieties, the effect should not be caused by intramolecular electron-withdrawing and/or conjugated effect of the fluorinated moieties, instead, the charge transfer in the indole-anion-π systems may arouse some influence to the indole groups.

6.2 The binding behavior of indole with anions in solution

Initially, indole molecule was employed as receptor to calculate the binding constants of it with several kinds of anions (Cl^-, Br^-, I^- or NO_3^-) which were introduced as TBA salts. The ^1H NMR titration results and corresponding K_a values were displayed in Figure 38.

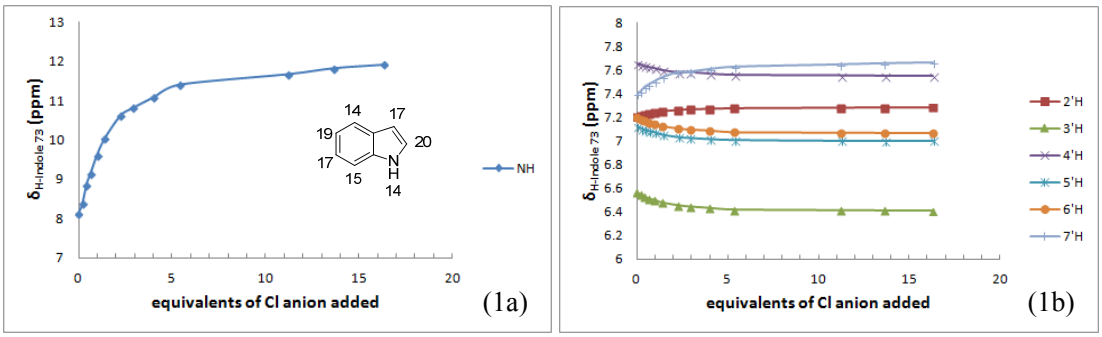

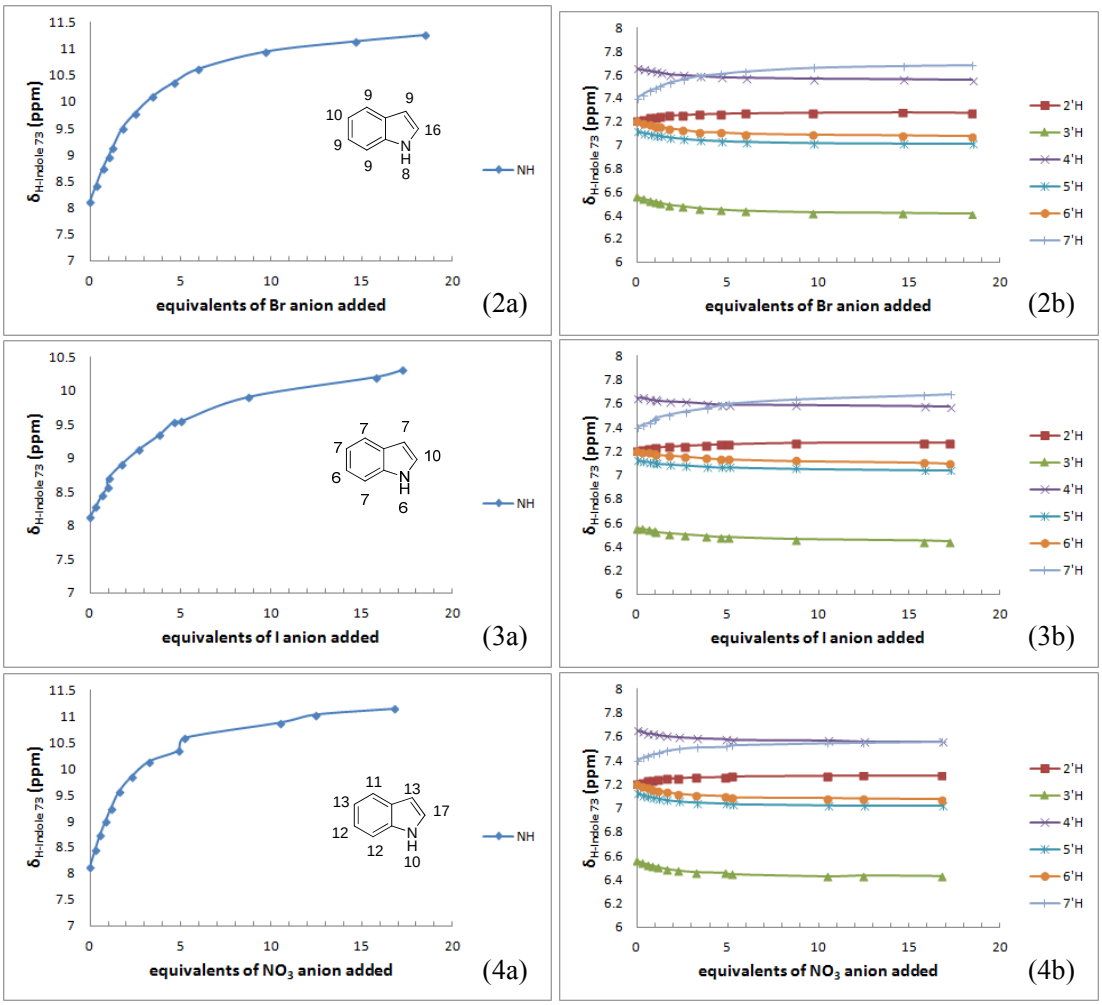

Figure 38. ^{1}H NMR chemical shifts of indole **73** with the addition of Cl^- (1a, 1b), Br^- (2a, 2b), I^- (3a, 3b) and NO_3^- (4a, 4b) in $CDCl_3$ at 298 K. The binding constants of hydrogen atoms of the indole molecule with anions were shown by the corresponding positions, respectively.

The changes of ^{1}H NMR chemical shifts with the addition of anions demonstrate there is non-covalent binding effect aroused between the indole molecule and anions. Especially, the Cl^- or NO_3^- induced much more obvious interactions to the indole than Br^- or I^-, which was revealed from the larger binding constants of indole with the former two kinds of anions. Although the NH undergoes the largest down-field shifting, the K_a of NH is not distinctly larger than any other hydrogen's. The 2′-H which has weaker acidity than that of NH generated the highest K_a in all of the four indole-anion systems. Analyzing the shifting direction of ^{1}H NMR chemical shifts, it is found that the ^{1}H NMR signals of 1′-, 2′- and 7′-H shifted to down-field and 3′-, 4′-, 5′- and 6′-H shows high-field shifting. These differences imply there should not be only hydrogen binding effect generated in indole-anion systems; otherwise all of the ^{1}H NMR signals would undergo down-field shifting. By a cooperative consideration to these experimental results, a possible binding model is depicted (Scheme 44).

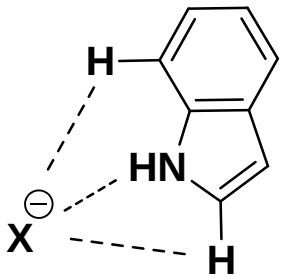

Scheme 44. Proposed model of indole-anion system. (X = Cl, Br, I, NO_3)

The anion is prior located in the front of the NH group of indole with hydrogen bonds to the 1′-, 2′- and 7′-H, but it is not fixed on the same plane of the indole aromatic ring. Due to the generation of hydrogen bonding combined with the polarization of aromatic π-bond by the introduction of anions, 1′-, 2′- and 7′-H shift to down-field and others are high-field shifting caused by the decrease of de-shielding. Because of the delocalization of conjugated π-bond which is different from that of σ-bond, it is reasonable to deduce the emergence of uneven-distribution of π-bond and the change of shielding effect. Therefore, the polarization of π-bond contributed to an increase of shielding effect by the side of NH group and made the largest down-field shifting to the NH signal, even though it does not associate with anions strongly.

6.3 The influence of fluorinated substituents on the ^{1}H NMR chemical shifts of indole

Compounds **74**-**79** bear various fluorinated moieties connecting to the indole unit. Besides the difference of pentafluorobenzyl and 3,5-bis(trifluoromethyl)benzyl groups, compound **74** or **77** with three methylene units and one ester unit connecting indole to fluorinated benzyl; while only one methylene and an ester unit exist between the indole and fluorinated unit as a linker in structure **75** or **78**. Different from compounds **74**, **75**, **77** and **78** which are substituted on the C3 position, derivative **76** or **79** exploits only an ester unit as a linker to bind the fluorinated aromatic unit on the C2 position of the indole moiety. ^{1}H NMR spectra of these derivatives show the fluorinated aromatics inducing an obvious effect to indole units (Figure 39).

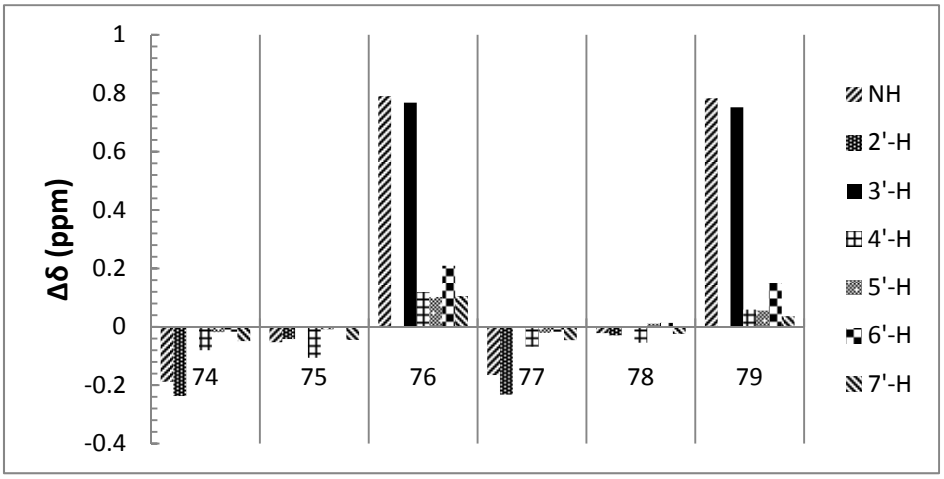

Figure 39. The chemical shift changes of ^{1}H NMR spectra of the indole units in derivatives **74**-**79**. The NMR experiments were performed in $CDCl_3$ for indole and all derivatives except **76** which was tested in acetone-d_6 (298 K). ($\Delta\delta = \delta_{derivative} - \delta_{indole}$)

Except 5′- and 6′-H of **78**, all of other ^{1}H NMR signals of C3-substituted derivatives are high-field shiftings. Especially, the NH and 2′-H of **74** or **77** obviously shift to high-field 0.2 ppm approximately. On the other hand, C2-substituted derivatives **76** and **79** display down-field shiftings and both the NH and 3′-H underwent about 0.8 ppm down-field shifting.

It is not surprising for the fluorinated electron-deficient aromatic derivatives bearing different linkers to make diverse influences to their indole units. Moreover, the different length linkers enable the derivatives to adjust feasible conformations in solution, so that the indole unit can interact with the electron-deficient aromatics though spacial electromagnetic field effect. Consequently, the indole units of C3-substituted derivatives are located in the shielding zone of electron-deficient arenes and high-field shifting can be induced. In compound **76** or **79**, due to the carbonyl directly connecting to the C2 position, the protons especially the NH and 3′-H of indole suffered intramolecular electron-withdrawing induced effect combined with shielding effect of fluorinated aromatics. Therefore, all the ^{1}H signals are down-field shifting.

6.4 The ^{1}H/^{19}F NMR-titration experiments of indole derivatives bearing C_6F_5/CF_3 electron-deficient aromatic units with anions

As indole derivatives are kinds of potential physiological activators, it is significant to study the anion binding behavior of indole derivatives in solution. Moreover, with the presence of fluorinated electron-deficient aromatic units in the structures, the interaction between indole and anions may benefit from some additional effect generated from the introduced fluorinated aromatics. Therefore, indole-anion-π system should be turned into an interesting research topic in supramolecular chemistry.

In this part, ^{1}H/^{19}F NMR-titration experiments were performed to gather the binding information in indole-anion-π systems. Different anions (Cl^-, Br^-, I^- and NO_3^-) were added as TBA salts into the systems and $CDCl_3$ or acetone-d_6 were used as solvent depending on the solubility. Consequently, similar ^{1}H/^{19}F NMR-titration results occurred for different anions with each indole derivative (Appendix, Figure S14-S25). Herein, only indole-chloride-π systems are shown as examples.

6.4.1 The binding behavior of compound **74** with anions

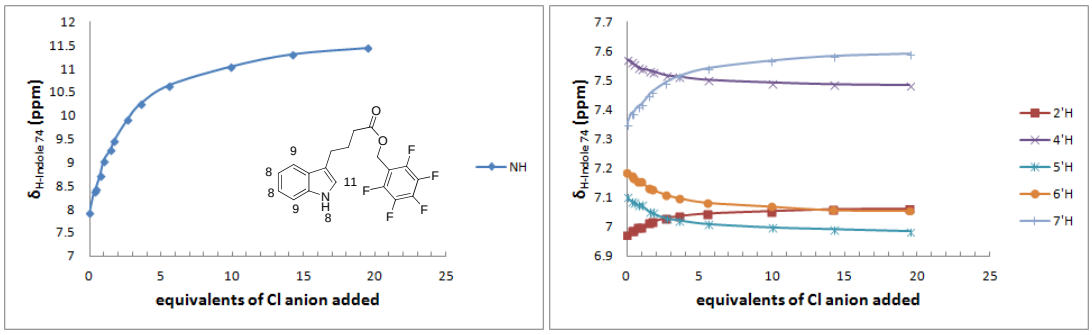

Figure 40. ^{1}H NMR-titration spectra of the derivative **74** with the addition of Cl^- in $CDCl_3$ (298 K). Only chemical shifts of protons on the indole unit are displayed. The binding constants of H/F with anions are shown by the corresponding positions, respectively.

As shown in Figure 40, although receptor **74** contains a long linker between indole and the C_6F_5

unit, the binding constants of hydrogen atoms with Cl^- suffered a distinct influence because of the electron-deficient aromatic unit. Comparing with indole **73**, all the K_a of hydrogen were reduced in regard to each kind of anion and much obviously for Cl^- or NO_3^- (Appendix, Figure S14). The down-field shifting of NH, 2′-H and 7′-H as well as the high-field shifting of 4′-H, 5′-H and 6′-H demonstrate the interaction between anions and the π-bond of indole units and this effect was weakened, which was revealed from the reduced binding constants.

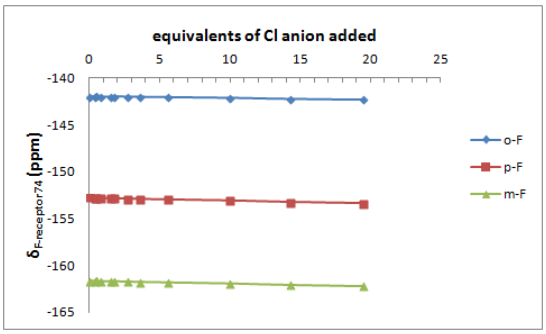

Figure 41. ^{19}F NMR-titration spectra of the derivative **74** with the addition of Cl^- in $CDCl_3$. (298 K)

The pentafluorobenzyl unit produced an obvious influence to the indole moiety with anions, but the ^{19}F NMR spectra show there is a faint effect between C_6F_5 and the anion added. The ^{19}F NMR chemical shifts display inconspicuous high-field shifting with the addition of anions with a linear relation (Figure 41, Appendix Figure S20).

6.4.2 The binding behavior of compound **75** with anions

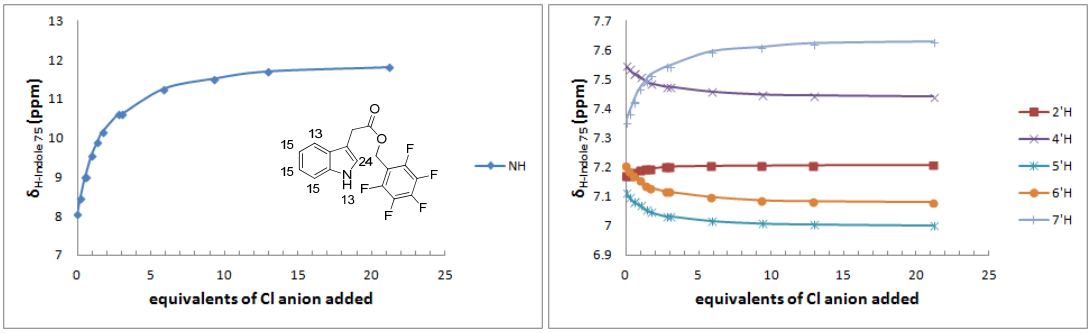

Figure 42. ^{1}H NMR-titration spectra of the derivative **75** with the addition of Cl^- in $CDCl_3$ (298 K). Only chemical shifts of protons on the indole unit are displayed. The binding constants of H/F with anions are shown by the corresponding positions, respectively.

In the structure of receptor **75**, the linker is shorter than in receptor **74** and the electron-deficient substituent made nearly no effect to the interaction of indole with anions. The binding constants of **75** with anions were almost equal to those of indole molecule with corresponding anions, although only the K_a of 2′-H with Br or Cl anion slightly increased (Figure 42, Appendix Figure S15).

Similar to compound **74**, the C_6F_5 unit of **75** did not display any binding effect and the ^{19}F NMR signals of **75** underwent high-field shifting with the anion added (Appendix Figure S21).

6.4.3 The binding behavior of compound **76** with anions

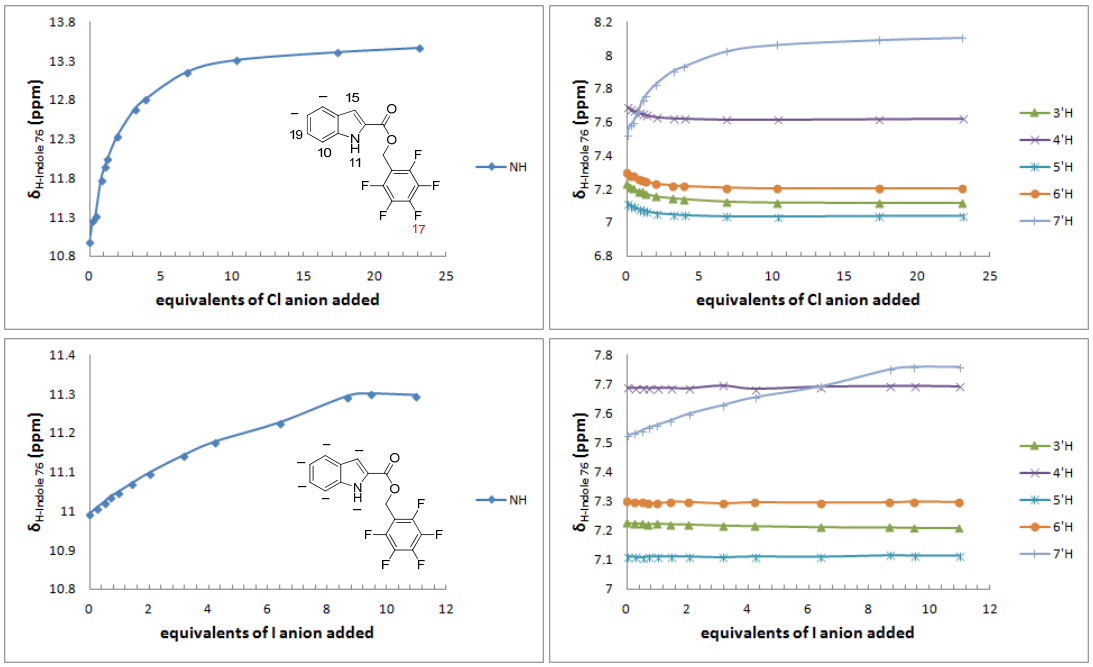

Figure 43. ^{1}H NMR-titration spectra of the derivative **76** with the addition of Cl^- or I^- in acetone-d_6 (298 K). Only chemical shifts of protons on the indole unit are displayed. The binding constants of H/F with anions are shown at the corresponding positions, respectively.

In acetone, the presence of 2′-substituted electron-withdrawing group in receptor **76** somewhat disturb the binding effect between the indole unit and anions. All of the 4′- and 5′-H did not show any binding effect with anions and others obtained decreased binding constants with Cl^-, Br^- and NO_3^-. The iodide anion interacted with NH and 7′-H and did not affect any other hydrogen atoms of the indole unit (Figure 43, Appendix Figure S16).

The anions interact with the indole unit of **76** with weaker effect, but it displays a micro binding effect with the π-bond of the electron-deficient aromatic unit, except iodide anion with which the ^{19}F NMR chemical shifts show a linear relation (Appendix, Figure S16 and S22).

6.4.4 The binding behavior of compound **77** with anions

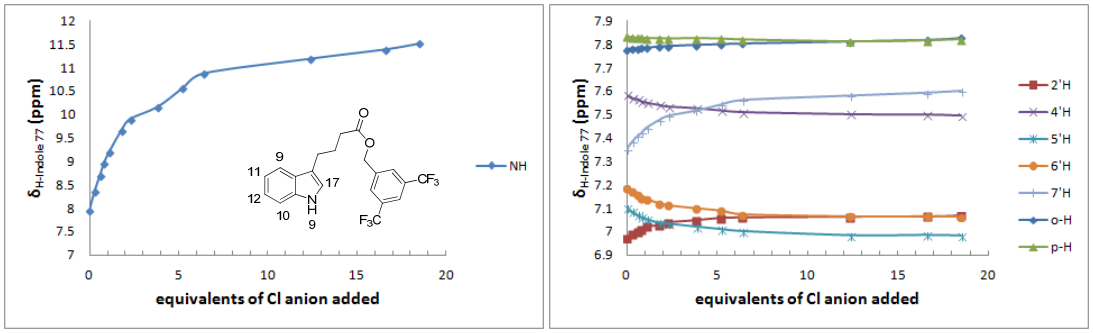

Figure 44. ^{1}H NMR-titration spectra of the derivative **77** with the addition of Cl^- in $CDCl_3$ (298 K). Only chemical shifts of protons on the indole unit are displayed. The binding constants of H/F with anions are shown by the corresponding positions, respectively.

To compound **77**, the CF_3 aromatic substituent similar with its C_6F_5 counterpart, reduced the affinity of indole unit with corresponding anion in solution. Moreover, the 3,5-bis(trifluoromethyl)phenyl unit was suffered comprehensive effect with anions. With all kinds of anions (Cl^-, Br^-, I^- and NO_3^-), the ortho-H shifted to down-field and the para-H performed high-field shifting and then displayed the same chemical shift when the anion was added exceed 10 equivalents (Figure 44, Appendix Figure S17). It is ambiguous that whether anion-π interaction exists between the CF_3 arene and anions, but it is obvious that there should not be only a hydrogen bonding effect be induced.

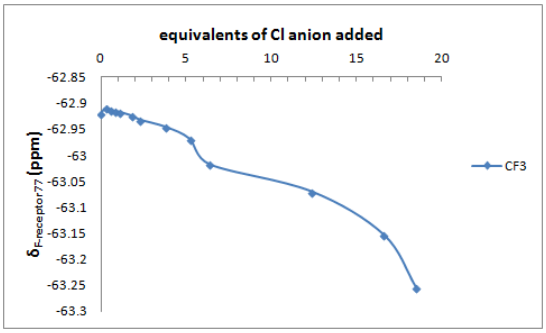

Figure 45. ^{19}F NMR-titration spectra of the derivative **77** with the addition of Cl^- in $CDCl_3$. (298 K)

Initially, when a few chloride anions were added, approximately less than 0.5 equivalents, the ^{19}F NMR signal of CF_3 underwent a slightly down-field shifting. However, excessive amount of anions led to a dramatic high-field shifting for the ^{19}F NMR peaks (Figure 45). The similar results can also be induced by other kinds of anions (Appendix Figure S23).

6.4.5 The binding behavior of compound **78** with anions

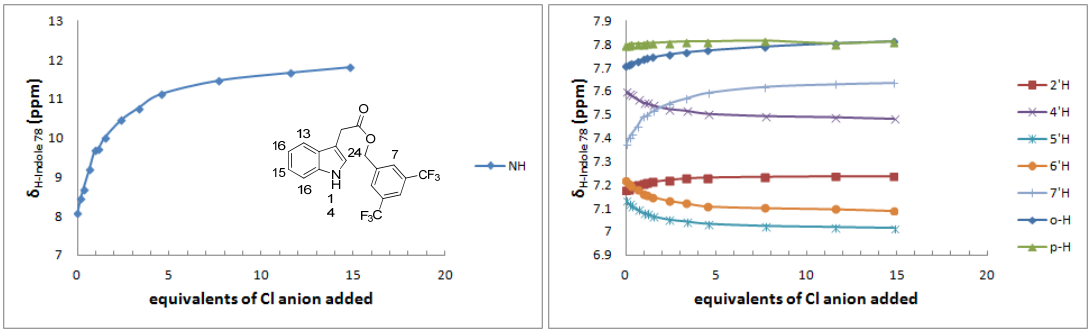

Figure 46. ^{1}H NMR-titration spectra of the derivative **78** with the addition of Cl^- in $CDCl_3$ (298 K). Only chemical shifts of protons on the indole unit are displayed. The binding constants of H/F with anions are shown by the corresponding positions, respectively.

The changes of ^{1}H NMR chemical shifts in receptor **78** with the addition of anions are similar to that in **77**, but the binding constants are not affected by the substituent and are close to the K_a of indole molecule with corresponding anions. In addition, the anions interact with the ortho-H of CF_3 aromatic unit by hydrogen binding but without influence of the para-H (Figure 46, Appendix Figure S18).

The initial down-field shifting of ^{19}F in **78** is more obvious than that in **77**, which might coincide with the hydrogen binding effect of the ortho-H with anions (Appendix Figure S24).

6.4.6 The binding behavior of compound **79** with anions

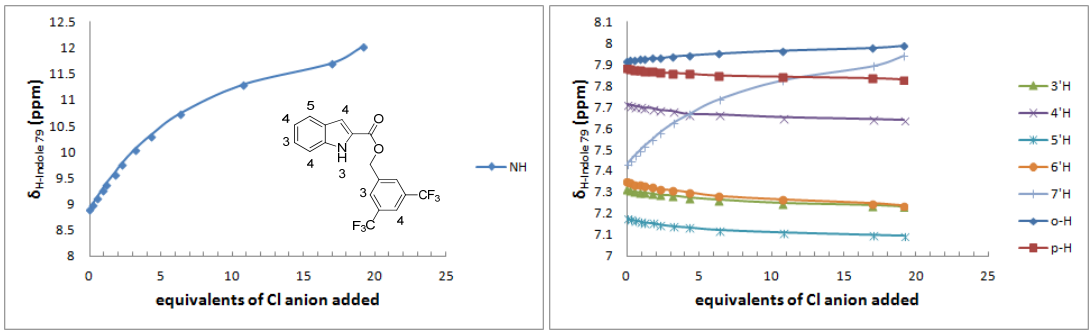

Figure 47. ^{1}H NMR-titration spectra of the derivative **79** with the addition of Cl^- in $CDCl_3$ (298 K). Only chemical shifts of protons on the indole unit are displayed. The binding constants of H/F with anions are shown by the corresponding positions, respectively.

The C2-substituted indole derivative **79** shows a reduced affinity to anions. All the ^{1}H NMR-titration results display more or less linear relations with the equivalents of anion added (Figure 47, Appendix Figure S19). Probably the electron-withdrawing carbonyl group which is directly connected to the indole unit plays a significant role in the reduction of the anion binding effect.

The ^{19}F NMR-titration spectra show an obvious down-field shifting when few equivalents of anions are added. A large amount of anions induces the high-field shifting of ^{19}F NMR signals (Appendix Figure S25).

6.5 Conclusion

A series of C_6F_5/CF_3 electron-deficient aromatic substituted indole derivatives **74-79** were synthesized. The anions (Cl^-, Br^-, I^- and NO_3^-) were introduced as TBA salts into the solution of these receptors and then these indole-anion-π systems were investigated by ^{1}H/^{19}F NMR-titration experiments. The C3-substituent with a longer linker in **74** and in **77** efficiently reduces the binding constants of the indole unit with anions and the substituent with a shorter linker in **75** and in **78** causes less influence to the indole unit related to the anion binding. The steric conformation of the C3-substituted indole derivative probably plays a pivotal role to the anion binding effect which existed in the indole-anion-π system, because the flexible methylene linker is not able to transfer the electronic effect between the indole unit and the electron-deficient aromatics. The C2-substituent in **76** and in **79** is bound to the indole unit directly with an electron-withdrawing ester group and reduces, even disturbs the binding effect of the indole unit with anions. Some interactions are revealed between the C_6F_5/CF_3 aromatic unit and anions, but they cannot be classified to any special non-covalent binding effect. Specifically, the pentafluorophenyl unit of receptor **76** demonstrates a weak anion-π binding effect with Br^-, Cl^- or NO_3^- in acetone, which shows an anion binding competition between indole unit and electron-deficient aromatic moiety, as the binding constants of indole with anions are distinctly reduced in this system.

This part of work represents a preliminary exploration, considering indole derivatives are of significance in physiological research, additional theoretical and experimental research work are valuable to be performed and will obtain much understanding to the indole-anion-π systems.

Chapter 7 Other C_6F_5/CF_3 π-receptors for anion binding and their crystal structures

According to previous research, the pentafluorophenyl group is able to participate in the construction of π-receptors for anions. Recently, 3,5-bis(trifluoromethyl)phenylated electron-deficient aromatics were studied as a kind of original binding hosts in regard to anion-π interactions. Both theoretical and experimental investigation suggest that these CF_3 aromatic compounds could become potential receptors for anions with favorable attraction by hydrogen binding effect and/or anion-π interaction both in the solid state and in solution. For exploring a broader scope of π-receptors which are able to be used for anion-π interactions, some compounds bearing C_6F_5 and/or 3,5-bis(trifluoromethyl)phenyl unit were synthesized and characterized by X-ray crystal structure diffraction.

7.1 Synthesis and crystal study of receptors bearing pentafluorophenyl and/or 3,5-bis(trifluoromethyl)phenyl groups

In the aforementioned chapter, some receptors bearing only one kind of electron-deficient aromatic unit (pentafluorophenyl or 3,5-bis(trifluoromethyl)phenyl group) were introduced as π-receptors and revealed binding effect with anions in solution. In this part, three compounds bearing both C_6F_5 and CF_3-aromatic units were synthesized from commercially available products. Because of the presence of electron-deficient aromatic units in their structures, they would be used as π-receptors for anions.

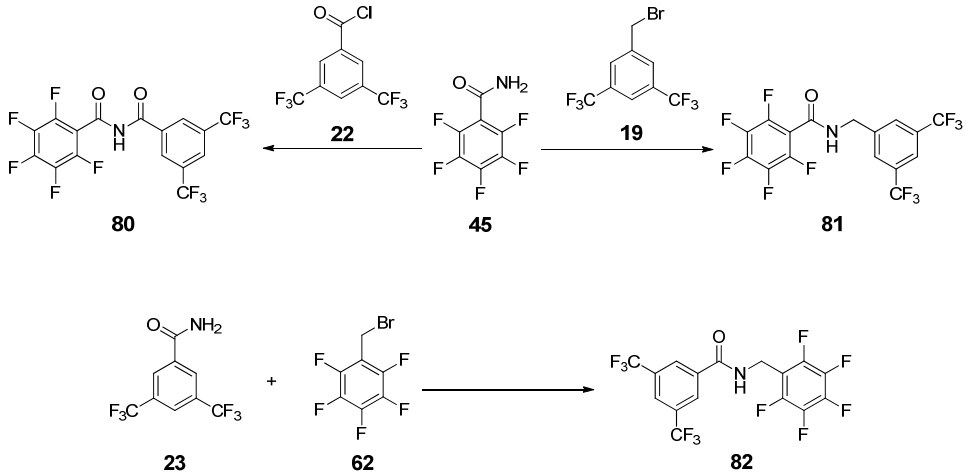

Scheme 45. The synthesis of compounds containing both pentafluorophenyl and 3,5-bis(trifluoromethyl)phenyl units in the structures.

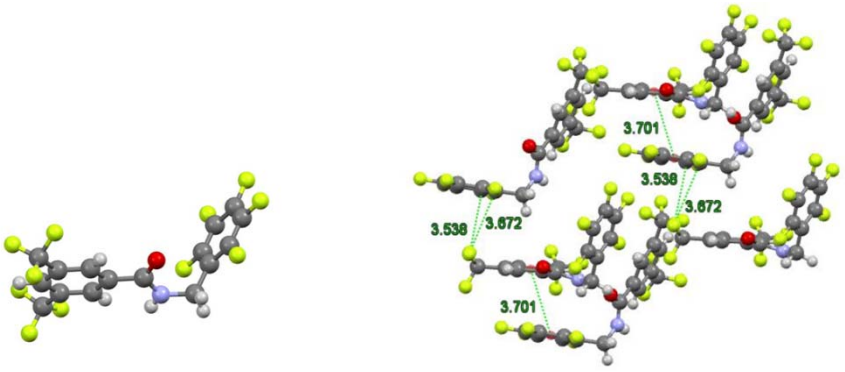

(a) (b)

Figure 48. The crystal structure of compound **82**. (black: C, gray: H, yellow-green: F, blue: N, red: O)

Figure 48 (a) shows the two fluorinated aromatic units of compound **82** are not in the same plane and the C_6F_5 of one molecule is stacked with the CF_3-aromtic unit of the other molecule nearby. Moreover, the F atoms of the latter interact with the third molecule by lone-pair electron-π interaction (Figure 48, b).

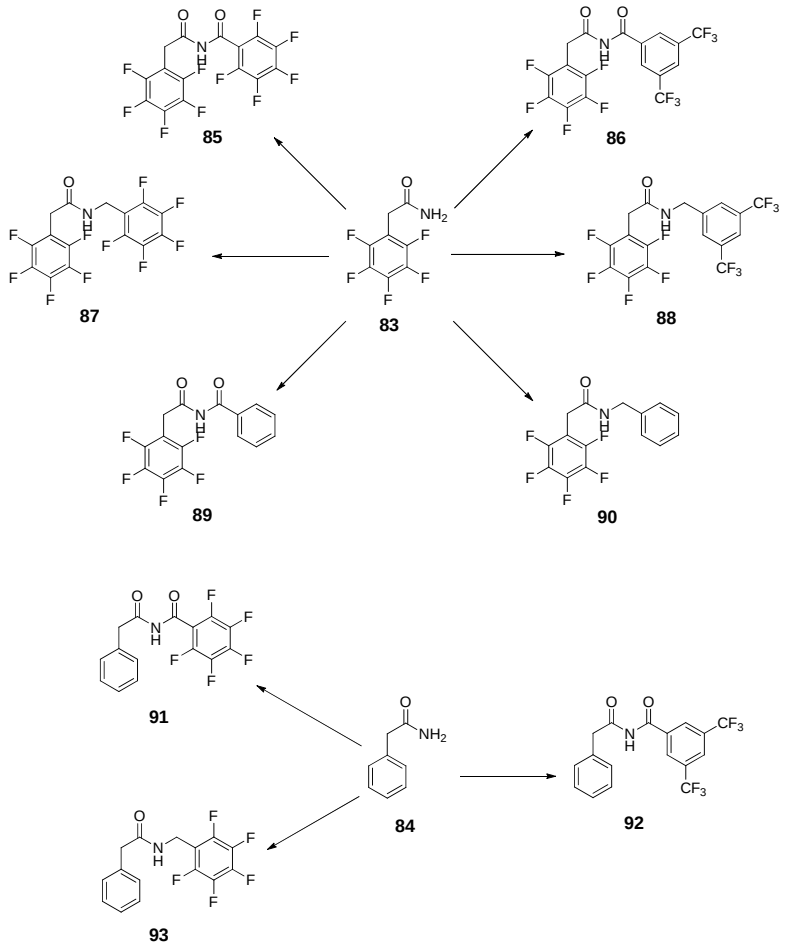

Scheme 46. The synthesis of anion receptors based on phenyl/pentafluorophenyl acetamide.

The methylene unit of the π-receptors shows a distinct influence to binding effect of

electron-deficient aromatic unit with anions, which is already discussed in the abovementioned chapters. Compounds **85-93** were obtained from prepared phenyl/pentafluorophenyl acetamide, so that a methylene unit is introduced between the carbonyl and an aromatic unit of the receptor (Scheme 46). The binding behavior of these compounds to anions may be different from the analogous structures studied previously, because of the methylene unit.

Additionally, some other fluorinated π-receptors **94-117** with ester/ether or amine/amide unit as a linker were prepared. Moreover, some of these receptors were investigated with X-ray crystal diffraction in the solid state.

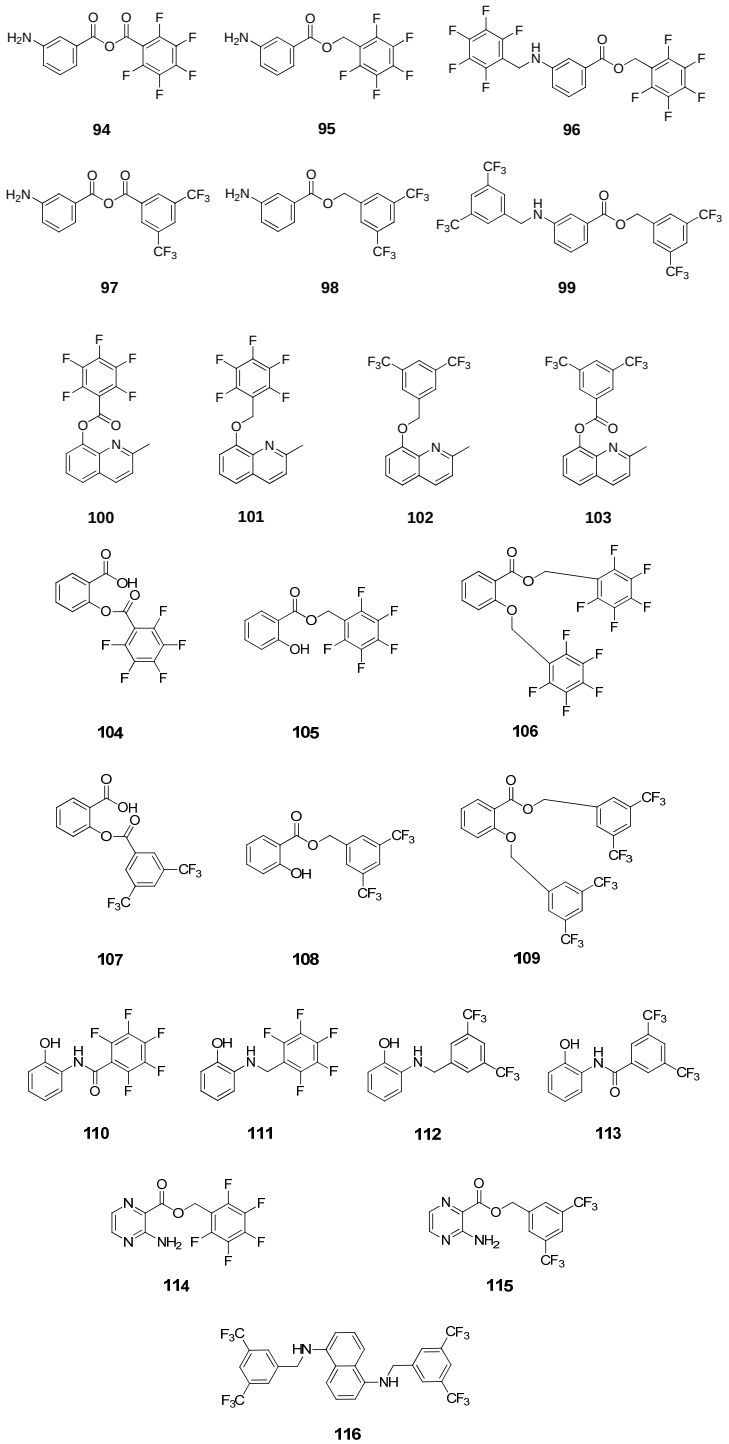

Scheme 47. Fluorinated π-receptors bearing two or three aromatic rings.

Compounds **94-99** were prepared from 3-aminobenzoic acid and fluorinated materials. Besides the electron-deficient aromatics, the amino group in the structure could react with anions by hydrogen bond which may strengthen the effect between the fluorinated aromatic unit and anions.

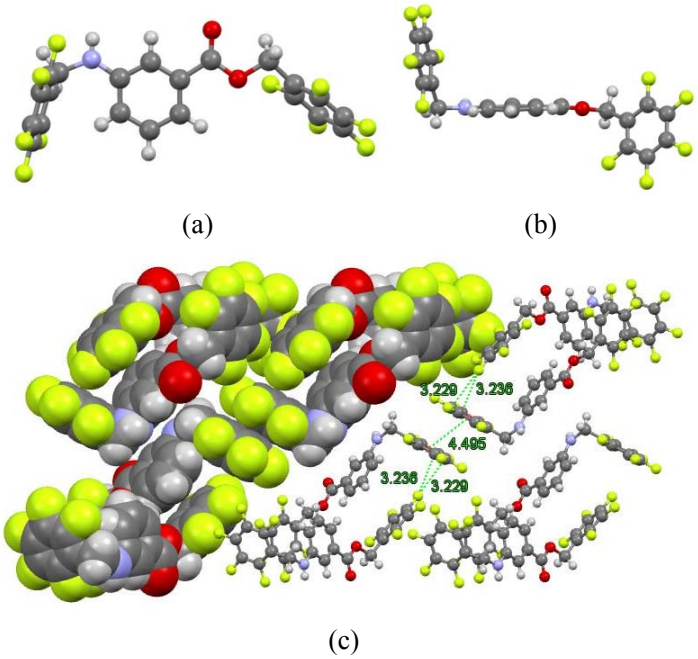

(a) (b)

(c)

Figure 49. The crystal structure of compound **96** shown from top (a) or side (b) view and the aggregation of molecules in crystals (c). (black: C, gray: H, yellow-green: F, blue: N, red: O)

The crystals of **96** were cultivated from DCM by slow evaporation of the solvent. As shown in Figure 49, the amino benzoic moiety spreads in the same plane and is orthogonal with the two C_6F_5 units. In crystals, two molecules approach to each other thereby forming a dimer with lone-pair electron-π interaction. Although C_6F_5 is proved to be an electron-deficient aromatic, a non-classical π-π stacking (4.50 Å) is still found between two pentafluorophenyl units which are closed face to face.

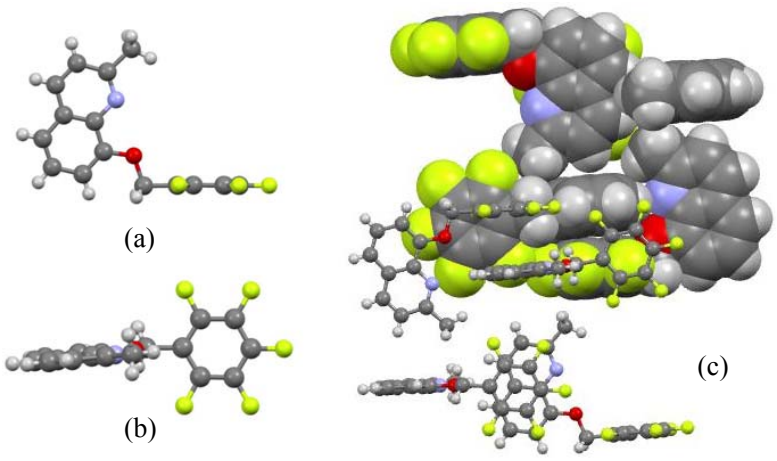

(a)

(b)

(c)

Figure 50. The crystal structure and part of the crystal lattice of **101** cultivated from the mixed solvent of ethyl acetate and hexane. (a: side view; b: top view) (black: C, gray: H, yellow-green: F, blue: N, red: O)

As shown in Figure 50, the quinoline unit is perpendicular to the pentafluorophenyl plane with an ether unit as a linker in the molecule **101**. The solid-state structure reveals π-π stacking of the pentafluorophenyl ring with the quinoline moiety of a second molecule. The intermolecular distance between the stacking systems is about 3.40 Å (Figure 50, c).

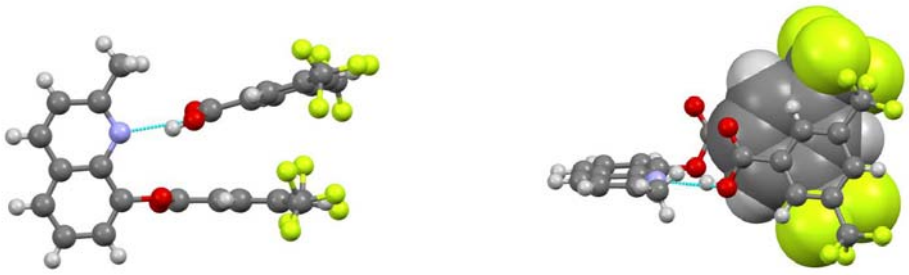

(a) (b)

Figure 51. (a) The crystal structure of compound **103** with a 3,5-bis(trifluoromethyl)benzoic acid co-crystallized. (b) The aromatic plane of the acid molecule stacking over the CF_3 aromatic plane of **103** which is shown in spacefill mode.

Quinoline derivative **103** which is bearing an ester unit was dissolved in the mixed solvent of ethanol/ethyl acetate (v/v =1:1). Colorless crystals were cultivated and their structure is shown in Figure 51. Obviously, some molecules of sample **103** decomposed in the solvent and 3,5-bis(trifluoromethyl)benzoic acid was produced. The acid is located above the CF_3 aromatic ring of **103** and fixed by N···H hydrogen bonding effect to a quinoline moiety (N···H = 1.87 Å). The quinoline aromatic formed an intramolecular angle of 80.89° to the 3,5-bis(trifluoromethyl)phenyl plane and the intermolecular angle between the 3,5-bis(trifluoromethyl)phenyl plane and the 3,5-bis(trifluoromethyl)benzoic acid plane is 16.06°.

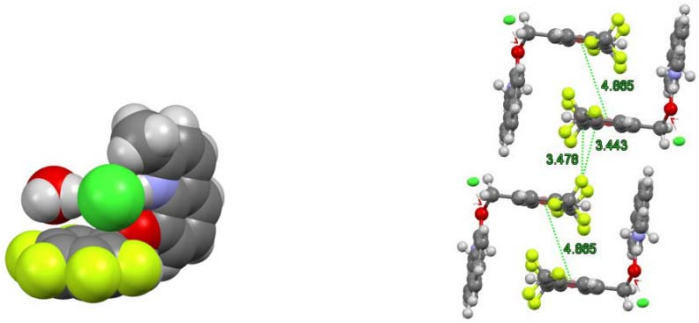

(a) (b)

Figure 52. (a) The structure of **101** chloride salt with a water crystallized. (b) Part of the crystal lattice of **102** chloride salt which was cultivated by the dispersion of Et_2O into the DMF solution.

Compound **101** or **102** was dissolved in ethanol solution of HCl and corresponding chloride salts were obtained separately after the solvent was removed. In the crystal of the pentafluorophenylated chloride salt obtained from DCM/hexane (V/V = 1:2), the Cl anion is fixed over the fluorinated aromatic ring by hydrogen bonding (NH···Cl = 2.27 Å, OH···Cl = 2.38 Å), which reveals anion-π interaction induced between the electron-deficient aromatic ring and anions

in co-crystals. In contrast, the Cl anion stays far away from the CF_3 aromatic ring in co-crystal salt of **102** and only contacts water molecules co-crystallized with hydrogen bonds. The solid-state structure reveals π-π stacking of two CF_3 aromatic rings and lone-pair electron-π effect between the CF_3 aromatic unit and the fluorine atom of the third cation.

Salicylic acid derivatives **104-109** were prepared by the binding of fluorinated benzoyl/benzyl chloride to the structure of 2-hydroxybenzoic acid. The fluorinated benzoyl chloride preferred to react with the OH group (for **104** and **107**), while the connecting of carboxyl group to the benzyl counterpart is prefered (for **105** and **108**). The di-substituted derivatives **106** and **109** were by-products of these reactions.

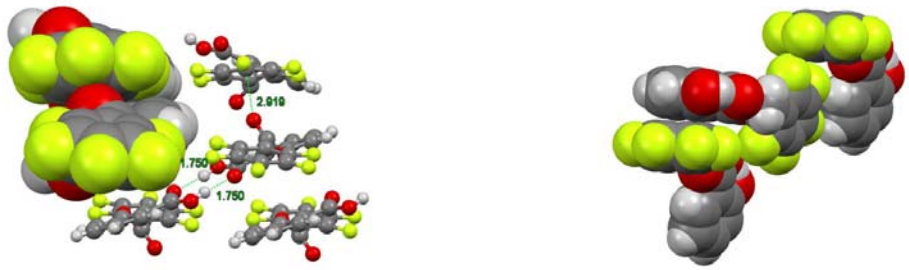

(a) (b)

Figure 53. (a) Part of the crystal lattice of **104**. (b) Spacefill mode structure of **105** showing π-π stacking and T-shaped CF-π interactions in crystals.

Compound **104** was crystallized from DMF/Et_2O in the space group $P2_1/c$. Its crystal structure is shown in Figure 53 (a). Hydrogen bonding is found between two carboxylic acid units, leading to a dimerization of the molecules. A dominating lone-pair electron-π interaction can be observed between the carbonyl oxygen and the carbon atom in the 4-position of the fluorinated ring, which prevents a parallel orientation of the aromatic units between molecules.

Compound **105** is the pentafluorobenzyl ester of salicylic acid and was crystallized from MeOH/Et_2O. Which is different from **104**, a parallel intermolecular π-π interaction is observed between C_6F_5 and the salicylic moiety. In addition, because of the distinct torsion between two aromatic rings in a molecule, T-shaped CF-π interactions are found between electron-deficient aromatic systems.

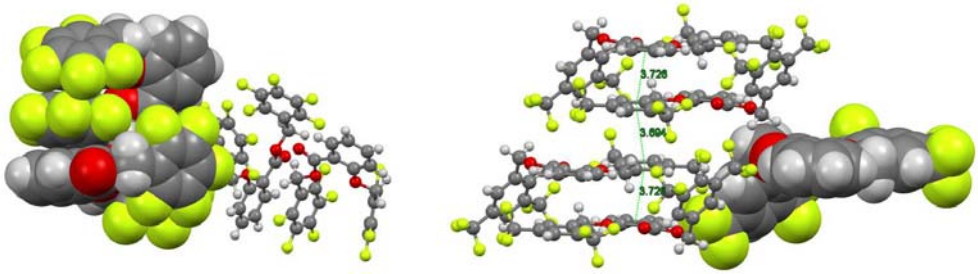

(a) (b)

Figure 54. (a) Part of the crystal lattice of **106**. (b) Spacefill mode structure showing the torsion of the molecule **109**. Ball-and-stick plots showing intermolecular π-π interactions between aromatic rings.

The di-substituted derivative **106** was crystallized from DMF/Et_2O in the chiral space group $P2_12_12_1$. The two benzylated oxygen atoms are forced into close proximity instead of repulsing

each other. The carbonyl oxygen atom of one neighboring molecule points into the tweezer space of the electron-deficient rings, which is undergoing lone-pair electron-π interaction with the carbon atoms of the two C_6F_5 rings. The two C_6F_5 rings are not in a parallel orientation, with the closest distance of corresponding carbon atoms of 3.47 Å and the longest of 4.98 Å. Moreover, the pentafluorophenyl group faces to the salicylic acid moiety of the other molecule nearby with attractive π-π interaction (Figure 54, a).

The molecular conformation of the CF_3 analogue **109** in crystals is not a tweezer form, as shown in Figure 54 (b). One of the CF_3-ring is in the same plane with the salicylic acid unit and the other one tilts with the angel of 61.51°. The CF_3 aromatic ring undergoes π-π stacking interaction with not only the salicylic ester unit of the second molecule but also another CF_3 aromatic ring of the third neighboring molecule. The centroid-to-centroid distances are about 3.73 Å and 3.69 Å, respectively.

The compounds **110-113** were produced though the nucleophilic reaction of 2-aminophenol with the fluorinated reactants in the presence of bases. The amino-substituted compound is the exclusive product without the phenolic derivatives.

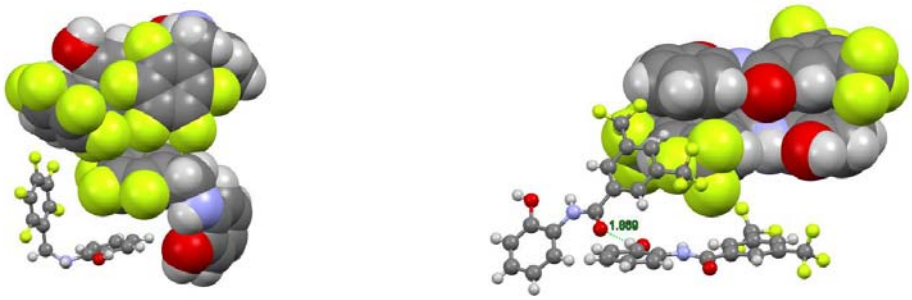

(a) (b)

Figure 55. (a) Spacefill mode structure showing the CF-π interaction of the electron-deficient aromatic rings in **111**. (b) Part of the crystal lattice of **113** cultivated from ethyl acetate/hexane showing hydrogen bonding and π-π stacking effect in solid state.

The crystal of compound **111** was obtained from ethyl acetate/hexane in the space group P_b2_1/a. The pentafluorophenyl group forms an interplanar angle of 81.08° with the plane of 2-aminophenol moiety. Intermolecular rather than intramolecular hydrogen-bonding of NH and OH can be observed (OH···NH = 1.93 Å) and the C_6F_5 ring is not parallel to the aminophenol unit of another molecule. The dominant effect is the CF-π interaction which is formed by the CF of two C_6F_5 rings pointing to the third pentafluorophenyl group with the closest distances of approximate 3.05 Å and 3.35 Å, respectively.

The two aromatic rings of trifluoromethylated compound **113** spread nearly in the same plane with the interplanar angle of 5.36°. The two molecules are in parallel arrangement with head-to-tail orientation and the centriod distance of this π-π stacking is 3.67 Å. In addition, intermolecular H-bond effect can be found between carbonyl oxygen atom and the phenolic hydroxyl group (C=O···HO = 1.87 Å).

The reaction of 3-aminopyrazine-2-carboxylic acid with pentafluorobenzyl/3,5-bis(trifluoromethyl)benzyl bromide generated fluorinated ester derivatives **114** or **115** as the only product. The crystal of **114** or **115** was obtained from ethyl acetate/hexane and the XRD structure is shown in Figure 56.

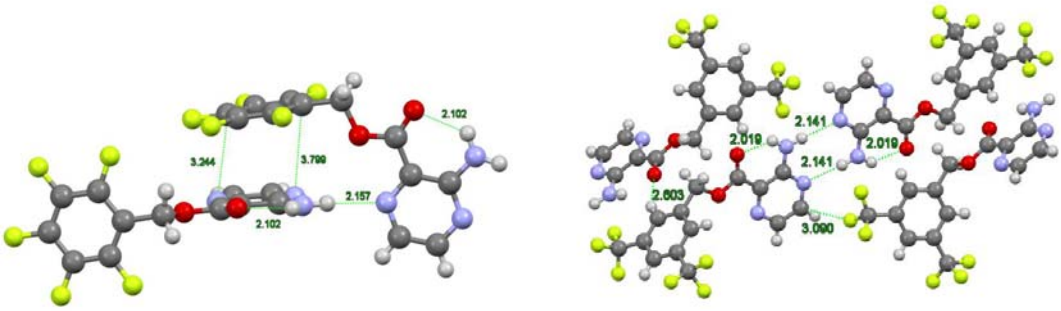

(a) (b)

Figure 56. (a) The crystal structure of **114** showing inter- and intramolecular interactions in solid state. (b) Part of the crystal lattice of **115** showing non-covalent interactions containing H-bonding and non-classical C=O···HC effect and CF-π interaction.

In the structure of **114**, the plane of pentafluorophenyl ring is orthogonal to the pyrazine unit with the interplanar angle of 89.92°. The intramolecular hydrogen binding effect can be found between the carbonyl oxygen atom and the amino group (C=O···HN = 2.10 Å). As the intermolecular H-bond (NH···N= 2.16 Å) exists between NH and the nitrogen atom of the pyrazine ring, the pentafluorophenyl unit is not parallel to the pyrazine ring of the neighboring molecule, but over the pyrazine unit with the closest distance between the carbon atom in the 4-position (C4) of the C_6F_5 and the nitrogen atom in the 3-position (N3) of the pyrazine ring of 3.24 Å and the longest distance between C1 and N6 of 3.80 Å (Figure 56, a).

In the CF_3 derivative **115**, a CF-π interaction (3.09 Å) between fluorine and C5 of the pyrazine ring of the second molecule can be observed rather than the emergence of π-π effect. In addition, inter-/intramolecular hydrogen bonding effect as well as short contact between CH of the fluorinated aromatic ring and the carbonyl oxygen atom of the neighboring molecule are found in the crystal structure (Figure 56, b).

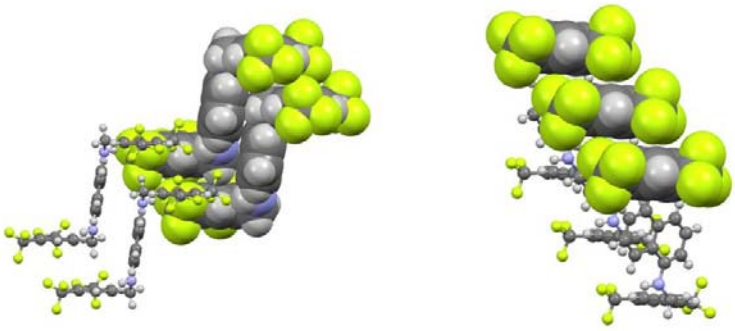

(a) (b)

Figure 57. (a) The "zigzag" conformation of compound **116** in crystals. (b) Spacefill mode of **116** showing the CF-π interaction between the neighboring 3,5-bis(trifluoromethyl)phenyl rings.

Di-substituted derivative **116** was synthesized from the reaction of naphthalene-1,5-diamine with 3,5-bis(trifluoromethyl)benzyl bromide. Figure 57 shows the "trans" conformation of the structure **116** crystallized from ethyl acetate/hexane with the intramolecular angle between the plane of fluorinated ring and naphthalene of 82.50°. Both fluorinated ring and naphthalene unit adopt parallel arrangement and π-π interaction can be found between the corresponding C1 or C5

of the closed naphthalene units (Figure 57, a). The trifluoromethylated aromatic rings are not only parallel to each other but also reveal CF-π interaction with shortest distance between (C)F and the carbon atom of the ring of 3.34 Å.

7.2 The crystal study of tert-amine or tert-amide derivatives bearing three or four aromatic rings

Pentafluorophenyl group is a significant aromatic unit in the research of supramolecular chemistry, as it can participate in the formation of various non-covalent interactions according to the previous study. In this part, several amine/amide derivatives **117-123** bearing the pentafluorophenyl group(s) were synthesized and their structures were investigated in crystals.

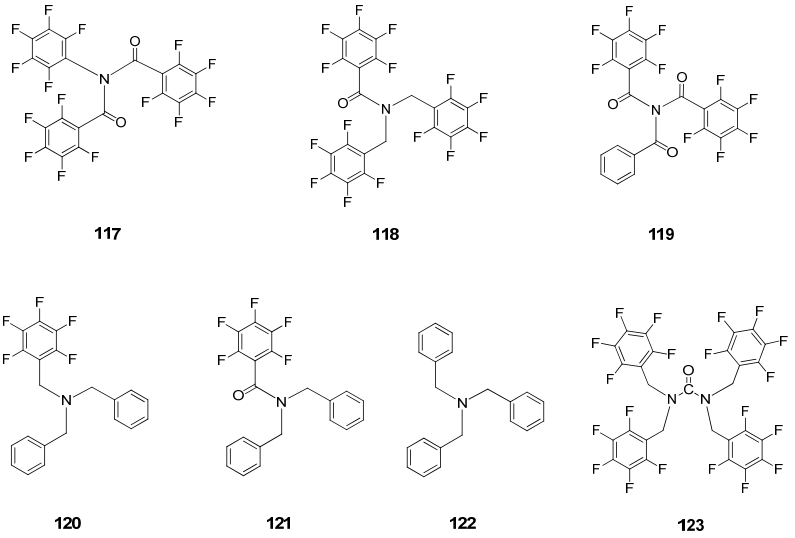

Scheme 48 Several amine/amide derivatives **117-123**.

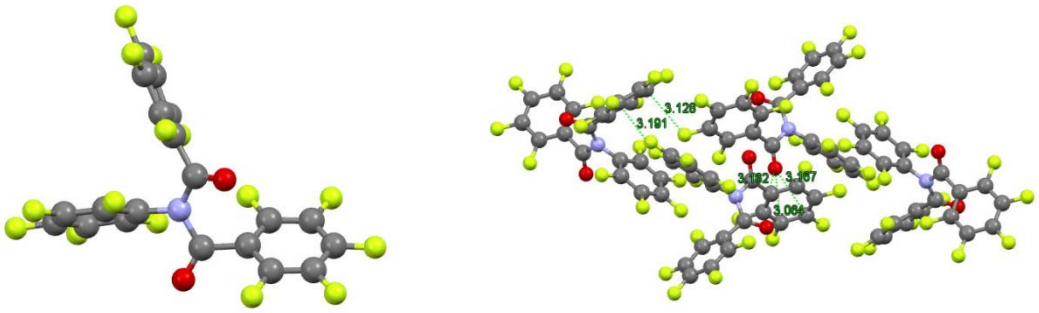

(a) (b)

Figure 58. (a) The crystal structure of **117**. (b) Part of the crystal lattice of **117** showing lone-pair electron-π and CF-π interactions between pentafluorophenyl ring and oxygen or fluorine atom.

The crystal of compound **117** was cultivated from EtOH/Et_2O in the space group $P2_1/c$. In the crystal structure of a molecule, one of the two pentafluorobenzoyl moieties and the pentafluoroaniline unit form a "V-shape" cavity, with an interplanar angle of 73.83°. The third plane of the pentafluorobenzoyl unit forms an angle of 68.69° or 52.78° with each plane of the "V-shape" cavity (Figure 58, a). Two molecules aggregate into a dimer by lone-pair electron-π interaction (C=O···π = 3.06, 3.16 and 3.17Å) between the carbonyl and the pentaflorobenzoyl ring

of a neighboring molecule. Every two of the other four electron-deficient rings point into the "V-shape" cavity of the third molecule nearby and the closest distance between (C)F of the two C_6F_5 rings and the carbon atom of the "V-shape" cavity is about 3.13 or 3.19Å, respectively (Figure 58, b).

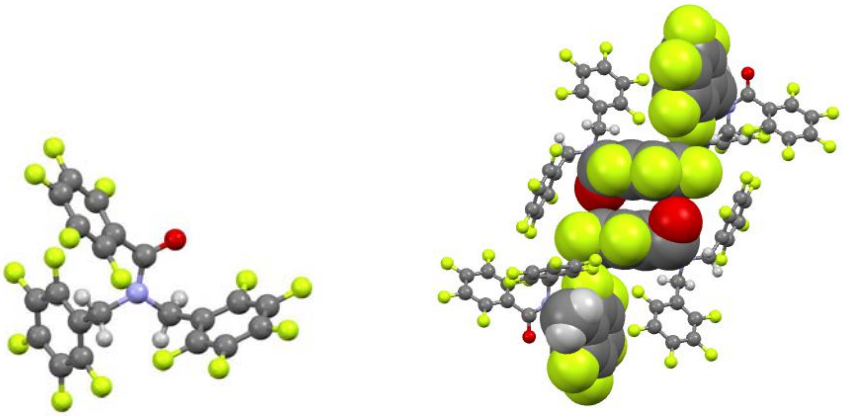

(a) (b)

Figure 59. (a) The structure of compound**118** in crystals. (b) Part of the crystal lattice of **118** showing the lone-pair electron-π and CF-π interactions with spacefill mode.

The compound **118** was crystallized from EtOH/Et_2O in the space group $P2_1/c$. The positions of the three pentafluorophenyl rings in the molecule are fixed asymmetrically and dominantly by the intermolecular interactions. As showing in Figure 59, the carbonyl group points to the plane of pentafluorophenyl of the second molecule with the closest distance between oxygen of the carbonyl and the carbon atom of the C_6F_5 of 2.90 Å; In addition, this C_6F_5 unit interacts to another pentafluorophenyl moiety of the third molecule with T-shaped CF-π interaction (CF⋯C = 2.94, 3.36 and 3.38 Å).

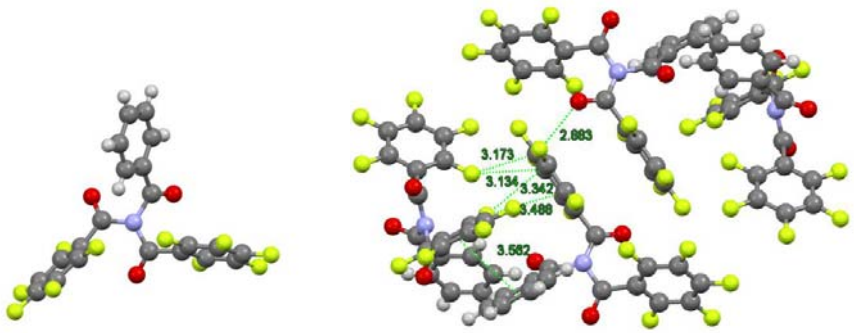

(a) (b)

Figure 60. (a) The crystal structure of **119**. (b) Part of the crystal lattice of **119** showing the lone-pair electron-π, CF-π and π-π interactions.

The crystal of compound **119** was cultivated from EtOH/Et_2O in the space group $P2_1/c$. The plane of phenyl unit forms two different angles (83.70° and 56.12°) with each pentafluorophenyl plane and an interplanar angle of 53.93° can be found between the two planes of C_6F_5 rings. Two pentafluorophenyl rings are in the parallel position compelled by the lone-pair electron-π attraction between the oxygen atom and the carbon atom in the 4-position of the C_6F_5 ring as well

as CF-π interaction. Intermolecular π-π stacking can be observed between the C_6F_5 unit and the C_6H_5 ring of the neighboring, with the centriod distance of 3.56 Å.

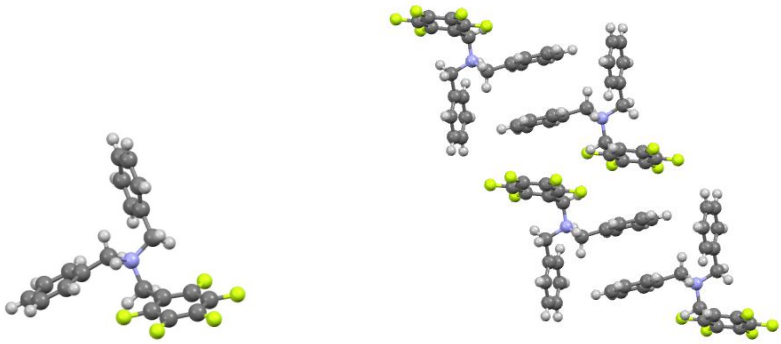

(a) (b)

Figure 61. (a) The crystal structure of **120**. (b) Part of the crystal lattice of **120**.

The crystal of compound **120** was cultivated from ethyl acetate/hexane in the space group $P2_1/n$. The plane of one C_6H_5 ring is not only orthometric to the other phenyl plane and the C_6F_5 ring of the molecule with interplanar angles of 73.79° or 89.43° respectively but also parallel to the phenyl ring of the neighboring molecule with a longer centriod distance of 3.86 Å. In the crystal of **120** (Figure 61, b), the pentafluorophenyl ring is not parallel to the phenyl ring and only short contact (C(F)···C(H) = 3.40 Å) can be found between the two carbon atoms in 4-positions of the two aromatic rings.

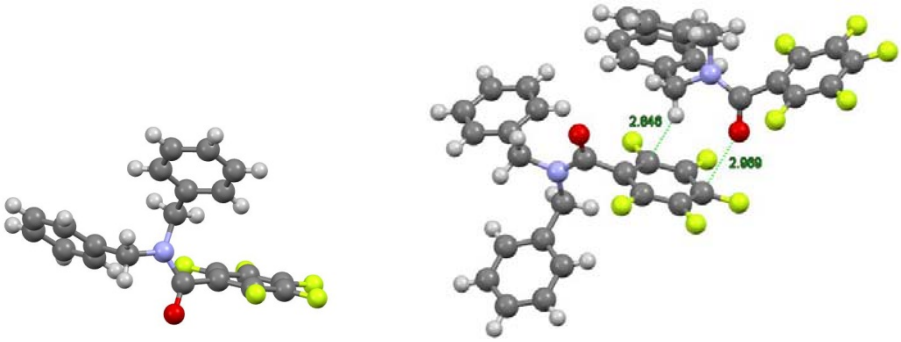

(a) (b)

Figure 62. (a) The crystal structure of **121**. (b) Part of the crystal lattice of **121** showing the CH-π and CO-π interactions.

The compound **121** was crystallized from EtOH/Et_2O in the space group $P2_1/c$. Because of the non-classical hydrogen binding effect (CH_2···O = 2.33 Å) between the oxygen atom of the carbonyl group and the hydrogen atom of the methlyene unit, the plane of pentafluorophenyl ring forms a smaller angle of 29.61° with one C_6H_5 ring and 44.89° with the other. The intermolecular CH-π and CO-π interactions as the dominant effects can be observed in the crystal structures (Figure 62, b).

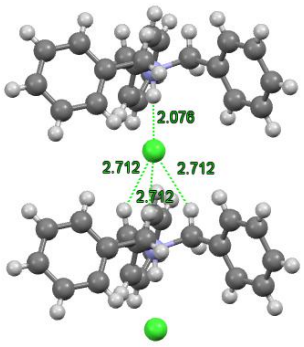

Figure 63. The crystal structure of the chloride salt of compound **122**.

Non-fluorinated derivative **122** was synthesized as a reference compound and its chloride salt was crystallized from EtOH in the space group *R*3. As shown in Figure 63, the chloride anion does not interact with the phenyl groups and only hydrogen bonding can be observed between Cl anion and NH as well as the non-classical hydrogen binding with the methylene units nearby.

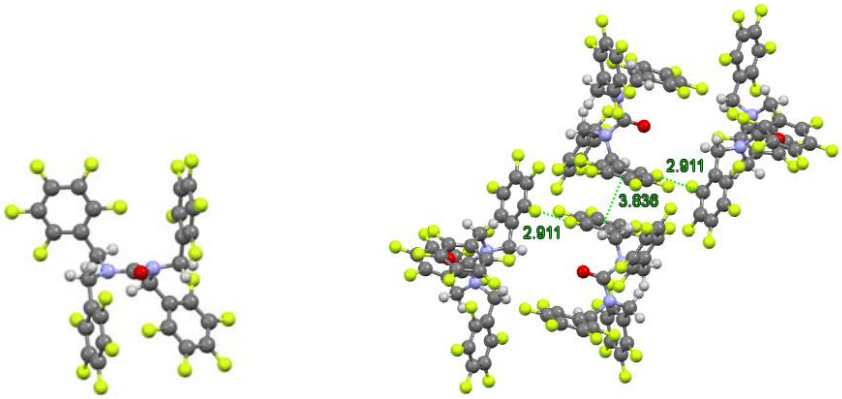

(a) (b)

Figure 64. (a) The crystal structure of **123**. (b) Part of the crystal lattice of **123** showing the CF-π and π-π interactions.

The crystal of 1,1,3,3-tetrakis((perfluorophenyl)methyl)urea **123** was obtained from ethyl acetate/hexane in the space group $P2_1/c$. Two trans-position pentafluorophenyl rings are parallel to each other and other two form an angle of 58.20°. In addition, an interplanar angle of 67.32° can be observed between the two C_6F_5 rings binding to the same nitrogen atom with methylene units. Intermolecular CF-π and π-π interactions are the significant binding existing in the solid state of compound **123** (Figure 64, b).

7.3 The synthesis and crystal structure of the trifluoromethylated imine derivative **126**

Pyridine-2,6-dicarbaldehyde **125** was obtained by the oxidation of pyridine-2,6-diyldimethanol **124**,[69] and then reacted with (3,5-bis(trifluoromethyl)phenyl)methanamine **21** in methanol to afford the condensation product **126**.

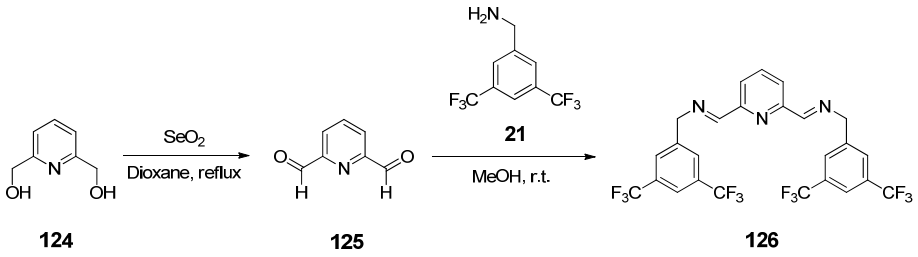

Scheme 49. The preparation of the trifluoromethylated imine derivative **126**.

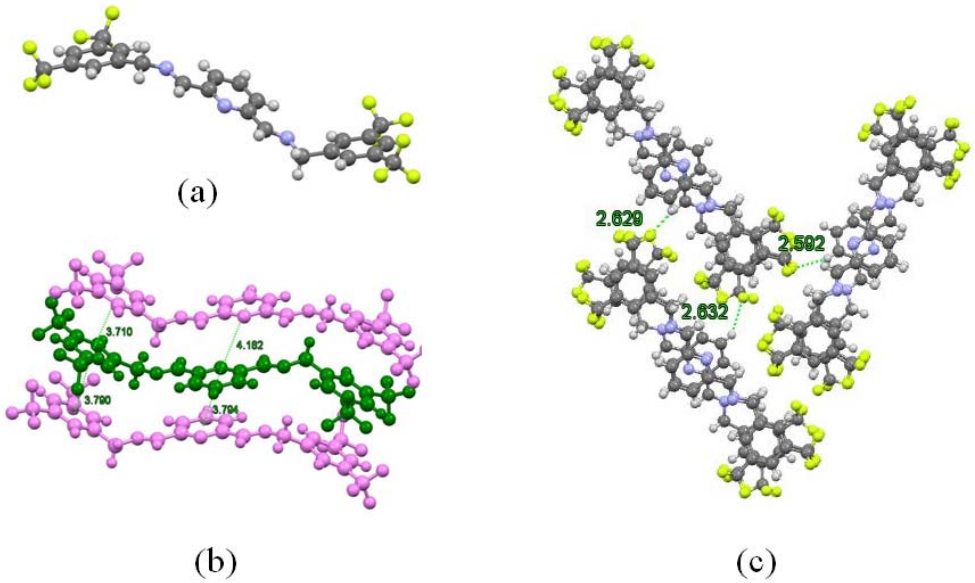

Figure 65. (a) The crystal structure of a single molecule for **126**. (b) The stacking of molecules in part of the crystal lattice of **126**. (c) Non-classical (C)F⋯H(C) hydrogen binding effect existing in the crystal structure.

Compound **126** was crystallized from MeOH/Et_2O in the space group $P2_1/n$. The planes of two 3,5-bis(trifluoromethyl)phenyl rings are not exactly parallel and a minor angle of 2.19° can be found between these two planes as well as interplanar angles of 32.04° and 32.83° with the plane of the pyridine unit, respectively. The molecules are located in different layers and the orientations of H-(C=N) units of two molecules in adjacent layers are opposite resulting in the unequal center-to-center distances (3.71, 3.79, 3.79 and 4.18 Å) between the stacking aromatic rings (Figure 65, b). The CF interact to the hydrogen atoms of the neighboring molecules with non-classical hydrogen bonds ((C)F⋯H(C4) = 2.63, (C)F⋯H(C3) = 2.59 and (C)F⋯H(C=N) = 2.63 Å), but no CF-π interaction can be observed in the crystal structure.

7.4 The synthesis and crystal structure of the trifluoromethylated calix[4]arene derivative **129**

The calix[4]arene **128** was synthesized from the commercially available material 4-tert-butylcalix[4]arene **127** by removing the four tert-butyl groups.[70] Afterwards, the 3,5-bis(trifluoromethyl)benzyl bromide **19** was introduced into the structure of **128** by substitution reaction, so that the trifluoromethylated calix[4]arene derivative **129** was produced sufficiently.[71]

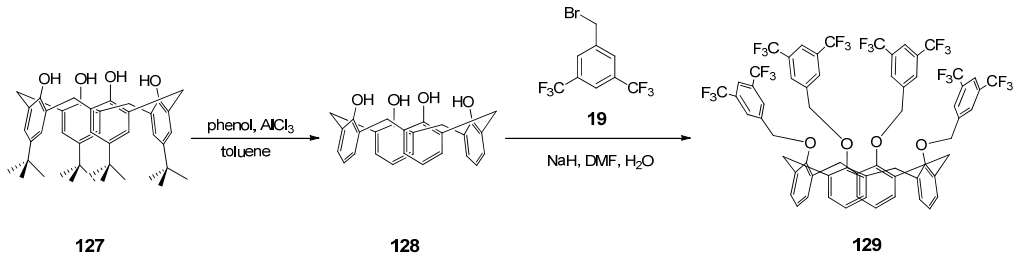

Scheme 50. The preparation of the trifluoromethylated calix[4]arene derivative **129**.

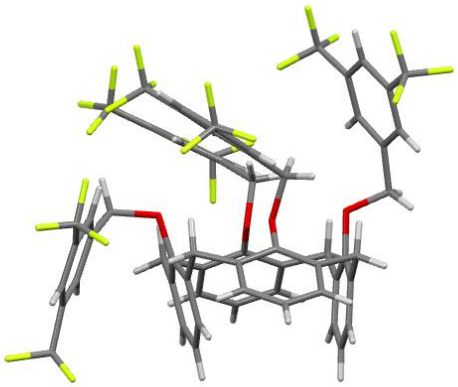

Figure 66. Capped sticks mode showing the structure of compound **129** in the crystal.

Compound **129** was crystallized from MeOH/Et_2O in the space group *P*-1. The attempt for cultivating co-crystals of **129** with diverse anions failed, because the four 3,5-Bis(trifluoromethyl)phenyl rings of the molecule cannot tune a cavity which could contain an anion due to the steric repulsive force of four CF_3 aromatic rings. For realizing the motif of a co-crystal with an anion fixed into the CF_3-arene cavity, a larger calyxarene should be introduced as the basis.

7.5 Conclusion

Some π-receptors bearing fluorinated electron-deficient aromatic rings were synthesized and some of their structures were investigated by X-ray crystal diffraction. Lone-pair electron-π and π-π interactions are the common effect existing in these crystal structures. Especially, a co-crystal containing two different neutral molecules cultivated from compound **103** dissolved in the mixed solvent of ethanol/ethyl acetate. It is quite rare that two diverse molecules are co-crystallized and the stacking of two 3,5-bis(trifluoromethyl)phenyl rings can be observed in crystals. The Cl^- co-crystal structures (**101**, **102** and **122**) reveal that anion-π interaction exists between the anion and the pentafluorophenyl ring, but it cannot be observed between Cl anion and 3,5-bis(trifluoromethyl)phenyl or non-fluorinated phenyl ring. Because of the lone-pair electron-π binding between the oxygen atom of the carbonyl and the carbon atom of pentafluorophenyl ring, the two electron-deficient C_6F_5 rings are fixed in a parallel position, which could be an interesting motif for crystal engineering in the future.

Chapter 8 Conclusion and perspective

Several kinds of fluorinated electron-deficient aromatic compounds bearing pentafluorophenyl or 3,5-bis(trifluoromethyl)phenyl group as well as perfluoro-1,1′-biphenyl or perfluoronaphthalene and their derivatives were synthesized and investigated both in crystals and in solution as π-receptors for anions.

By ^{19}F NMR-titration experiments, ^{19}F high-field shifting of perfluoro-1,1′-biphenyl or perfluoronaphthalene with the addition of anions can be found in solution. However, the linear relation of ^{19}F NMR chemical shifts with anion added does not reveal anion-π interactions between the electron-deficient aromatic unit and anions. In fact, the anion-π interaction has not been found between perfluoro-1,1′-biphenyl or perfluoronaphthalene and anions by experimental research up to now, although theoretical calculation demonstrate that anion-π interaction can be possible between the perfluoronaphthalene molecule and anions. On the other hand, DABCO substituted cations show an attractive effect to bromide anion which can be fixed above the aromatic ring by Br···H interaction showing η^4-type anion-π interactions in the solid state.

3,5-Bis(trifluoromethyl)phenylated compounds were firstly studied as π-receptors for anions in crystals. The chloride anion interacts with the hydrogen atoms of the 3,5-bis(trifluoromethyl)phenyl unit by hydrogen binding and no anion-π interaction can be observed between Cl^- and the aromatic ring in the solid state. Probably because of the larger polarizability, the bromide anion can be able to induce anion-π interaction with the CF_3 electron-deficient aromatic ring.

The solution research of anion-π interactions demonstrates that only a linear relation of the ^{19}F NMR chemical shifts of the amine derivatives with the addition of anions can be observed rather than anion-π interaction, while the amide derivatives not only show anion-π interactions with diverse anions in solution but also induce a stronger attractive effect in acetone than in chloroform. It obviously shows that the active hydrogen can more efficiently fix the anion above the electron-deficient ring by hydrogen binding with a saturated mode. In addition, the different directions of ^{19}F NMR chemical shifts for the ortho-F (down-field shifting), meta- and para-F (high-field shifting) of pentafluorophenyl units as well as of ^1H NMR chemical shifts for the ortho-H (down-field shifting) and para-H (high-field shifting) of the CF_3-aromatic rings reveal the uneven-distribution of the π-bond induced by the anion added.

Different acid-base systems can adjust the existence and the strength of anion-π interactions in solution, which has been confirmed by the research of zwitterions as host-guest systems themselves. Moreover, the fluorinated electron-deficient aromatic moieties connecting to the 2′- or 3′-position of the indole molecule are able to influence the binding behavior of indole to anions in solution. These preliminary results provide some possible references for the practical research in bio-chemistry or material science etc..

Crystal study is significant in these research subjects. Either pentafluorophenyl ring or 3,5-bis(trifluoromethyl)phenyl unit not only interact with anions by non-covalent binding effect but also induce π-π stacking or T-shaped CF-π interactions with the neighboring aromatic rings. It is reasonable for the pentafluorophenyl unit to locate in a parallel position above the electron-rich ring nearby because of the electron-deficient property of the pentafluorophenyl ring. Interestingly, the parallel motif can also be found between two pentafluorophenyl rings or between two

3,5-bis(trifluoromethyl)phenyl rings which are both electron-deficient aromatics. In fact, with the crystal structure analysis aforementioned of C=O–π interaction (for pentafluorobenzoyl) or CF–π interaction (for CF_3 aromatics), consequently, it is feasible to compel the two electron-deficient aromatic rings locating in a parallel mode which is counterintuitive but may be interesting in crystal engineering.

3,5-Bis(trifuoromethyl)phenyl unit has been investigated as a new kind of building block related to π-receptors for anions. Because of the presence of both CF_3 groups and hydrogen atoms in the structure, according to the abovementioned research work, it is not an easy task to investigate or separate the pure anion-π interaction or hydrogen binding effect from the comprehensive non-covalent effect. Since the CF_3 aromatic units can afford diverse binding effects simultaneously, why not exploit them as a kind of versatile non-covalent bond donator?

Experimental section

General experiment conditions

All commercially available reagents were used as received. All solvents were distilled and used without further purification, except THF which was dried by filtration over activated alumina (basic) in a column.

^{1}H (300 MHz or 400 MHz) and ^{19}F (282 or 376 MHz) NMR spectra were obtained with a Varian Mercury 300 or Inova 400 spectrometer in deuterated solvents and ^{1}H or ^{19}F NMR yield determination with an internal standerd TMS or $CFCl_3$, respectively. The mass spectrometric data were recorded with a Finnigan SSQ 7000 and a Thermo Deca XP system by using EI (70 eV) or ESI. The infrared spectra were measured with a PerkinElmer FTIR spectrometer (Spectrum 100) and the samples were measured in KBr (4000－650 cm^{-1}). Elemental analyses were performed with a CHN-O-Rapid Vario EL system from Heraeus. HRMS were performed with a Thermo Scientific LTQ XL system. The melting points were measured with a Büchi B-540 system and were not corrected.

Single crystal X-ray data were collected at 173(2) or 123(2) K using an Agilent SuperNova diffractometer or a Bruker-Nonius KappaCCD diffractometer with an APEX-II detector and utilizing monochromatized Mo-Kα (λ = 0.71073 Å) or Cu-Kα (λ = 1.54184 Å) radiation. The data collection, data reduction and multi-scan absorption correction for samples were made by program CrysAlisPro.[72] The program COLLECT[73] or HKL DENZO AND SCALE-PACK were used for the data collection (θ and ω scans), DENZO-SMN[74] for the processing and SADABS[75] for multi-scan absorption correction for data. The structures were solved by direct methods with SIR2004[76] or SHELXS and refined by full-matrix least-squares methods with the OLEX2 or WinGX-software,[77] which utilizes the SHELXL-2013 or SHELXL-97 module.[78] (The X-ray single crystal diffraction was determined by Prof. Kari Rissanen and co-workers)

$^{1}H/^{19}F$ NMR-titration experiments

In each group of $^{1}H/^{19}F$ NMR-titration experiment, the amount of the receptor as hosts was 0.025 mmol and the amount of each TBA salt was successively increased as guests. The volume of the tested solution in each NMR tube was kept for 0.6 mL and all the $^{1}H/^{19}F$ NMR-titration experiments were processed at 298 K.

Synthesis of compounds

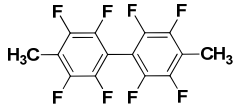

28

2,2',3,3',5,5',6,6'-Octafluoro-4,4'-dimethyl-1,1'-biphenyl 28. Under nitrogen atmosphere, perfluoro-1,1'-biphenyl **24** (2.3 g, 7.0 mmol) was dissolved in THF (7.0 mL) and cooled to

0 °C. Methyllithium (14.0 mmol, 1.6 M sol. in diethyl ether) was added dropwise into the solution. The mixture was stirred overnight at the same temperature and then was allowed to warm to room temperature. After completion of reaction, the mixture was washed with saturated NaCl aqueous solution (3 × 20 mL) and extracted with ethyl acetate (3 × 15 mL). The organic layers were combined and dried with Na_2SO_4, filtered. Then the organic solution was removed under vacuum, finally the residue was obtained and separated by column chromatography on a silica gel using Hexane as eluent. Compound **28** was obtained as a white solid with yield of 88% (2.021 g, 6.2 mmol). m.p.: 142.3-143.9 °C; ^{1}H NMR (300 MHz, $CDCl_3$): δ = 2.29 (t, *J* = 2.1 Hz, 6H); ^{19}F NMR (282 MHz, $CDCl_3$): δ = -140.29 (dd, *J* = 16.4, 8.2 Hz, 4F), -142.90 (d, *J* = 9.9 Hz, 4F); EI-MS: m/z: 326.3 (52.77%), 325.4 (56.73%), 324.3 (63.83%), 162.6 (100%), 160.9 (86.05%); IR(KBr, cm^{-1}): 2933, 2336, 2072, 1743, 1654, 1593, 1466, 1373, 1251, 1134, 1067, 1009, 941, 906, 717; Anal. Calcd. for $C_{14}H_6F_8$: C, 51.55; H, 1.85; Found: C, 51.64; H, 2.08.

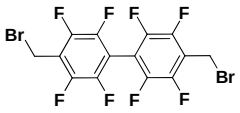

29

4,4'-Bis(bromomethyl)-2,2',3,3',5,5',6,6'-octafluoro-1,1'-biphenyl 29. A mixture of compound **28** (1.6 g, 5.0 mmol) and *N*-bromosuccinimide (1.8 g, 10.0 mmol) in CCl_4 (10.0 mL) was refluxing for 10 h. After completion of reaction, the mixture was washed with saturated NaCl aqueous solution (3 × 20 mL) and extracted with ethyl acetate (3 × 15 mL). The organic layers were combined and dried with Na_2SO_4, filtered. The solvent was evaporated and the residue was purified by column chromatography on a silica gel using hexane as eluent to afford the **29** as a white solid (1.159 g, 48%). m.p.: 146.4-147.6 °C; ^{1}H NMR (300 MHz, $CDCl_3$): δ = 4.51 (s, 4H); ^{19}F NMR (282 MHz, $CDCl_3$): δ = -137.45 (dd, *J* = 16.4, 8.5 Hz, 4F), -141.57 (d, *J* = 8.7 Hz); EI-MS: 405.0 (8.90%), 403.4 (14.96%), 324.5 (100.00%), 162.0 (30.99%), 161.0 (43.25%), 160.2 (25.52%); IR(KBr, cm^{-1}): 1470, 1321, 1268, 1222, 1167, 1120, 1068, 1026, 976, 929, 861, 805, 759, 721; Anal. Calcd. for $C_{14}H_4Br_2F_8$: C, 34.74; H, 0.83; Found: C, 35.38; H, 1.18; HRMS (ESI) m/z Calcd. for $C_{14}H_4Br_2F_8$: 481.8547; Found: 481.8536.

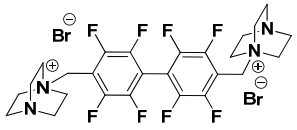

26

1,1'-((Perfluoro-[1,1'-biphenyl]-4,4'-diyl)bis(methylene))bis(1,4-diazabicyclo[2.2.2]octan-1-ium) bromide 26. Compound **29** (1.0 g, 2.0 mmol) was dissolved in dichloromethane (2.0 mL), then DABCO (0.4 g, 4.0 mmol) was added and stirred at room temperature. After 10 min, white precipitate was generated from the solution. The mixture was continued to stir overnight and the white solid was filtered and dried under vacuum to obtain pure compound **26** (1.343 g, 95%). m.p.: > 270 °C decomposed; ^{1}H NMR (300 MHz, DMSO-d_6): δ = 3.05 (t, *J* = 6.9 Hz, 12H), 3.50 (t, *J* = 6.9 Hz, 12H), 4.75 (s, 4H); ^{19}F NMR (282 MHz, DMSO-d_6): δ= -134.04 (d, *J* = 12.1 Hz, 4F), -138.03 (dd, *J* = 18.3, 7.9

Hz, 4F); ESI-MS: 274.1 $[3\text{-}2Br^-]^{2+}$, 627.1 $[3\text{-}Br^-]^+$; IR(KBr, cm^{-1}): 3417, 2954, 2889, 2798, 2594, 2317, 2191, 2030, 1971, 1654, 1469, 1381, 1334, 1264, 1188, 1057, 992, 936, 886, 844, 793, 722, 663.

The dicationic derivative **26** was crystallized in the chiral space group *C*2 by diffusing Et_2O into the methanol solution of the sample.

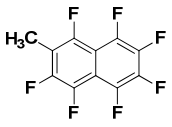

30

1,2,3,4,5,6,8-Heptafluoro-7-methylnaphthalene 30. Under nitrogen atmosphere, perfluoronaphthalene **25** (1.9 g, 7.0 mmol) was dissolved in Et_2O (7.0 mL) and cooled to 0 °C. Methyllithium (7.0 mmol, 1.6 M sol. in diethyl ether) was added dropwise into the solution. The mixture was stirred overnight at the same temperature and then was allowed to warm to room temperature. After completion of reaction, the mixture was washed with saturated NaCl aqueous solution (3 × 20 mL) and extracted with ethyl acetate (3 × 15 mL). The organic layers were combined and dried with Na_2SO_4, filtered. Then the organic solution was removed under vacuum, finally the residue was obtained and separated by column chromatography on a silica gel using hexane as eluent. Compound **30** was obtained as a white solid with yield of 82% (1.528 g, 5.7 mmol). m.p.: 53.1-53.9 °C; ^{1}H NMR (400 MHz, $CDCl_3$): δ = 2.41 (t, *J* = 2.4 Hz, 3H); ^{19}F NMR (376 MHz, $CDCl_3$): δ = -121.62 (d, *J* = 18.8 Hz, 0.5F), -121.80 (d, *J* = 18.8 Hz, 0.5F), -137.27 (d, *J* = 12.8 Hz, 1F), -145.08 (dd, *J* =35.0, 16.9 Hz, 1F), -146.57 (td, *J* = 17.3, 4.1 Hz, 0.5F), -146.73 (td, *J* = 17.3, 4.1 Hz, 0.5F), -150.23 (m, 1F), -155.11 (t, *J* = 18.8 Hz, 1F), -156.44 (m, 1F); EI-MS: 268.1 (12.45%), 85.4 (34.96%), 83.3 (44.68%), 71.5 (53.44%), 57.5 (100.00%); IR(KBr, cm^{-1}): 3422, 2949, 1653, 1472, 1406, 1262, 1172, 1104, 1056, 1000, 947, 901, 844, 770, 671; Anal. Calcd. for $C_{11}H_3F_7 \cdot 0.5H_2O$: C, 47.67; H, 1.45; Found: C, 47.68; H, 1.68.

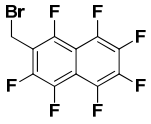

31

2-(Bromomethyl)-1,3,4,5,6,7,8-heptafluoronaphthalene 31. A mixture of compound **30** (1.3 g, 5.0 mmol) and *N*-bromosuccinimide (0.9 g, 5.0 mmol) in CCl_4 (10.0 mL) was refluxing for 6 h. After completion of reaction, the mixture was washed with saturated NaCl aqueous solution (3 × 20 mL) and extracted with ethyl acetate (3 × 15 mL). The organic layers were combined and dried with Na_2SO_4, filtered. The solvent was evaporated and the residue was purified by column chromatography on a silica gel using hexane as eluent to afford the **31** as a white solid (0.677 g, 39%). m.p.: 71.8-73.2 °C; ^{1}H NMR (400 MHz, $CDCl_3$): δ = 4.65 (t, *J* = 1.6 Hz, 2H); ^{19}F NMR (376 MHz, $CDCl_3$): δ = -120.01 (d, *J* = 19.2 Hz, 0.5F), -120.19 (d, *J* = 19.2 Hz, 0.5F), -138.96 (d, *J* = 16.2 Hz, 1F), -143.29 (t, *J* = 16.9 Hz, 0.5F), -143.47 (t, *J* = 16.9 Hz, 0.5F), -145.42 (t, *J* = 16.9 Hz, 0.5F), -145.57 (t, *J* = 16.9 Hz, 0.5F), -147.98 (m, 1F), -151.89 (t, *J* = 16.9 Hz, 1F), -154.75 (m, 1F); EI-MS: 347.6 (2.11%), 346.1 (4.10%), 267.0 (32.92%), 265.5 (100.00%); IR(KBr, cm^{-1}): 3422,

2946, 2655, 2335, 2098, 1742, 1651, 1473, 1396, 1265, 1217, 1177, 1107, 1055, 1014, 948, 869, 778, 715.

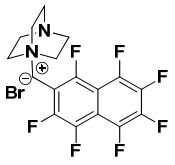

27

1-((Perfluoronaphthalen-2-yl)methyl)-1,4-diazabicyclo-[2.2.2]octan-1-ium bromide 27. Compound **31** (0.5 g, 1.5 mmol) was dissolved in dichloromethane (1.0 mL), then DABCO (0.2 g, 1.5 mmol) was added and stirred at room temperature. After 10 min, white precipitate was generated from the solution. The mixture was continued to stir overnight and the white solid was filtered and dried under vacuum to obtain pure compound **27** (0.668 g, 97%). m.p.: 260 °C decompose; ^{1}H NMR (300 MHz, DMSO-d_6): δ = 3.02 (dt, J = 9.3 Hz, J = 5.1 Hz, 6H), 3.47 (m, 6H), 4.79 (s, 2H); ^{19}F NMR (282 MHz, DMSO-d_6): δ = -112.27 (dd, J = 68.8, 17.5 Hz, 1F), -133.03 (d, J = 17.2 Hz, 1F), -144.04 (dt, J = 68.8, 17.2 Hz, 1F), -147.18 (dt, J = 55.8, 16.9 Hz, 1F), -149.37 (dt, J = 55.8, 18.3 Hz, 1F), -150.92 (t, J = 19.7 Hz, 1F), -154.76 (t, J = 18.3 Hz, 1F); ESI-MS: 379.1 [4-Br^-]$^+$; IR(KBr, cm^{-1}): 2980, 2893, 2594, 2187, 2017, 1976, 1656, 1614, 1533, 1494, 1404, 1327, 1264, 1174, 1113, 1058, 1031, 982, 930, 887, 849, 785, 726, 672; HRMS (ESI) m/z Calcd. for $C_{17}H_{13}N_2BrF_7$ $(M-H)^-$: 457.0145; Found: 457.0153.

The complex **27** was crystallized in the space group *Pbca* with a methanol molecule co-crystallized by slow evaporation as methanol solvate.

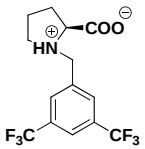

34

(2S)-1-(3,5-Bis(trifluoromethyl)benzyl)pyrrolidin-1-ium-2-carboxylate 34. To a dry 100 mL flask, L-proline **33** (2.3 g, 20.0 mmol) and potassium carbonate (8.3 g, 60.0 mmol) were dissolved in isopropanol (27.0 mL) and heated to 40 ^{o}C. 3,5-Bis(trifluoromethyl)benzyl bromide **19** (2.4 mL, 20.0 mmol) was added dropwise. The reaction mixture was stirred overnight at the same temperature and then was allowed to cool to room temperature. Concentrated HCl was added until the solution became slightly acidic. Chloroform (40 mL) was added and the reaction mixture was allowed to stir at room temperature for 6 h. The reaction mixturewas filtered to remove the white precipitate and the precipitate was washed with chloroform (3 × 15 mL). The organic layers were combined and washed with brine and dryed with anhydrous Na_2SO_4. The solvent was removed under vacuum and the residual liquid was treated with acetone (25 mL). A large amount of white solid appeared. The mixture was further cooled to 0 ^{o}C, and then was filtered and the precipitate was washed with cold acetone (3×10 mL). The solid was dried under vacuum to give the zwitterion **34** (5.456 g, 80%) as a white solid. m.p. : 199.3-200.7℃; ^{1}H NMR (300 MHz, methanol-d_4): δ 2.05-2.23 (m, 4H), 2.58-2.68 (m, 1H), 3.68-3.46 (m, 1H), 3.57-3.61 (m, 1H), 4.33-4.42 (m, 1H), 4.57 (d, J = 13.0 Hz, 1H), 4.73 (d, J = 13.0 Hz, 1H), 8.14 (s, 1H), 8.22 (s, 1H);

^{19}F NMR (282 MHz, methanol-d_4): δ -64.46 (s, 6F); ESI-MS: 342.09 $[M+H]^+$; IR (KBr, cm^{-1}): 2952, 2745, 2407, 2103, 1722, 1458, 1371, 1276, 1129, 979, 896, 681; Anal. Calcd. For $C_{14}H_{13}F_6NO_2 \cdot 2H_2O$: C, 44.57; H, 4.54; N, 3.71; Found: C, 43.63; H, 4.14; N, 3.97.

The chloride salt **35** was crystallized in the space group $P2_12_12_1$ by the acidification of **34** with ethanol solution of HCl and the slow evaporation of solvent at room temperature.

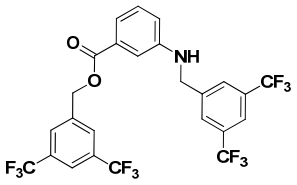

37

3,5-Bis(trifluoromethyl)benzyl 3-((3,5-bis(trifluoromethyl)benzyl)amino)benzoate 37. The mixture of 3-aminobenzoic acid **36** (0.14 g, 1.0 mmol), 1-(bromomethyl)-3,5-bis(trifluoromethyl)benzene **19** (0.36 mL, 2.0 mmol) and potassium carbonate (0.55 g, 4.0 mmol) in THF (7.0 mL) was stirred at r.t. and monitored by TLC. After completion of the reaction, the mixture was washed with saturated NaCl aqueous solution and extracted with ethyl acetate, the organic layer were combined and dried with Na_2SO_4 then filtered. The organic solvent was removed under vacuum and the residue was chromatographed on silica gel (ethyl acetate/hexane = 1:10) affording pure **37** (0.406 g, 69%) as a white solid. m.p.: 97.8-99.6℃; ^{1}H NMR (400 MHz, $CDCl_3$): δ 4.37 (s, 1H), 4.52 (s, 2H), 5.42 (s, 2H), 6.81 (d, J = 8.0 Hz, 1H), 7.23 (s, 1H), 7.30 (s, 1H), 7.32 (t, J = 2.0 Hz, 1H), 7.48 (d, J = 8.0 Hz, 1H), 7.80 (s, 1H), 7.83 (s, 2H), 7.86 (s, 1H), 7.88 (s, 2H); ^{19}F NMR (376 MHz, $CDCl_3$): δ -62.95 (s, 6F), -62.93 (s, 6F); EI-MS: m/z: 589.0 (100%); IR (KBr, cm^{-1}): 3642, 3304, 3097, 3001, 2869, 2664, 2550, 2052, 1684, 1595, 1560, 1448, 1375, 1274, 1136, 908, 846, 758, 679; HRMS (ESI) m/z Calcd. for $C_{25}H_{16}O_2NF_{12}$: 590.09839; Found: 590.09930.

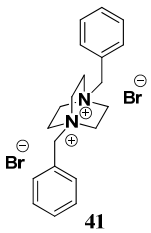

41

1,4-Dibenzyl-1,4-diazabicyclo[2.2.2]octane-1,4-diium bromide 41. (Bromomethyl)benzene **40** (0.342 g, 2.0 mmol) and 1,4- diazabicyclo[2.2.2]octane **39** (0.112 g, 1.0 mmol) were dissolved in DCM (1.5 mL). After the mixture was stirred overnight, the white solid was filtered and dried in vacuum to give the pure product **41** (0.449 g, 99%). m.p. : 264.2-265.1℃; ^{1}H NMR (400 MHz, methanol-d_4): δ 3.19 (t, J = 7.5 Hz, 6H), 3.43 (t, J = 7.5 Hz, 6H), 4.01 (s, 4H), 7.52-7.59 (m, 10H); EI-MS: m/z: 203.0 (2.12%), 169.8 (4.68%), 90.9 (100.00%), 88.8 (18.54%), 80.7 (14.36%), 78.7 (12.28%), 64.9 (29.66%), 62.9 (28.74%); IR (KBr, cm^{-1}): 3852, 3443, 2964, 2650, 2482, 2289, 2177, 2055, 1898, 1741, 1576, 1459, 1375, 1314, 1216, 1065, 1003, 899, 850, 766, 700; Anal. Calcd. For $C_{20}H_{26}Br_2N_2$: C, 52.88; H, 5.77; N, 6.17; Found: C, 51.41; H, 6.44; N, 7.83.

The salt **41** was crystallized in the space group *Pbca* by diffusing Et_2O into the methanol solution of the sample.

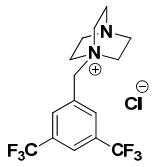

42

1-(3,5-Bis(trifluoromethyl)benzyl)-1,4-diazabicyclo[2.2.2]octan-1-ium chloride 42. 1-(Chloromethyl)-3,5-bis(trifluoromethyl)benzene **20** (0.307 g, 1.0 mmol) and 1,4-diazabicyclo[2.2.2]octane **39** (0.112 g, 1.0 mmol) were dissolved in DCM (1.0 mL). After the mixture was stirred overnight, the white solid was filtered and dried in vacuum to give the pure product **42**. m.p. : > 240℃ decomposed; ^{1}H NMR (300 MHz, DMSO-d_6): δ 3.02 (t, J = 7.5 Hz, 6H), 3.35 (s, 6H), 4.81 (s, 2H), 8.31 (s, 3H); ^{19}F NMR (282 MHz, DMSO-d_6): δ -61.21 (s, 6F); EI-MS: m/z: 374.0 (1.94%), 339.1 (7.41%), 337.9 (30.97%), 324.9 (26.25%), 281.9 (29.22%), 226.9 (100.00%); IR (KBr, cm^{-1}): 3413, 2977, 2805, 2274, 2047, 1993, 1628, 1466, 1372, 1276, 1122, 988, 899, 845, 790, 701; Anal. Calcd. For $C_{15}H_{17}ClF_6N_2 \cdot 2H_2O$: C, 43.86; H, 5.15; N, 6.82; Found: C, 43.73; H, 5.38; N, 6.96.

The salt **42** was crystallized in the space group *pbca* by diffusing Et_2O into the methanol solution of the sample.

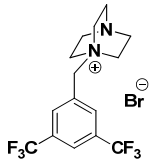

43

1-(3,5-Bis(trifluoromethyl)benzyl)-1,4-diazabicyclo[2.2.2]octan-1-ium bromide 43. The synthesis method was similar with **42.** m.p. : > 300℃ decomposed; ^{1}H NMR (300 MHz, methanol-d_4): δ 3.19 (t, J = 7.5 Hz, 6H), 3.46 (t, J = 7.5 Hz, 6H), 4.73 (s, 2H), 7.90 (s, 1H), 8.22 (s, 3H); ^{19}F NMR (282 MHz, methanol-d_4): δ -64.35 (s, 6F); EI-MS: m/z: 339.1 (62.72%), 338.1 (32.96%), 227.1 (88.80%); IR (KBr, cm^{-1}): 3037, 2975, 2896, 2312, 1894, 1622, 1538, 1466, 1374, 1330, 1280, 1177, 1127, 1058, 992, 928, 888, 844, 796, 711, 680; Anal. Calcd. For $C_{15}H_{17}BrF_6N_2$: C, 42.98; H, 4.09; N, 6.68; Found: C, 42.73; H, 4.46; N, 6.42.

The salt **43** was crystallized in the space group *pbca* by diffusing Et_2O into the acetonitrile solution of the sample.

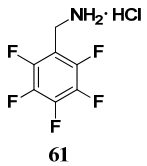

61

This compound **61** was prepared as reported in the literature.[79]

Compounds **46**—**51**, **53**—**56** and **71** were synthesized by the similar methods with 2.2 equivalents (for **46**) or 1.1 equivalents (for **47**-**51**, **71**) of NaH (60% in mineral oil) as base, respectively. The general synthetic methods are described with the preparation of the compound **46** as a representative example.

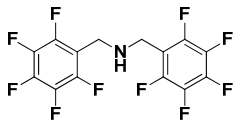

46

Bis((perfluorophenyl)methyl)amine 46. To a suspension of (perfluorophenyl)methanamine hydrochloride **61** (0.23 g, 1.0 mmol), NaH (60% in mineral oil, 1.10 g, 2.2 mmol) in anhydrous THF (5 mL), 1-(bromomethyl)-2,3,4,5,6-pentafluorobenzene **62** (0.26 g, 1.0 mmol) was added dropwise. The reaction mixture was stirred at r.t. and monitored by TLC. After completion of the reaction, the mixture was washed with saturated NaCl aqueous solution and extracted with ethyl acetate, the organic layer were combined and dried with Na_2SO_4 then filtered. The organic solvent was removed under vacuum and the residue was chromatographed on silica gel (ethyl acetate/hexane 1:10) affording pure **46** (0.256 g, 68%) as colourless liquid. ^{1}H NMR (400 MHz, $CDCl_3$): δ 1.73 (s, 1H), 3.93 (s, 4H); ^{19}F NMR (376 MHz, $CDCl_3$): δ -161.70 (td, *J* = 26.3, 11.3 Hz, 4F), -154.73 (t, *J* = 26.3 Hz, 2F), -144.17 (d, *J* = 26.3 Hz, 4F); EI-MS: m/z: 377.0 (68.94%), 376.0 (42.89%), 210.0 (17.19%), 181.0 (100.00%), 163.0 (10.97%); IR (KBr, cm^{-1}): 3360, 2945, 2865, 2649, 2327, 2094, 1739, 1654, 1501, 1361, 1303, 1220, 1115, 944, 778; HRMS (ESI) m/z Calcd. for $C_{14}H_6F_{10}N$: 378.03351; Found: 378.03195.

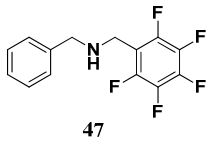

47

***N*-Benzyl-1-(perfluorophenyl)methanamine 47**. Yield: 77% as a pale yellow solid. m.p.: 39.9-40.4℃; ^{1}H NMR (300 MHz, $CDCl_3$): δ 1.91 (s, 1H), 3.79 (s, 2H), 3.94 (s, 2H), 7.22-7.36 (m, 5H); ^{19}F NMR (282 MHz, $CDCl_3$): δ -162.12 (t, *J* = 20.0 Hz, 2F), -155.52 (d, *J* = 20.0 Hz, 1F), -143.90 (s, 2F); EI-MS: m/z: 287.1 (64.87%), 286.0 (100%), 209.9 (12.58%), 195.9 (23.69%), 180.9 (61.15%), 91.0 (10.51%); IR (KBr, cm^{-1}): 3304, 3032, 2924, 2853, 2629, 2416, 2058, 1979, 1738, 1656, 1499, 1360, 1297, 1214, 1113, 949, 818, 739; HRMS (ESI) m/z Calcd. for $C_{14}H_{11}F_5N$: 288.08062; Found: 288.07990.

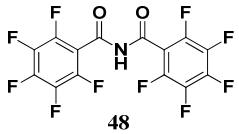

48

2,3,4,5,6-Pentafluoro-*N*-(perfluorobenzoyl)benzamide 48. Yield: 70% as a white solid. m.p.: 157.6-158.1℃; ^{1}H NMR (300 MHz, $CDCl_3$): δ 8.79 (s, 1H); ^{19}F NMR (282 MHz, $CDCl_3$): δ -158.91 (td, *J* = 20.0, 5.0 Hz, 2F), -146.68 (t, *J* = 20.0 Hz, 1F), -139.56 (d, *J* = 20.0 Hz, 2F); EI-MS: m/z: 405.0 (47.91%), 195.0 (100.00%), 167.0 (36.79%), 117.0 (23.78%); IR (KBr, cm^{-1}): 3265, 3181, 1745, 1650, 1496, 1415, 1319, 1263, 1196, 1107, 1071, 994, 927, 811, 761, 728, 689; Anal. Calcd. for $C_{14}HF_{10}NO_2$: C, 41.50; H, 0.25; N, 3.46; Found: C, 41.54; H, 0.026; N, 3.312.

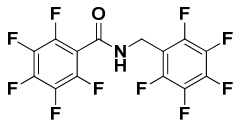

49

2,3,4,5,6-Pentafluoro-*N*-((perfluorophenyl)methyl)benzamide 49. Yield: 22% as a white solid. m.p.: 154.0-154.6℃; ^{1}H NMR (300 MHz, $CDCl_3$): δ 6.42 (s, 1H), 4.75 (d, *J* = 6.0 Hz, 2H); ^{19}F NMR (282 MHz, $CDCl_3$): δ -140.10 (d, *J* = 17.6 Hz, 2F), -142.64 (dd, *J* = 21.8, 7.7 Hz, 2F), -149.35 (t, *J* = 20.7 Hz, 1F), -153.39 (t, *J* = 20.8 Hz, 1F), -159.58 (qd, *J* = 11.5, 5.2 Hz, 2F), -161.14 (td, *J* = 21.3, 7.8 Hz, 2F); EI-MS: m/z: 392.0 (72.07%), 391.0 (100.00%), 371.9 (45.90%), 195.0 (82.00%), 181.0 (22.98%); IR (KBr, cm^{-1}): 3286, 3106, 2924, 1736, 1660, 1565, 1499, 1416, 1365, 1325, 1259, 1117, 1040, 989, 894, 750, 686; Anal. Calcd. for $C_{14}H_3F_{10}NO$: C, 42.99; H, 0.77; N, 3.58; Found: C, 43.16; H, 0.89; N, 3.65.

The compound **49** was crystallized in the space group $P2_1/c$ by diffusing Et_2O into the methanol solution of the sample.

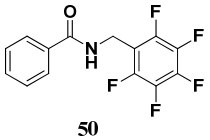

50

***N*-((Perfluorophenyl)methyl)benzamide 50**. Yield: 22% as a white solid. m.p.: 172.7-173.1℃; ^{1}H NMR (300 MHz, $CDCl_3$): δ 7.90 – 7.64 (m, 2H), 7.52 (ddd, *J* = 6.5, 3.7, 1.3 Hz, 1H), 7.47 – 7.38 (m, 2H), 6.58 (s, 1H), 4.75 (d, *J* = 5.9 Hz, 2H); ^{19}F NMR (282 MHz, $CDCl_3$): δ -142.83 (dd, *J* = 21.9, 7.7 Hz, 2F), -154.55 (t, *J* = 20.8 Hz, 1F), -161.65 (td, *J* = 21.6, 8.0 Hz, 2F); EI-MS: m/z: 302.1 (17.05%), 301.1 (100.00%), 105.2 (43.16%), 104.5 (10.68%), 77.2 (24.09%); IR (KBr, cm^{-1}): 3269, 3081, 1741, 1642, 1497, 1365, 1299, 1123, 1063, 1014, 933, 805, 749, 689; HRMS (ESI) m/z Calcd. for $C_{14}H_9ONF_5$: 302.05988; Found: 302.05969.

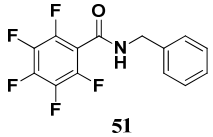

51

***N*-Benzyl-2,3,4,5,6-pentafluorobenzamide 51**. Yield: 19% as a white solid. m.p.: 144.6-145.3℃; ^{1}H NMR (300 MHz, $CDCl_3$): δ 7.52 – 7.26 (m, 5H), 6.24 (s, 1H), 4.65 (d, *J* = 5.7 Hz, 2H); ^{19}F NMR (282 MHz, $CDCl_3$): δ -140.27 (d, *J* = 15.8 Hz, 2F), -150.45 (t, *J* = 20.7 Hz, 1F), -159.90 (qd, *J* = 11.3, 4.7 Hz, 2F); EI-MS: m/z: 302.0 (36.82%), 301.0 (100.00%), 282.0 (30.77%), 194.9 (40.84%), 166.9 (10.03%); IR (KBr, cm^{-1}): 3848, 3232, 3068, 2918, 2698, 2501, 2315, 2184, 2086, 2010, 1977, 1901, 1741, 1651, 1570, 1498, 1451, 1329, 1246, 1118, 1061, 988, 928, 894, 815, 735, 695; HRMS (ESI) m/z Calcd. for $C_{14}H_8ONF_5Na$: 324.04183; Found: 324.04144.

The compound **51** was crystallized in the space group $P2_1/c$ by diffusing Et_2O into the methanol solution of the sample.

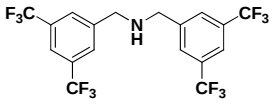

52

This compound **52** was prepared as reported in the literature.[61]

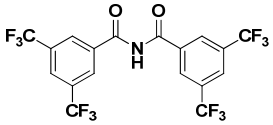

53

***N*-(3,5-Bis(trifluoromethyl)benzoyl)-3,5-bis(trifluoromethyl)benzamide 53**. Yield: 74% as a white solid. m.p.: 132.1-133.3℃; ^{1}H NMR (400 MHz, acetone-d_6): δ 11.26 (s, 1H), 8.58 (s, 4H), 8.34 (s, 2H); ^{19}F NMR (376 MHz, acetone-d_6): δ -63.43 (s, 12F); EI-MS: m/z: 498.0 (9.89%), 496.9 (56.35%), 477.9 (28.44%), 241.0 (100.00%), 213.0 (29.40%); IR (KBr, cm^{-1}): 3846, 3270, 3180, 3099, 2923, 2693, 2507, 2282, 2099, 1981, 1728, 1623, 1509, 1460, 1372, 1275, 1211, 1128, 912, 846, 774, 683; HRMS (ESI) m/z Calcd. for $C_{18}H_7O_2NF_{12}Na$: 520.01774; Found: 520.01740.

The compound **53** was crystallized in the space group *P*-1 by diffusing Et_2O into the DMSO solution of the sample.

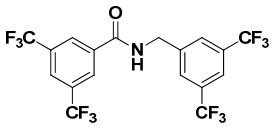

54

***N*-(3,5-Bis(trifluoromethyl)benzyl)-3,5-bis(trifluoromethyl)benzamide 54**. Yield: 76% as a white solid. m.p.: 132.1-133.3℃; ^{1}H NMR (400 MHz, $CDCl_3$): δ 8.25 (s, 2H), 8.04 (s, 1H), 7.83 (s, 3H), 6.80 (s, 1H), 4.80 (d, J = 6.0 Hz, 2H); ^{19}F NMR (376 MHz, $CDCl_3$): δ -62.95 (s, 6F), -63.01 (s, 6F); EI-MS: m/z: 484.1 (36.64%), 483.1 (79.21%), 482.1 (31.59%), 464.1 (26.06%), 241.0 (100.00%), 213.0 (35.22%); IR (KBr, cm^{-1}): 3848, 3639, 3280, 3087, 2923, 2704, 2466, 2269, 2023, 1981, 1894, 1738, 1649, 1545, 1455, 1370, 1274, 1117, 900, 847, 763, 681; Anal. Calcd. for $C_{18}H_9F_{12}NO$: C, 44.74; H, 1.88; N, 2.90; Found: C, 44.80; H, 2.03; N, 2.72.

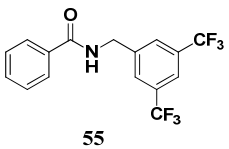

55

***N*-(3,5-Bis(trifluoromethyl)benzyl)benzamide 55**. Yield: 36% as a white solid. m.p.: 87.5-88.3℃; ^{1}H NMR (300 MHz, Acetone-d_6): δ 8.53 (s, 1H), 8.06 (s, 2H), 7.96 (s, 1H), 7.94 (d, J = 1.5 Hz, 2H), 7.61 – 7.52 (m, 1H), 7.52 – 7.42 (m, 2H), 4.82 (d, J = 6.1 Hz, 2H); ^{19}F NMR (282 MHz, Acetone-d_6): δ -63.37 (s, 6F); EI-MS: m/z: 348.1 (89.05%), 347.1 (75.90%), 346.1 (22.67%), 328.1 (12.42%), 105.1 (100.00%), 77.2 (29.30%); IR (KBr, cm^{-1}): 3302, 3074, 2922, 2856, 2240, 1739, 1643, 1528, 1461, 1377, 1278, 1163, 1117, 999, 890, 846, 683;

Anal. Calcd. for $C_{16}H_{11}F_6NO$: C, 55.34; H, 3.19; N, 4.03; Found: C, 55.51; H, 3.24; N, 3.96.

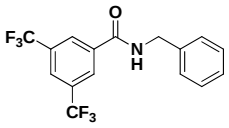

56

***N*-Benzyl-3,5-bis(trifluoromethyl)benzamide 56**. Yield: 48% as a white solid. m.p.: 109.3-109.6℃; ^{1}H NMR (400 MHz, acetone-d_6): δ 8.71 (s, 1H), 8.56 (s, 2H), 8.23 (s, 1H), 7.41 (d, J = 7.5 Hz, 2H), 7.37 – 7.30 (m, 2H), 7.29 – 7.23 (m, 1H), 4.66 (d, J = 5.9 Hz, 2H); ^{19}F NMR (376 MHz, acetone-d_6): δ -63.44 (s, 6F); EI-MS: m/z: 348.1 (35.75%), 347.1 (100.00%), 346.1 (20.77%), 241.0 (47.18%), 213.1 (22.23%), 106.1 (24.38%), 91.1 (13.43%); IR (KBr, cm^{-1}): 3843, 3625, 3289, 3087, 2931, 2706, 2473, 2288, 2051, 1983, 1740, 1648, 1551, 1456, 1379, 1275, 1124, 1035, 907, 845, 810, 738, 681; HRMS (ESI) m/z Calcd. for $C_{16}H_{12}ONF_6$: 348.08176; Found: 348.08176.

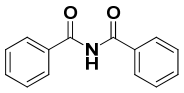

71

***N*-Benzoylbenzamide 71.** Yield: 55% as a white solid. m.p.: 131.4-131.8℃; ^{1}H NMR (400 MHz, $CDCl_3$): δ, 8.97 (s, 1H), 7.86-7.89 (m, 4H), 7.60-7.64 (m, 2H), 7.49-7.54 (m, 4H); EI-MS: m/z: 225.0 (6.38%), 105.0 (66.28%), 77.1 (100.00%), 51.1 (68.98%); IR (KBr, cm^{-1}): 3241, 3063, 2931, 2719, 2322, 2061, 1912, 1693, 1599, 1468, 1304, 1219, 1109, 1022, 956, 793, 698; Elemental analysis calcd. for $C_{14}H_{11}NO_2$: C, 74.65; H, 4.92; N, 6.22; found: C, 74.77; H, 4.57; N, 5.88.

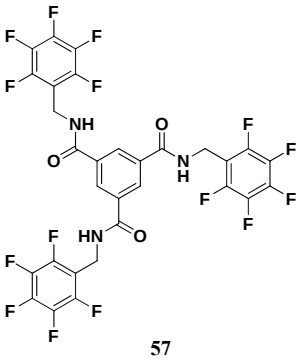

57

***N*^{1},*N*^{3},*N*^{5}-Tris((perfluorophenyl)methyl)benzene-1,3,5-tricarboxamide 57**. Benzene-1,3,5-tricarbonyl trichloride **68** (0.133 g, 0.5 mmol) and 2,3,4,5,6 -pentafluorobenzylamine hydrochloride **61** (0.350 g, 1.5 mmol) were dissolved in 15.0 mL DCM and DIPEA (3.0 mmol, 0.52 mL) was used as a base. The reaction was stirred on refluxing for 8 h and monitored by TLC. After the end of the reaction, the mixture was washed with saturated NaCl aqueous solution and extracted with ethyl acetate, the organic layers were combined and dried with Na_2SO_4, filtered. Then the organic solution was removed under vacuum, finally the residue was obtained and re-crystallized in acetone. The target product **57** was obtained with yield of 94%

as a white solid. m.p.: > 310℃ decomposed; ^{1}H NMR (300 MHz, acetone-d_6): δ 8.66 (s, 3H), 8.42 (s, 3H), 4.76 (d, J = 5.4 Hz, 6H); ^{19}F NMR (282 MHz, acetone-d_6): δ -144.00 (dd, J = 21.05, 7.61 Hz, 6H), -158.41 (t, J = 21.05 Hz, 3H), -165.41 (td, J = 21.05, 7.61 Hz, 6H); ESI-MS: 782.03 $[M+Cl]^-$; IR (KBr, cm^{-1}): 3240, 3070, 2966, 1738, 1644, 1554, 1504, 1365, 1294, 1123, 1053, 950, 801, 679; Elemental analysis calcd. for $C_{30}H_{12}F_{15}N_3O_3$: C, 48.21; H, 1.62; N, 5.62; found: C, 48.00; H, 2.26; N, 5.32.

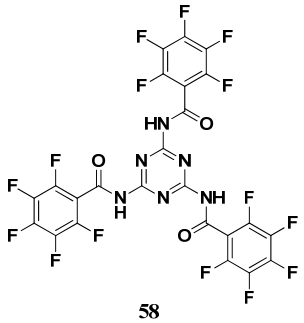

58

***N*,*N*',*N*''-(1,3,5-Triazine-2,4,6-triyl)tris(2,3,4,5,6-pentafluorobenzamide) 58**. 2,4,6-Trichloro-1,3,5-triazine **67** (0.184 g, 1.0 mmol) and 2,3,4,5,6-pentafluorobenzamide **45** (0.633 g, 3.0 mmol) were dissolved in anhydrous THF (10.0 mL), NaH (60% in mineral oil, 0.144 g, 3.6 mmol)was used as a base. The reaction was stirred on refluxing and monitored by TLC. After completion of the reaction, the mixture was washed with saturated NaCl aqueous solution and extracted with ethyl acetate, the organic layer were combined and dried with Na_2SO_4 then filtered. The organic solvent was removed under vacuum and the residue was chromatographed on silica gel (ethyl acetate/hexane 1:3) affording pure **58** (0.463 g, 65%) as a white solid. m.p.: 262.9-263.6℃; ^{1}H NMR (400 MHz, acetone-d_6): δ 10.52 (s, 1H); ^{19}F NMR (376 MHz, acetone-d_6): δ -144.12 (d, J = 17.7 Hz, 6F), -154.27 (s, 3F), -163.49 (dd, J = 19.9, 15.1 Hz, 6F); ESI-MS: 730.99 $[M+Na]^+$; IR (KBr, cm^{-1}): 3747, 3264, 3073, 2963, 2925, 2855, 2663, 2192, 2088, 2022, 1994, 1963, 1740, 1691, 1659, 1616, 1579, 1499, 1414, 1319, 1255, 1189, 1108, 1053, 992, 889, 816, 716, 686; Elemental analysis calcd. for $C_{24}H_3F_{15}N_6O_3$: C, 40.70; H, 0.43; N, 11.87; found: C, 40.71; H, 0.44; N, 11.98.

The compound **58** was crystallized in the space group *P*-1 by diffusing Et_2O into the methanol solution of the sample.

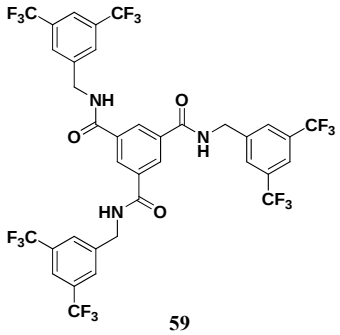

59

***N*^{1},*N*^{3},*N*^{5}-Tris(3,5-Bis(trifluoromethyl)benzyl)benzene-1,3,5-tricarboxamide 59**. Benzene-1,3,5-tricarbonyl trichloride **68** (0.265 g, 1.0 mmol) and (3,5-Bis(trifluoromethyl)phenyl)methanamine **21** (0.729 g, 3.0 mmol) were refluxed in present of

Et_3N (0.42 ml, 3.0 mmol) in 15 mL DCM. After completion of the reaction, the mixture was washed with saturated NaCl aqueous solution and extracted with ethyl acetate, the organic layer were combined and dried with Na_2SO_4 then filtered. The organic solvent was removed under vacuum and the residue was chromatographed on silica gel (ethyl acetate/hexane 1:2) affording pure **59** (0.700 g, 79%) as a white solid. m.p.: 241.6-242.3℃; ^{1}H NMR (400 MHz, acetone-d_6): δ 8.86 (t, J = 6.0 Hz, 3H), 8.57 (s, 3H), 8.09 (s, 6H), 7.95 (s, 3H), 4.86 (d, J = 6.0 Hz, 6H); ^{19}F NMR (376 MHz, acetone-d_6): δ -63.35 (s, 18F); ESI-MS: 886.14 $[M+H]^+$; IR (KBr, cm^{-1}): 3298, 1646, 1535, 1429, 1378, 1275, 1123, 1016, 896, 846, 790, 684; Elemental analysis calcd. for $C_{36}H_{21}F_{18}N_3O_3$: C, 48.83; H, 2.39; N, 4.75; found: C, 48.79; H, 2.03; N, 4.69.

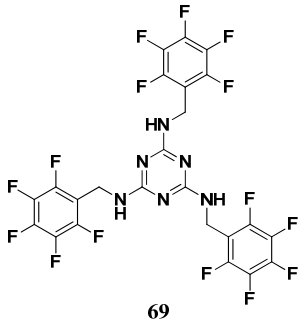

69

***N*^{2},*N*^{4},*N*^{6}-Tris((perfluorophenyl)methyl)-1,3,5-triazine-2,4,6-triamine 69**. The reaction of 2,4,6-trichloro-1,3,5-triazine **67** (0.092 g, 0.5 mmol) and 2,3,4,5,6–pentafluorobenzylamine hydrochloride **61** (0.350 g, 1.5 mmol) in present of K_2CO_3 (0.021 g, 1.5 mmol), 18-crown-6 (0.004 g, 0.015 mmol) and DIPEA (0.26 ml, 1.5 mmol) in 5.0 mL toluene was refluxed under the N_2 atmosphere. After completion of the reaction, the mixture was washed with saturated NaCl aqueous solution and extracted with ethyl acetate, the organic layer were combined and dried with Na_2SO_4 then filtered. The organic solvent was removed under vacuum and the residue was chromatographed on silica gel (ethyl acetate/hexane 1:8) affording pure **69** (0.227 g, 68%) as a white solid. m.p.: 170.7-171.5℃; ^{1}H NMR (300 MHz, acetone-d_6): δ 6.51 (s, 2H), 6.40 (s, 1H), 4.77 (s, 4H), 4.60 (s, 2H); ^{19}F NMR (376 MHz, acetone-d_6) δ -144.28 (d, J = 16.0 Hz, 3F), -144.64 (d, J = 14.9 Hz, 3F), -158.75 – -159.37 (m, 3F), -165.54 (dd, J = 19.6, 12.3 Hz, 6F); ESI-MS: 667.07 $[M+H]^+$; IR (KBr, cm^{-1}): 3469, 3274, 2954, 1739, 1573, 1495, 1345, 1229, 1163, 1120, 994, 919, 807, 662; Elemental analysis calcd. for $C_{24}H_9F_{15}N_6$: C, 43.26; H, 1.36; N, 12.61; found: C, 43.28; H, 1.87; N, 11.89.

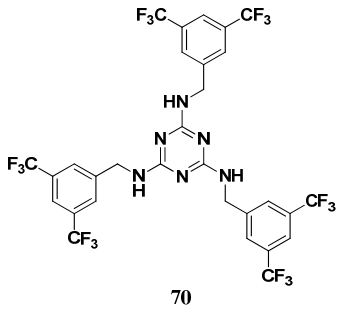

70

***N*^{2},*N*^{4},*N*^{6}-Tris(3,5-Bis(trifluoromethyl)benzyl)-1,3,5-triazine-2,4,6-triamine 70**. The synthesis method of **70** is similar with that of compound **69**. Yield: 58% as a white solid.

m.p.: 146.3-147.1℃; ^{1}H NMR (400 MHz, $CDCl_3$): δ 7.76 (s, 6H), 7.70 (s, 3H), 5.58 (s, 3H), 4.61 (s, 6H); ^{19}F NMR (376 MHz, $CDCl_3$): δ -62.99 (s, 18F); ESI-MS: 805.14 $[M+H]^+$; IR (KBr, cm^{-1}): 3446, 3264, 3110, 2952, 2180, 1738, 1623, 1536, 1415, 1341, 1274, 1113, 960, 897, 814, 683; Elemental analysis calcd. for $C_{30}H_{18}F_{18}N_6$: C, 44.79; H, 2.26; N, 10.45; found: C, 44.90; H, 2.56; N, 10.23.

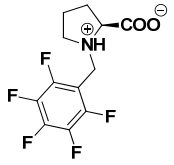

72

(2S)-1-((Perfluorophenyl)methyl)pyrrolidin-1-ium-2-carboxylate 72. To a dry 100 mL flask, L-proline **33** (2.3 g, 20.0 mmol) and potassium carbonate (8.3 g, 60.0 mmol) were dissolved in isopropanol (27.0 mL) and heated to 40 ^{o}C. pentafluorobenzyl bromide **62** (2.2 mL, 20.0 mmol) was added dropwise. The reaction mixture was stirred overnight at the same temperature and then was allowed to cool to room temperature. Concentrated HCl was added until the solution became slightly acidic. Chloroform (40 mL) was added and the reaction mixture was allowed to stir at room temperature for 6 h. The reaction mixturewas filtered to remove the white precipitate and the precipitate was washed with chloroform (3×15 mL). The organic layers were combined and washed with brine and dryed with anhydrous Na_2SO_4. The solvent was removed under vacuum and the residual liquid was treated with acetone (25 mL). A large amount of white solid appeared. The mixture was further cooled to 0 ^{o}C, and then was filtered and the precipitate was washed with cold acetone (3×10 mL). The solid was dried under vacuum to give the zwitterion **72** (5.13 g, 87%) as a white solid. m.p.: > 135℃ decomposed; ^{1}H NMR (300 MHz, methanol-d_4): δ 4.44 (m, 2H), 3.76 (dd, J = 9.6, 6.3 Hz, 1H), 3.50 (m, 1H), 3.06 (dd, J = 17.4, 6.3 Hz, 1H), 2.43 (m, 1H), 1.99 (m, 3H); ^{19}F NMR (282 MHz, methanol-d_4): δ -141.41 (d, J = 16.1 Hz, 2F), -154.79 (t, J = 19.5 Hz, 1F), -164.29 (td, J = 20.0 Hz, J = 6.2 Hz, 2F); EI-MS: m/z: 296.1 (3.39%), 295.0 (1.79%), 251.1 (12.61%), 250.1 (100.00%), 181.0 (52.47%); IR (KBr, cm^{-1}): 3035, 3000, 2331, 1612, 1504, 1447, 1372, 1345, 1296, 1240; Anal. Calcd. for $C_{12}H_{10}F_5NO_2$: C, 48.82; H, 3.41; N, 4.74; Found: C, 48.60; H: 3.30; N, 4.65.

The zwitterion **72** was crystallized in the space group $P2_12_12_1$ by diffusing Et_2O into the methanol solution of the sample.

Compounds **74-79** were synthesized with the similar methods. The general synthetic methods are described with the preparation of the compound **74** as a representative example.

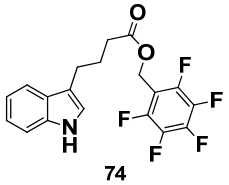

74

(Perfluorophenyl)methyl 4-(1*H*-indol-3-yl)butanoate 74. 1-(Bromomethyl)-2,3,4,5,6-penta-fluorobenzene **62** (0.14 mL, 1.0 mmol) and indole-3-butyric acid **73a** (0.20 g, 1.0 mmol) were dissolved in 15.0 mL THF and KOH (0.130 g, 2.4 mmol) was used as base. The reaction was

stirred on refluxing and monitored by TLC. After completion of the reaction, the mixture was washed with saturated NaCl aqueous solution and extracted with ethyl acetate, the organic layer were combined and dried with Na_2SO_4 then filtered. The organic solvent was removed under vacuum and the residue was separated by column chromatography. The target product **74** was obtained with yield of 91% (0.349 g). m.p.: 129.6-130.6℃; ^{1}H NMR (400 MHz, $CDCl_3$): δ 7.93 (s, 1H), 7.57 (d, *J* = 8.0 Hz, 1H), 7.35 (d, *J* = 8.1 Hz, 1H), 7.21 – 7.15 (m, 1H), 7.13 – 7.07 (m, 1H), 7.00 – 6.94 (m, 1H), 5.18 (d, *J* = 1.4 Hz, 2H), 2.85 – 2.74 (m, 2H), 2.40 (t, *J* = 7.5 Hz, 2H), 2.04 (p, *J* = 7.5 Hz, 2H); ^{19}F NMR (376 MHz, $CDCl_3$): δ -141.84 – -142.09 (m, 2F), -152.69 (t, *J* = 20.8 Hz, 1F), -161.63 (td, *J* = 21.3, 7.9 Hz, 2F); EI-MS: m/z: 384.2 (18.19%), 383.1 (95.66%), 186.1 (19.35%), 180.9 (22.62%), 130.1 (100.00%); IR (KBr, cm^{-1}): 3899, 3454, 3336, 2967, 2664, 2324, 2097, 1736, 1507, 1439, 1366, 1218, 1098, 927, 797, 741; Anal. Calcd. for $C_{19}H_{14}F_5NO_2$: C, 59.53; H, 3.68; N, 3.65; Found: C, 59.53; H: 3.68; N, 3.64.

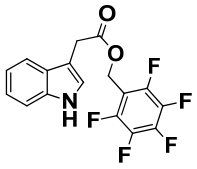

75

(Perfluorophenyl)methyl 2-(1*H*-indol-3-yl)acetate 75. Yield: 91% as a white solid. m.p.: 130.8-131.5℃; ^{1}H NMR (300 MHz, $CDCl_3$): δ 8.07 (s, 1H), 7.54 (dd, *J* = 7.9, 0.6 Hz, 1H), 7.35 (d, *J* = 8.1 Hz,1H), 7.20 (d, *J* = 1.2 Hz, 1H), 7.16 (d, *J* = 2.4 Hz, 1H), 7.11 (d, *J* = 0.8 Hz, 1H), 5.22 (t, *J* = 1.5 Hz, 2H), 3.80 (d, *J* = 0.7 Hz, 2H); ^{19}F NMR (282 MHz, $CDCl_3$): δ -141.75 (dd, *J* = 21.8, 7.8 Hz, 2F), -152.64 (t, *J* = 20.8 Hz, 1F), -161.67 (dt, *J* = 21.3, 7.8 Hz, 2F); EI-MS: m/z: 356.1 (11.76%), 355.1 (66.43%), 181.0 (11.41%), 130.1 (100.00%); IR (KBr, cm^{-1}): 3866, 3412, 3146, 2975, 2928, 2648, 2397, 2293, 2106, 2050, 1930, 1730, 1658, 1503, 1429, 1374, 1304, 1245, 1126, 1058, 992, 944, 812, 743, 667; Anal. Calcd. for $C_{17}H_{10}F_5NO_2$: C, 57.47; H, 2.84; N, 3.94; Found: C, 57.16; H: 2.86; N, 3.87.

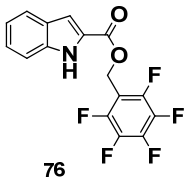

76

(Perfluorophenyl)methyl 1*H*-indole-2-carboxylate 76. Yield: 86% as a white solid. m.p.: 199.4-200.6℃; ^{1}H NMR (300 MHz, acetone-d_6): δ 10.99 (s, 1H), 7.69 (d, *J* = 8.1 Hz, 1H), 7.53 (ddd, *J* = 8.4, 2.6, 1.7 Hz, 1H), 7.30 (ddd, *J* = 8.2, 7.1, 1.2 Hz, 1H), 7.23 (dd, *J* = 2.9, 1.6 Hz, 1H), 7.16 – 7.07 (m, 1H), 5.55 (t, *J* = 1.5 Hz, 2H); ^{19}F NMR (282 MHz, acetone-d_6): δ -143.51 (dd, *J* = 21.4, 7.4 Hz, 2F), -155.69 (t, *J* = 20.3 Hz, 1F), -164.52 (td, *J* = 20.9, 7.5 Hz, 2F); EI-MS: m/z: 342.1 (17.13%), 341.1 (100.00%), 181.0 (58.90%), 143.1 (68.35%); IR (KBr, cm^{-1}): 3340, 2961, 2304, 2107, 1907, 1690, 1506, 1438, 1392, 1358, 1308, 1241, 1189, 1129, 1053, 968, 931, 819, 748, 663; Anal. Calcd. for $C_{16}H_8F_5NO_2 \cdot 0.5H_2O$: C, 54.87; H, 2.59; N, 4.00; Found: C, 54.55; H: 2.57; N, 3.99.

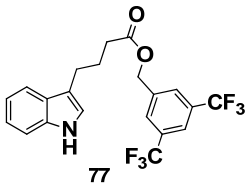

77

3,5-Bis(trifluoromethyl)benzyl 4-(1*H*-indol-3-yl)butanoate 77. Yield: 73% as a yellow solid. m.p.: 62.5-63.1℃; ^{1}H NMR (400 MHz, $CDCl_3$): δ 7.96 (s, 1H), 7.83 (s, 1H), 7.78 (s, 2H), 7.58 (d, *J* = 7.9 Hz, 1H), 7.35 (d, *J* = 8.1 Hz, 1H), 7.18 (t, *J* = 7.6 Hz, 1H), 7.12 – 7.07 (m, 1H), 6.98 (d, *J* = 1.3 Hz, 1H), 5.15 (s, 2H), 2.90 – 2.77 (m, 2H), 2.47 (t, *J* = 7.4 Hz, 2H), 2.14 – 2.01 (m, 2H); ^{19}F NMR (376 MHz, $CDCl_3$): δ -62.92 (s, 6F); EI-MS: m/z: 430.3 (16.14%), 429.3 (66.19%), 131.2 (12.05%), 130.2 (100.00%); IR (KBr, cm^{-1}): 3356, 3068, 2930, 2875, 2842, 2329, 2087, 2002, 1816, 1722, 1623, 1460, 1395, 1352, 1321, 1278, 1169, 1122, 1000, 910, 887, 843, 786, 736, 704, 682; Anal. Calcd. for $C_{21}H_{17}F_6NO_2$: C, 58.74; H, 3.99; N, 3.26; Found: C, 58.35; H: 4.06; N, 2.92.

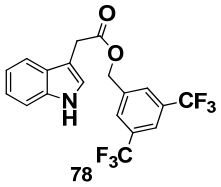

78

3,5-Bis(trifluoromethyl)benzyl 2-(1*H*-indol-3-yl)acetate 78. Yield: 67% as a white solid. m.p.: 114.6-115.6℃; ^{1}H NMR (400 MHz, $CDCl_3$): δ 8.14 (s, 1H), 7.80 (s, 1H), 7.71 (s, 2H), 7.61 – 7.57 (m, 1H), 7.37 (d, *J* = 8.1 Hz, 1H), 7.24 – 7.19 (m, 1H), 7.18 (d, *J* = 2.4 Hz, 1H), 7.15 – 7.10 (m, 1H), 5.23 (s, 2H), 3.88 (d, *J* = 0.7 Hz, 2H); ^{19}F NMR (376 MHz, $CDCl_3$): δ -62.96 (s, 6F); EI-MS: m/z: 402.1 (12.34%), 401.1 (60.99%), 130.1 (100.00%); IR (KBr, cm^{-1}): 3378, 3065, 2916, 2284, 2039, 1717, 1626, 1460, 1330, 1279, 1121, 982, 892, 840, 803, 748, 682; Anal. Calcd. for $C_{19}H_{13}F_6NO_2$: C, 56.87; H, 3.27; N, 3.49; Found: C, 56.50; H: 3.18; N, 3.37.

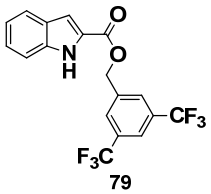

79

3,5-Bis(trifluoromethyl)benzyl 1*H*-indole-2-carboxylate 79. Yield: 94% as a white solid. m.p.: 123.9-125.1℃; ^{1}H NMR (400 MHz, $CDCl_3$): δ 8.93 (s, 1H), 7.92 (s, 2H), 7.88 (s, 1H), 7.71 (d, *J* = 8.1 Hz, 1H), 7.43 (dd, *J* = 8.4, 0.8 Hz, 1H), 7.38 – 7.32 (m, 1H), 7.31 (d, *J* = 1.3 Hz, 1H), 7.17 (t, *J* = 7.5 Hz, 1H), 5.48 (s, 2H); ^{19}F NMR (376 MHz, $CDCl_3$): δ -62.92 (s, 6F); EI-MS: m/z: 388.2 (19.14%), 387.1 (100.00%), 227.0 (32.99%), 143.0 (94.38%); IR (KBr, cm^{-1}): 3328, 3068, 2962, 2290, 2042, 1695, 1624, 1525, 1446, 1393, 1350, 1259, 1114, 1018, 883, 807, 747, 679; Anal. Calcd. for $C_{18}H_{11}F_6NO_2$: C, 55.82; H, 2.86; N, 3.62; Found: C, 54.17; H: 3.12; N, 3.24.

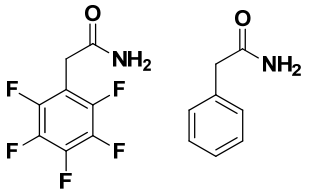

83 **84**

Compound **83** and **84** were prepared as reported in the literature.[80]

Compounds **80**-**82** and **85**-**94** were synthesized with the similar methods as compound **46**.

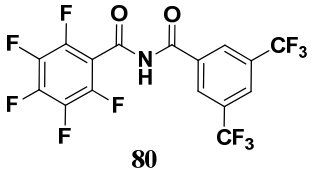

80

***N*-(3,5-Bis(trifluoromethyl)benzoyl)-2,3,4,5,6-pentafluorobenzamide 80**. Yield: 35% as a white solid. m.p.: 180.6-181.5℃; ^{1}H NMR (400 MHz, acetone-d_6): δ 11.53 (s, 1H), 8.63 (s, 2H), 8.39 (s, 1H); ^{19}F NMR (376 MHz, acetone-d_6): δ -63.53 (s, 6F), -143.67 (ddd, J = 8.6, 6.1, 2.9 Hz, 2F), -153.34 (t, J = 20.2 Hz, 1F), -162.88 – -163.63 (m, 2F); EI-MS: m/z: 452.1 (16.37%), 451.1 (92.96%), 241.0 (100.00%), 213.0 (30.39%), 195.0 (34.01%); IR (KBr, cm^{-1}): 3846, 3262, 3177, 2942, 2704, 2486, 2278, 2085, 1736, 1653, 1509, 1380, 1329, 1277, 1244, 1145, 998, 910, 847, 812, 761, 685; HRMS (ESI) m/z Calcd. for $C_{16}H_4O_2NF_{11}Na$: 473.99586; Found: 473.99585.

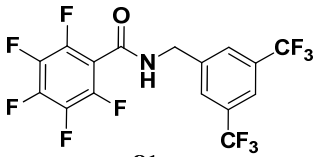

81

***N*-(3,5-Bis(trifluoromethyl)benzyl)-2,3,4,5,6-pentafluorobenzamide 81**. Yield: 24% as a white solid. m.p.: 82.7-83.0℃; ^{1}H NMR (300 MHz, $CDCl_3$): δ 7.82 (s, 2H), 7.59 (s, 1H), 6.47 (s, 1H), 4.79 (s, 2H); ^{19}F NMR (282 MHz, $CDCl_3$): δ -62.82 (s, 6F), -140.45 (t, J = 40.8 Hz, 2F), -153.18 (t, J = 20.5 Hz, 1F), -161.08 – -161.93 (m, 2F); EI-MS: m/z: 438.0 (41.79%), 437.0 (100.00%), 419.0 (17.03%), 417.9 (95.15%), 227.0 (33.18%), 195.0 (88.78%); IR (KBr, cm^{-1}): 3308, 3089, 2931, 2652, 2308, 2078, 1896, 1664, 1501, 1360, 1274, 1119, 988, 900, 682; HRMS (ESI) m/z Calcd. for $C_{16}H_6ONF_{11}Na$: 460.01660; Found: 460.01666.

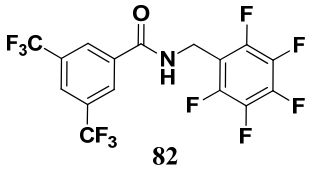

82

***N*-((Perfluorophenyl)methyl)-3,5-bis(trifluoromethyl)benzamide 82**. Yield: 53% as a white solid. m.p.: 145.2-146.4℃; ^{1}H NMR (300 MHz, $CDCl_3$): δ 8.20 (dd, J = 1.1, 0.5 Hz, 2H), 8.06 –

7.97 (m, 1H), 6.75 (s, 1H), 4.78 (d, J = 5.9 Hz, 2H); ^{19}F NMR (282 MHz, $CDCl_3$): δ -63.04 (s, 6F), -142.60 (dd, J = 22.0, 7.9 Hz, 2F), -153.61 (t, J = 20.7 Hz, 1F), -161.17 (td, J = 21.5, 7.9 Hz, 2F); EI-MS: m/z: 438.1 (25.24%), 437.1 (100.00%), 418.1 (15.48%), 241.0 (96.43%), 213.0 (31.42%), 177.0 (12.44%); IR (KBr, cm^{-1}): 3848, 3624, 3292, 3093, 2933, 2703, 2482, 2283, 2042, 1980, 1893, 1740, 1651, 1556, 1509, 1456, 1369, 1275, 1132, 1060, 1020, 951, 912, 847, 792, 696; HRMS (ESI) m/z Calcd. for $C_{16}H_6ONF_{11}Na$: 460.01660; Found: 460.01633.

Compound **82** was crystallized in the space group *C*c by diffusing Et_2O into the methanol solution of the sample.

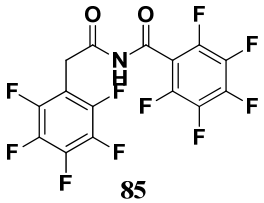

85

2,3,4,5,6-Pentafluoro-*N*-(2-(perfluorophenyl)acetyl)benzamide 85. Yield: 23% as a white solid. m.p.: 172.9-173.7℃; ^{1}H NMR (300 MHz, $CDCl_3$): δ 8.89 (s, 1H), 4.27 (s, 2H); ^{19}F NMR (282 MHz, $CDCl_3$): δ -139.17 (d, J = 17.3 Hz, 2F), -141.98 (dd, J = 21.7, 7.5 Hz, 2F), -146.78 (s, 1F), -154.14 (t, J = 20.7 Hz, 1F), -158.77 (t, J = 17.6 Hz, 2F), -161.89 (td, J = 21.2, 7.3 Hz, 2F); EI-MS: m/z: 420.1 (4.68%), 419.1 (25.60%), 212.1 (10.68%), 208.1 (72.16%), 195.0 (100.00%), 181.0 (35.73%), 167.0 (30.55%), 117.1 (19.88%); IR (KBr, cm^{-1}): 3841, 3258, 3179, 2989, 2661, 2433, 2284, 2040, 1895, 1738, 1654, 1497, 1416, 1321, 1215, 1148, 1091, 987, 909, 804, 763, 713; HRMS (ESI) m/z Calcd. for $C_{15}H_3O_2NF_{10}Na$: 441.98963; Found: 441.98981.

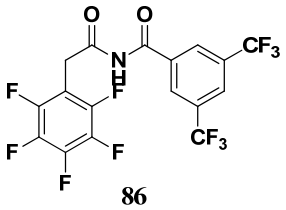

86

***N*-(2-(Perfluorophenyl)acetyl)-3,5-bis(trifluoromethyl)benzamide 86**. Yield: 29% as a white solid. m.p.: 177.7-178.7℃; ^{1}H NMR (400 MHz, $CDCl_3$): δ 9.41 (s, 1H), 8.35 (d, J = 0.5 Hz, 2H), 8.13 (d, J = 0.7 Hz, 1H), 4.45 (s, 2H); ^{19}F NMR (376 MHz, $CDCl_3$): δ -63.20 (s, 6F), -142.25 (dd, J = 21.9, 7.9 Hz, 2F), -154.75 (t, J = 20.7 Hz, 1F), -162.22 (td, J = 21.5, 7.8 Hz, 2F); EI-MS: m/z: 465.1 (23.37%), 446.1 (12.41%), 241.1 (52.42%), 213.1 (37.23%), 208.0 (100.00%), 181.0 (31.14%), 180.0 (17.18%); IR (KBr, cm^{-1}): 3842, 3270, 3187, 3017, 2656, 2490, 2184, 2082, 1739, 1622, 1513, 1379, 1279, 1247, 1134, 1012, 976, 910, 847, 802, 765, 683; Anal. Calcd. for $C_{17}H_6F_{11}NO_2$: C, 43.89; H, 1.30; N, 3.01; Found: C, 43.65; H: 1.92; N, 2.98.

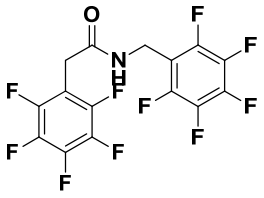

87

2-(Perfluorophenyl)-*N*-((perfluorophenyl)methyl)acetamide 87. Yield: 32% as a white solid. m.p.: 197.3-197.8℃; ^{1}H NMR (300 MHz, DMSO-d_6): δ 8.88 (d, J = 5.1 Hz, 1H), 4.38 (d, J = 5.1 Hz, 2H), 3.63 (s, 2H); ^{19}F NMR (282 MHz, DMSO-d_6): δ -142.66 (dd, J = 23.3, 6.7 Hz, 2F), -142.97 (dd, J = 23.2, 7.1 Hz, 2F), -156.09 (t, J = 22.1 Hz, 1F), -156.95 (t, J = 22.1 Hz, 1F), -163.27 (td, J = 22.9, 7.4 Hz, 2F), -163.63 (td, J = 22.9, 7.0 Hz, 2F); EI-MS: m/z: 405.1 (26.55%), 181.0 (100.00%), 161.1 (10.13%); IR (KBr, cm^{-1}): 3847, 3296, 3095, 2928, 2703, 2431, 2319, 2087, 1922, 1740, 1656, 1561, 1502, 1443, 1349, 1308, 1256, 1189, 1120, 1051, 1001, 947, 912, 802, 704; HRMS (ESI) m/z Calcd. for $C_{15}H_5ONF_{10}Na$: 428.01037; Found: 428.01031.

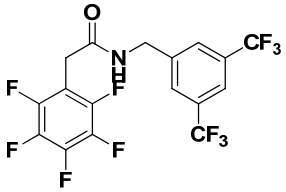

88

***N*-(3,5-Bis(trifluoromethyl)benzyl)-2-(perfluorophenyl)acetamide 88**. Yield: 25% as a white solid. m.p.: 126.0-126.4℃; ^{1}H NMR (400 MHz, $CDCl_3$): δ 7.80 (s, 1H), 7.71 (s, 2H), 6.15 (s, 1H), 4.59 (d, J = 6.1 Hz, 2H), 3.70 (s, 2H); ^{19}F NMR (376 MHz, $CDCl_3$): δ -63.06 (d, J = 9.7 Hz, 6F), -142.31 (dd, J = 21.9, 8.0 Hz, 2F), -154.63 (t, J = 20.8 Hz, 1F), -161.69 (td, J = 21.4, 7.6 Hz, 2F); EI-MS: m/z: 451.1 (4.85%), 450.1 (21.16%), 407.1 (15.73%), 242.0 (15.61%), 227.1 (100%), 181.0 (11.18%); IR (KBr, cm^{-1}): 3845, 3287, 3073, 2898, 2652, 2441, 2286, 2061, 1650, 1509, 1376, 1279, 1122, 1004, 902, 691; HRMS (ESI) m/z Calcd. for $C_{17}H_8ONF_{11}Na$: 474.03225; Found: 474.03229.

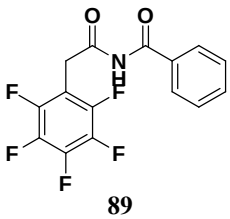

89

***N*-(2-(Perfluorophenyl)acetyl)benzamide 89**. Yield: 54% as a white solid. m.p.: 111.6-112.9℃; ^{1}H NMR (300 MHz, $CDCl_3$): δ 9.45 (s, 1H), 8.13 (ddd, J = 7.2, 2.9, 1.6 Hz, 2H), 7.70 – 7.52 (m, 1H), 7.52 – 7.43 (m, 2H), 4.49 (s, 2H); ^{19}F NMR (282 MHz, $CDCl_3$): δ -141.99 (dd, J = 22.1, 7.7 Hz, 2F), -155.78 (t, J = 20.8 Hz, 1F), -162.83 (td, J = 21.7, 7.9 Hz, 2F); EI-MS: m/z: 329.0 (35.61%), 208.0 (31.18%), 181.0 (14.62%), 122.1 (24.41%), 105.1 (100.00%), 77.2 (37.40%); IR (KBr, cm^{-1}): 3849, 3639, 3266, 3074, 2951, 2657, 2497, 2285, 2086, 1917, 1684,

1597, 1505, 1359, 1300, 1239, 1201, 1120, 1003, 909, 770, 698; Anal. Calcd. for $C_{15}H_8F_5NO_2$: C, 54.72; H, 2.45; N, 4.25; Found: C, 53.87; H: 2.74; N, 4.08.

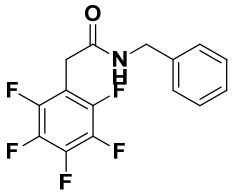

90

***N*-Benzyl-2-(perfluorophenyl)acetamide 90**. Yield: 24% as a white solid. m.p.: 164.9-165.3℃; ^{1}H NMR (300 MHz, $CDCl_3$): δ 7.40 – 7.22 (m, 5H), 5.88 (s, 1H), 4.46 (d, *J* = 5.6 Hz, 2H), 3.64 (s, 2H); ^{19}F NMR (282 MHz, $CDCl_3$): δ -142.16 (dd, *J* = 22.0, 7.7 Hz, 2F), -155.22 (t, *J* = 20.9 Hz, 2F), -162.05 (td, *J* = 21.7, 7.9 Hz, 2F); EI-MS: m/z: 316.1 (13.85%), 315.1 (51.41%), 181.0 (11.07%), 91.1 (100.00%); IR (KBr, cm^{-1}): 3849, 3628, 3287, 3088, 2929, 2699, 2475, 2289, 2081, 1892, 1740, 1650, 1506, 1446, 1364, 1307, 1193, 1119, 1006, 915, 800, 738, 702; HRMS (ESI) m/z Calcd. for $C_{15}H_{10}ONF_5Na$: 338.05748; Found: 338.05737.

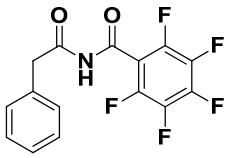

91

2,3,4,5,6-Pentafluoro-*N*-(2-phenylacetyl)benzamide 91. Yield: 47% as a white solid. m.p.: 113.4-114.5℃; ^{1}H NMR (400 MHz, $CDCl_3$): δ 8.82 (s, 1H), 7.42 – 7.26 (m, 5H), 3.96 (s, 2H); ^{19}F NMR (376 MHz, $CDCl_3$): δ -136.62 (qd, *J* = 12.2, 6.1 Hz, 2F), -146.75 (tt, *J* = 20.9, 5.6 Hz, 1F), -159.96 – -160.16 (m, 1F); EI-MS: m/z: 329.0 (33.33%), 195.0 (43.72%), 181.0 (100.00%), 91.1 (34.32%), 90.1 (11.11%), 65.1 (10.45%); IR (KBr, cm^{-1}): 3259, 3176, 2994, 2926, 2637, 2492, 2239, 2113, 1732, 1652, 1494, 1418, 1363, 1320, 1217, 1135, 1093, 995, 915, 805, 733, 698; Anal. Calcd. for $C_{15}H_8F_5NO_2$: C, 54.72; H, 2.45; N, 4.25; Found: C, 54.54; H: 3.11; N, 4.28.

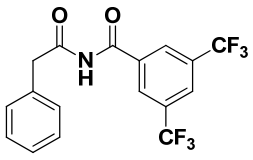

92

***N*-(2-Phenylacetyl)-3,5-bis(trifluoromethyl)benzamide 92**. Yield: 20% as a white solid. m.p.: 171.7-172.5℃; ^{1}H NMR (400 MHz, $CDCl_3$): δ 9.31 (s, 1H), 8.30 (s, 2H), 8.09 (s, 1H), 7.39 – 7.27 (m, 5H), 4.28 (s, 2H); ^{19}F NMR (376 MHz, $CDCl_3$): δ -63.04 (s, 6F); EI-MS: m/z: 375.1 (21.87%), 241.0 (28.60%), 213.0 (20.46%), 118.0 (100.00%), 91.1 (27.78%), 90.1 (15.28%); IR (KBr, cm^{-1}): 3268, 3178, 2921, 2858, 2620, 2517, 2317, 1724, 1622, 1511, 1458, 1369, 1279, 1122, 912, 846, 803, 684; Anal. Calcd. for $C_{17}H_{11}F_6NO_2$: C, 54.41; H, 2.95; N, 3.73; Found: C, 53.91; H: 3.53; N, 3.56.

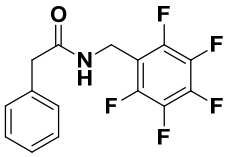

93

***N*-((Perfluorophenyl)methyl)-2-phenylacetamide 93**. Yield: 26% as a white solid. m.p.: 151.5-151.9℃; ^{1}H NMR (400 MHz, $CDCl_3$): δ 7.39 – 7.33 (m, 2H), 7.31 (ddd, *J* = 7.4, 3.6, 1.5 Hz, 1H), 7.24 – 7.20 (m, 2H), 5.79 (s, 1H), 4.49 (d, *J* = 6.0 Hz, 2H), 3.57 (s, 2H); ^{19}F NMR (376 MHz, $CDCl_3$): δ -143.08 (dd, *J* = 22.4, 8.2 Hz, 2F), -154.73 (t, *J* = 20.8 Hz, 2F), -161.80 (td, *J* = 21.6, 8.1 Hz, 2F); EI-MS: m/z: 316.1 (27.74%), 315.1 (74.55%), 181.0 (66.39%), 105.0 (16.42%), 91.1 (100.00%), 65.1 (21.90%); IR (KBr, cm^{-1}): 3847, 3628, 3409, 3286, 3080, 2936, 2650, 2472, 2291, 2025, 1895, 1742, 1650, 1502, 1446, 1333, 1253, 1121, 1053, 953, 884, 695; HRMS (ESI) m/z Calcd. for $C_{15}H_{10}ONF_5Na$: 338.05748; Found: 338.05719.

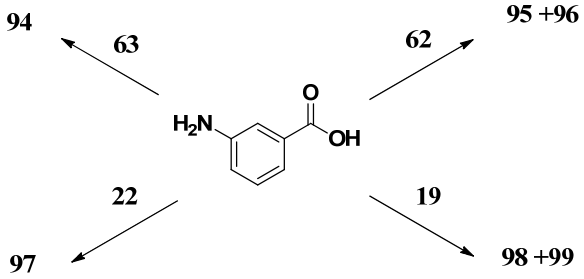

Compounds **94-99** were synthesized with similar methods.The general synthetic methods are described with the preparation of the compounds **94** or **95** as a representative example.

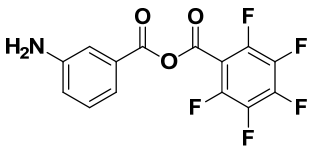

94

3-Aminobenzoic 2,3,4,5,6-pentafluorobenzoic anhydride 94. 3-Aminobenzoic acid (0.137 g, 1.0 mmol) and 2,3,4,5,6-pentafluorobenzoyl chloride **63** (0.14 mL, 1.0 mmol) were dissolved in THF (10 mL). The mixture was tirred at room temperature overnight and some precipitates were produced. These precipitates were filtered and then dried under vaccum to obtain the product **94**. Yield: 69% as a brown solid. m.p.: > 280℃ decomposed; ^{1}H NMR (400 MHz, acetone-d_6): δ 10.21 (s, 2H), 8.44 (s, 1H), 8.05 – 7.98 (m, 1H), 7.90 – 7.84 (m, 1H), 7.56 (t, *J* = 8.0 Hz, 1H); ^{19}F NMR (376 MHz, acetone-d_6): δ -142.86 – -143.13 (m, 2F), -154.16 (td, *J* = 20.3, 8.5 Hz, 1F), -162.93 – -163.20 (m, 2F); EI-MS: m/z: 332.2 (11.00%), 331.2 (69.48%), 195.1 (100.00%), 167.1 (26.83%), 117.1 (10.20%); IR (KBr, cm^{-1}): 3394, 3100, 2935, 2191, 1708, 1609, 1520, 1491, 1377, 1322, 1277, 1113, 1008, 886, 842, 749, 680; Anal. Calcd. for $C_{14}H_6F_5NO_3$: C, 50.77; H, 1.83; N, 4.23; Found: C, 50.52; H: 2.66; N, 4.42.

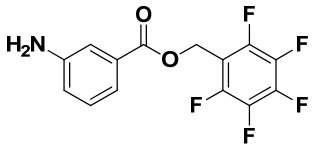

95

(Perfluorophenyl)methyl 3-aminobenzoate 95. 1-(Bromomethyl)-2,3,4,5,6-penta-fluorobenzene **62** (0.14 mL, 1.0 mmol) and 3-aminobenzoic acid (0.137 g, 1.0 mmol) were dissolved in 15.0 mL THF and K_2CO_3 (0.552 g, 4.0 mmol) was used as base. The reaction was stirred at r.t. and monitored by TLC. After completion of the reaction, the mixture was washed with saturated NaCl aqueous solution and extracted with ethyl acetate, the organic layer were combined and dried with Na_2SO_4 then filtered. The organic solvent was removed under vacuum and the residue was separated by column chromatography. The product **95** was obtained with yield of 40% as a white solid. m.p.: 101.9-102.3℃; ^{1}H NMR (400 MHz, $CDCl_3$): δ 7.42 – 7.36 (m, 1H), 7.33 – 7.28 (m, 1H), 7.20 (t, *J* = 7.9 Hz, 1H), 6.87 (ddd, *J* = 8.0, 2.5, 1.0 Hz, 1H), 5.42 (t, *J* = 1.4 Hz, 2H), 3.80 (s, 2H); ^{19}F NMR (376 MHz, $CDCl_3$): δ -141.67 (dd, *J* = 22.4, 8.1 Hz, 2F), -152.61 (t, *J* = 20.7 Hz, 2F), -161.58 (td, *J* = 21.2, 7.7 Hz, 2F); EI-MS: m/z: 318.1 (23.16%), 317.1 (100.00%); IR (KBr, cm^{-1}): 3853, 3640, 3498, 3396, 3217, 3018, 2929, 2652, 2450, 2292, 2157, 2058, 1941, 1709, 1658, 1619, 1502, 1460, 1382, 1307, 1228, 1119, 1048, 930, 821, 751, 682; Anal. Calcd. for $C_{14}H_8F_5NO_2$: C, 53.01; H, 2.54; N, 4.42; Found: C, 53.02; H: 3.73; N, 4.34.

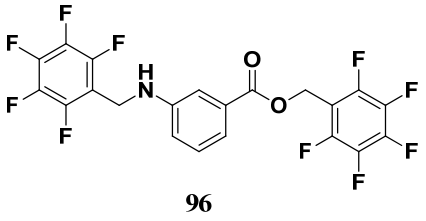

96

(Perfluorophenyl)methyl 3-(((perfluorophenyl)methyl)amino)benzoate 96. Yield: 36% as the second product of the reaction for compound **95**. m.p.: 105.4-105.8℃; ^{1}H NMR (400 MHz, $CDCl_3$): δ 7.43 – 7.36 (m, 1H), 7.33 – 7.27 (m, 1H), 7.23 (d, *J* = 7.8 Hz, 1H), 6.86 (ddd, *J* = 8.1, 2.5, 0.9 Hz, 1H), 5.42 (t, *J* = 1.4 Hz, 2H), 4.50 (s, 2H), 4.23 (s, 1H); ^{19}F NMR (376 MHz, $CDCl_3$): δ -141.78 (dd, *J* = 21.8, 8.2 Hz, 2F), -143.77 (dd, *J* = 22.4, 8.1 Hz, 2F), -152.58 (t, *J* = 20.7 Hz, 1F), -154.35 (t, *J* = 20.8 Hz, 1F), -161.27 – -161.96 (m, 4F); EI-MS: m/z: 498.1 (21.93%), 496.9 (100.00%); IR (KBr, cm^{-1}): 3640, 3391, 3044, 2950, 2649, 2449, 2196, 2026, 1711, 1656, 1608, 1496, 1423, 1377, 1322, 1275, 1227, 1104, 1024, 976, 931, 811, 744, 675; Anal. Calcd. for $C_{21}H_9F_{10}NO_2$: C, 50.72; H, 1.82; N, 2.82; Found: C, 50.27; H: 2.30; N, 3.28.

Compound **96** was crystallized in the space group $P2_1/c$ from DCM by slow evaporation of the solvent.

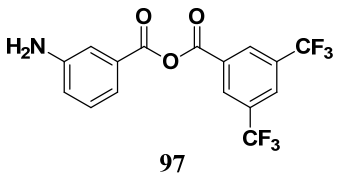

97

3-Aminobenzoic 3,5-bis(trifluoromethyl)benzoic anhydride 97. The synthesis of **97** was similar to that of **94**. Yield: 92% as a white solid. m.p.: 274.2-274.6℃; ^{1}H NMR (400 MHz,

acetone-d_6): δ 10.15 (s, 2H), 8.67 (s, 2H), 8.48 (dd, J = 3.4, 1.6 Hz, 1H), 8.30 (s, 1H), 8.15 (ddd, J = 8.1, 3.1, 1.9 Hz, 1H), 7.88 – 7.81 (m, 1H), 7.54 (t, J = 7.9 Hz, 1H); ^{19}F NMR (376 MHz, acetone-d_6): δ -63.38 (s, 6F); EI-MS: m/z: 378.3 (12.58%), 377.2 (71.64%), 241.1 (100.00%), 213.2 (45.81%); IR (KBr, cm^{-1}): 3305, 3097, 3000, 2866, 2554, 2064, 1831, 1684, 1594, 1560, 1448, 1376, 1273, 1135, 907, 846, 817, 758, 676; Anal. Calcd. for $C_{16}H_9F_6NO_3$: C, 50.94; H, 2.40; N, 3.71; Found: C, 50.70; H: 2.81; N, 4.00.

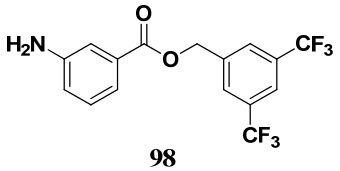

98

3,5-Bis(trifluoromethyl)benzyl 3-aminobenzoate 98. The synthesis of **98** was similar to that of **94**. Yield: 43% as a yellow solid. m.p.: 137.5-138.1℃; ^{1}H NMR (400 MHz, $CDCl_3$): δ 7.89 (s, 2H), 7.86 (s, 1H), 7.46 (d, J = 7.7 Hz, 1H), 7.37 (s, 1H), 7.28 – 7.21 (m, 1H), 6.90 (d, J = 7.9 Hz, 1H), 5.43 (s, 2H), 3.88 (s, 2H); ^{19}F NMR (376 MHz, $CDCl_3$): δ -62.92 (s, 6F); EI-MS: m/z: 364.1 (25.02%), 363.1(100.00%), 120.1 (21.70%), 93.2 (11.76%), 92.2 (42.63%), 65.2 (36.86%); IR (KBr, cm^{-1}): 3448, 3317, 3213, 3099, 2925, 2647, 2202, 2043, 1715, 1626, 1593, 1463, 1369, 1282, 1242, 1163, 1115, 1011, 909, 881, 843, 808, 747, 681; Anal. Calcd. for $C_{16}H_{11}F_6NO_2$: C, 52.90; H, 3.05; N, 3.86; Found: C, 53.26; H: 3.01; N, 3.62.

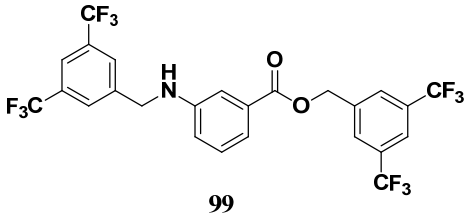

99

3,5-Bis(trifluoromethyl)benzyl 3-((3,5-Bis(trifluoromethyl)benzyl)amino)benzoate 99. The synthesis of **99** was similar to that of **94**. Yield: 35% as a yellow solid. m.p.: 97.8-99.6℃; ^{1}H NMR (400 MHz, $CDCl_3$): δ 7.87 (s, 2H), 7.86 (s, 1H), 7.83 (s, 2H), 7.80 (s, 1H), 7.48 (d, J = 7.8 Hz, 1H), 7.36 – 7.20 (m, 1H), 6.81 (dd, J = 8.1, 1.7 Hz, 1H), 5.42 (s, 2H), 4.52 (s, 2H), 4.37 (s, 1H); ^{19}F NMR (376 MHz, $CDCl_3$): δ -62.93 (s, 6F), -62.95 (s, 6F); EI-MS: m/z: 590.1 (23.81%), 589.0 (100.00%); IR (KBr, cm^{-1}): 3642, 3304, 3097, 3001, 2869, 2664, 2550, 2052, 1684, 1595, 1560, 1448, 1375, 1274, 1136, 908, 846, 758, 679; HRMS (ESI) m/z Calcd. for $C_{25}H_{16}O_2NF_{12}$: 590.09839; Found: 590.09930.

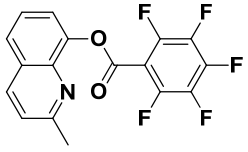

100

2-Methylquinolin-8-yl 2,3,4,5,6-pentafluorobenzoate 100. 2-Methylquinolin-8-ol (0.159 g, 1.0 mmol) and 2,3,4,5,6-pentafluorobenzoyl chloride **63** (0.14 mL, 1.0 mmol) were dissolved in THF (15 mL). The mixture was stirred at room temperature overnight and some precipitates were

produced. These precipitates were filtered and then dried under vaccum to obtain the product **100**. Yield: 89% as a yellow solid. m.p.: 206.4-207.5℃; ^{1}H NMR (400 MHz, $CDCl_3$): δ 8.70 (d, *J* = 8.6 Hz, 1H), 8.02 (dd, *J* = 7.5, 2.0 Hz, 1H), 7.90 (d, *J* = 0.8 Hz, 1H), 7.71 – 7.68 (m, 1H), 7.61 – 7.56 (m, 1H), 3.38 (s, 3H); ^{19}F NMR (376 MHz, $CDCl_3$): δ -133.85 – -134.78 (m, 2F), -146.40 (tt, *J* = 21.2, 6.4 Hz, 1F), -160.36 – -161.24 (m, 2F); EI-MS: m/z: 353.0 (62.77%), 194.9 (100.00%), 166.9 (45.81%); IR (KBr, cm^{-1}): 3651, 3106, 3011, 2436, 2313, 2139, 2096, 2033, 1740, 1644, 1496, 1425, 1370, 1332, 1200, 1097, 1049, 995, 923, 844, 759, 700; Anal. Calcd. for $C_{17}H_8F_5NO_2 \cdot 1.3H_2O$: C, 54.21; H, 2.84; N, 3.72; Found: C, 54.06; H: 3.13; N, 4.34.

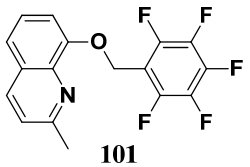

101

2-Methyl-8-((perfluorophenyl)methoxy)quinoline 101.

1-(Bromomethyl)-2,3,4,5,6-penta-fluorobenzene **62** (0.14 mL, 1.0 mmol) and 2-methylquinolin-8-ol (0.159 g, 1.0 mmol) were dissolved in 15.0 mL THF and KOH (0.067 g, 1.2 mmol) was used as base. The reaction was stirred at r.t. and monitored by TLC. After completion of the reaction, the mixture was washed with saturated NaCl aqueous solution and extracted with ethyl acetate, the organic layer were combined and dried with Na_2SO_4 then filtered. The organic solvent was removed under vacuum and the residua were separated with column chromatography. The product **95** was obtained with yield of 81% as a brown solid. m.p.: 164.0-164.4℃; ^{1}H NMR (400 MHz, $CDCl_3$): δ 8.02 (d, *J* = 8.4 Hz, 1H), 7.45 (dd, *J* = 8.2, 1.3 Hz, 1H), 7.38 (t, *J* = 7.9 Hz, 1H), 7.30 (d, *J* = 8.4 Hz, 1H), 7.20 (dd, *J* = 7.6, 1.3 Hz, 1H), 5.49 (d, *J* = 1.4 Hz, 2H), 2.76 (s, 3H); ^{19}F NMR (376 MHz, cdcl$_3$) δ -140.97 – -141.77 (m, 2F), -153.30 (t, *J* = 20.8 Hz, 1F), -162.06 (td, *J* = 22.1, 8.3 Hz, 2F); EI-MS: m/z: 340.1 (26.91%), 339.0 (100.00%), 338.0 (16.34%), 143.0 (75.56%), 130.0 (39.81%); IR (KBr, cm^{-1}): 3027, 2928, 2867, 2649, 2288, 2092, 1740, 1658, 1607, 1564, 1504, 1432, 1373, 1266, 1169, 1104, 1006, 973, 936, 900, 832, 763, 681; Anal. Calcd. for $C_{17}H_{10}F_5NO$: C, 60.18; H, 2.97; N, 4.13; Found: C, 60.28; H: 3.03; N, 4.06.

Compound **101** was crystallized in the space group *Pbca* from ethyl acetate/hexane by slow evaporation of the solvent.

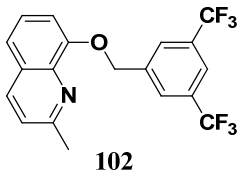

102

8-((3,5-Bis(trifluoromethyl)benzyl)oxy)-2-methylquinoline 102. The synthesis of **102** was similar to that of **101**. Yield: 96% as a brown solid. m.p.: 93.9-94.9℃; ^{1}H NMR (400 MHz, $CDCl_3$): δ 8.08 (s, 2H), 8.06 (s, 0.5H), 8.04 (s, 0.5H), 7.83 (s, 1H), 7.43 (d, *J* = 8.2 Hz, 1H), 7.38 – 7.31 (m, 2H), 7.07 – 7.01 (m, 1H), 5.52 (s, 2H), 2.82 (s, 3H); ^{19}F NMR (376 MHz, $CDCl_3$): δ -62.88 (s, 6F); EI-MS: m/z: 386.1 (24.86%), 385.1 (100.00%), 384.1 (66.16%), 366.1 (12.85%), 172.0 (45.86%); IR (KBr, cm^{-1}): 3028, 2928, 2866, 2289, 2044, 1741, 1611, 1566, 1504, 1469,

1361, 1278, 1164, 1108, 1009, 972, 898, 826, 743, 682; Anal. Calcd. for $C_{19}H_{13}F_6NO$: C, 59.23; H, 3.40; N, 3.64; Found: C, 59.46; H: 4.13; N, 3.67.

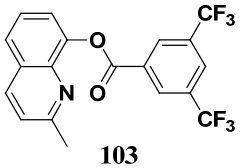

103

2-Methylquinolin-8-yl 3,5-bis(trifluoromethyl)benzoate 103. The synthesis of **103** was similar to that of **100**. Yield: 91% as a pale yellow solid. m.p.: >200℃ decomposed; ^{1}H NMR (400 MHz, $CDCl_3$): δ 8.86 (s, 2H), 8.71 (d, J = 8.6 Hz, 1H), 8.13 (s, 1H), 8.03 (dd, J = 8.1, 1.3 Hz, 1H), 7.88 (t, J = 7.9 Hz, 1H), 7.81 (dd, J = 7.7, 1.3 Hz, 1H), 7.70 (d, J = 8.6 Hz, 1H), 3.36 (s, 3H); ^{19}F NMR (376 MHz, $CDCl_3$): δ -62.84 (s, 6F); EI-MS: m/z: 399.1 (66.15%), 241.0 (100.00%), 213.0 (31.26%), 159.0 (18.58%), 131.0 (10.28%); IR (KBr, cm^{-1}): 3612, 3218, 3097, 2922, 2498, 2061, 1997, 1923, 1752, 1614, 1466, 1376, 1280, 1220, 1128, 913, 849, 758, 683. Compound **103** with a 3,5-Bis(trifluoromethyl)benzoic acid was co-crystallized from the mixed solvent of ethanol/ethyl acetate (v/v =1:1) in the space group $P2_1/n$.

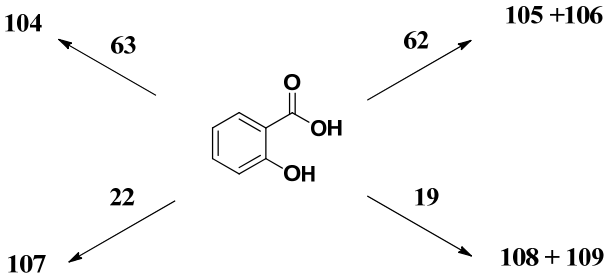

Compounds **104-109** were synthesized with similar methods.The general synthetic methods are described with the preparation of the compound **104** as a representative example.

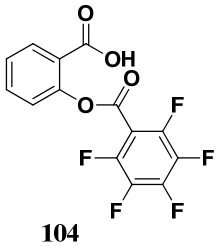

104

2-((Perfluorobenzoyl)oxy)benzoic acid 104. 2,3,4,5,6-Pentafluorobenzoyl chloride **63** (0.14 mL, 1.0 mmol) and 2-hydroxybenzoic acid (0.138 g, 1.0 mmol) were dissolved in 15.0 mL THF and KOH (0.067 g, 1.2 mmol) was used as base. The reaction was stirred at r.t. and monitored by TLC. After completion of the reaction, the mixture was washed with saturated NaCl aqueous solution and extracted with ethyl acetate, the organic layer were combined and dried with Na_2SO_4 then filtered. The organic solvent was removed under vacuum and the residua were separated with column chromatography. The product **104** was obtained with yield of 83% as a white solid. m.p.: 74.2-75.1℃; ^{1}H NMR (400 MHz, $CDCl_3$): δ 8.20 (dd, J = 7.9, 1.7 Hz, 1H), 7.76 – 7.67 (m, 1H), 7.46 (td, J = 7.7, 1.2 Hz, 1H), 7.28 (dd, J = 8.1, 1.1 Hz, 1H); ^{19}F NMR

(376 MHz, $CDCl_3$): δ -136.55 (t, *J* = 22.5 Hz, 2F), -146.42 – -147.18 (m, 1F), -159.62 – -160.52 (m, 2F); EI-MS: m/z: 332.1 (3.81%), 195.0 (100.00%), 167.0 (26.27%), 121.1 (10.08%), 120.1 (80.41%), 117.1 (10.69%); IR (KBr, cm^{-1}): 2923, 2642, 2551, 2053, 1704, 1651, 1496, 1418, 1321, 1261, 1201, 1094, 996, 919, 796, 738; Anal. Calcd. for $C_{14}H_5F_5O_4$: C, 50.62; H, 1.52; Found: C, 50.56; H: 1.66.

Compound **104** was crystallized from DMF/Et_2O in the space group $P2_1/c$.

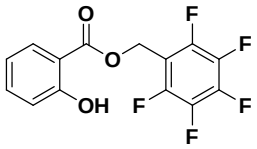

105

(Perfluorophenyl)methyl 2-hydroxybenzoate 105. The synthesis of **105** was similar to that of **104**. Yield: 73% as a white solid. m.p.: 105.8-106.1℃; ^{1}H NMR (400 MHz, $CDCl_3$): δ 10.49 – 10.45 (m, 1H), 7.80 – 7.74 (m, 1H), 7.51 – 7.43 (m, 1H), 7.02 – 6.95 (m, 1H), 6.87 (ddd, *J* = 8.2, 7.2, 1.1 Hz, 1H), 5.48 (t, *J* = 1.4 Hz, 2H); ^{19}F NMR (376 MHz, $CDCl_3$): δ -141.52 (dd, *J* = 22.5, 8.3 Hz, 2F), -151.77 (t, *J* = 20.7 Hz, 1F), -161.19 (qd, *J* = 10.0, 2.6 Hz, 2F); EI-MS: m/z: 318.1 (48.93%), 181.0 (100.00%), 120.0 (28.76%); IR (KBr, cm^{-1}): 3225, 2924, 2653, 2282, 2165, 2083, 1916, 1681, 1610, 1504, 1400, 1301, 1251, 1197, 1133, 1046, 965, 929, 874, 804, 761, 707; Anal. Calcd. for $C_{14}H_7F_5O_3$: C, 52.84; H, 2.22; Found: C, 52.98; H: 2.28.

Compound **105** was crystallized in the space group *P*-1 by diffusing Et_2O into the methanol solution of the sample.

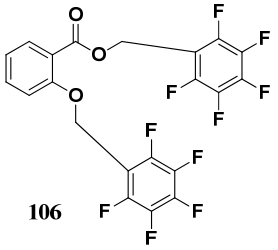

106

(Perfluorophenyl)methyl 2-((perfluorophenyl)methoxy)benzoate 106. Yield: 9% as the second product of the reaction for compound **105**. m.p.: 93.1-94.3℃; ^{1}H NMR (400 MHz, $CDCl_3$): δ 7.81 (dd, *J* = 7.6, 1.8 Hz, 1H), 7.58 – 7.46 (m, 1H), 7.08 (t, *J* = 7.7 Hz, 2H), 5.35 (t, *J* = 1.5 Hz, 2H), 5.17 (s, 2H); ^{19}F NMR (376 MHz, $CDCl_3$): δ -142.06 (dd, *J* = 21.8, 8.3 Hz, 2F), -142.31 (dd, *J* = 21.8, 8.2 Hz, 2F), -152.37 (t, *J* = 20.7 Hz, 1F), -152.60 (t, *J* = 20.7 Hz, 1F), -161.62 (dt, *J* = 21.8, 8.1 Hz, 2F), -161.82 (dt, *J* = 21.5, 8.1 Hz, 2F); EI-MS: m/z: 499.2 (66.40%), 498.2 (43.73%), 317.1 (32.92%), 181.0 (100.00%); IR (KBr, cm^{-1}): 3394, 2925, 2651, 2325, 2079, 1705, 1659, 1601, 1506, 1453, 1384, 1299, 1238, 1131, 1051, 974, 936, 870, 834, 759, 696, 662; Anal. Calcd. for $C_{21}H_8F_{10}O_3$: C, 50.62; H, 1.62; Found: C, 50.73; H: 1.81.

Compound **106** was crystallized from the space group $P2_12_12_1$ by diffusing Et_2O into the DMF solution of the sample.

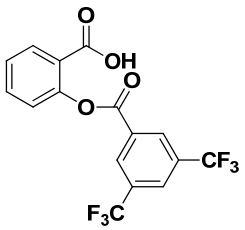

107

2-((3,5-Bis(trifluoromethyl)benzoyl)oxy)benzoic acid 107. The synthesis of **107** was similar to that of **104**. Yield: 79% as a white solid. m.p.: 166.1-166.2℃; ^{1}H NMR (300 MHz, $CDCl_3$): δ 8.66 – 8.63 (m, 2H), 8.16 (dd, *J* = 7.9, 1.5 Hz, 2H), 7.70 (ddd, *J* = 8.1, 7.5, 1.8 Hz, 1H), 7.47 – 7.40 (m, 1H), 7.31 – 7.26 (m, 1H); ^{19}F NMR (282 MHz, $CDCl_3$): δ -63.00 (s, 6F); EI-MS: m/z: 378.1 (1.15%), 362.1 (15.11%), 361.0 (91.74%), 241.0 (100.00%), 213.0 (36.03%), 120.0 (31.27%); IR (KBr, cm^{-1}): 3069, 2826, 2662, 2546, 2199, 2077, 1866, 1739, 1696, 1611, 1492, 1459, 1417, 1280, 1244, 1171, 1118, 918, 844, 801, 743, 683; Anal. Calcd. for $C_{21}H_8F_{10}O_3$: C, 50.81; H, 2.13; Found: C, 50.22; H: 2.14.

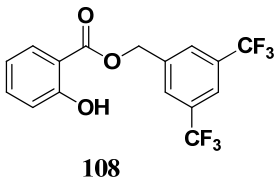

108

3,5-Bis(trifluoromethyl)benzyl 2-hydroxybenzoate 108. The synthesis of **108** was similar to that of **104**. Yield: 21% as a white solid. m.p.: 48.4-48.9℃; ^{1}H NMR (300 MHz, $CDCl_3$): δ 10.54 (s, 1H), 8.03 – 7.77 (m, 4H), 7.56 – 7.43 (m, 1H), 7.01 (dd, *J* = 8.3, 0.9 Hz, 1H), 6.96 – 6.83 (m, 1H), 5.48 (s, 2H); ^{19}F NMR (282 MHz, $CDCl_3$): δ -62.92 (s, 6F); EI-MS: m/z: 364.3 (4.35%), 363.2 (19.04%), 227.1 (100.00%), 177.1 (13.97%), 121.1 (71.22%), 120.1 (10.06%); IR (KBr, cm^{-1}): 3229, 2955, 2222, 1977, 1678, 1613, 1475, 1394, 1270, 1120, 1031, 928, 878, 803, 756, 685; Anal. Calcd. for $C_{16}H_{10}F_6O_3$: C, 52.76; H, 2.77; Found: C, 52.66; H: 3.35.

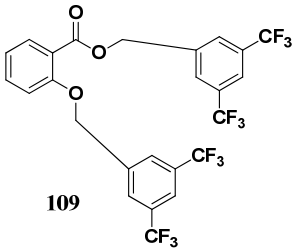

109

3,5-Bis(trifluoromethyl)benzyl 2-((3,5-bis(trifluoromethyl)benzyl)oxy)benzoate 109. Yield: 15% as the second product of the reaction for compound **108**. m.p.: 92.1-92.5℃; ^{1}H NMR (400 MHz, $CDCl_3$); δ 7.99 (s, 2H), 7.93 (dd, *J* = 7.8, 1.8 Hz, 1H), 7.86 (s, 2H), 7.81 (d, *J* = 4.9 Hz, 2H), 7.54 (ddd, *J* = 8.4, 7.4, 1.8 Hz, 1H), 7.11 (td, *J* = 7.6, 1.0 Hz, 1H), 7.04 (d, *J* = 8.4 Hz, 1H), 5.48 (s,2H), 5.29 (s, 2H); ^{19}F NMR (376 MHz, $CDCl_3$): δ -63.05 (s, 6F), -63.07 (s, 6F); EI-MS: m/z: 592.3 (11.20%), 591.3 (45.55%), 590.3 (18.86%), 363.1 (33.17%), 347.1 (12.00%), 228.1 (10.20%), 227.1 (100.00%), 120.9 (21.59%); IR (KBr, cm^{-1}): 3072, 2961, 1719, 1600, 1492, 1450, 1363, 1274, 1234, 1114, 1062, 891, 843, 803, 760, 691; Anal. Calcd. for $C_{25}H_{14}F_{12}O_3$: C, 50.86; H, 2.39; Found: C, 51.12; H: 3.43.

Compound **109** was crystallized from ethyl acetate/hexane in the space group *P*-1.

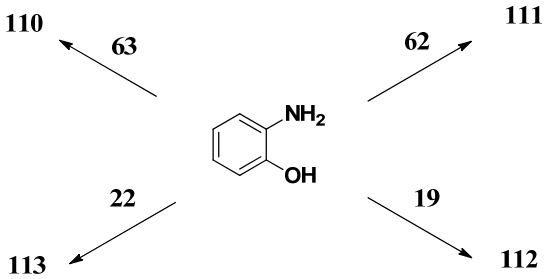

Compounds **110-113** were synthesized with similar methods.The general synthetic methods are described by the preparation of the compound **110** as a representative example.

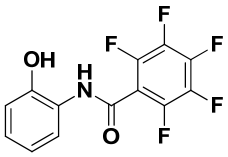

110

2,3,4,5,6-Pentafluoro-*N*-(2-hydroxyphenyl)benzamide 110. 2,3,4,5,6-Pentafluorobenzoyl chloride **63** (0.14 mL, 1.0 mmol) and 2-aminophenol (0.109 g, 1.0 mmol) were dissolved in 15.0 mL THF. The mixture was stirred at r.t. and monitored by TLC. After completion of the reaction, the mixture was washed with saturated NaCl aqueous solution and extracted with ethyl acetate, the organic layer were combined and dried with Na_2SO_4 then filtered. The organic solvent was removed under vacuum and the residua were separated with column chromatography. The product **110** was obtained with yield of 81% as a brown solid. m.p.: 211.5-212.4℃; ^{1}H NMR (300 MHz, acetone-d_6): δ 9.44 (s, 1H), 8.16 (dt, *J* = 8.0, 1.5 Hz, 1H), 7.06 (ddd, *J* = 8.1, 7.2, 1.6 Hz, 1H), 7.01 – 6.81 (m, 2H); ^{19}F NMR (282 MHz, acetone-d_6): δ -143.02 – -143.74 (m, 2F), -155.12 (t, *J* = 20.2 Hz, 1F), -162.96 – -164.28 (m, 2F); EI-MS: m/z: 303.4 (39.32%), 302.9 (100.00%), 590.3 (18.86%), 363.1 (33.17%), 347.1 (12.00%), 228.1 (10.20%), 227.1 (100.00%), 302.0 (29.21%), 195.5 (39.84%), 194.3 (58.74%), 80.2 (31.91%); IR (KBr, cm^{-1}): 3758, 3290, 3103, 2321, 2171, 2106, 2031, 1976, 1863, 1740, 1663, 1597, 1545, 1495, 1453, 1342, 1281, 1228, 1188, 1104, 993, 829, 745; Anal. Calcd. for $C_{13}H_6F_5NO_2$: C, 51.50; H, 1.99; N, 4.62; Found: C, 51.03; H:1.93; N, 4.47.

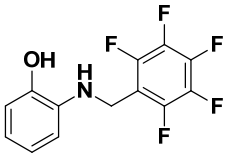

111

2-(((Perfluorophenyl)methyl)amino)phenol 111. The synthesis of **111** was similar to that of **110**. Yield: 45% as a pale yellow solid. m.p.: 121.4-122.7℃; ^{1}H NMR (300 MHz, $CDCl_3$): δ 6.87 (ddd, *J* = 8.0, 6.5, 2.1 Hz, 1H), 6.82 – 6.76 (m, 1H), 6.75 – 6.65 (m, 2H), 4.70 (s, 1H), 4.47 (s, 2H); ^{19}F NMR (282 MHz, $CDCl_3$): δ -143.67 (dd, *J* = 22.5, 8.1 Hz, 2F), -154.96 (t, *J* = 20.8 Hz, 1F),

-161.84 (td, J = 22.0, 8.3 Hz, 2F); EI-MS: m/z: 290.7 (19.51%), 289.7 (100.00%), 288.3 (95.17%); IR (KBr, cm^{-1}): 3644, 3327, 3029, 2841, 2703, 2596, 2437, 2290, 2051, 1774, 1656, 1600, 1499, 1355, 1278, 1239, 1186, 1112, 1056, 1018, 926, 865, 748, 684; Anal. Calcd. for $C_{13}H_8F_5NO$: C, 53.99; H, 2.79; N, 4.84; Found: C, 53.86; H:3.66; N, 5.00.
Compound **111** was crystallized from ethyl acetate/hexane in the space group P_b2_1/a.

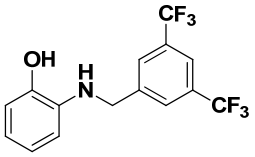

112

2-((3,5-Bis(trifluoromethyl)benzyl)amino)phenol 112. The synthesis of **112** was similar to that of **110**. Yield: 41% as a red solid. m.p.: 88.1-88.5℃; ^{1}H NMR (400 MHz, $CDCl_3$): δ 7.85 (s, 2H), 7.79 (s, 1H), 6.81 (td, J = 7.7, 1.4 Hz, 1H), 6.75 (dd, J = 7.8, 1.4 Hz, 1H), 6.66 (td, J = 7.6, 1.4 Hz, 1H), 6.51 (dd, J = 7.9, 1.4 Hz, 1H), 4.70 (s, 2H), 4.49 (s, 2H); ^{19}F NMR (376 MHz, $CDCl_3$): δ -62.84 (s, 6F); EI-MS: m/z: 336.5 (13.67%), 335.5 (97.42%), 334.2 (100.00%); IR (KBr, cm^{-1}): 3328, 3103, 2867, 2709, 2599, 2177, 2043, 1976, 1830, 1742, 1599, 1511, 1472, 1438, 1379, 1279, 1239, 1116, 1048, 994, 946, 895, 841, 794, 749, 707, 676; Anal. Calcd. for $C_{15}H_{11}F_6NO$: C, 53.74; H, 3.31; N, 4.18; Found: C, 55.12; H:3.48; N, 4.27.

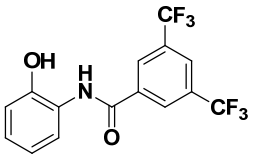

113

***N*-(2-Hydroxyphenyl)-3,5-bis(trifluoromethyl)benzamide 113**. The synthesis of **113** was similar to that of **110**. Yield: 96% as a white solid. m.p.: 174.6-175.2℃; ^{1}H NMR (300 MHz, acetone-d_6): δ 9.79 (s, 1H), 8.65 (s, 2H), 8.31 (s, 1H), 7.76 (dd, J = 8.0, 1.8 Hz, 1H), 7.13 (ddd, J = 8.1, 7.3, 1.6 Hz, 1H), 7.00 (dd, J = 8.1, 1.4 Hz, 1H), 6.96 – 6.87 (m, 1H); ^{19}F NMR (282 MHz, acetone-d_6): δ -63.42 (s, 6F); EI-MS: m/z: 349.1 (88.47%), 240.8 (100.00%), 213.4 (30.11%); IR (KBr, cm^{-1}): 3422, 3197, 2175, 2010, 1904, 1714, 1655, 1601, 1542, 1452, 1363, 1271, 1121, 902, 846, 753, 684; Anal. Calcd. for $C_{15}H_9F_6NO_2$: C, 51.59; H, 2.60; N, 4.01; Found: C, 51.46; H:2.96; N, 3.95.
Compound **113** was crystallized from ethyl acetate/hexane in the space group $P2_1/n$.

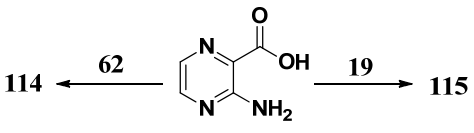

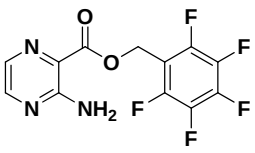

114

(Perfluorophenyl)methyl 3-aminopyrazine-2-carboxylate 114. To a suspension of 3-aminopyrazine-2-carboxylic acid (0.139 g, 1.0 mmol), NaH (60% in mineral oil, 0.10 g,

1.2 mmol) in DMF (5 mL), 1-(bromomethyl)-2,3,4,5,6-pentafluorobenzene **62** (0.14 mL, 1.0 mmol) was added dropwise. The reaction mixture was stirred at r.t. and monitored by TLC. After completion of the reaction, the mixture was washed with saturated NaCl aqueous solution and extracted with ethyl acetate, the organic layer were combined and dried with Na_2SO_4 then filtered. The organic solvent was removed under vacuum and the residue was chromatographed on silica gel (ethyl acetate/hexane 1:4) affording pure **114** (0.254 g, 80%) as a white solid. m.p.: 155.7-156.0℃; ^{1}H NMR (300 MHz, $CDCl_3$): δ 8.22 (d, J = 2.1 Hz, 1H), 8.01 (d, J = 2.2 Hz, 1H), 6.48 (s, 2H), 5.49 (d, J = 1.2 Hz, 2H); ^{19}F NMR (282 MHz, $CDCl_3$): δ -141.09 (d, J = 21.1 Hz, 2F), -152.19 (t, J = 20.2 Hz, 1F), -161.49 (t, J = 16.7 Hz, 2F); EI-MS: m/z: 320.2 (31.37%), 319.2 (46.76%), 181.1 (100.00%), 123.1 (64.58%), 95.2 (69.07%), 94.2 (25.30%), 67.3 (27.73%); IR (KBr, cm^{-1}): 3461, 3263, 3151, 2636, 2229, 2078, 1696, 1609, 1508, 1431, 1386, 1301, 1197, 1107, 978, 925, 839, 737, 662; Anal. Calcd. for $C_{12}H_6F_5N_3O_2$: C, 45.15; H, 1.89; N, 13.16; Found: C, 45.23; H:1.78; N, 13.16.
Compound **114** was crystallized from ethyl acetate/hexane in the space group $P2_1/c$.

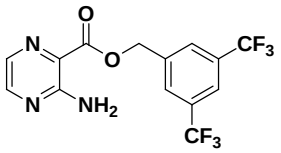

115

3,5-Bis(trifluoromethyl)benzyl 3-aminopyrazine-2-carboxylate 115. The synthesis of **115** was similar to that of **114**. Yield: 74% as a white solid. m.p.: 160.6-161.1℃; ^{1}H NMR (300 MHz, $CDCl_3$): δ 8.24 (d, J = 2.2 Hz, 1H), 8.04 (d, J = 2.2 Hz, 1H), 7.95 (s, 2H), 7.86 (s, 1H), 6.40 (s, 2H), 5.52 (s, 2H); ^{19}F NMR (282 MHz, $CDCl_3$): δ -62.92 (s, 6F); EI-MS: m/z: 365.2 (30.41%), 227.2 (49.66%), 123.1 (69.57%), 95.2 (100.00%), 94.2 (18.76%), 67.3 (15.35%); IR (KBr, cm^{-1}): 3454, 3275, 3154, 2643, 2231, 2044, 1827, 1684, 1621, 1542, 1467, 1397, 1280, 1161, 1110, 896, 843, 685; Anal. Calcd. for $C_{14}H_9F_6N_3O_2$: C, 46.04; H, 2.48; N, 11.51; Found: C, 46.02; H:2.59; N, 11.56.
Compound **115** was crystallized from ethyl acetate/hexane in the space group $P2_1/n$.

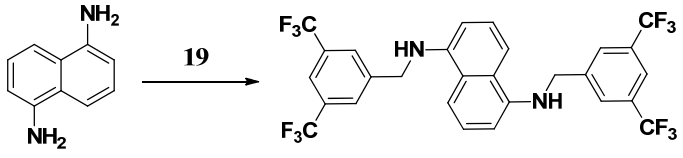

116

***N*^{1},*N*^{5}-Bis(3,5-bis(trifluoromethyl)benzyl)naphthalene-1,5-diamine 116**.
1-(Bromomethyl)-3,5-bis(trifluoromethyl)benzene **19** (0.36 mL, 2.0 mmol) and naphthalene-1,5-diamine (0.158 g, 1.0 mmol) were dissolved in 7.0 mL THF and NaH (60% in mineral oil, 0.20 g, 2.4 mmol) was used as base. The reaction was stirred at r.t. and monitored by TLC. After completion of the reaction, the mixture was washed with saturated NaCl aqueous solution and extracted with ethyl acetate, the organic layer were combined and dried with Na_2SO_4 then filtered. The organic solvent was removed under vacuum and the residua were separated with column chromatography. The product **116** was obtained with yield of 61% as a brown solid. m.p.: 215.9-216.4℃; ^{1}H NMR (400 MHz, acetone-d_6): δ 8.13

(s, 4H), 7.91 (s, 2H), 7.50 (d, J = 8.5 Hz, 2H), 7.19 (t, J = 8.0 Hz, 2H), 6.51 (d, J = 7.6 Hz, 2H), 6.39 (t, J = 5.8 Hz, 2H), 4.83 (d, J = 5.5 Hz, 4H); ^{19}F NMR (376 MHz, acetone-d_6): δ -63.32 (s, 6F); ESI-MS: 609.12 $[M-H]^-$; IR (KBr, cm^{-1}): 3307, 2930, 2086, 1664, 1547, 1494, 1427, 1380, 1332, 1277, 1170, 1114, 1061, 988, 902, 845, 811, 757, 704, 679; Elemental analysis calcd. for $C_{28}H_{18}F_{12}N_2$: C, 55.09; H, 2.97; N, 4.59; found: C, 55.01; H, 3.10; N, 4.53.
Compound **116** was crystallized from ethyl acetate/hexane.

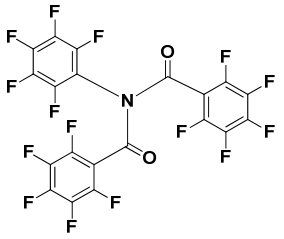

117

2,3,4,5,6-Pentafluoro-*N*-(perfluorobenzoyl)-*N*-(perfluorophenyl)benzamide 117.
2,3,4,5,6-Pentafluorobenzoyl chloride **63** (0.14 mL, 1.0 mmol) and 1-(perfluorophenyl)urea (0.226 g, 1.0 mmol) were dissolved in 4.0 mL THF and NaH (60% in mineral oil, 0.048 g, 1.2 mmol) was used as base. The reaction was stirred at r.t. and monitored by TLC. After completion of the reaction, the mixture was washed with saturated NaCl aqueous solution and extracted with ethyl acetate, the organic layer were combined and dried with Na_2SO_4 then filtered. The organic solvent was removed under vacuum and the residua were separated with column chromatography. The product **117** was obtained with yield of 28% as a white solid. m.p.: 121.6-122.3℃; ^{19}F NMR (282 MHz, $CDCl_3$): δ -139.01 (s, 4F), -141.94 (s, 2F), -145.75 (s, 2F), -147.46 (s, 1F), -158.10 – -159.20 (m, 6F); EI-MS: m/z: 570.9 (24.02%), 196.0 (10.17%), 194.9 (100.00%), 166.9 (38.77%), 116.9 (17.33%); IR (KBr, cm^{-1}): 3745, 3444, 2962, 2651, 2324, 2161, 2103, 2007, 1956, 1733, 1653, 1508, 1423, 1326, 1254, 1208, 1161, 1114, 1084, 994, 959, 859, 812, 769, 730, 703; Anal. Calcd. for $C_{20}F_{15}NO_2$: C, 42.05; N, 2.45; Found: C, 41.99; N, 2.33.
Compound **117** was crystallized in the space group $P2_1/c$ by diffusing Et_2O into the ethanol solution of the sample.

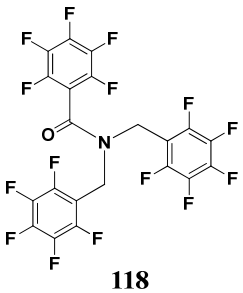

118

2,3,4,5,6-Pentafluoro-*N*,*N*-bis((perfluorophenyl)methyl)benzamide 118. A white solid; Yield: 37% as the second product of the reaction for compound **49**. m.p.: 159.3-159.7; ^{1}H NMR (400 MHz, $CDCl_3$): δ 4.74 (s, 2H), 4.63 (s, 2H); ^{19}F NMR (376 MHz, $CDCl_3$): δ -149.56 (t, J = 20.9 Hz, 1F), -150.49 (t, J = 20.9 Hz, 1F), -152.88 (t, J = 20.8 Hz, 1F), -159.09 (dt, J = 20.4, 10.2 Hz, 4F), -159.63 (td, J = 20.4, 6.9 Hz, 4F), -161.20 (td, J = 21.0, 7.2 Hz, 4F); EI-MS: m/z: 572.1 (18.27%), 570.9 (80.99%), 389.9 (31.91%), 195.0 (100.00%), 181.0 (20.29%), 167.0 (10.73%); IR

(KBr, cm^{-1}): 2981, 2786, 2643, 2229, 2086, 2004, 1663, 1501, 1432, 1363, 1320, 1232, 1180, 1119, 1047, 990, 961, 911, 841, 811, 774, 728, 695; Anal. Calcd. for $C_{21}H_4F_{15}NO$: C, 44.15; H, 0.71; N, 2.45; Found: C, 44.64; H:0.86; N, 2.55.

Compound **118** was crystallized in the space group $P2_1/c$ by diffusing Et_2O into the ethanol solution of the sample.

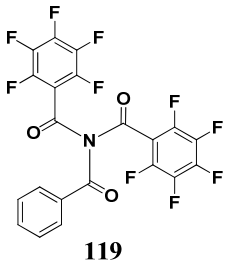

119

***N*-Benzoyl-2,3,4,5,6-pentafluoro-*N*-(perfluorobenzoyl)benzamide 119**.

2,3,4,5,6-Pentafluorobenzoyl chloride **63** (0.28 mL, 2.0 mmol) and benzamide **65** (0.121 g, 1.0 mmol) were dissolved in 4.0 mL THF and NaH (60% in mineral oil, 0.096 g, 2.2 mmol) was used as base. The reaction was stirred at r.t. and monitored by TLC. After completion of the reaction, the mixture was washed with saturated NaCl aqueous solution and extracted with ethyl acetate, the organic layer were combined and dried with Na_2SO_4 then filtered. The organic solvent was removed under vacuum and the residua were separated with column chromatography. The product **119** was obtained with yield of 51% as a white solid. m.p.: 139.8-140.6℃; ^{1}H NMR (400 MHz, $CDCl_3$): δ 7.88 – 7.82 (m, 2H), 7.68 – 7.61 (m, 1H), 7.54 – 7.46 (m, 2H); ^{19}F NMR (376 MHz, $CDCl_3$): δ -138.91 – -139.98 (m, 2F), -146.17 (dd, J = 29.3, 12.5 Hz, 1F), -159.04 (dd, J = 20.8, 14.6 Hz, 2F); EI-MS: m/z: 509.3 (7.40%), 195.2 (41.19%), 167.1 (19.78%), 105.2 (100.00%), 77.3 (54.24%), 51.6 (17.12%); IR (KBr, cm^{-1}): 3427, 2927, 2659, 2479, 2168, 1720, 1654, 1595, 1503, 1424, 1325, 1208, 1120, 1041, 993, 958, 905, 796, 693; Anal. Calcd. for $C_{21}H_5F_{10}NO_3$: C, 49.53; H, 0.99; N, 2.75; Found: C, 49.77; H:1.21; N, 2.74.

Compound **119** was crystallized in the space group $P2_1/c$ by diffusing Et_2O into the ethanol solution of the sample.

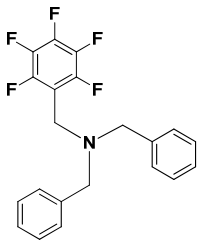

120

***N*,*N*-Dibenzyl-1-(perfluorophenyl)methanamine 120**. (Bromomethyl)benzene **64** (0.48 mL, 4.0 mmol) and (perfluorophenyl)methanaminium chloride **61** (0.466 g, 2.0 mmol) were dissolved in 4.0 mL THF and NaH (60% in mineral oil, 0.300 g, 6.0 mmol) was used as base. The reaction was stirred at r.t. and monitored by TLC. After completion of the reaction, the mixture was washed with saturated NaCl aqueous solution and extracted with ethyl acetate, the organic layer were combined and dried with Na_2SO_4 then filtered. The organic solvent was removed under vacuum and the residua were separated with column chromatography. The

product **120** was obtained with yield of 48% as a white solid. m.p.: 85.8-86.2℃; EI-MS: m/z: 378.3 (35.62%), 377.3 (100.00%), 300.2 (43.17%), 286.2 (69.39%), 181.1 (30.99%), 91.2 (22.63%); ^{1}H NMR (300 MHz, $CDCl_3$): δ 7.37 (d, *J* = 7.1 Hz, 4H), 7.30 (t, *J* = 7.1 Hz, 4H), 7.22 (t, *J* = 6.9 Hz, 2H), 3.73 (s, 2H), 3.59 (s, 4H); ^{19}F NMR (282 MHz, $CDCl_3$): δ -141.29 (d, *J* = 17.1 Hz, 2F), -155.57 (t, *J* = 19.0 Hz, 1F), -162.82 (d, *J* = 15.9 Hz, 2F); EI-MS: m/z: 509.3 (7.40%), 195.2 (41.19%), 167.1 (19.78%), 105.2 (100.00%), 77.3 (54.24%), 51.6 (17.12%); IR (KBr, cm^{-1}): 3227, 3033, 2951, 2803, 2713, 2604, 2322, 2187, 2084, 1997, 1951, 1881, 1810, 1709, 1651, 1601, 1518, 1491, 1453, 1402, 1370, 1332, 1296, 1248, 1207, 1180, 1105, 1009, 979, 933, 913, 854, 809, 746, 694; Anal. Calcd. for $C_{21}H_{16}F_5N$: C, 66.84; H, 4.27; N, 3.71; Found: C, 65.61; H:4.53; N, 3.44.
The crystal of compound **120** was cultivated from ethyl acetate/hexane in the space group $P2_1/n$.

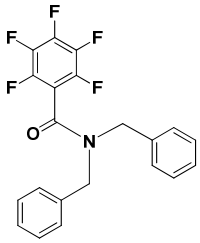

121

***N*,*N*-Dibenzyl-2,3,4,5,6-pentafluorobenzamide 121**. A white solid; Yield: 35% as the second product of the reaction for compound **51**. m.p.: 94.8-95.6℃; ^{1}H NMR (300 MHz, $CDCl_3$): δ 7.43 – 7.22 (m, 8H), 7.13 – 7.04 (m, 2H), 4.72 (s, 2H), 4.30 (s, 2H); ^{19}F NMR (282 MHz, $CDCl_3$): δ -140.29 (dd, *J* = 20.9, 6.1 Hz, 2F), -151.71 (t, *J* = 20.6 Hz, 1F), -159.28 – -159.72 (m, 2F); EI-MS: m/z: 392.1 (32.22%), 391.1 (89.50%), 300.0 (100.00%), 195.0 (83.16%), 107.1 (10.91%), 91.1 (27.84%); IR (KBr, cm^{-1}): 3039, 2924, 2637, 2321, 2082, 1810, 1643, 1449, 1318, 1215, 1099, 989, 811, 762, 691; Anal. Calcd. for $C_{21}H_{14}F_5NO$: C, 64.45; H, 3.61; N, 3.58; Found: C, 64.43; H:3.94; N, 3.83.
Compound **121** was crystallized in the space group $P2_1/c$ by diffusing Et_2O into the ethanol solution of the sample.

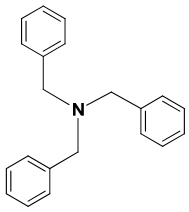

122

Tribenzylamine 122. (Bromomethyl)benzene **64** (0.24 mL, 2.0 mmol) and phenylmethanamine **60** (0.11 mL, 1.0 mmol) were dissolved in 5.0 mL THF and NaH (60% in mineral oil, 0.100 g, 1.2 mmol) was used as base. The reaction was stirred at r.t. and monitored by TLC. After completion of the reaction, the mixture was washed with saturated NaCl aqueous solution and extracted with ethyl acetate, the organic layer were combined and dried with Na_2SO_4 then filtered. The organic solvent was removed under vacuum and the residua were separated with column chromatography. The product **122** was obtained with yield of 70% as a white solid. m.p.: 91.5-92.3℃; ^{1}H NMR (300 MHz, $CDCl_3$): δ 7.41 (d, *J* = 7.2 Hz, 6H), 7.31 (t, *J* = 7.3 Hz, 6H), 7.23 (dd, *J* = 12.3, 5.2 Hz, 3H), 3.55 (s, 6H); EI-MS: m/z: 288.2 (33.94%),

287.2 (100.00%), 210.2 (63.01%), 196.2 (36.97%), 91.2 (49.92%); IR (KBr, cm^{-1}): 3062, 3030, 2925, 2883, 2801, 2715, 2325, 2170, 2083, 1996, 1949, 1877, 1811, 1658, 1600, 1492, 1448, 1368, 1316, 1246, 1203, 1121, 1072, 1027, 972, 906, 880, 808, 739, 694; Anal. Calcd. for $C_{21}H_{21}N$: C, 87.76; H, 7.36; N, 4.87; Found: C, 85.32; H, 7.57; N, 4.57.

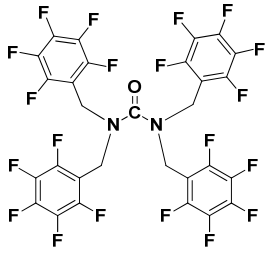

123

1,1,3,3-Tetrakis((perfluorophenyl)methyl)urea 123. To a suspension of Biuret (0.103 g, 1.0 mmol), NaH (60% in mineral oil, 0.10 g, 1.2 mmol) in DMF (5 mL), 1-(bromomethyl)-2,3,4,5,6-pentafluorobenzene **62** (0.14 mL, 1.0 mmol) was added dropwise. The reaction mixture was stirred at r.t. and monitored by TLC. After completion of the reaction, the mixture was washed with saturated NaCl aqueous solution and extracted with ethyl acetate, the organic layer were combined and dried with Na_2SO_4 then filtered. The organic solvent was removed under vacuum and the residua were chromatographed on silica gel (ethyl acetate/hexane 1:8) affording pure **123** (0.097 g, 50%) as a white solid. m.p.: 115.6-116.3℃; ^{1}H NMR (300 MHz, $CDCl_3$): δ 4.47 (s, 8H); ^{19}F NMR (282 MHz, $CDCl_3$): δ -141.10 (dd, J = 21.6, 7.5 Hz, 8F), -152.22 (t, J = 20.7 Hz, 4F), -160.51 – -162.76 (m, 8F); EI-MS: m/z: 779.6 (1.24%), 419.7 (10.89%), 375.7 (36.45%), 221.9 (31.04%), 180.9 (100.00%); IR (KBr, cm^{-1}): 2930, 2648, 2082, 1714, 1682, 1656, 1501, 1424, 1343, 1307, 1239, 1122, 1045, 1015, 953, 919, 790, 726, 676.

The crystal of compound **123** was cultivated from ethyl acetate/hexane in the space group $P2_1/c$.

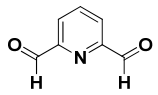

125

Compound **125** was prepared as reported in the literature.[69]

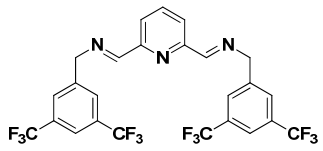

126

(*N*,*N*'*E*,*N*,*N*'*E*)-*N*,*N*'-(Pyridine-2,6-diylbis(methanylylidene))bis(1-(3,5-bis(trifluoromethyl)phenyl)methanamine) 126. Pyridine-2,6-dicarbaldehyde **125** (0.135 g, 1.0 mmol) and (3,5-Bis(trifluoromethyl)phenyl)methanamine **21** (0.486 g, 2.0 mmol) were dissolved in MeOH (8 mL). The mixture was tirred at room temperature overnight and some precipitates were produced. These precipitates were filtered and then dried under vaccum to obtain the product **126**. Yield: 66% as a white solid. m.p.: 116.6-117.0℃; ^{1}H NMR (300 MHz, DMSO-d_6): δ 8.65 (s, 2H), 8.12 (m,

6H), 8.06 – 7.97 (m, 3H), 5.08 (s, 4H); ^{19}F NMR (282 MHz, DMSO-d_6): δ -61.29 (s, 12F); ESI-MS: 586.1110 $[M+H]^+$; IR (KBr, cm^{-1}): 2878, 2812, 2083, 1998, 1793, 1647, 1567, 1460, 1421, 1385, 1357, 1276, 1159, 1112, 1043, 995, 959, 902, 872, 843, 808, 733, 702, 682; Elemental analysis calcd. for $C_{25}H_{15}F_{12}N_3$: C, 51.29; H, 2.58; N, 7.18; found: C, 51.28; H, 2.60; N, 7.07.

Compound **126** was crystallized in the space group $P2_1/n$ by diffusing Et_2O into the methanol solution of the sample.

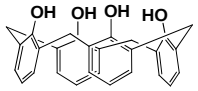

128

Compound **128** was prepared according to the literature.[70]

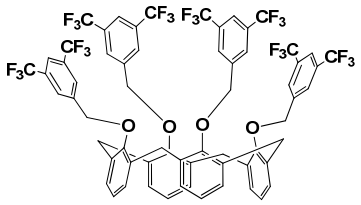

129

Trifluoromethylated calix[4]arene 129.[71] A suspension of compound **128** (0.532 g, 1.25 mmol), NaH (60% in mineral oil, 0.487 g, 9.75 mmol) in DMF (80 mL) was stirred for 15 min at r.t. 1-(bromomethyl)-3,5-Bis(trifluoromethyl)benzene **19** (1.34 mL, 7.45 mmol) was added into this mixture and the reaction was stirred at -15℃ for 30 min. Then water (180 mL) was added and extracted with DCM. The organic layer were combined and dried with Na_2SO_4 then filtered. The organic solvent was removed under vacuum and the residua were chromatographed on silica gel (DCM/hexane 1:4) affording pure **129** (1.561 g, 94%) as a white solid. m.p.: 171.0-171.7℃; ^{1}H NMR (300 MHz, $CDCl_3$): δ 7.83 (s, 4H), 7.60 (d, J = 1.5 Hz, 8H), 6.70 – 6.42 (m, 12H), 5.08 (s, 8H), 3.88 (d, J = 13.7 Hz, 4H), 2.82 (d, J = 13.8 Hz, 4H); ^{19}F NMR (282 MHz, $CDCl_3$): δ -63.10 (s, 24F); ESI-MS: 1351.2421 $[M+H]^+$; IR (KBr, cm^{-1}): 3941, 3220, 3066, 2981, 2929, 2878, 2576, 2327, 2196, 2088, 1998, 1930, 1806, 1697, 1625, 1586, 1458, 1383, 1354, 1277, 1164, 1128, 997, 890, 842, 804, 767, 732, 704, 679; Elemental analysis calcd. for $C_{64}H_{40}F_{24}O_4$: C, 57.84; H, 3.03; found: C, 57.20; H, 3.18.

Compound **129** was crystallized in the space group P-1 by diffusing Et_2O into the methanol solution of the sample.

References

[1] D. Quiñonero, C. Garau, C. Rotger, A. Frontera, P. Ballester, A. Costa, P. M. Deyà, *Angew. Chem. Int. Ed.*, **2002**, *41*, 3389.

[2] Mark Mascal, Alan Armstrong, Michael D. Bartberger, *J. Am. Chem. Soc.*, **2002**, *124*, 6274.

[3] Paul de Hoog, Patrick Gamez, Ilpo Mutikainen, Urho Turpeinen, Jan Reedijk, *Angew. Chem. Int. Ed.*, **2004**, *43*, 5815.

[4] Serhiy Demeshko, Sebastian Dechert, Franc Meyer, *J. Am. Chem. Soc.*, **2004**, *126*, 4508.

[5] M. Luhmer, A. Bartik, A. Dejaegere, P. Bovy, J. Reisse, *Bull. Soc. Chim. Fr.*, **1994**, *131*, 603.

[6] J. H. Williams, *Acc. Chem. Res.*, **1993**, *26*, 593.

[7] C. Garau, A. Frontera, D. Quiñonero, P. Ballester, A. Costa, P. M. Deyà, "*Anion-π Interactions, in Recent Research Developments in Chemical Physics*", ed. S. G. Pandalai, Transworld Research Network, Kerala, India, 2004, vol. 5, pp. 227 and references therein.

[8] Laura M. Salonen, Manuel Ellermann, Franois Diederich, *Angew. Chem. Int. Ed.*, **2011**, *50*, 4808.

[9] C. Garau, A. Frontera, D. Quiñonero, P. Ballester, A. Costa, P. M. Deyà, *ChemPhysChem*, **2003**, *4*, 1344.

[10] C. Garau, A. Frontera, D. Quiñonero, P. Ballester, A. Costa, P. M. Deyà, *J. Phys. Chem. A*, **2004**, *108*, 9423

[11] (a) J.-M. Lehn, "*Supramolecular Chemistry: Concepts and Perspectives*" (VCH, Weinheim, **1995**); (b) J.-M. Lehn, "*SUPRAMOLECULAR CHEMISTRY-SCOPE AND PERSPECTIVES MOLECULES-SUPERMOLECULES-MOLECULAR DEVICES*", Nobel lecture, December 8, **1987**.

[12] (a) D. Kim, P. Tarakeshwar, K. S. Kim, *J. Phys. Chem. A*, **2004**, *108*, 1250; (b) D. Quiñonero, C. Garau, A. Frontera, P. Ballester, A. Costa, P. M. Deyà, *J. Phys. Chem. A*, **2005**, *109*, 4632.

[13] G. A. Jeffrey, "*An Introduction to Hydrogen Bonding*", Oxford University Press, Oxford, **1997**.

[14] J. C. Ma, D. A. Dougherty, *Chem. Rev.*, **1997**, *97*, 1303.

[15] C. Janiak, *J. Chem. Soc.*, *Dalton Trans.*, **2000**, 3885.

[16] A. Robertazzi, F. Krull, E.-W. Knapp, P. Gamez, *CrystEngComm*, **2011**, *13*, 3293 and references therein.

[17] A. Ebrahimi, M. H. Khorassani, H. R. Masoodi, *Chemical Physics Letters*, **2011**, *504*, 118.

[18] C. Estarellas, A. Bauzá, A. Frontera, D. Quiñonero, P. M. Deyà, *Phys. Chem. Chem. Phys.*, **2011**, *13*, 5696.

[19] G. Shi, J. Yang, Y. Ding, H. Fang, *ChemPhysChem*, **2014**, *15*, 2588.

[20] L. Adriaenssens, C. Estarellas, A. V. Jentzsch, M. M. Belmonte, S. Matile, P. Ballester, *J. Am. Chem. Soc.*, **2013**, *135*, 8324.

[21] D. Wang, S. Fa, Y. Liu, B. Hou, M. Wang, *Chem. Commun.*, **2012**, *48*, 11458.

[22] W. Liu, Q.-Q. WANG, Y. Wang, Z.-T. Huang, D.-X. Wang, *RSC Adv.*, **2014**, *4*, 9339.

[23] (a)Q. He, Z. Huang, D. Wang, *Chem. Commun.*, **2014**, *50*, 12958; (b) Q. He, Y. Han, Y. Wang, Z. Huang, D. Wang, *Chem. Eur. J.*, **2014**, *20*, 7486.

[24] (a) P. Manna, S. K. Seth, M. Mitra, A. Das, N. J. Singh, S. R. Choudhury, T. Kar, S. Mukhopadhyay, *CrystEngComm*, **2013**, *15*, 7879; (b) P. Manna, S. K. Seth, A. Bauzá, M.

Mitra, S. R. Choudhury, A. Frontera, S. Mukhopadhyay, *Cryst. Growth. Des.*, **2014**, *14*, 747; (c) P. Manna, S. K. Seth, M. Mitra, S. R. Choudhury, A. Bauzá, A. Frontera, S. Mukhopadhyay, *Cryst. Growth. Des.*, **2014**, *14*, 5812.

[25] F. Orvay, A. Bauzá, M. Barceló-Oliver, A. Garcia-Raso, J. J. Fiol, A. Costa, E. Molins, I. Mata, A. Frontera, *CrystEngComm*, **2014**, *16*, 9043.

[26] C. Wang, G. Li, Q. Zhang, *Tetrahedron Letters*, **2013**, *54*, 2633.

[27] J. Zhao, G. Li, C. Wang, W. Chen, S. C. J. Loo, Q. Zhang, *RSC Adv.*, **2013**, *3*, 9653.

[28] S. Li, D. Wang, M. Wang, *Tetrahedron Letters*, **2012**, *53*, 6226.

[29] S. P. Mahanta, B. S. Kumar, S. Baskaran, C. Sivasankar, P. K. Panda, *Org. Lett.*, **2012**, *14*, 548.

[30] (a) Y. Zhao, Y. Domoto, E. Orentas, C. Beuchat, D. Emery, J. Mareda, N. Sakai, S. Matile, *Angew. Chem. Int. Ed.*, **2013**, *52*, 9940; (b) Y. Zhao, C. Beuchat, Y. Domoto, J. Gajewy, A. Wilson, J. Mareda, N. Sakai, S. Matile, *J. Am. Chem. Soc.*, **2014**, *136*, 2101; (c) T. Lu, S. E. Wheeler, *Org. Lett.*, **2014**, *16*, 3268.

[31] (a) A. S. Degtyarenko, K. V. Domasevitch, *Acta Cryst.*, **2014**, *C70*, 173; (b) K. Chen, C. E. Strasser, J. C. Schmitt, J. Shearer, V. J. Catalano, *Inorg. Chem.*, **2012**, *51*, 1207; (c) P. Cañellas, M. Torres, A. Bauzá, M. M. Cánaves, K. Sánchez, M. I. Cabra, A. García-Raso, J. J. Fiol, P. M. Deyà, E. Molins, I. Mata, A. Frontera, *Eur. J. Inorg. Chem.*, **2012**, 3995; (d) P. Cañellas, A. Bauzá, A. García-Raso, J. J. Fiol, P. M. Deyà, E. Molins, I. Mata, A. Frontera, *Dalton Trans.*, **2012**, *41*, 11161; (e) Z. Setifi, K. V. Domasevitch, F. Setifi, P. Mach, S. W. Ng, V. Petříček, M. Dušek, *Acta Cryst.*, **2013**, *C69*, 1351.

[32] G. J. Jones, A. Robertazzi, J. A. Platts, *J. Phys. Chem. B*, **2013**, *117*, 3315.

[33] C. Estarellas, A. Frontera, D. Quiñonero, P. M. Deyà, *Angew. Chem. Int. Ed.*, **2011**, *50*, 415.

[34] V. Philip, J. Harris, R. Adams, D. Nguyen, J. Spiers, J. Baudry, E. E. Howell, R. J. Hinde, *Biochemistry*, **2011**, *50*, 2939.

[35] C. Estarellas, A. Frontera, D. Quiñonero, P. M. Deyà, *Chem. Asian. J.*, **2011**, *6*, 2316.

[36] S. Chakravarty, Z. Sheng, B. Iverson, B. Moore, *FEBS Letters*, **2012**, *586*, 4180.

[37] J. P. Schwans, F. Sunden, J. K. Lassila, A. Gonzalez, Y. Tsai, D. Herschlag, *PNAS*, **2013**, *110*, 11308.

[38] A. Bauzá, D. Quiñonero, P. M. Deyà, A. Frontera, *Chem. Asian. J.*, **2013**, *8*, 2708.

[39] A. Bauzá, D. Quiñonero, P. M. Deyà, A. Frontera, *Chem. Eur. J.*, **2014**, *20*, 6985.

[40] Y. Chen, D. Wang, Z. Huang, M. Wang, *Chem. Commun.*, **2011**, *47*, 8112.

[41] O. Perraud, V. Robert, H. Gornitzka, A. Martinez, J. P. Dutasta, *Angew. Chem. Int. Ed.*, **2012**, *51*, 504.

[42] A. Bauzá, D. Quiñonero, P. M. Deyà, A. Frontera, *Chemical Physics Letters*, **2012**, *530*, 145.

[43] M. Albrecht, C. Wessel, M. de Groot, K. Rissanen, A. Lüchow, *Angew. Chem. Int. Ed.*, **2008**, *130*, 4600.

[44] M. Giese, M. Albrecht, A. Valkonen, K. Rissanen, *Chem. Sci.*, **2015**, *6*, 354.

[45] (a) S. V. Druzhinin, E. S. Balenkova, V. G. Nenajdenko, *Tetrahedron*, **2007**, *63*, 7753; (b) C. G Béguin, In "*Enantiocontrolled synthesis of fluoro-organic compounds*"; (c) V. A. Soloshonok, Ed.; Wiley: Chichester, U.K., **1999**; (d) M. Schlosser, *Angew. Chem. Int. Ed.*, **2006**, *45*, 5432.

[46] I. Alkorta, I. Rozas, J. Elguero, *J. Am. Chem. Soc.*, **2002**, *124*, 8593.

[47] (a) A. J. Ilott, S. Palucha, A. S. Batsanov, M. R. Wilson, P. Hodgkinson, *J. Am. Chem. Soc.*,

2010, *132*, 5179. (b) M. J. Molski, M. A. Khanfar, H. Shorafa, K. Seppelt, *Eur. J. Org. Chem.*, **2013**, 3131. (c) K. Kasai, M. Fujita, *Chem. Eur. J.*, **2007**, *13*, 3089. (d) J. C. Collings, K. P. Roscoe, R. Ll. Thomas, A. S. Batsanov, L. M. Stimson, J. A. K. Howard, T. B. Marder, *New. J. Chem.*, **2001**, *25*, 1410. (e) D. W. Shin, S. Y. Lee, C. H. Lee, K. Lee, C. H. Park, J. E. McGrath, M. Zhang, R. B. Moore, M. D. Lingwood, L. A. Madsen, Y. T. Kim, I. Hwang, Y. M. Lee, *Macromolecules*, **2013**, *46*, 7797. (f) Y. Chen, C. H. Lee, J. R. Rowlett, J. E. McGrath, *Polymer*, **2012**, *53*, 3143. (g) T. Öberg, M. S. Iqbal, *Chemosphere*, **2012**, *87*, 975. (h) A. Voege, V. A. Deimede, J. K. Kallitsis, *J. Polymer Science, Part A: Polymer Chemistry*, **2012**, *50*, 207. (i) J. Kerres, F. Schoenberger, A. Chromik, T. Haering, Q. Li, J. O. Jensen, C. Pan, P. Noye, N. J. Bjerrum, *Fuel Cells*, **2008**, *8*, 175.

[48] M. Albrecht, M. Müller, O. Mergel, K. Rissanen, A. Valkonen, *Chem. Eur. J.*, **2010**, *16*, 5062.

[49] C. G Béguin, In V. A. Soloshonok (Editor) "*Enantiocontrolled synthesis of fluoro-organic compounds*", Wiley: Chichester, U.K., **1999**.

[50] (a) B. E. Smart, *J. Fluorine Chem.*, **2001**, *109*, 3; (b) N. Iwai, R. Sakai, S. Tsuchida, M. Kitazume, T. Kitazume, *J. Fluorine Chem.*, **2009**, *130*, 434; (c) W. R. Dolbier Jr. , *J. Fluorine Chem.*, **2005**, *126*, 157; (d) C. Isanbor, D. O'Hagan, *J. Fluorine Chem.*, **2006**, *127*, 303; (e) Manfred Schlosser, *Angew. Chem. Int. Ed.*, **2006**, *45*, 5432.

[51] (a) R. Loska, M. Majcher, M. Makosza, *J. Org. Chem.*, **2007**, *72*, 5574; (b) T. Hosokawa, A. Matsumura, T. Katagiri, K. Uniyama, *J. Org. Chem.*, **2008**, *73*, 1468; (c) L. E. Kiss, H. S. Ferreira, D. A. Learmonth, *Org. Lett.*, **2008**, *10*, 1835; (d) B. I. Usachev, D. L. Obydennov, G. Röschenthaler, V. Y. Sosnovskikh, *Org. Lett.*, **2008**, *10*, 2857; (e) B. Jiang, Y. Si, *J. Org. Chem.*, **2002**, *67*, 9449; (f) J. Azizian, B. Mirza, M. M. Mojtahedi, M. S. Abaee, M. Sargordan, *J. Fluorine Chem.*, **2008**, *129*, 1083.

[52] S. Purser, P. R. Moore, S. Swallow, V. Gouverneur, *Chem. Soc. Rev.*, **2008**, *37*, 320.

[53] (a) Z. Hu, Y. Li, K. Liu, Q. Shen, *J. Org. Chem.*, **2012**, *77*, 7957; (b) X. Wang, B. List, *Angew. Chem. Int. Ed.*, **2008**, *47*, 1119.

[54] (a) C. Garau, D. Quiñonero, A. Frontera, P. Ballester, A. Costa, P. M. Deyà, *J. Phys. Chem. A*, **2005**, *109*, 9341; (b) B. L. Schottel, H. T. Chifotides, K. R. Dunbar, *Chem. Soc. Rev.*, **2008**, *37*, 68.

[55] B. P. Hay, V. S. Bryantsev, *Chem. Commun*., **2008**, 2417.

[56] M. Albrecht, H. Yi, O. Köksal, G. Raabe, F. Pan, A. Valkonen, K. Rissanen, in preparation.

[57] (a) Y. Dong, X. Mao, X. Jiang, J. Hou, Y. Cheng, C. Zhu. *Chem. Commun.*, **2011**, *47*, 9450.; (b) H. Liu, L. Peng, T. Zhang, Y. Li. *New J. Chem.*, **2003**, ***27***, 1159.; (c) A. Lu, P. Cotanda, J. P. Patterson, D. A. Longbottom, R. K. O'Reilly. *Chem. Commun.*, **2012**, *48*, 9699.

[58] M. Giese, M. Albrecht, T. Krappitz, M. Peters, V. Gossen, G. Raabe, A. Valkonen, K. Rissanen, *Chem. Commun.*, **2012**, 9983.

[59] (a) M. Giese, M. Albrecht, T. Krappitz, M. Prters, V. Gossen, G. Raabe, A. Valkonen, K. Rissanen, *Chem. Commun.*, **2012**, *48*, 9983; (b) M. Müller, M. Albrecht, J. Sackmann, A. Hoffmann, F. Dierkes, A. Valkonen, K. Rissanen, *Dalton Trans.*, **2010**, *39*, 11329; (c) M. Giese, M. Albrecht, T. Repenko, J. Sackmann, A. Valkonen, K. Rissanen, *Eur. J. Org. Chem.*, **2014**, 2435.

[60] M. Giese, M. Albrecht, K. Wiemer, G. Kubik, A. Valkonen, K. Rissanen, *Eur. J. Inorg. Chem.*, **2012**, 2995.

[61] (a) M. Horn, J. Ihringer, P. T. Glink, J. F. Stoddart, *Chem. Eur. J.*, **2003**, *9*, 4046; (b) A. R.

Williams, B. H. Northrop, K. N. Houk, J. F. Stoddart, D. J. Williams, *Chem. Eur. J.*, **2004**, *10*, 5406; (c) J. M. Mitchell, N. S. Finney, *Tetrahedron Lett.*, **2000**, *41*, 8431.

[62] (a) Y. Dong, X. Mao, X. Jiang, J. Hou, Y. Cheng, C. Zhu, *Chem. Commun.*, **2011**, *47*, 9450; (b) H. Liu, L. Peng, T. Zhang, Y. Li, *New J. Chem.*, **2003**, ***27***, 1159; (c) A. Lu, P. Cotanda, J. P. Patterson, D. A. Longbottom, R. K. O'Reilly, *Chem. Commun.*, **2012**, *48*, 9699.

[63] Y. Tang, J. Lu, X. Wang, L. Shao, *Tetrahedron*, **2010**, *66*, 7970.

[64] R. B. Van Order, H. G. Lindwall, *Chem. Rev.*, **1942**, *30*, 69.

[65] (a) K. N. Skala, K. G. Perkins, A. Ali, R. Kutlik, A. M. Summitt, S. Swamy-Mruthinti, F. A. Khan, M. Fujita, *Tetrahedron Lett.*, **2010**, **51**, 6516; (b) J. P. Gallivan, D. A. Dougherty, *Proc. Natl. Acad. Sci. U. S. A.*, **1999**, *96*, 9459.

[66] (a) Y. Chen, C. Tseng, Y. Chen, T. Hwang, C. Tzeng, *Int. J. Mol. Sci.*, **2015**, *16*, 6532; (b) Z. Liu, W. Li, T. Kang, L. He, Q. Liu, *Org. Lett.*, 2015, 17, 150; (c) A. Rajendran, C. Karthikeyan, K. Rajathi, D. Ragupathy, *American Journal of Organic Chemistry*, **2012**, *2*, 9.

[67] (a) T. Sato, H. Yamaguchi, T. Kogawa, T. Abe, N. Mano, *J. Pharm. Pharm. Sci.*, **2014**, *17*, 475; (b) Y. Son, S. Gwon, S. Kim, *MOL. CRYST. LIQUID CRYST.*, **2014**, *600*, 189; (c) J. A. Carrazana-Garcia, E. M. Cabaleiro-Lago, A. Campo-Cacharron, J. Rodriguez-Otero, *Org. Biomo. Chem.*, **2014**, *12*, 9145.

[68] (a) Z. Sun, M. Albrecht, F. Pan, M. Waringo, *Synthesis*, **2015**, *47*, 861; (b) Z. Sun, M. Albrecht, M. Giese, F. Pan, K. Rissanen, *Synlett*, **2014**, *25*, 2075; (c) D. Makuc, M. Albrecht, J. Plavec, *Supramol. Chem.*, **2010**, *22*, 603.

[69] Alam, MD. Mahbubul, *Journal of Bangladesh Academy of Sciences*, **2011**, *35*, 61.

[70] R. Rathore, S. H. Abdelwahed, I. A. Guzei, *J. Am. Chem. Soc.*, **2004**, *126*, 13582.

[71] A. V. Jentzsch, D. Emery, J. Mareda, P. Metrangolo, G. Resnati, S. Matile, *Angew. Chem. Int. Ed.*, **2011**, *50*, 11675.

[72] *CrysalisPro*, Agilent Technologies, Oxford, UK, **2013**.

[73] *COLLECT*, Bruker AXS, Inc., Madison, Wisconsin, USA, **2008**.

[74] Z. Otwinowski, W. Minor, *Methods in Enzymology*, vol. *276*, *Macromolecular Crystallography*, Part A, eds. C. W. Carter Jr, R. M. Sweet, Academic Press, New York, **1997**, 307.

[75] G. M. Sheldrick, SADABS, University of Göttingen, Germany, **1996**.

[76] M. C. Burla, R. Caliandro, M. Camalli, B. Carrozzini, G. L. Cascarano, L. De Caro, C. Giacovazzo, G. Polidori, R. Spagna, *J. Appl. Crystallogr.*, **2005**, *38*, 381.

[77] L. J. Farrugia, *J. Appl. Crystallogr.*, **2012**, *45*, 849.

[78] G. M. Sheldrick, *Acta Crystallogr., Sect. A: Found. Crystallogr.*, **2008**, *64*, 112.

[79] Y. El-Azizi, J. E. Zakarian, L. Bouillerand, A. R. Schmitzer, S. K. Collins, *Adv. Synth. Catal.* , **2008**, *350*, 2219.

[80] J. H. Hall, M. Gisler, *J. Org. Chem.*, **1976**, *41*, 3769.

Appendix

Part 1 $^{1}H/^{19}F$ NMR-titration curves of C_6F_5/CF_3 receptors with anions in solution

1.1 The interactions between C_6F_5-receptors and anions in solution

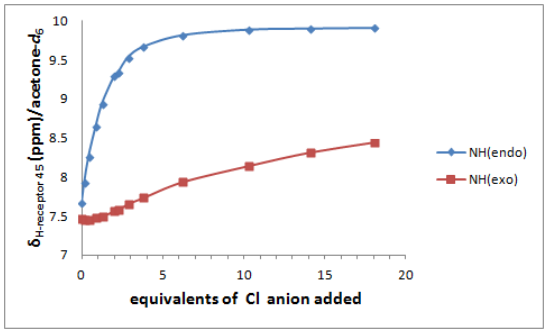

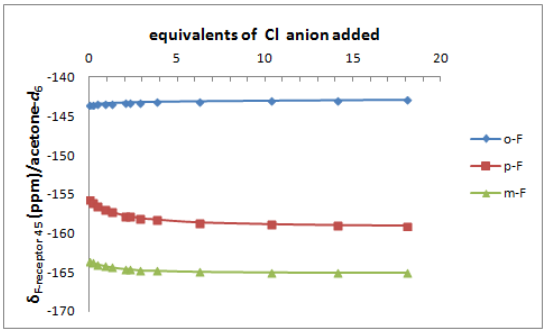

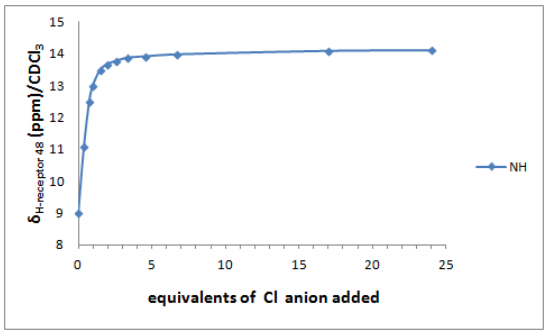

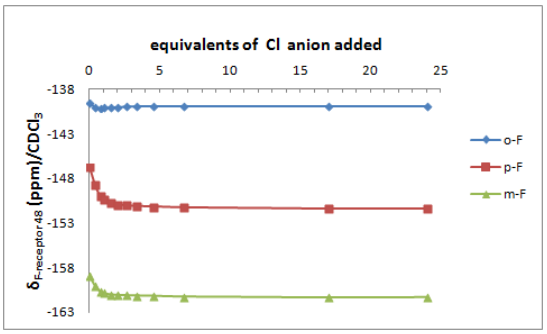

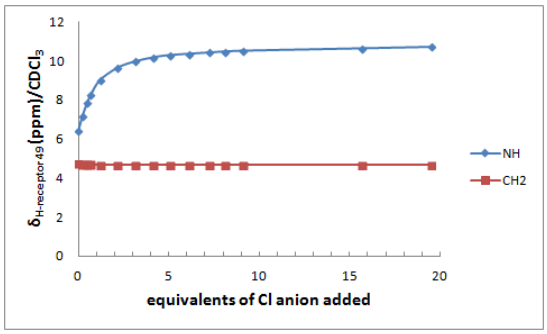

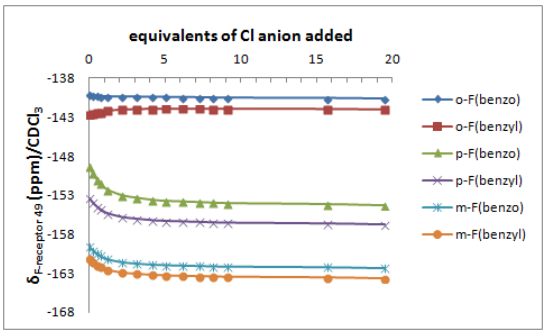

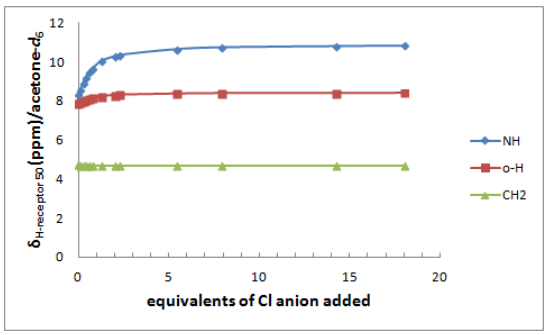

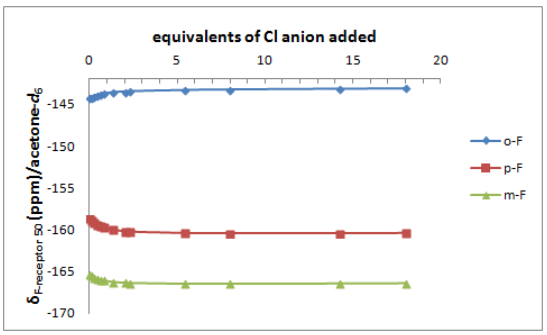

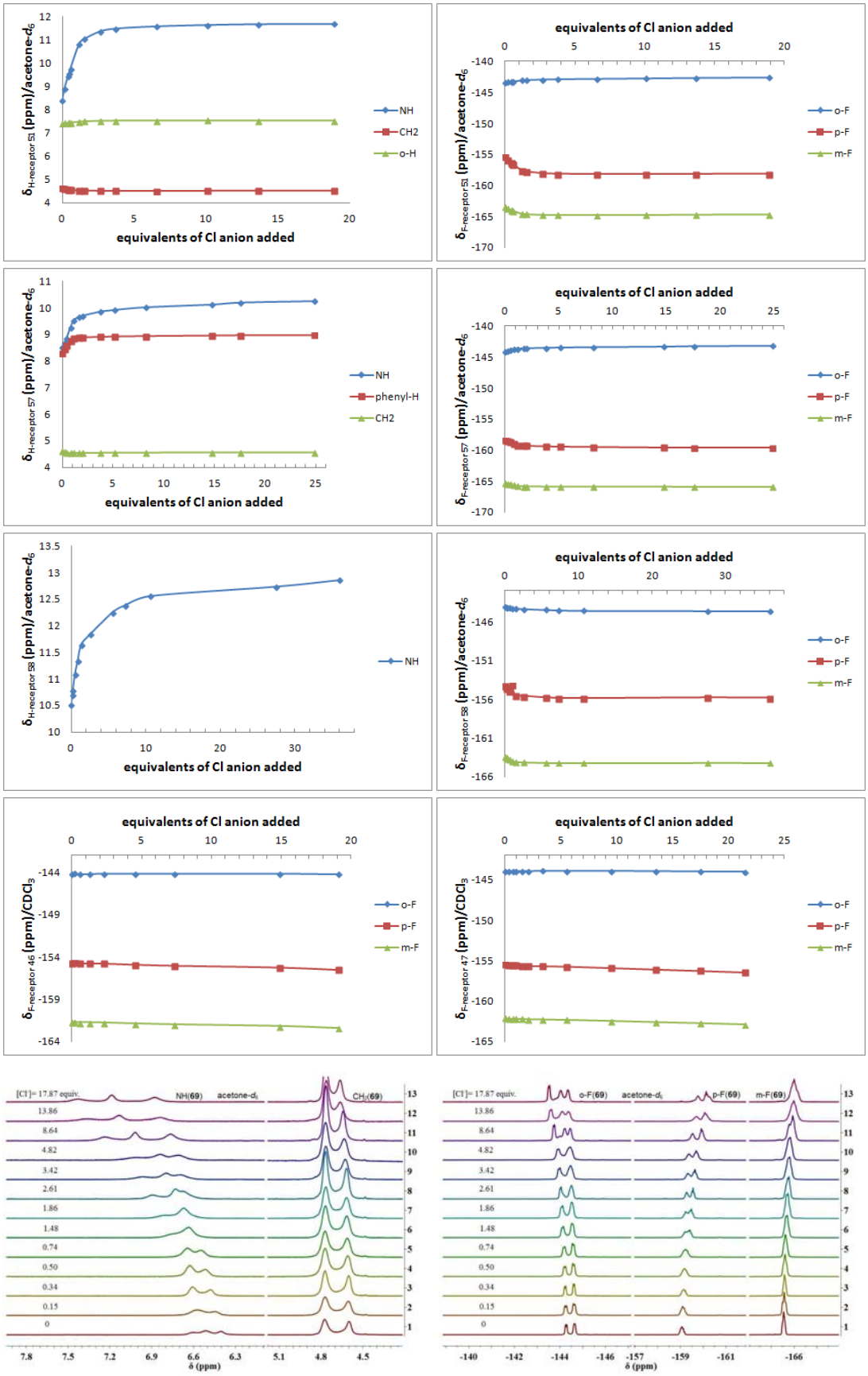

Figure S1. $^{1}H/^{19}F$ NMR chemical shifts of C_6F_5 receptors with the addition of TBA·Cl in $CDCl_3$ or acetone-d_6. (298 K)

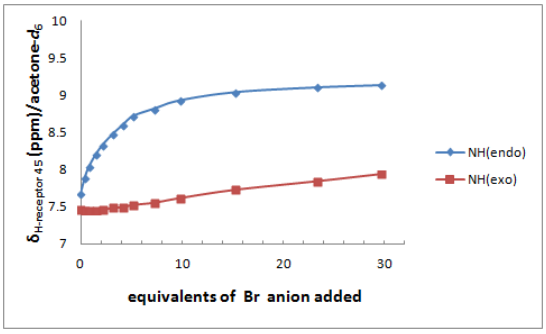
δH-receptor 45 (ppm)/acetone-d6
equivalents of Br anion added
NH(endo)
NH(exo)

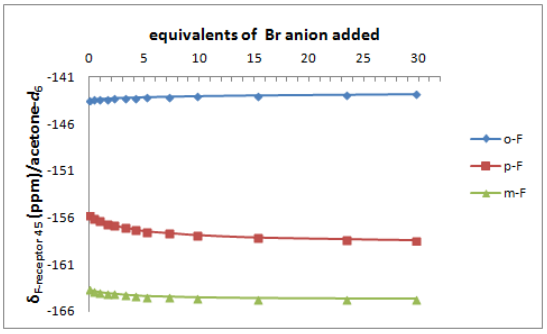
equivalents of Br anion added
δF-receptor 45 (ppm)/acetone-d6
o-F
p-F
m-F

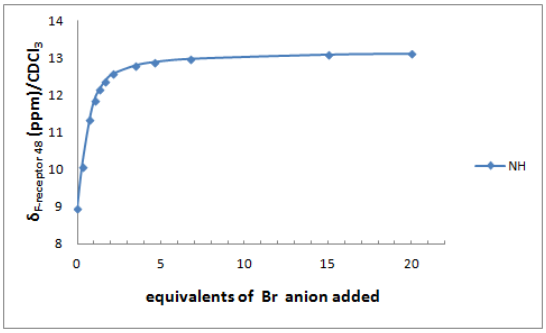
δF-receptor 48 (ppm)/CDCl3
equivalents of Br anion added
NH

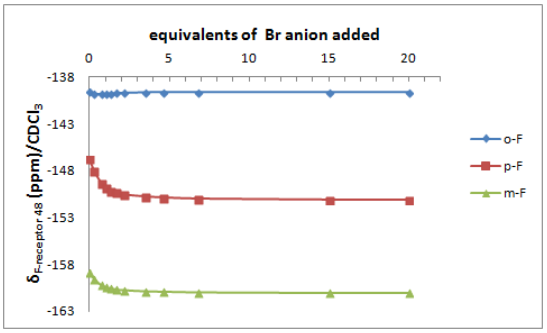
equivalents of Br anion added
δF-receptor 48 (ppm)/CDCl3
o-F
p-F
m-F

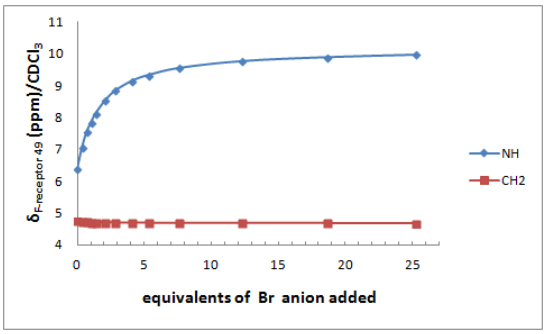
δF-receptor 49 (ppm)/CDCl3
equivalents of Br anion added
NH
CH2

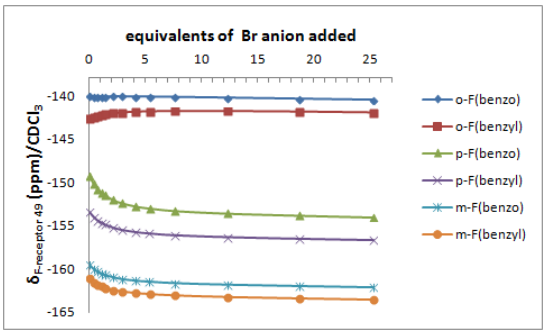
equivalents of Br anion added
δF-receptor 49 (ppm)/CDCl3
o-F(benzo)
o-F(benzyl)
p-F(benzo)
p-F(benzyl)
m-F(benzo)
m-F(benzyl)

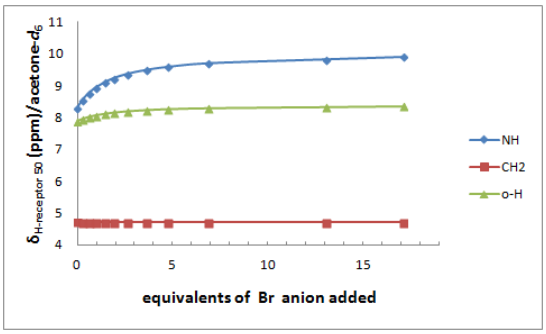
δH-receptor 50 (ppm)/acetone-d6
equivalents of Br anion added
NH
CH2
o-H

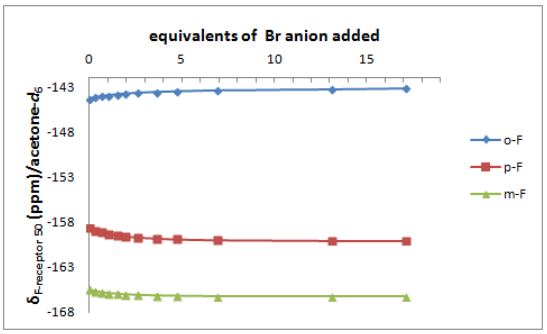
equivalents of Br anion added
δF-receptor 50 (ppm)/acetone-d6
o-F
p-F
m-F

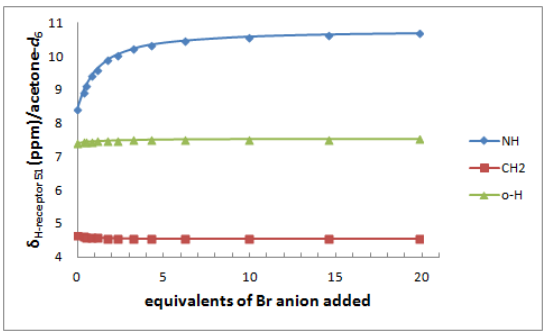
δH-receptor 51 (ppm)/acetone-d6
equivalents of Br anion added
NH
CH2
o-H

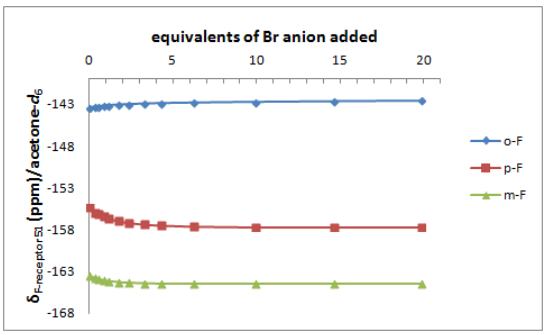
equivalents of Br anion added
δF-receptor 51 (ppm)/acetone-d6
o-F
p-F
m-F

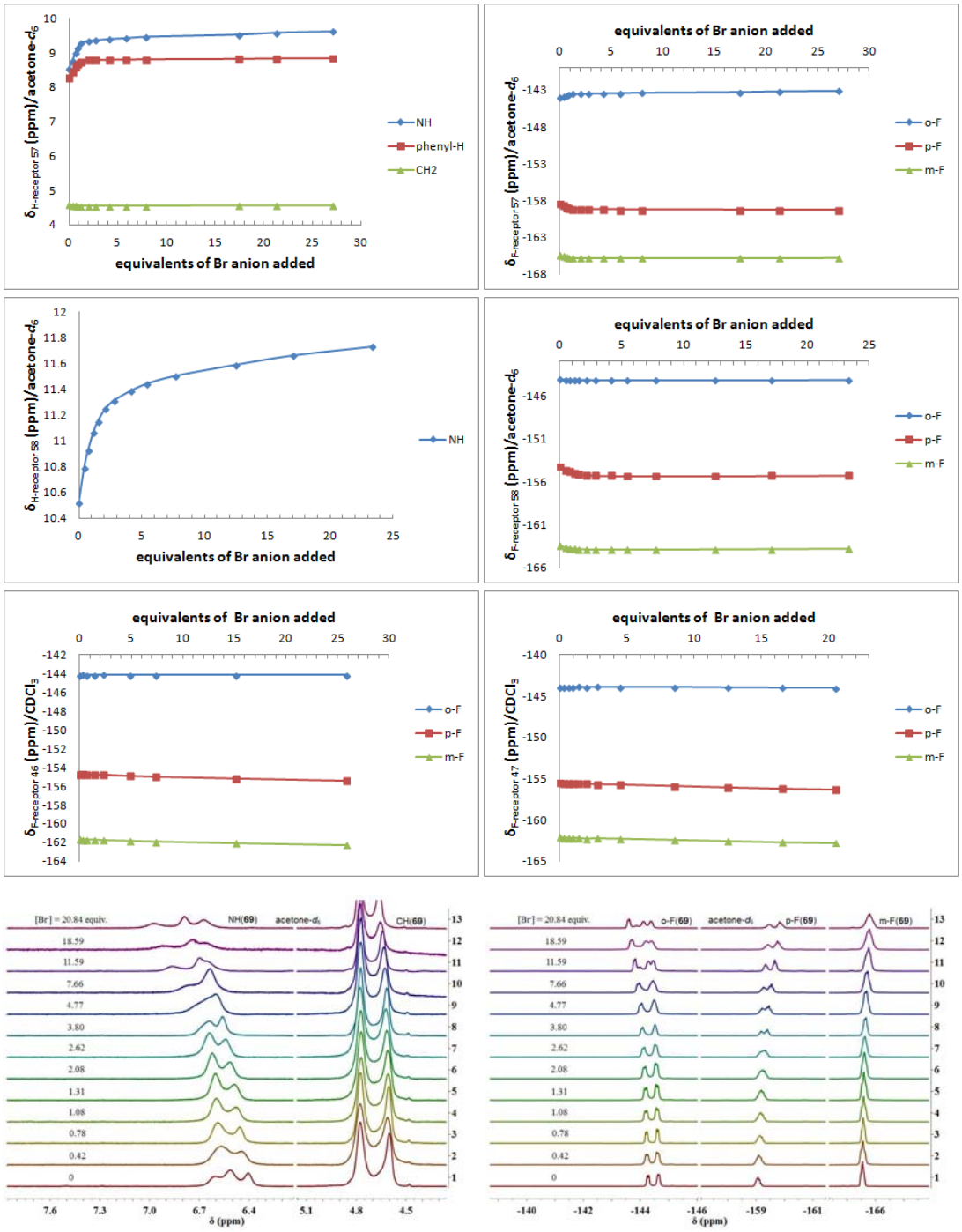

Figure S2. $^{1}H/^{19}F$ NMR chemical shifts of C_6F_5 receptors with the addition of TBA·Br in $CDCl_3$ or acetone-d_6. (298 K)

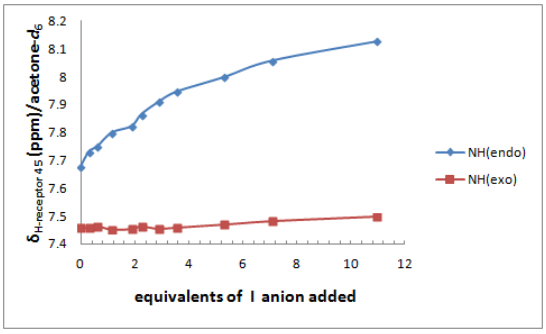
δH-receptor 45 (ppm)/acetone-d6
NH(endo)
NH(exo)
equivalents of I anion added

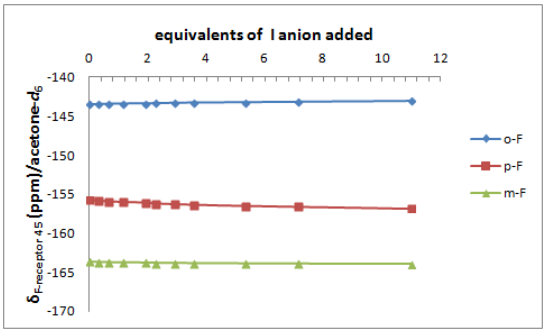
equivalents of I anion added
δF-receptor 45 (ppm)/acetone-d6
o-F
p-F
m-F

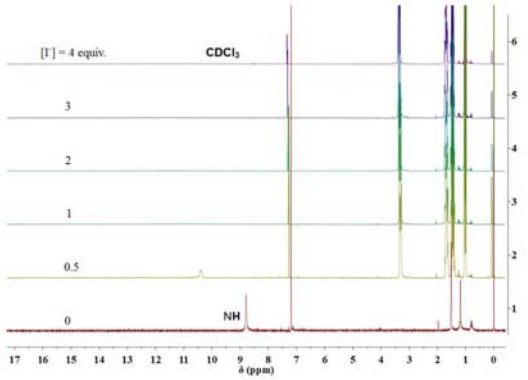
[I⁻] = 4 equiv.
CDCl3
3
2
1
0.5
0
NH
δ (ppm)

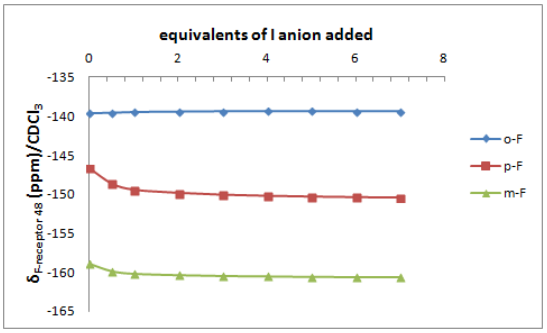
equivalents of I anion added
δF-receptor 48 (ppm)/CDCl3
o-F
p-F
m-F

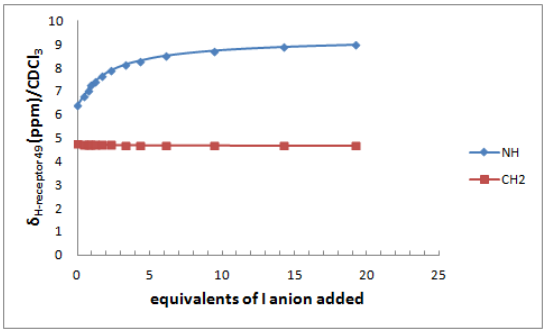
δH-receptor 49 (ppm)/CDCl3
NH
CH2
equivalents of I anion added

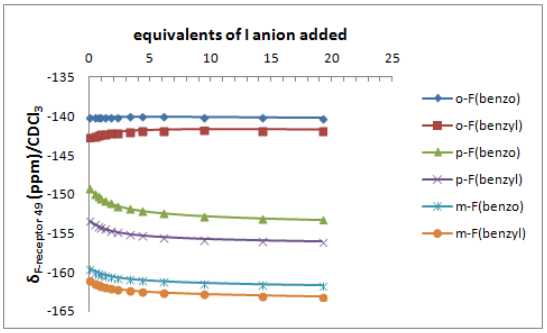
equivalents of I anion added
δF-receptor 49 (ppm)/CDCl3
o-F(benzo)
o-F(benzyl)
p-F(benzo)
p-F(benzyl)
m-F(benzo)
m-F(benzyl)

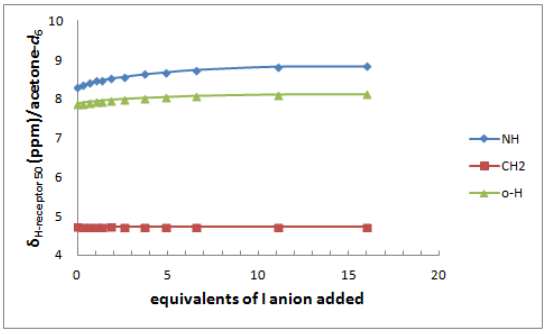
δH-receptor 50 (ppm)/acetone-d6
NH
CH2
o-H
equivalents of I anion added

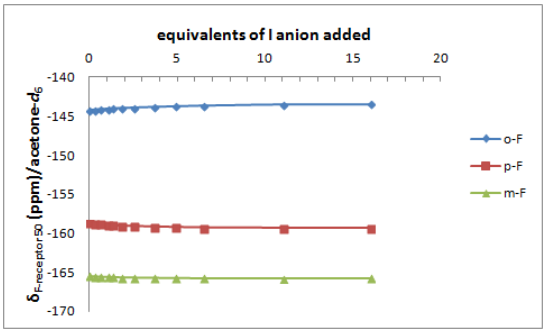
equivalents of I anion added
δF-receptor 50 (ppm)/acetone-d6
o-F
p-F
m-F

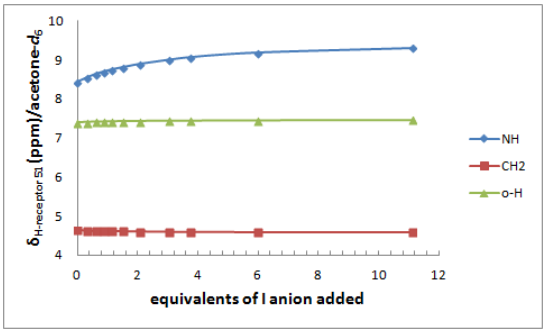
δH-receptor 51 (ppm)/acetone-d6
NH
CH2
o-H
equivalents of I anion added

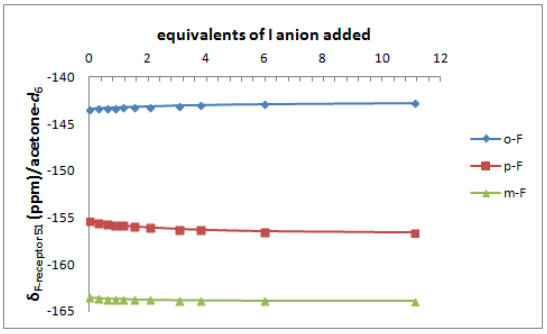
equivalents of I anion added
δF-receptor 51 (ppm)/acetone-d6
o-F
p-F
m-F

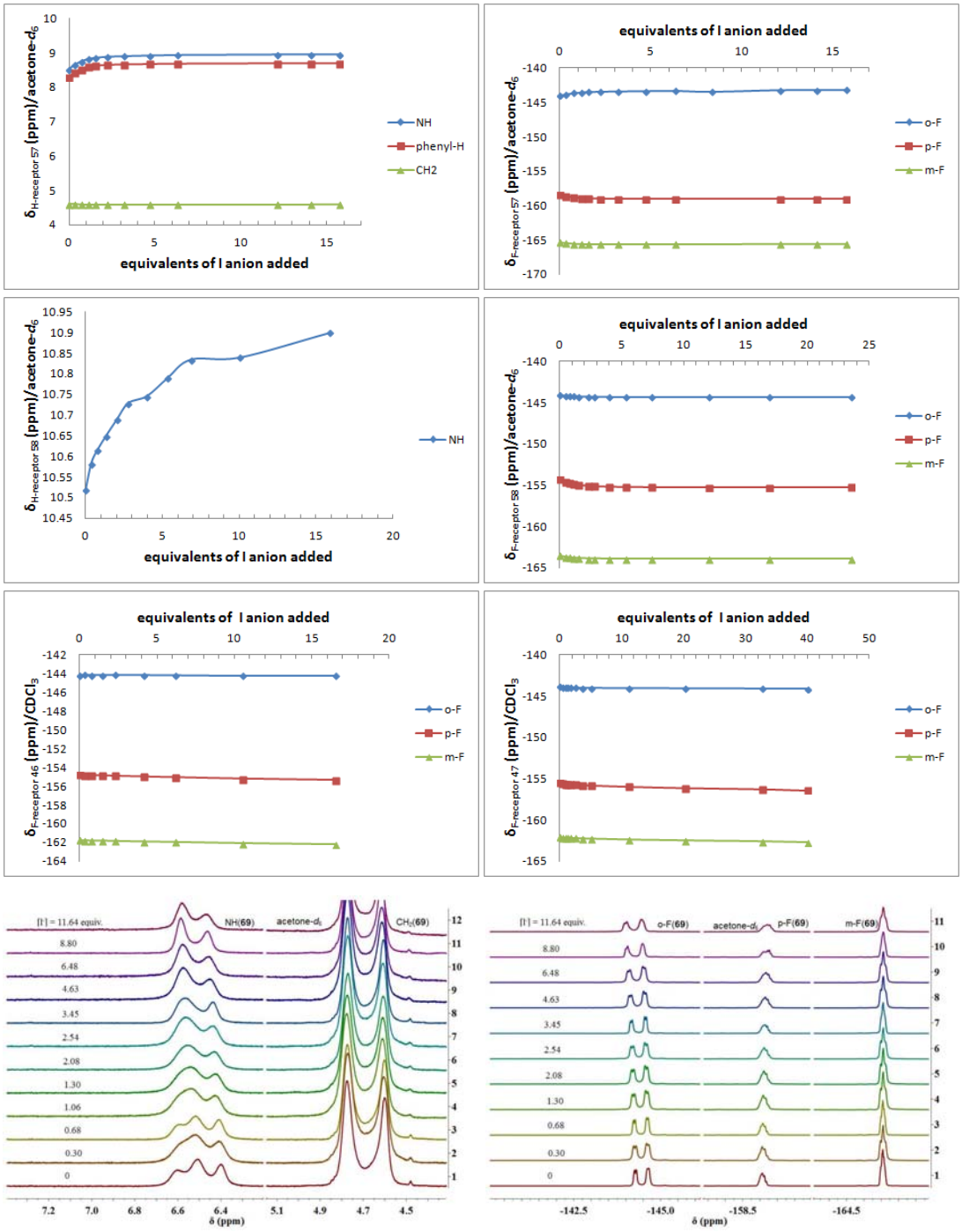

Figure S3. $^{1}H/^{19}F$ NMR chemical shifts of C_6F_5 receptors with the addition of TBA·I in $CDCl_3$ or acetone-d_6. (298 K)

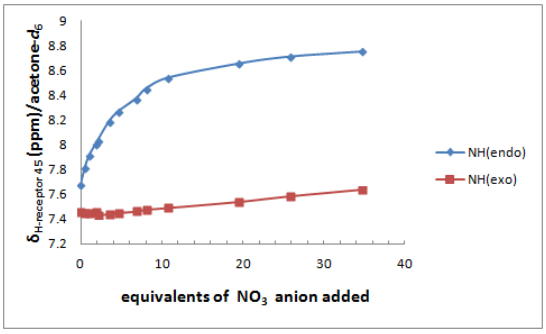
δH-receptor 45 (ppm)/acetone-d6
equivalents of NO3 anion added
NH(endo)
NH(exo)

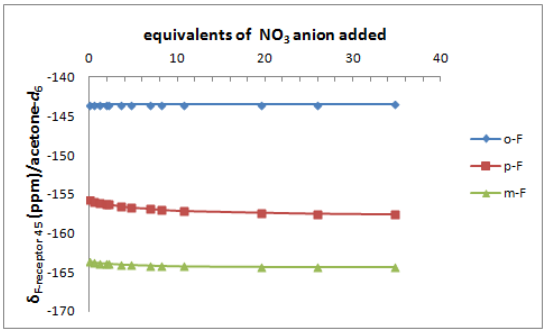
equivalents of NO3 anion added
δF-receptor 45 (ppm)/acetone-d6
o-F
p-F
m-F

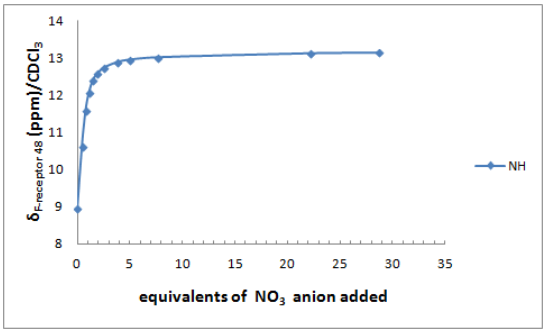
δF-receptor 48 (ppm)/CDCl3
equivalents of NO3 anion added
NH

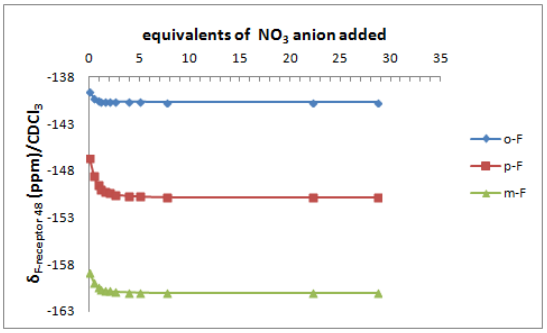
equivalents of NO3 anion added
δF-receptor 48 (ppm)/CDCl3
o-F
p-F
m-F

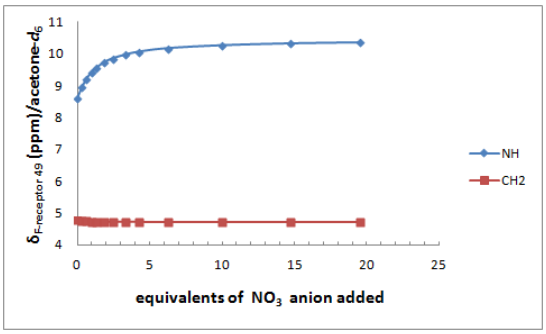
δF-receptor 49 (ppm)/acetone-d6
equivalents of NO3 anion added
NH
CH2

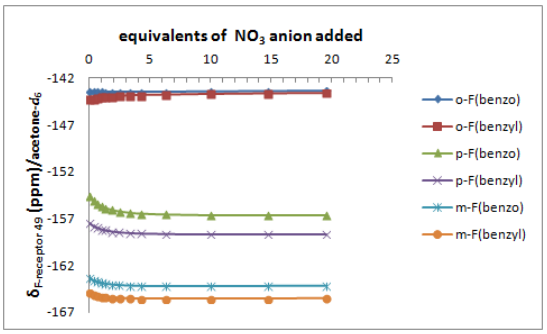
equivalents of NO3 anion added
δF-receptor 49 (ppm)/acetone-d6
o-F(benzo)
o-F(benzyl)
p-F(benzo)
p-F(benzyl)
m-F(benzo)
m-F(benzyl)

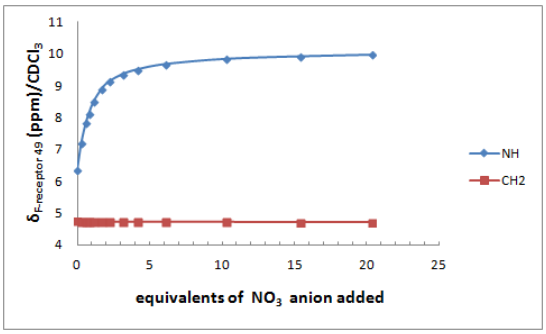
δF-receptor 49 (ppm)/CDCl3
equivalents of NO3 anion added
NH
CH2

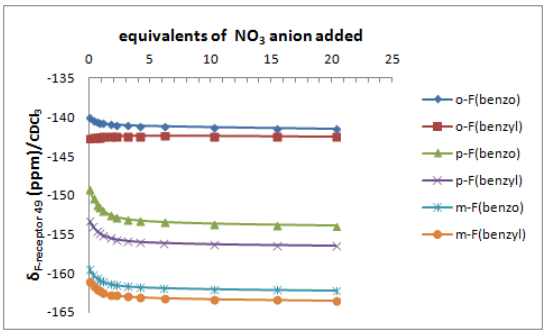
equivalents of NO3 anion added
δF-receptor 49 (ppm)/CDCl3
o-F(benzo)
o-F(benzyl)
p-F(benzo)
p-F(benzyl)
m-F(benzo)
m-F(benzyl)

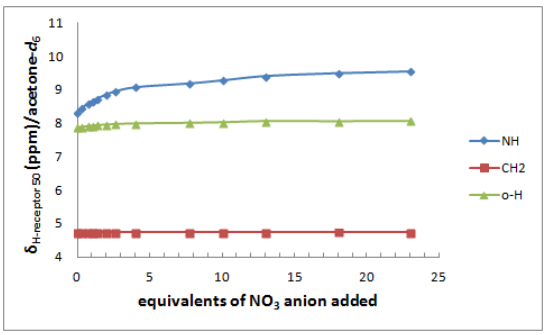
δH-receptor 50 (ppm)/acetone-d6
equivalents of NO3 anion added
NH
CH2
o-H

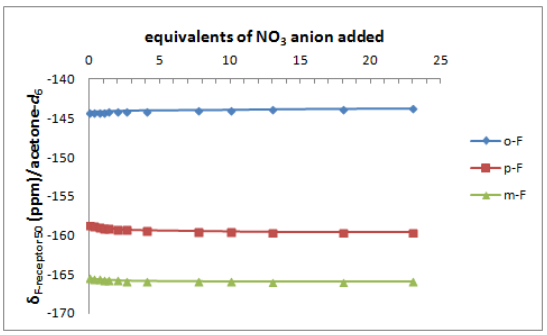
equivalents of NO3 anion added
δF-receptor 50 (ppm)/acetone-d6
o-F
p-F
m-F

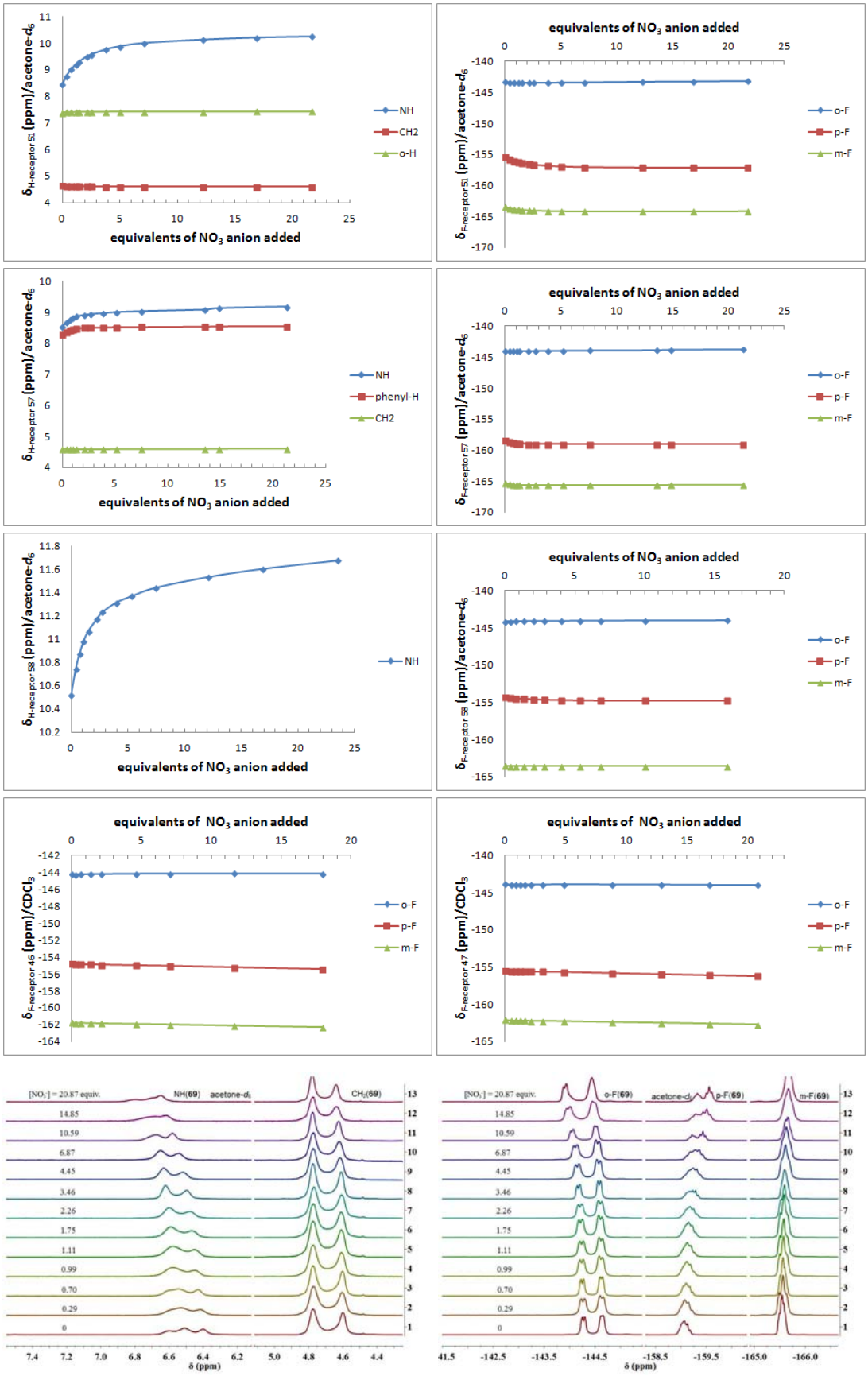

Figure S4. $^{1}H/^{19}F$ NMR chemical shifts of C_6F_5 receptors with the addition of TBA·NO_3 in $CDCl_3$ or acetone-d_6. (298 K)

1.2 The interactions between CF_3-receptors and anions in $CDCl_3$

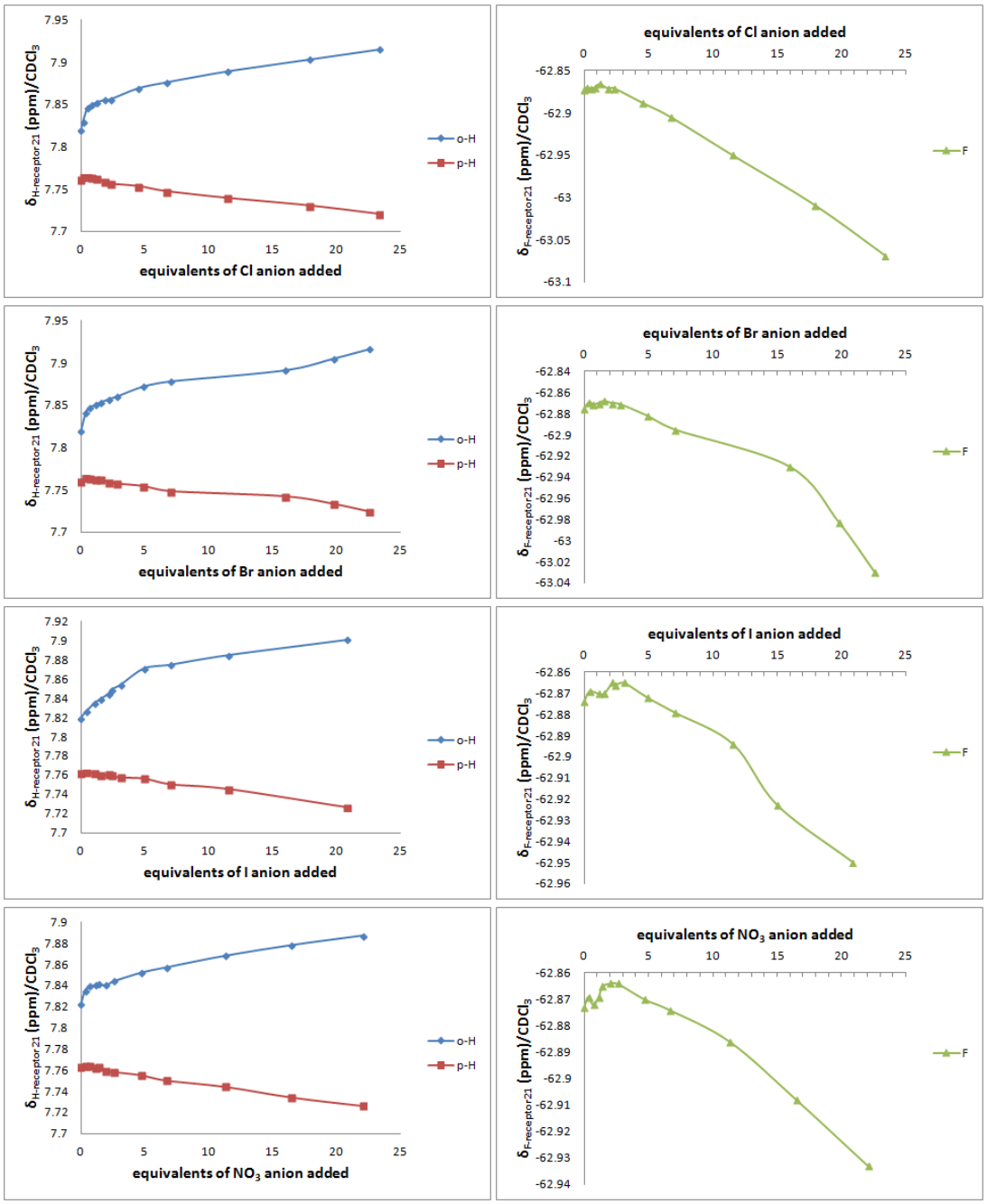

Figure S5. $^{1}H/^{19}F$ NMR chemical shifts of CF_3-receptor **21** with the addition of TBA·X (X = Cl, Br, I and NO_3) in $CDCl_3$. (298 K)

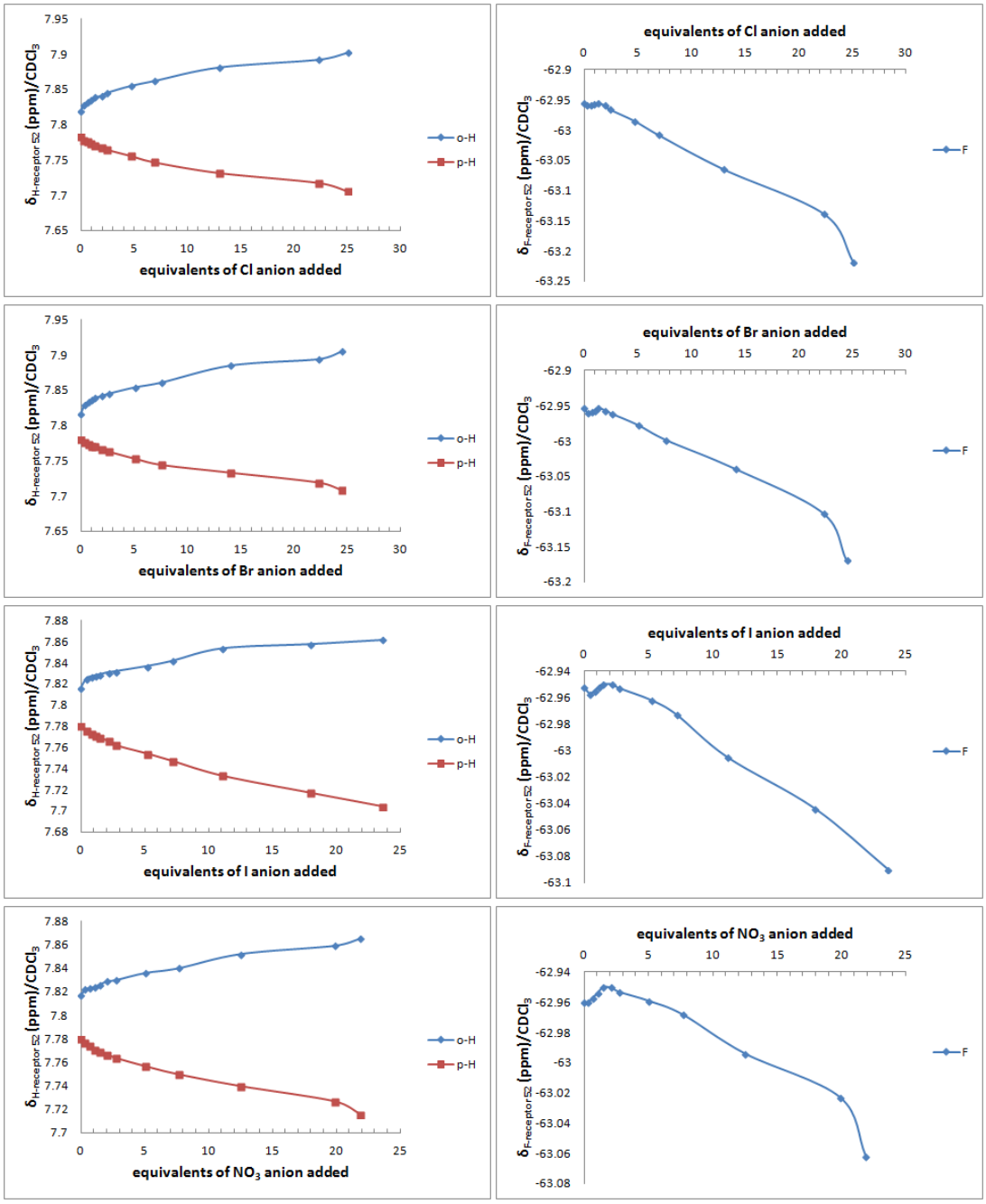

Figure S6. $^{1}H/^{19}F$ NMR chemical shifts of CF_3-receptor **52** with the addition of TBA·X (X = Cl, Br, I and NO_3) in $CDCl_3$. (298 K)

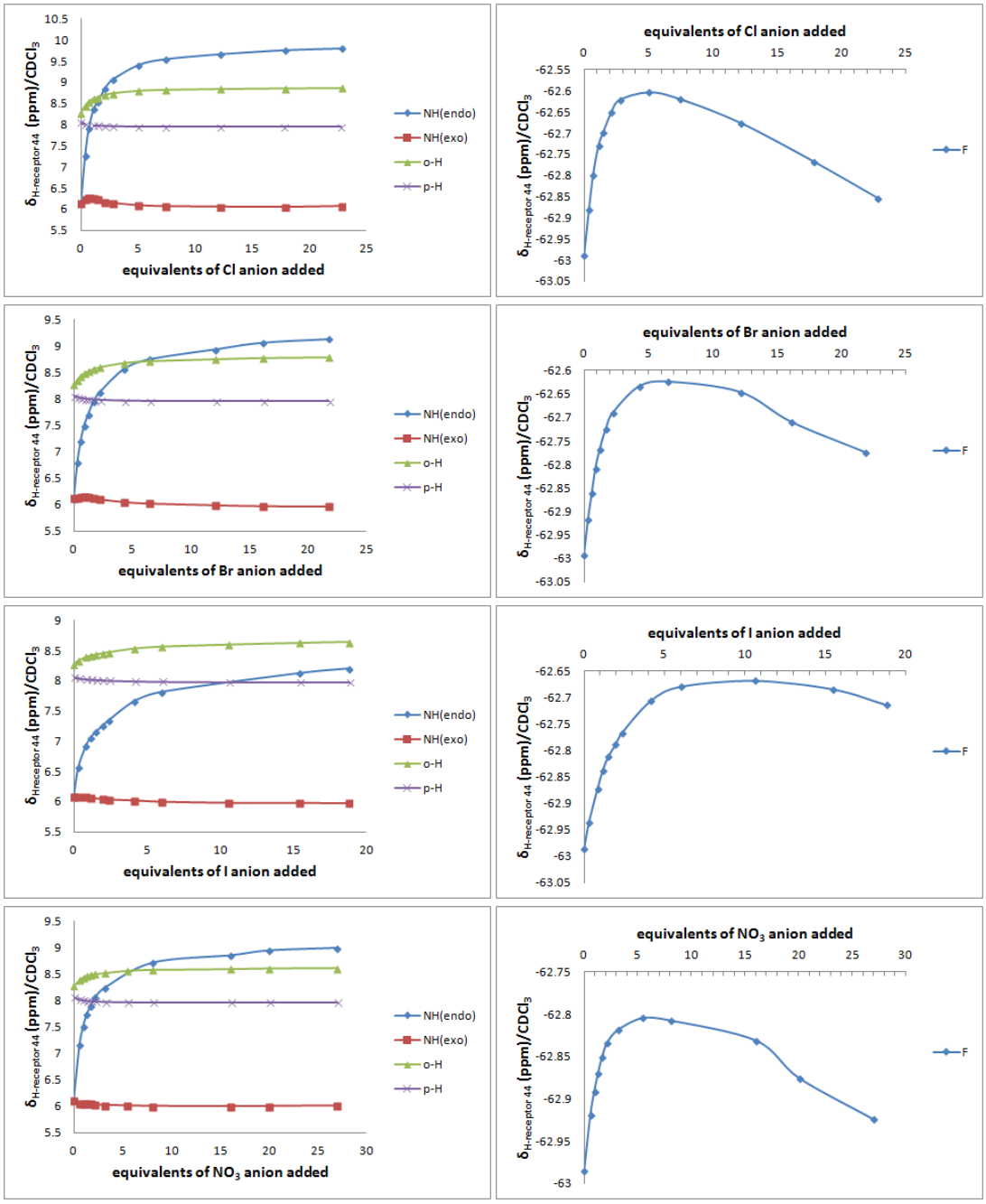

Figure S7. $^{1}H/^{19}F$ NMR chemical shifts of CF_3-receptor **44** with the addition of TBA·X (X = Cl, Br, I and NO_3) in $CDCl_3$. (298 K)

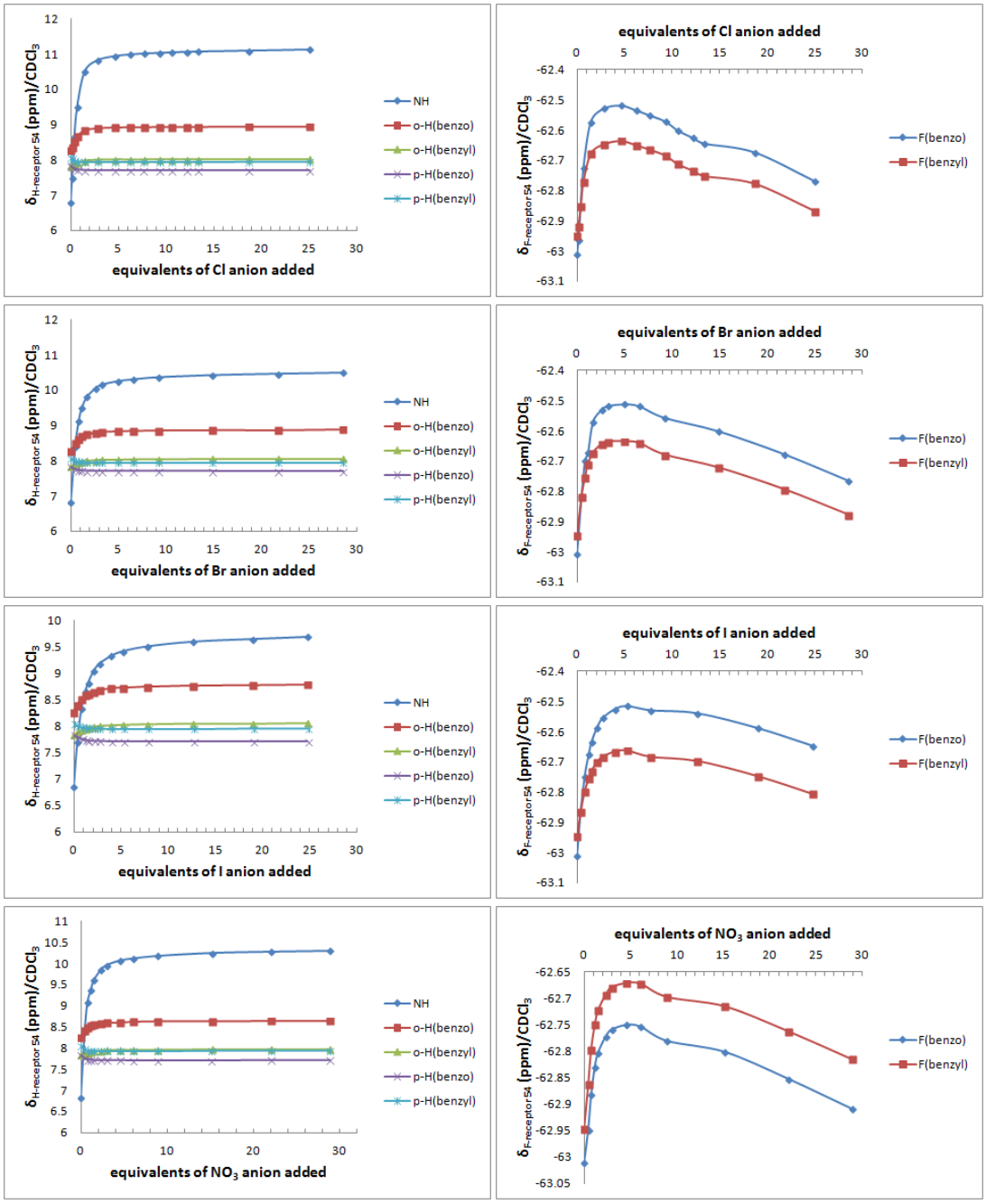

Figure S8. $^{1}H/^{19}F$ NMR chemical shifts of CF_3-receptor **54** with the addition of TBA·X (X = Cl, Br, I and NO_3) in $CDCl_3$. (298 K)

1.3 The interactions between CF_3-receptors and anions in acetone-d_6

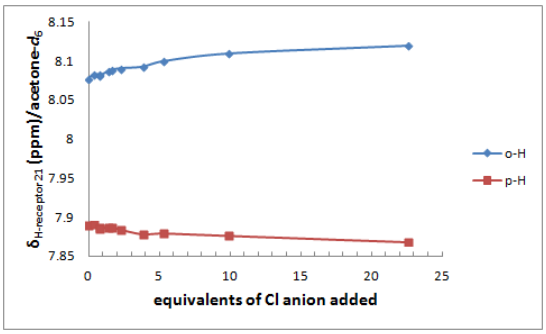

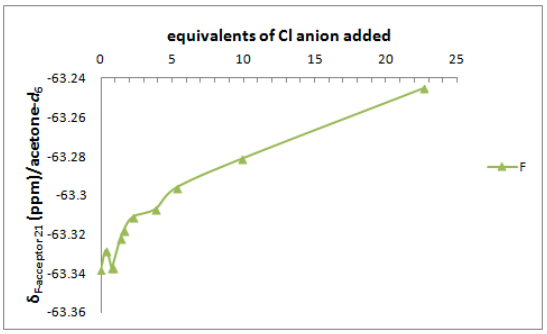

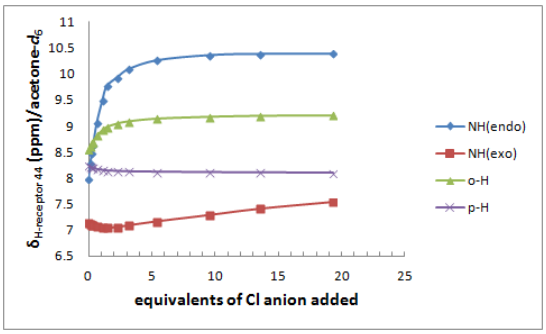

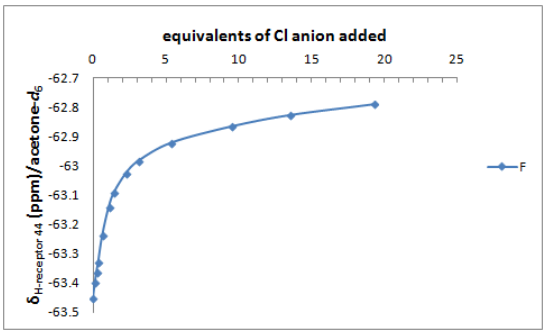

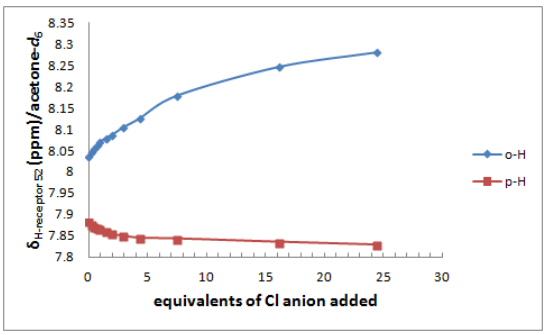

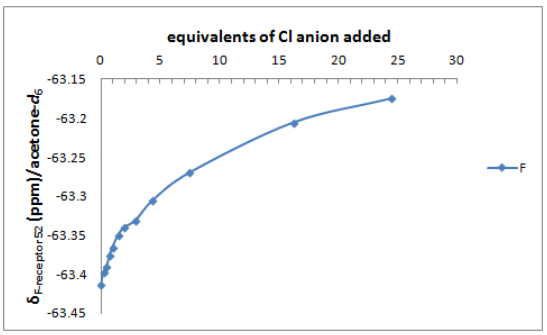

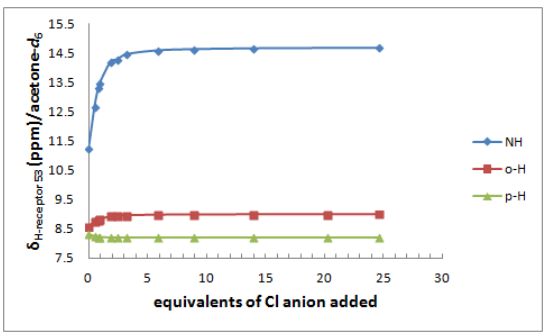

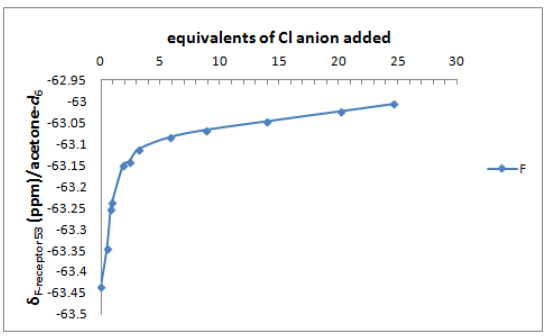

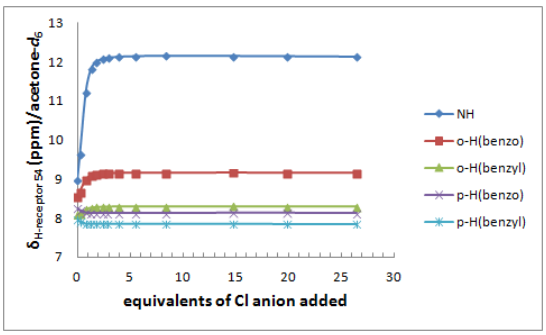

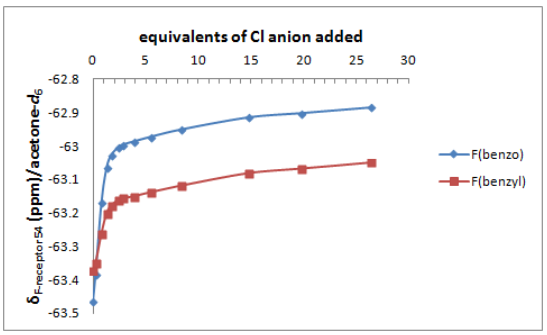

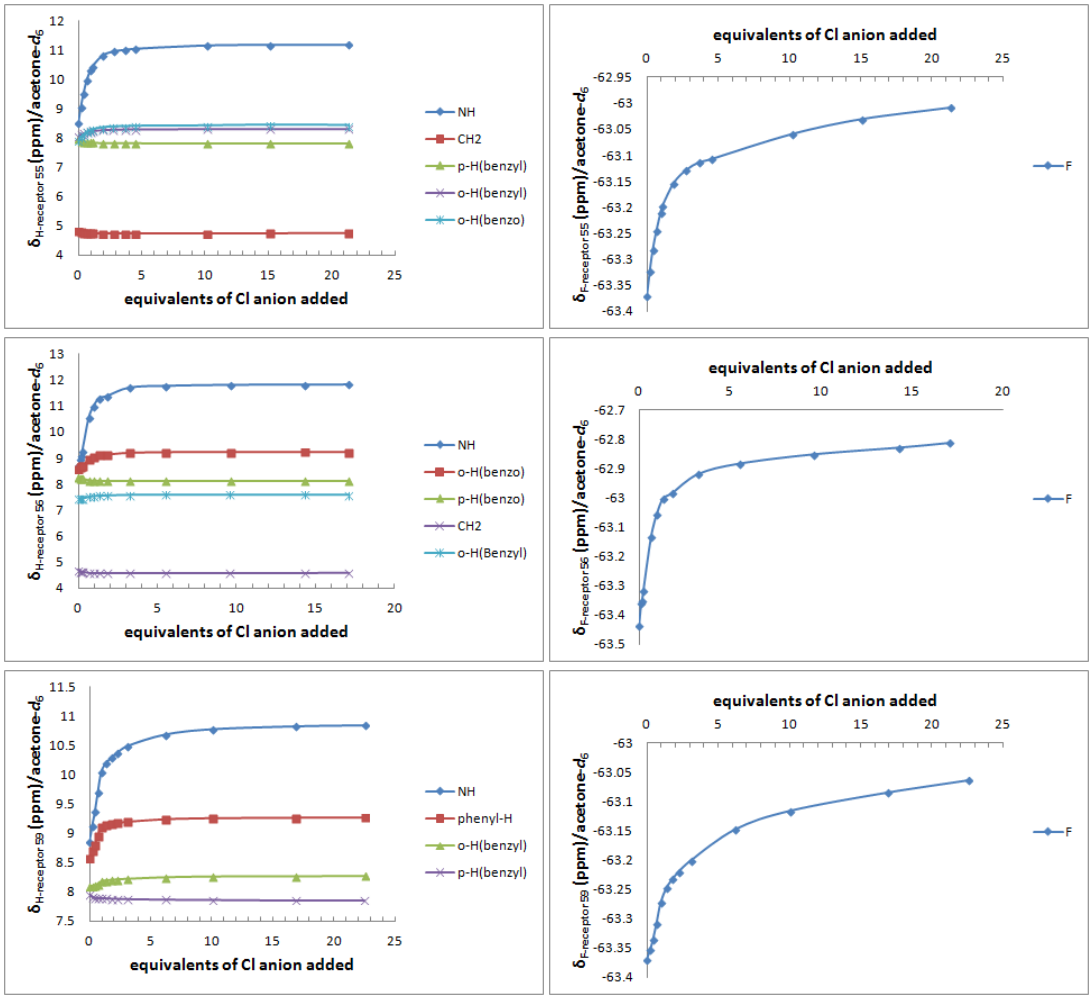

Figure S9. $^{1}H/^{19}F$ NMR chemical shifts of CF_3-receptors with the addition of TBA·Cl in acetone-d_6. (298 K)

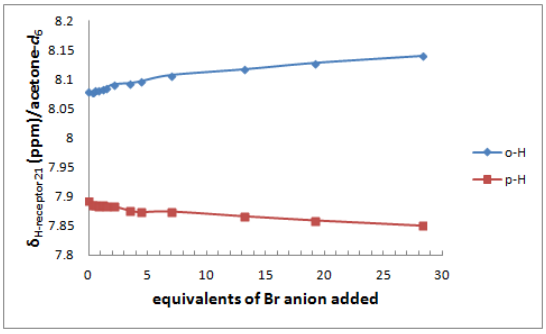
δH-receptor 21 (ppm)/acetone-d6
equivalents of Br anion added
o-H
p-H

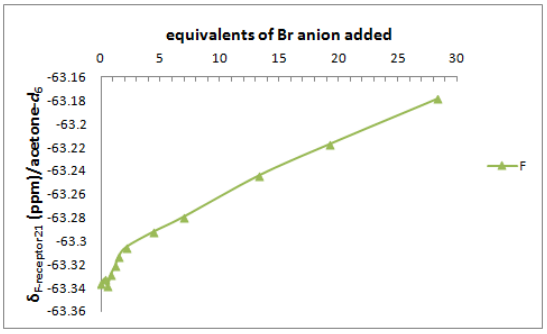
equivalents of Br anion added
δF-receptor 21 (ppm)/acetone-d6
F

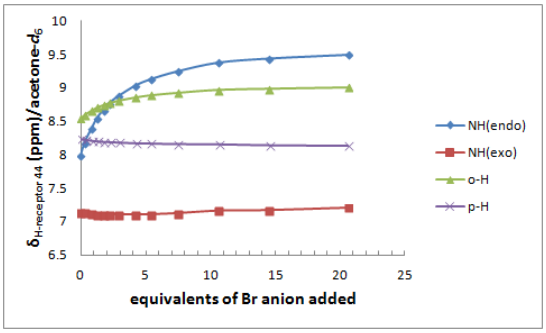
δH-receptor 44 (ppm)/acetone-d6
equivalents of Br anion added
NH(endo)
NH(exo)
o-H
p-H

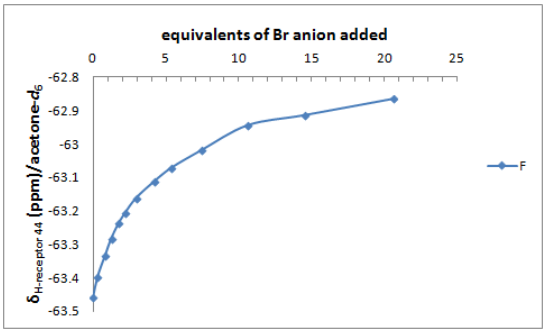
equivalents of Br anion added
δH-receptor 44 (ppm)/acetone-d6
F

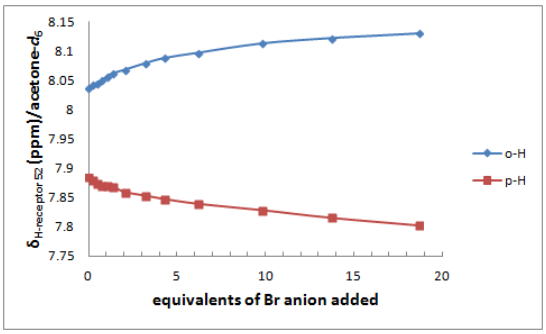
δH-receptor 52 (ppm)/acetone-d6
equivalents of Br anion added
o-H
p-H

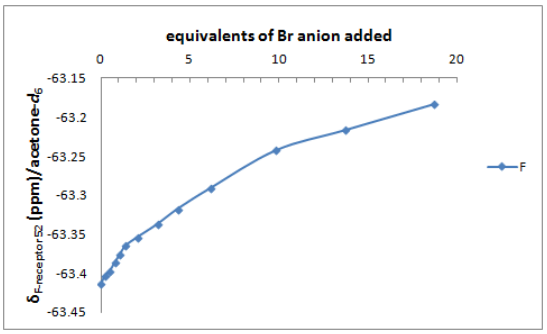
equivalents of Br anion added
δF-receptor 52 (ppm)/acetone-d6
F

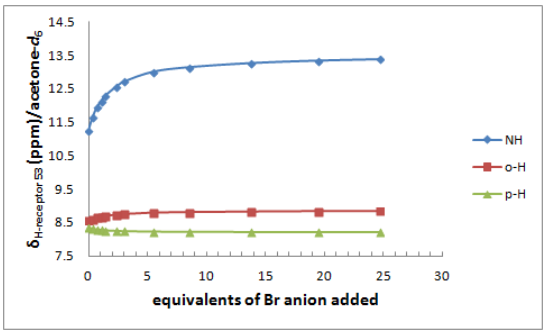
δH-receptor 53 (ppm)/acetone-d6
equivalents of Br anion added
NH
o-H
p-H

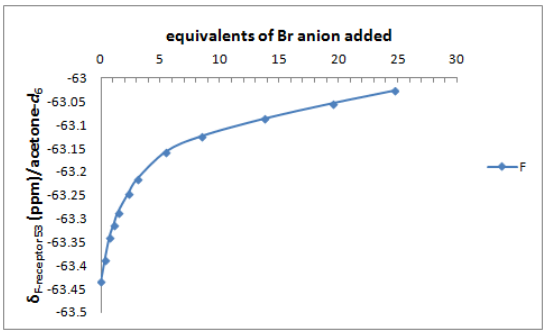
equivalents of Br anion added
δF-receptor 53 (ppm)/acetone-d6
F

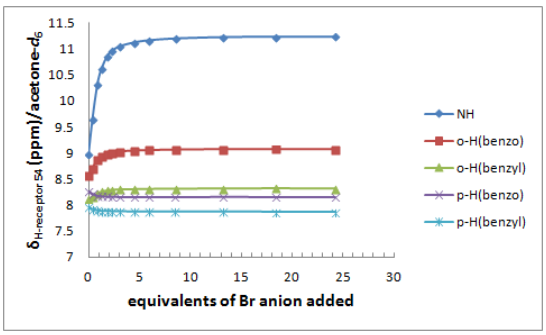
δH-receptor 54 (ppm)/acetone-d6
equivalents of Br anion added
NH
o-H(benzo)
o-H(benzyl)
p-H(benzo)
p-H(benzyl)

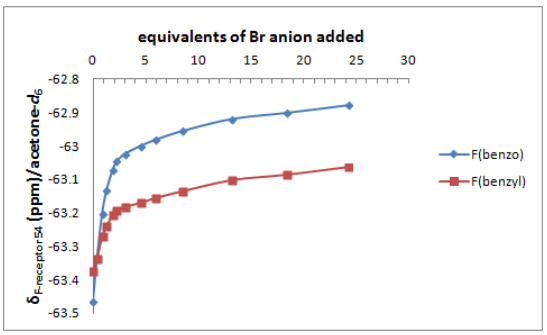
equivalents of Br anion added
δF-receptor 54 (ppm)/acetone-d6
F(benzo)
F(benzyl)

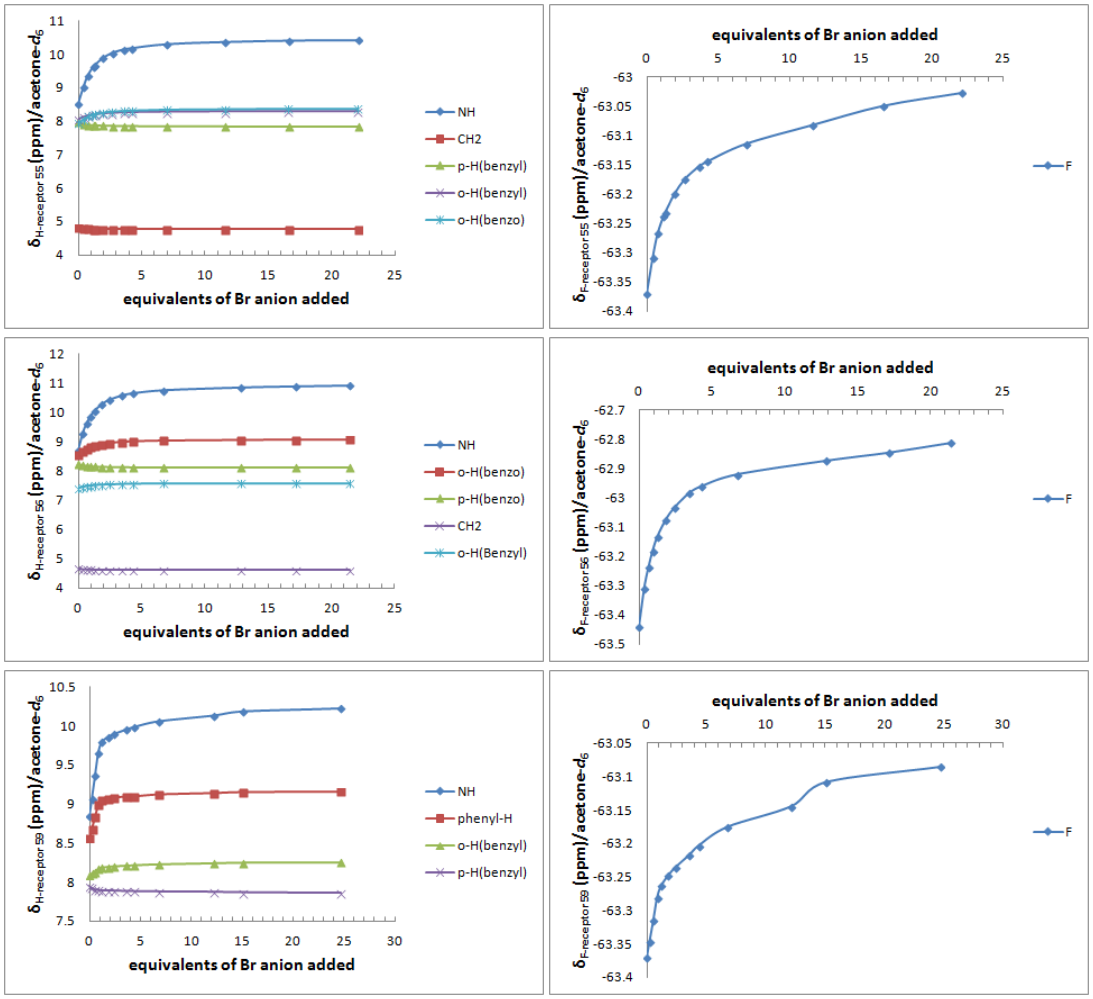

Figure S10. $^{1}H/^{19}F$ NMR chemical shifts of CF_3-receptors with the addition of TBA·Br in acetone-d_6. (298 K)

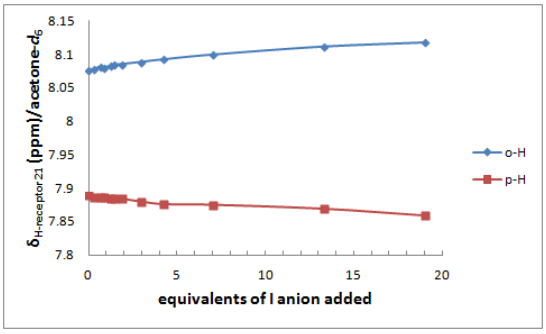
δH-receptor 21 (ppm)/acetone-d6
8.15
8.1
8.05
8
7.95
7.9
7.85
7.8
0
5
10
15
20
equivalents of I anion added
o-H
p-H

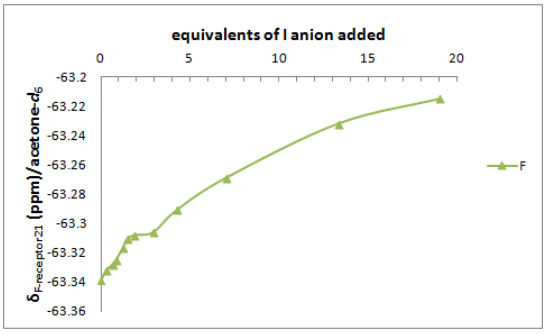
equivalents of I anion added
0
5
10
15
20
δF-receptor 21 (ppm)/acetone-d6
-63.2
-63.22
-63.24
-63.26
-63.28
-63.3
-63.32
-63.34
-63.36
F

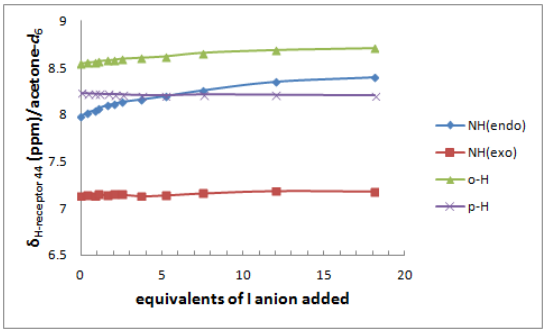
δH-receptor 44 (ppm)/acetone-d6
9
8.5
8
7.5
7
6.5
0
5
10
15
20
equivalents of I anion added
NH(endo)
NH(exo)
o-H
p-H

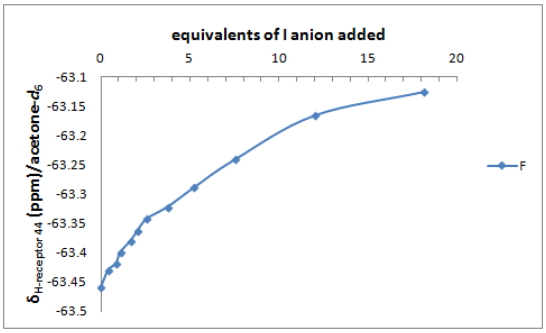
equivalents of I anion added
0
5
10
15
20
δF-receptor 44 (ppm)/acetone-d6
-63.1
-63.15
-63.2
-63.25
-63.3
-63.35
-63.4
-63.45
-63.5
F

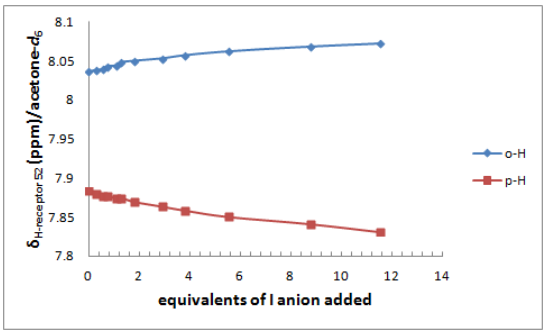
δH-receptor 52 (ppm)/acetone-d6
8.1
8.05
8
7.95
7.9
7.85
7.8
0
2
4
6
8
10
12
14
equivalents of I anion added
o-H
p-H

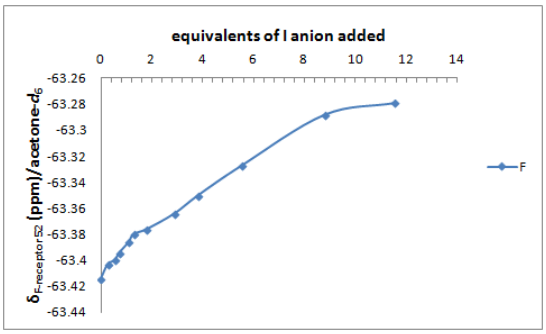
equivalents of I anion added
0
2
4
6
8
10
12
14
δF-receptor 52 (ppm)/acetone-d6
-63.26
-63.28
-63.3
-63.32
-63.34
-63.36
-63.38
-63.4
-63.42
-63.44
F

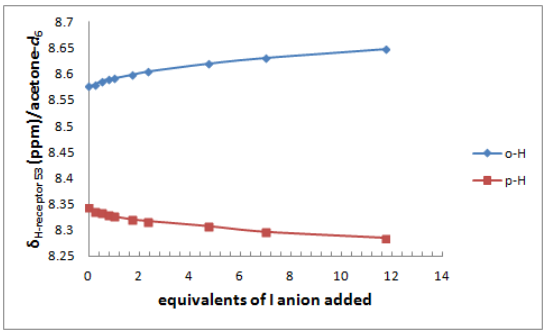
δH-receptor 53 (ppm)/acetone-d6
8.7
8.65
8.6
8.55
8.5
8.45
8.4
8.35
8.3
8.25
0
2
4
6
8
10
12
14
equivalents of I anion added
o-H
p-H

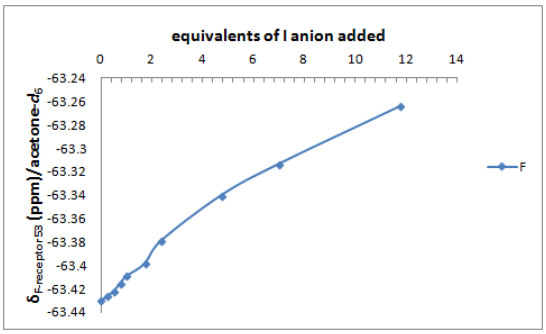
equivalents of I anion added
0
2
4
6
8
10
12
14
δF-receptor 53 (ppm)/acetone-d6
-63.24
-63.26
-63.28
-63.3
-63.32
-63.34
-63.36
-63.38
-63.4
-63.42
-63.44
F

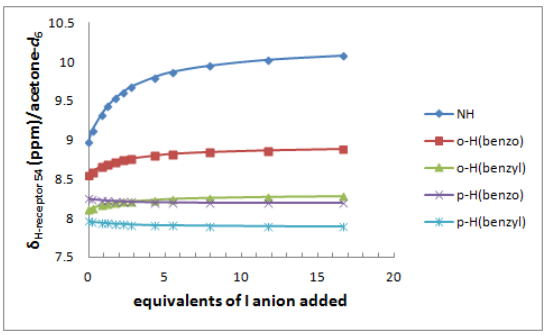
δH-receptor 54 (ppm)/acetone-d6
10.5
10
9.5
9
8.5
8
7.5
0
5
10
15
20
equivalents of I anion added
NH
o-H(benzo)
o-H(benzyl)
p-H(benzo)
p-H(benzyl)

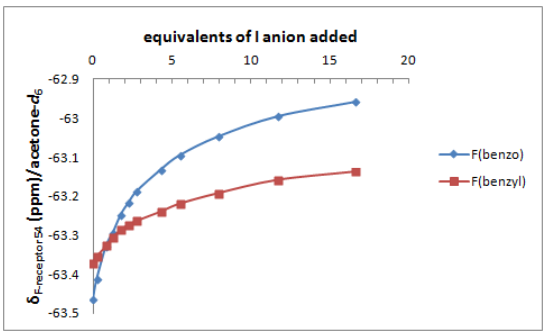
equivalents of I anion added
0
5
10
15
20
δF-receptor 54 (ppm)/acetone-d6
-62.9
-63
-63.1
-63.2
-63.3
-63.4
-63.5
F(benzo)
F(benzyl)

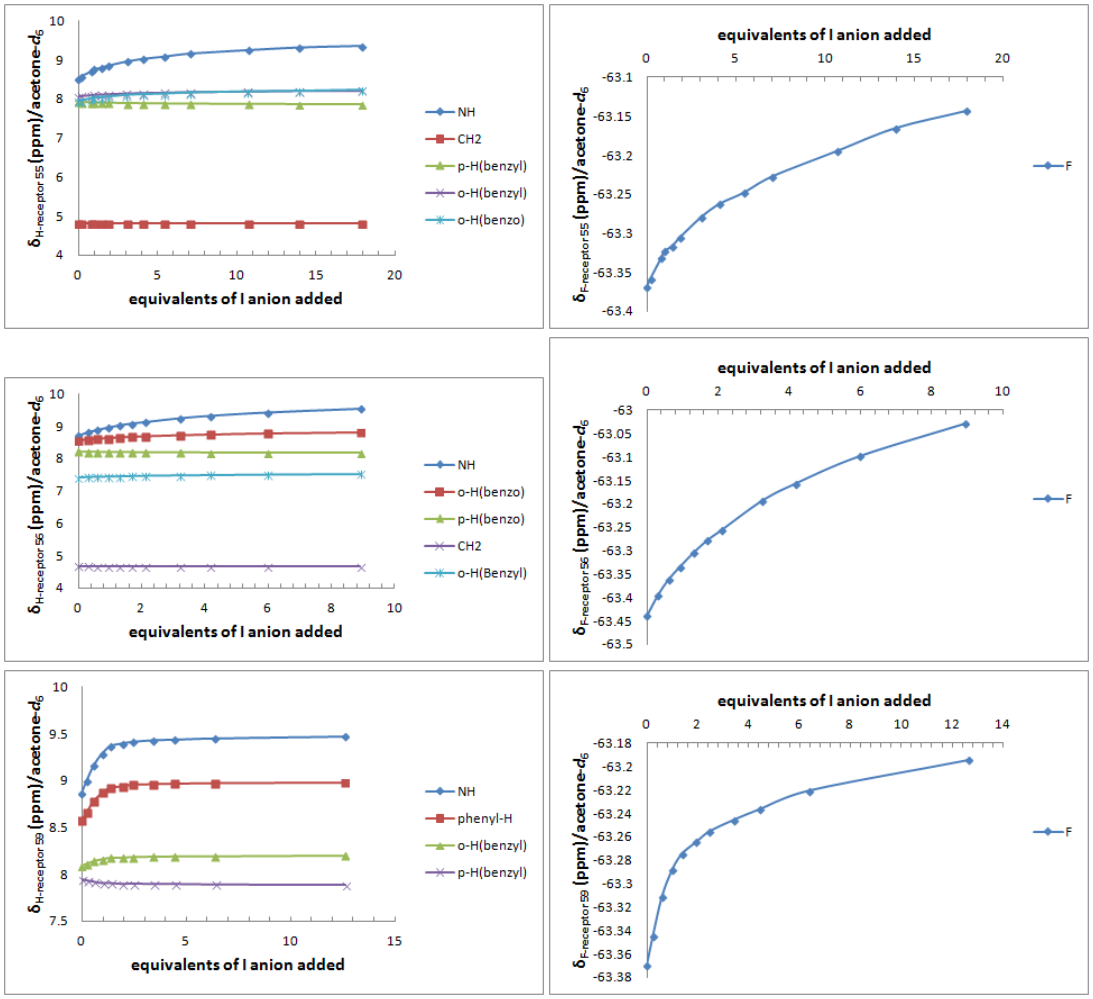

Figure S11. $^{1}H/^{19}F$ NMR chemical shifts of CF_3-receptors with the addition of TBA·I in acetone-d_6. (298 K)

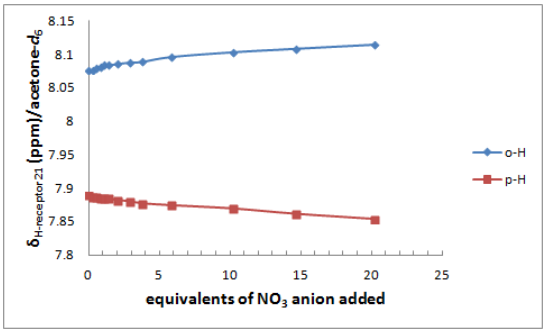
δH-receptor 21 (ppm)/acetone-d6
equivalents of NO3 anion added
o-H
p-H

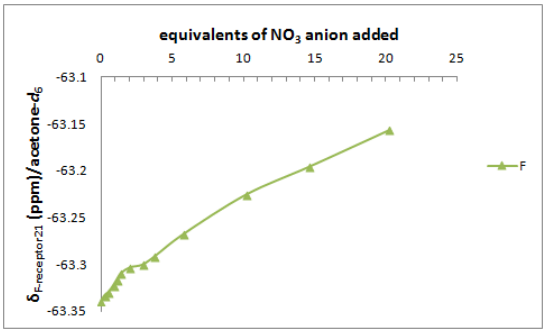
equivalents of NO3 anion added
δF-receptor 21 (ppm)/acetone-d6
F

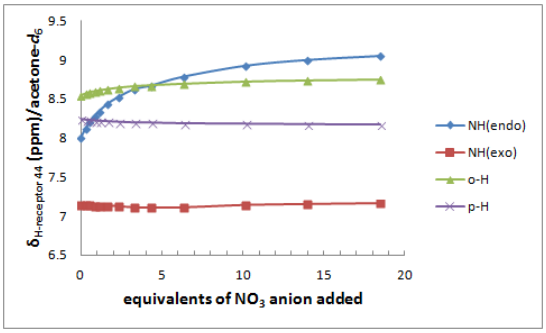
δH-receptor 44 (ppm)/acetone-d6
equivalents of NO3 anion added
NH(endo)
NH(exo)
o-H
p-H

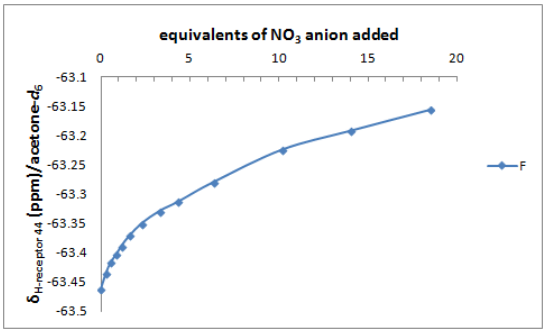
equivalents of NO3 anion added
δH-receptor 44 (ppm)/acetone-d6
F

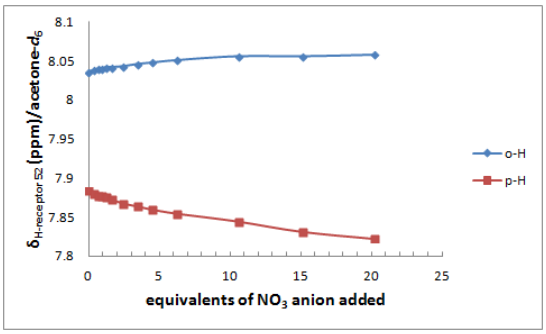
δH-receptor 52 (ppm)/acetone-d6
equivalents of NO3 anion added
o-H
p-H

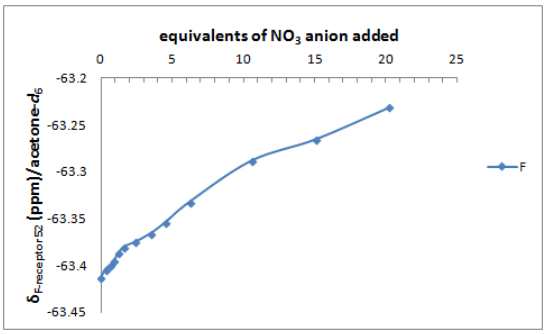
equivalents of NO3 anion added
δF-receptor 52 (ppm)/acetone-d6
F

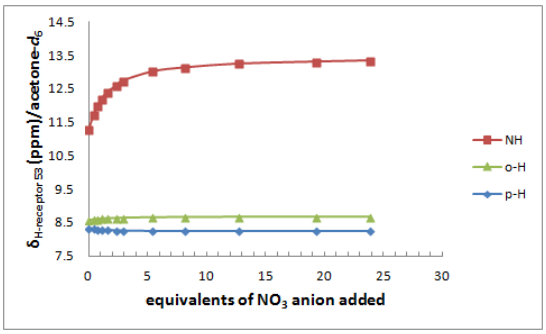
δH-receptor 53 (ppm)/acetone-d6
equivalents of NO3 anion added
NH
o-H
p-H

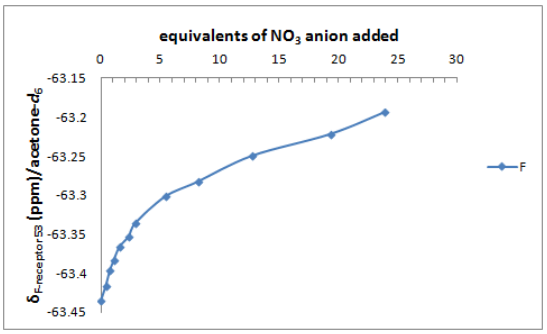
equivalents of NO3 anion added
δF-receptor 53 (ppm)/acetone-d6
F

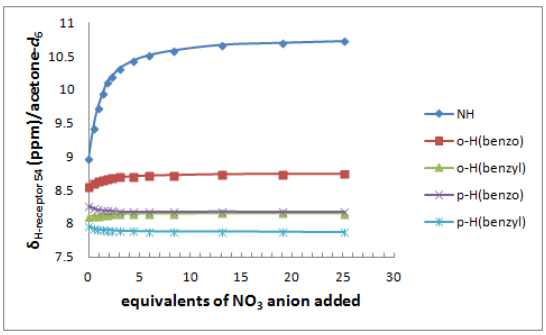
δH-receptor 54 (ppm)/acetone-d6
equivalents of NO3 anion added
NH
o-H(benzo)
o-H(benzyl)
p-H(benzo)
p-H(benzyl)

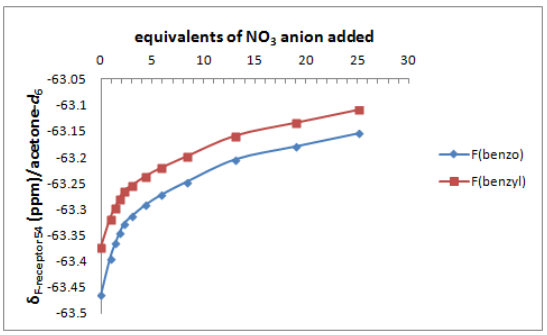
equivalents of NO3 anion added
δF-receptor 54 (ppm)/acetone-d6
F(benzo)
F(benzyl)

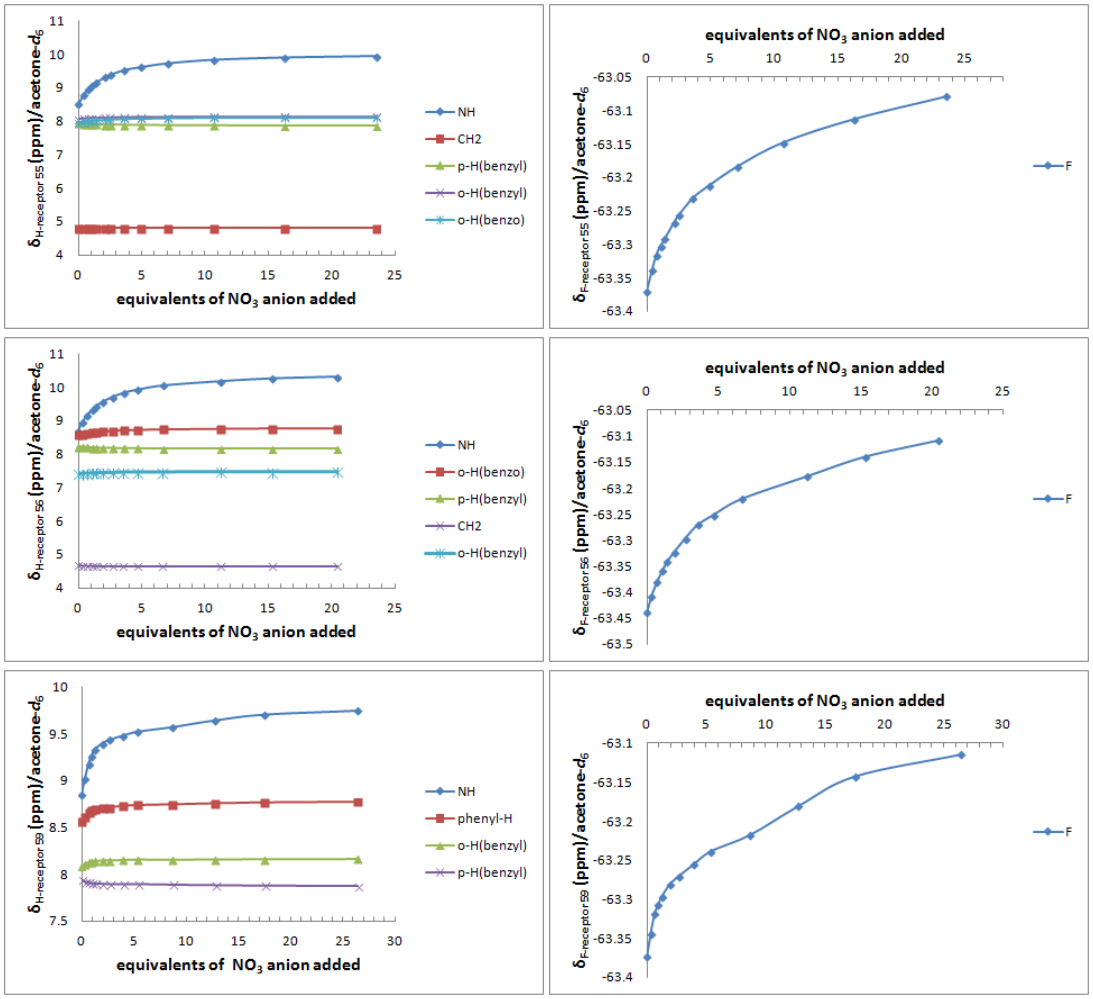

Figure S12. $^{1}H/^{19}F$ NMR chemical shifts of CF_3-receptors with the addition of TBA·NO_3 in acetone-d_6. (298 K)

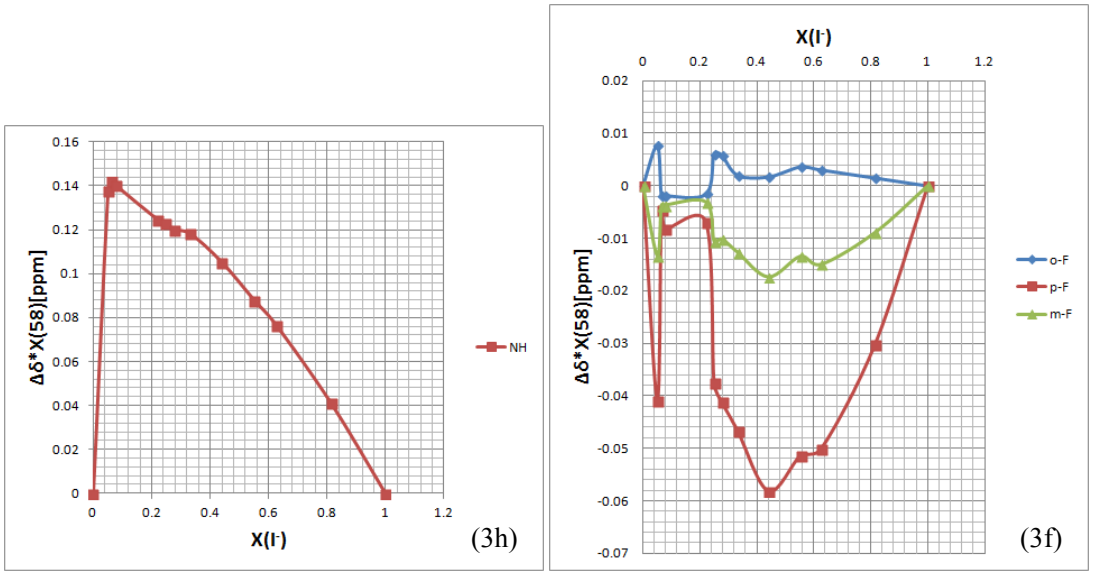

Figure S13. Job-plots of receptor **58** with I⁻. The data calculated were obtained from $^{1}H/^{19}F$ NMR spectra in acetone-d_6 at room temperature.

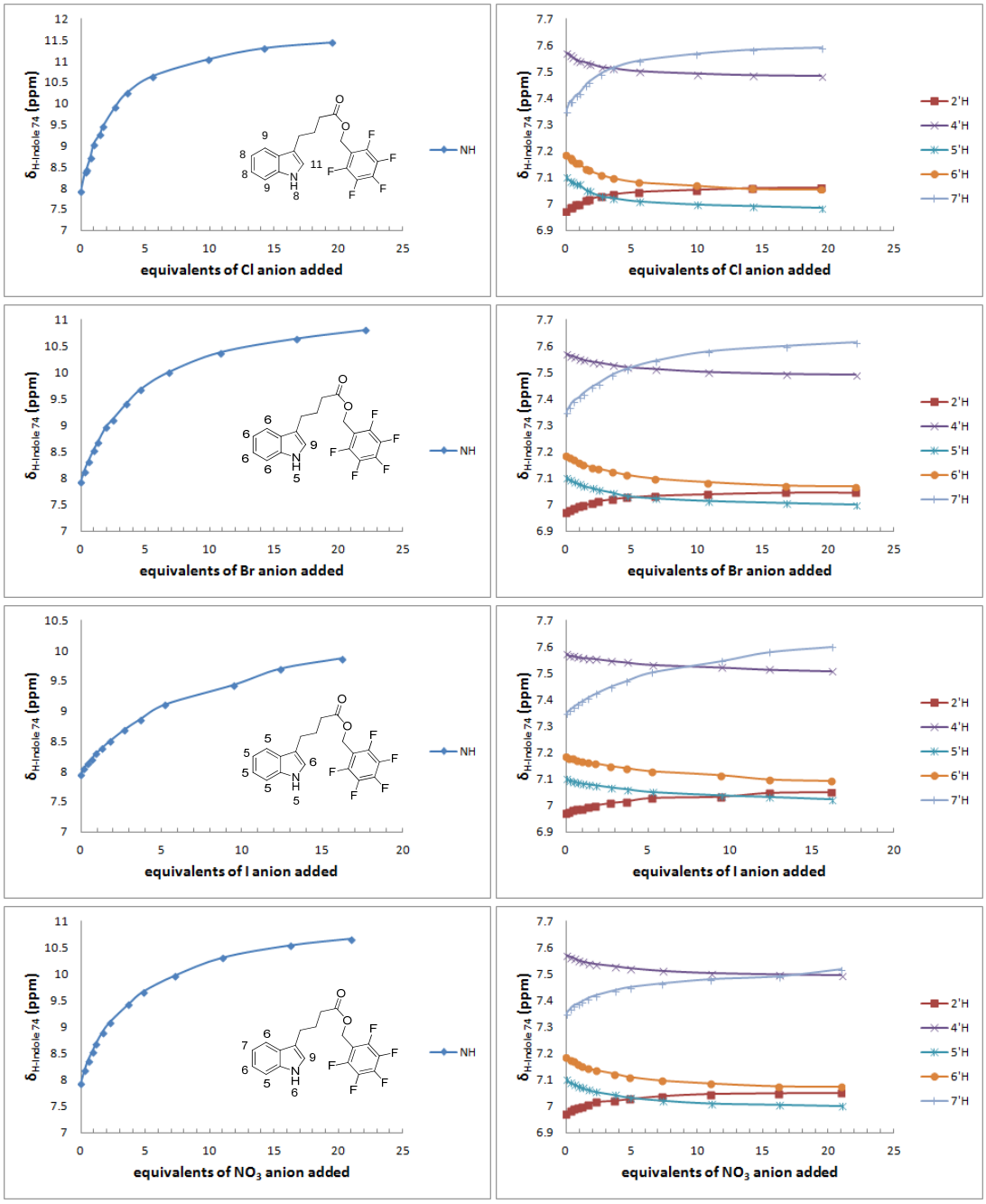

Figure S14. ^{1}H NMR-titration spectra of the derivative **74** with the addition of anions in $CDCl_3$ (298 K). Only chemical shifts of protons on the indole unit are displayed. The binding constants of H/F with anions are shown by the corresponding positions, respectively.

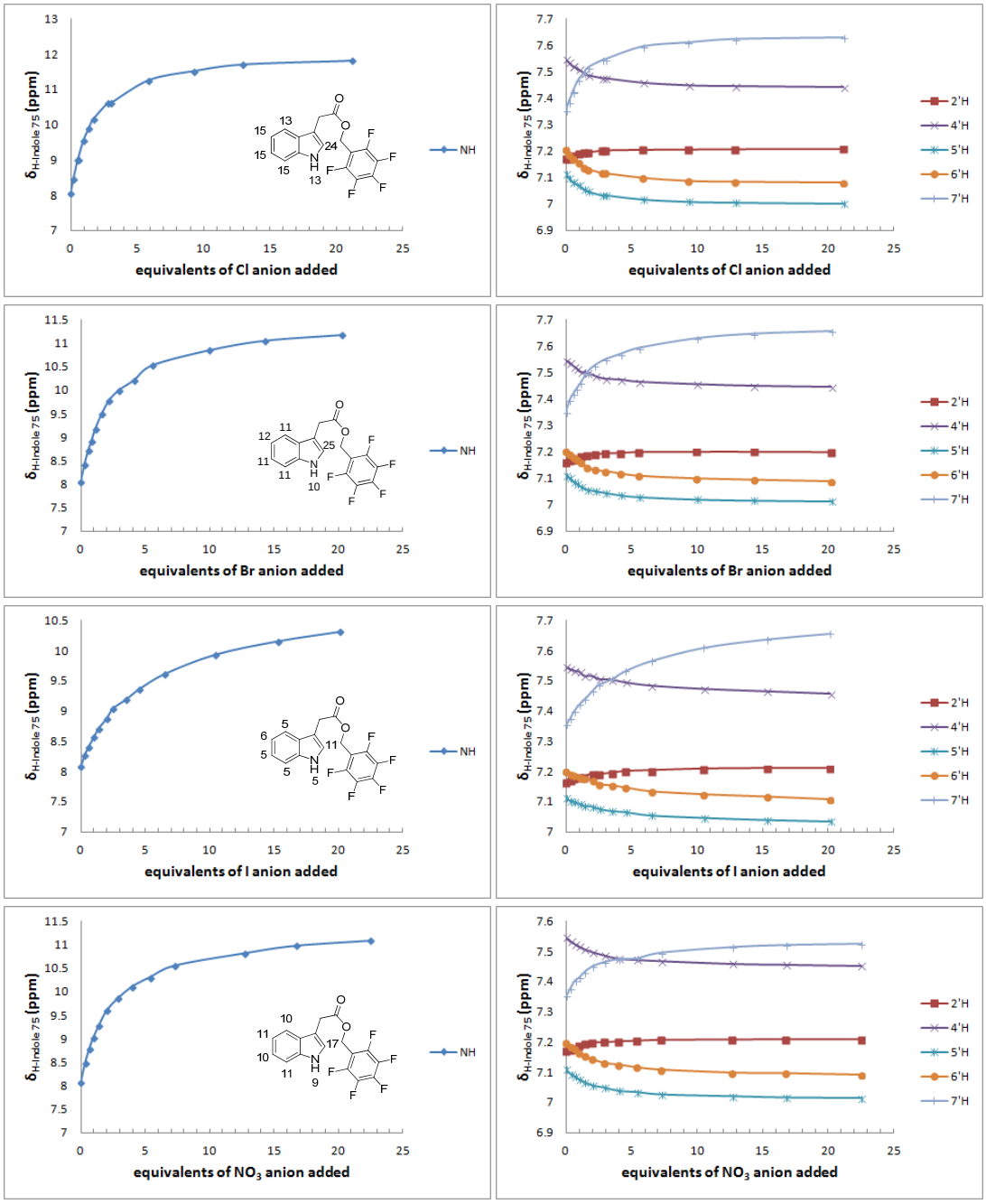

Figure S15. ^{1}H NMR-titration spectra of the derivative **75** with the addition of anions in $CDCl_3$ (298 K). Only chemical shifts of protons on the indole unit are displayed. The binding constants of H/F with anions are shown by the corresponding positions, respectively.

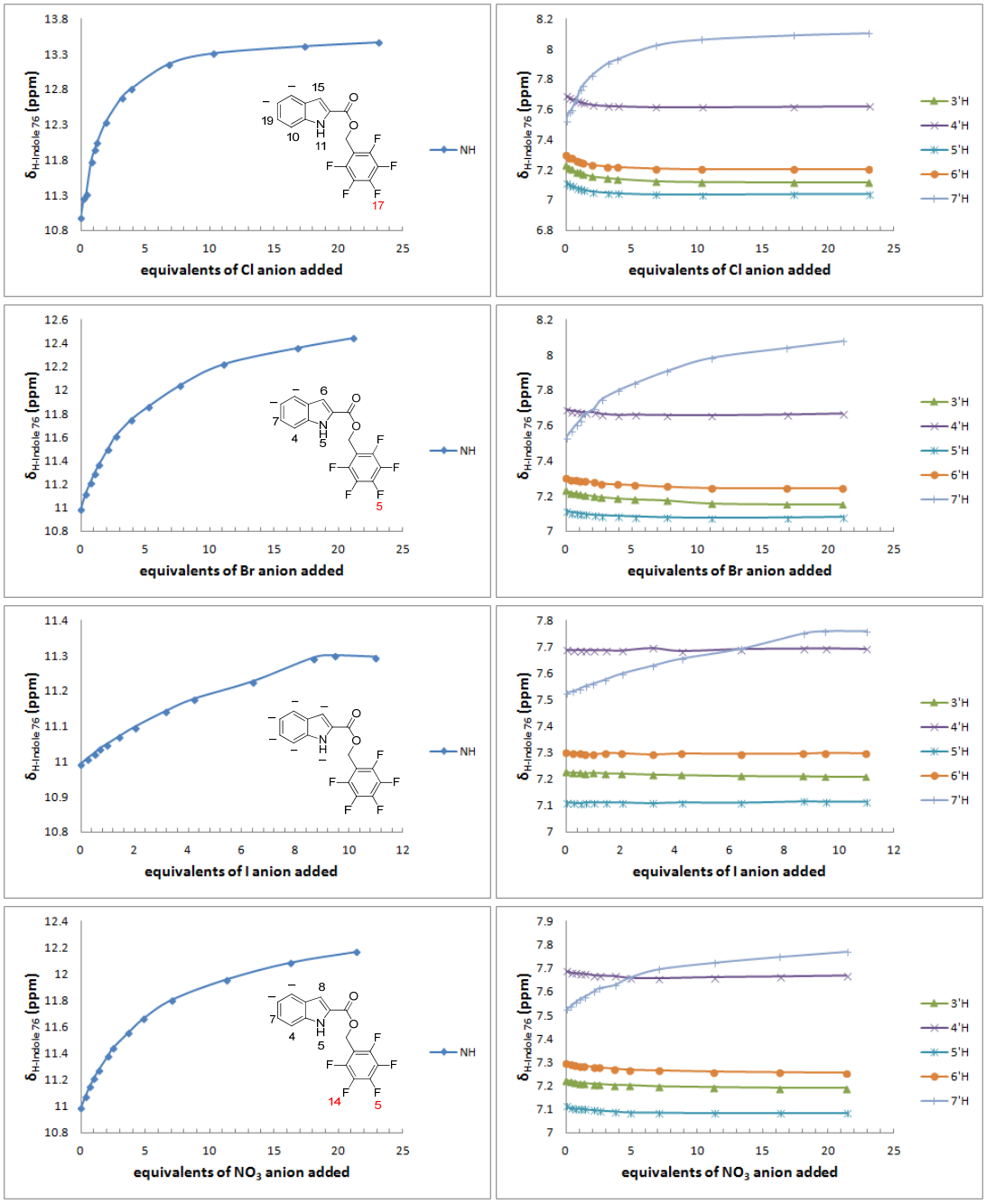

Figure S16. ^{1}H NMR-titration spectra of the derivative **76** with the addition of anions in acetone-d_6 (298 K). Only chemical shifts of protons on the indole unit are displayed. The binding constants of H/F with anions are shown at the corresponding positions, respectively.

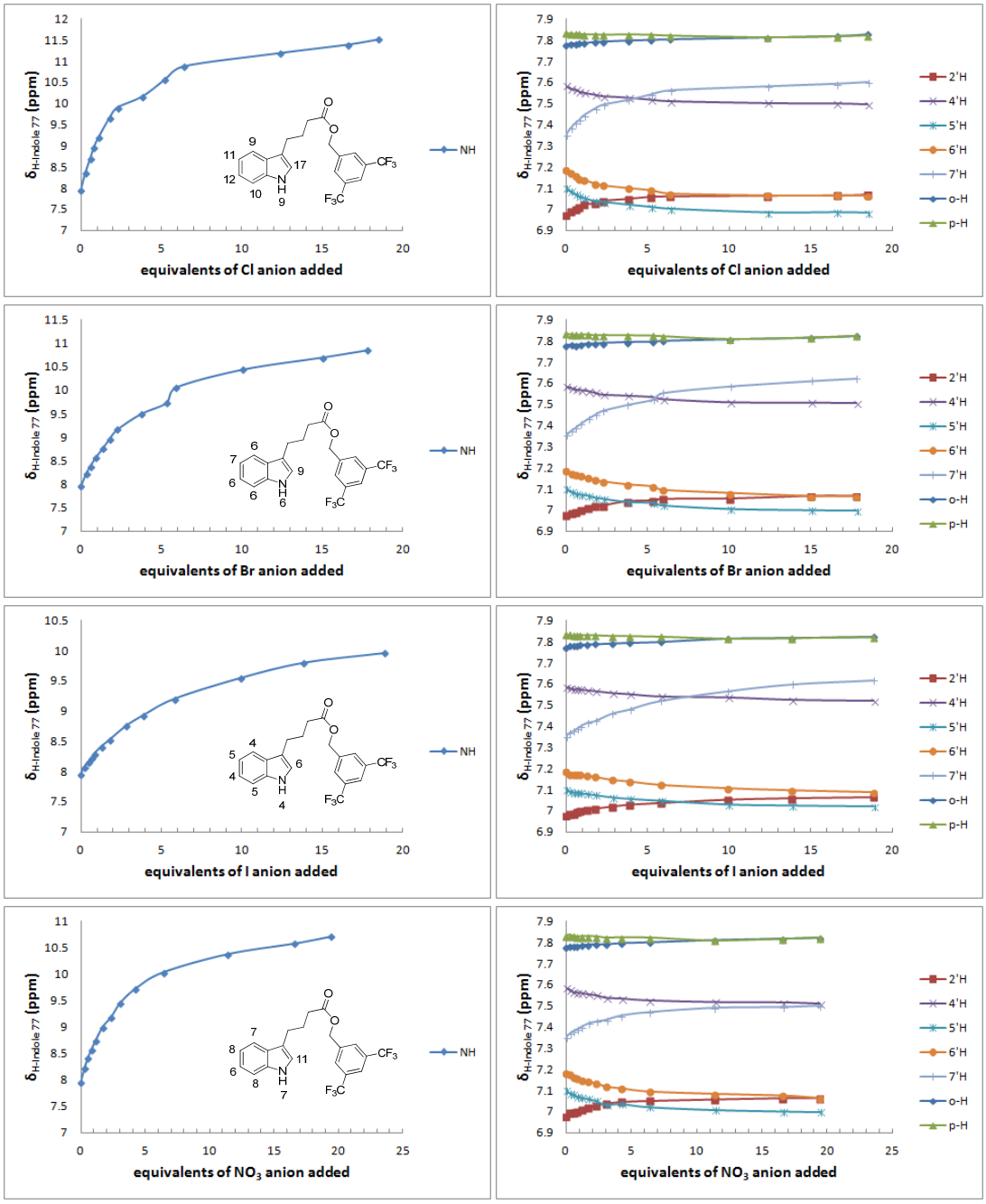

Figure S17. ^{1}H NMR-titration spectra of the derivative **77** with the addition of anions in $CDCl_3$ (298 K). Only chemical shifts of protons on the indole unit are displayed. The binding constants of H/F with anions are shown by the corresponding positions, respectively.

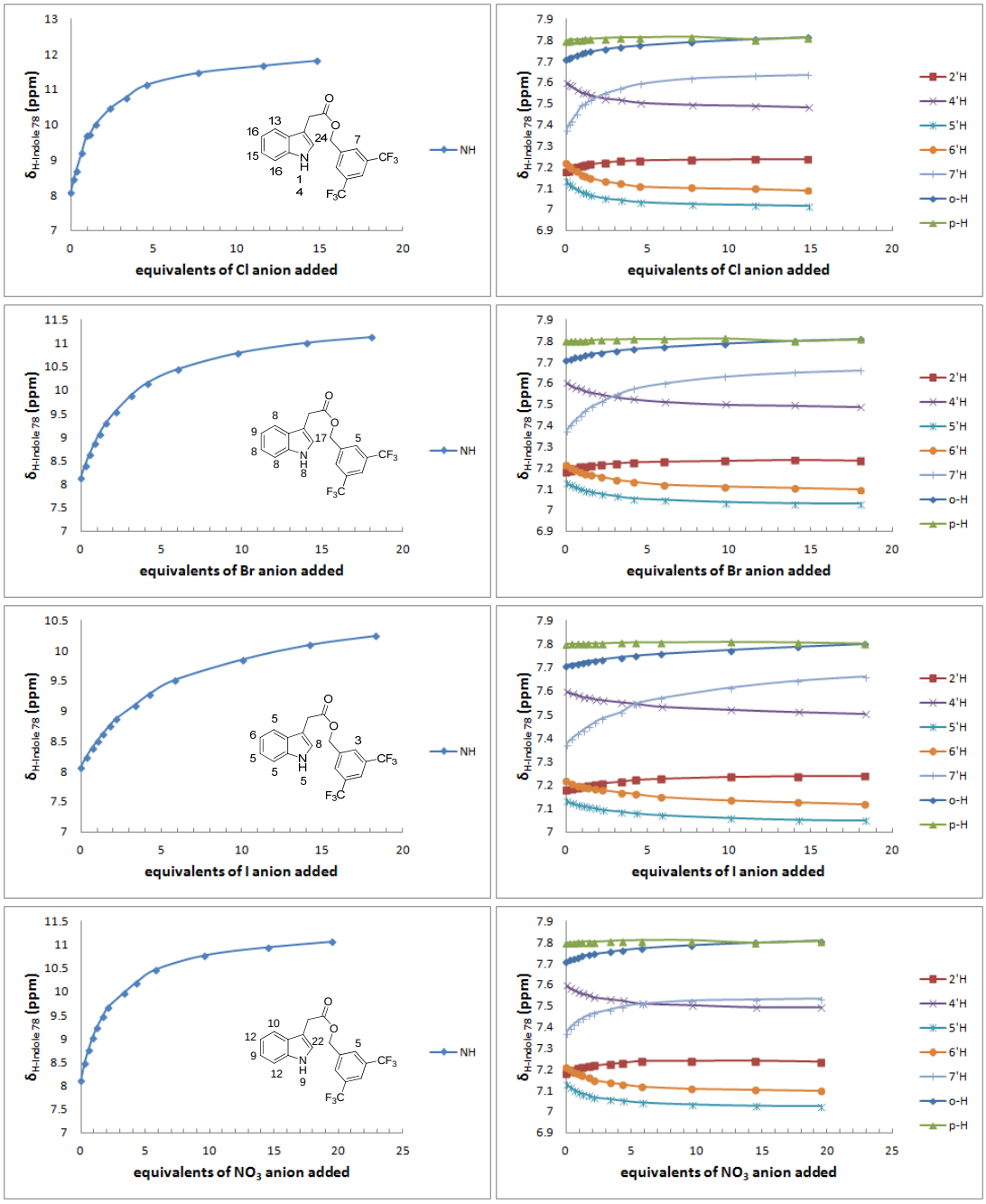

Figure S18. ^{1}H NMR-titration spectra of the derivative **78** with the addition of anions in $CDCl_3$ (298 K). Only chemical shifts of protons on the indole unit are displayed. The binding constants of H/F with anions are shown by the corresponding positions, respectively.

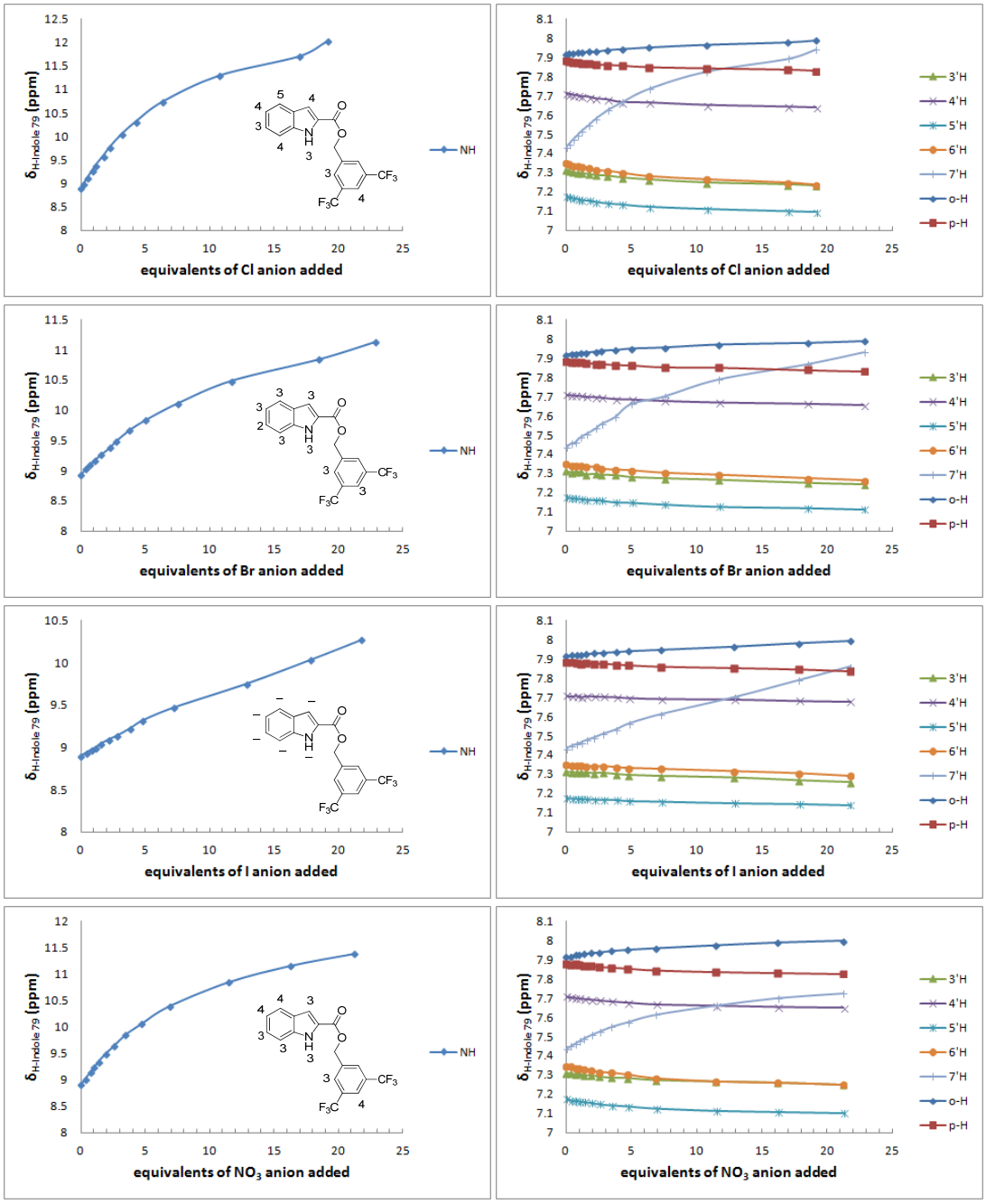

Figure S19. ^{1}H NMR-titration spectra of the derivative **79** with the addition of anions in $CDCl_3$ (298 K). Only chemical shifts of protons on the indole unit are displayed. The binding constants of H/F with anions are shown by the corresponding positions, respectively.

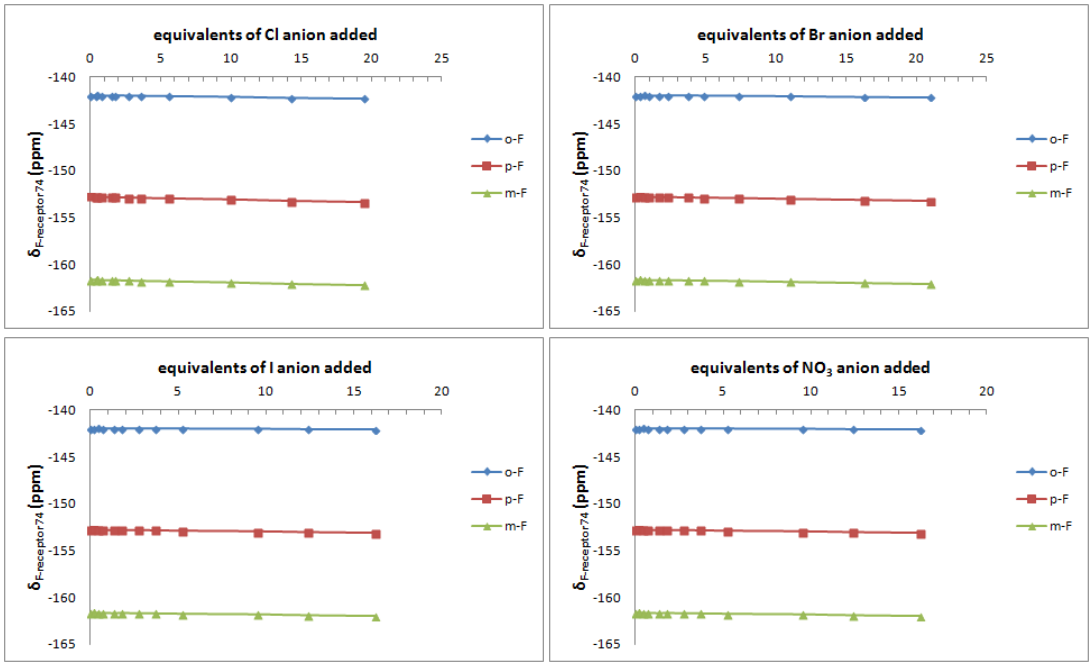

Figure S20. ^{19}F NMR-titration spectra of the derivative **74** with the addition of anions in $CDCl_3$. (298 K)

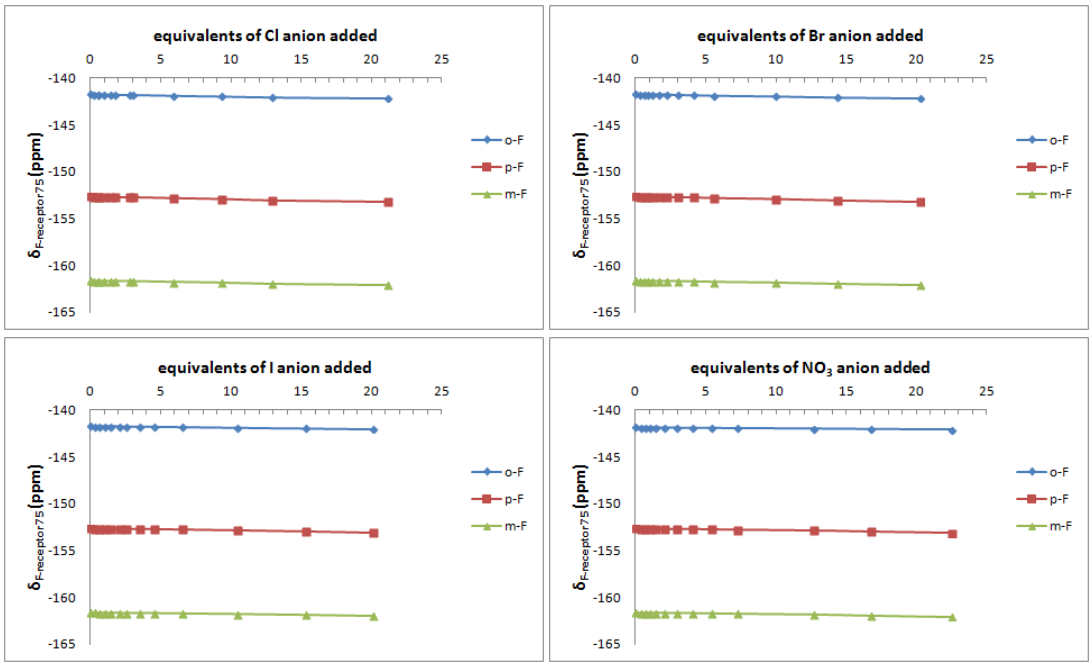

Figure S21. ^{19}F NMR-titration spectra of the derivative **75** with the addition of anions in $CDCl_3$. (298 K)

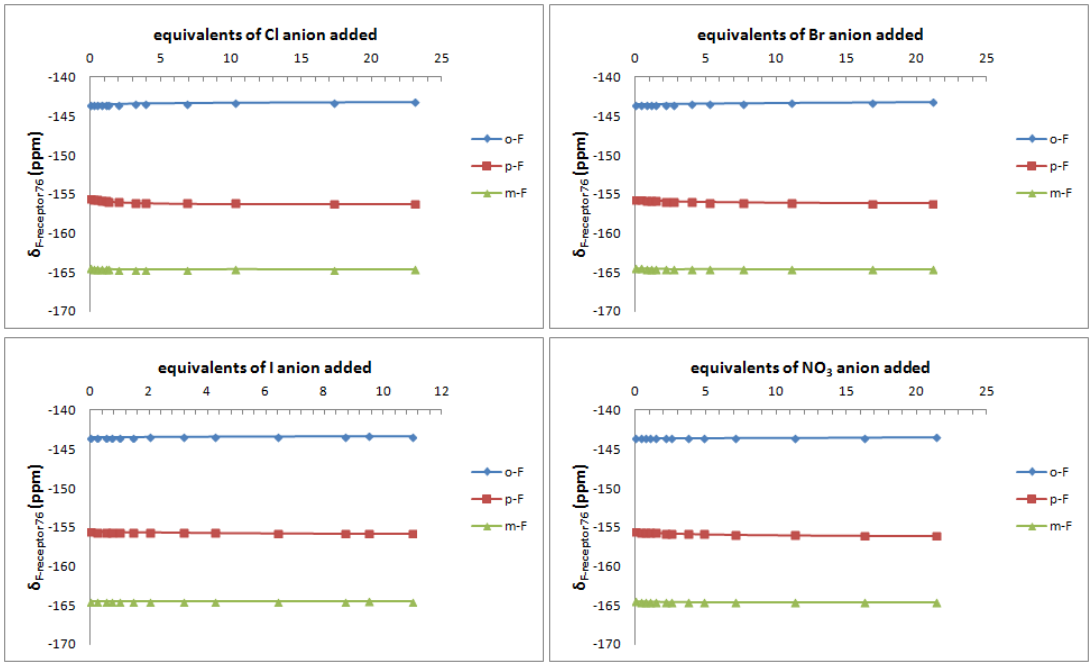

Figure S22. ^{19}F NMR-titration spectra of the derivative **76** with the addition of anions in acetone-d_6. (298 K)

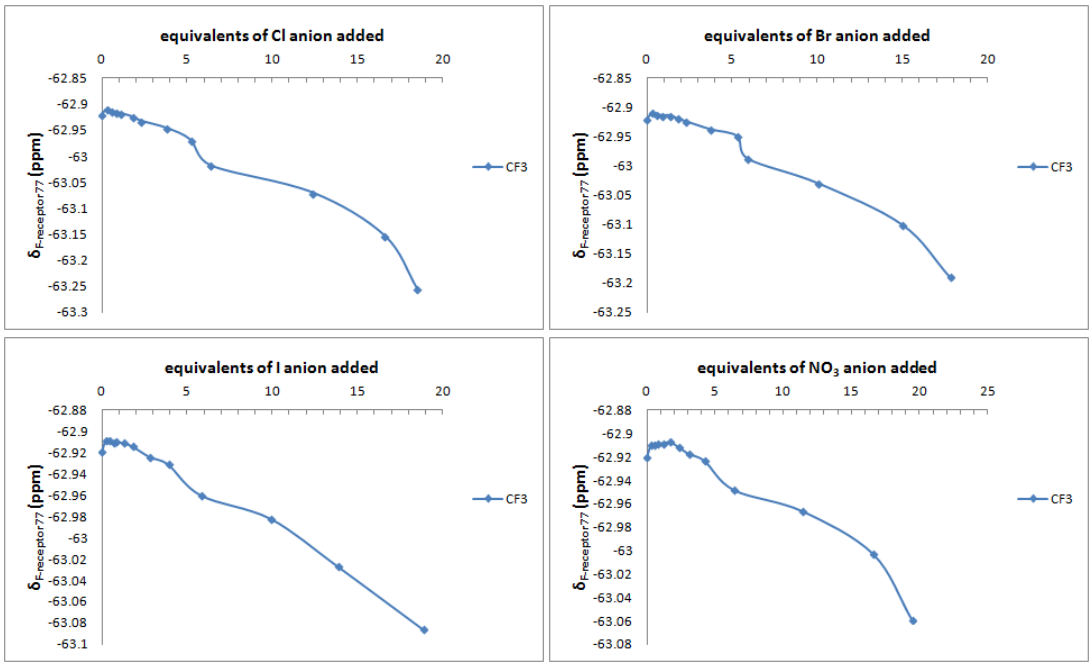

Figure S23. ^{19}F NMR-titration spectra of the derivative **77** with the addition of anions in $CDCl_3$. (298 K)

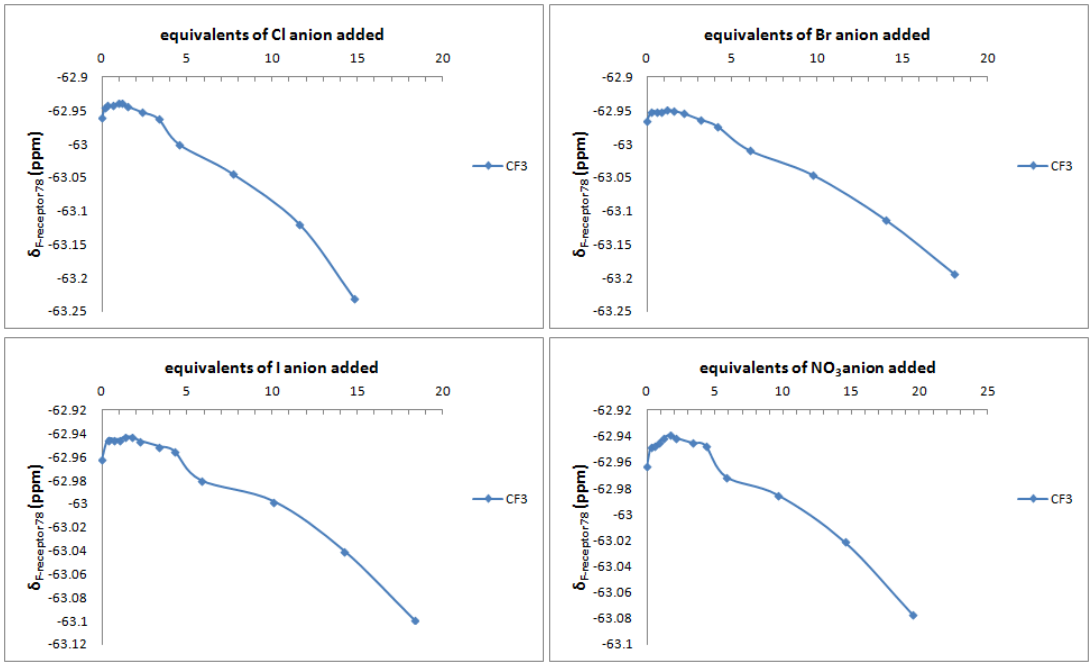

Figure S24. ^{19}F NMR-titration spectra of the derivative **78** with the addition of anions in $CDCl_3$. (298 K).

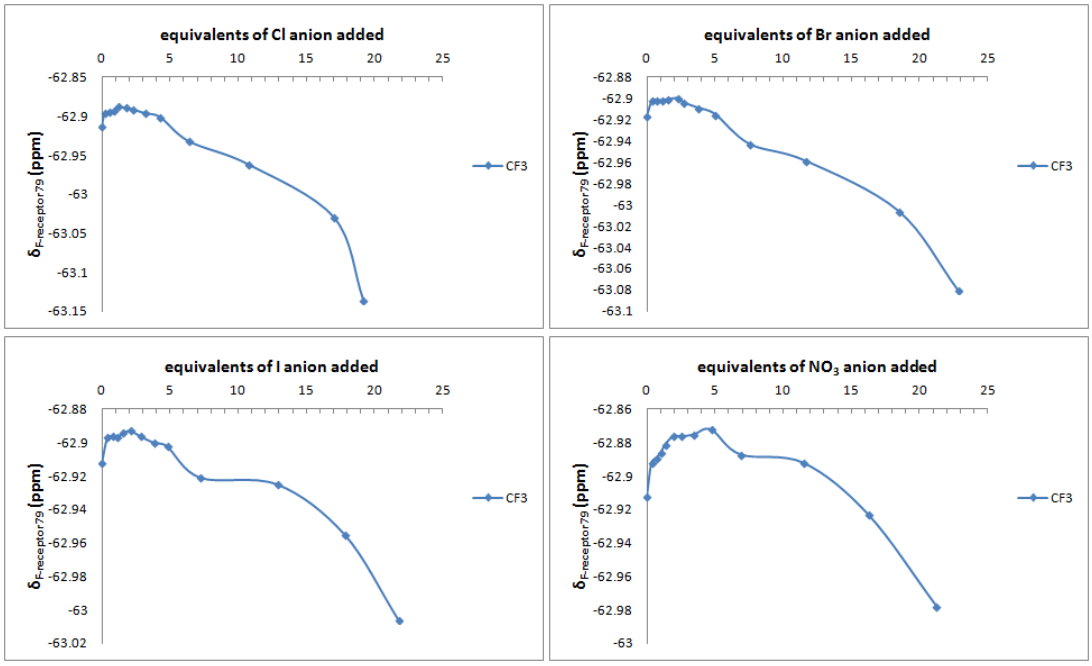

Figure S25. ^{19}F NMR-titration spectra of the derivative **79** with the addition of anions in $CDCl_3$ (298 K).

Part 2 Publications during doctorial study

1. "*CF_3: An electron withdrawing substituent for aromatic anion-acceptors? 'Side-on' versus 'on-top' binding of anions*", Markus Albrecht*, **Hai Yi**, Okan Köksal, Gerhard Raabe, Fangfang Pan, Arto Valkonen, Kari Rissanen, submitted.
2. "*Connecting Electro-Deficient and Electro-Rich Aromatics to Support Intermolecular Interactions in Crystals*", Markus Albrecht*, **Hai Yi**, Fangfang Pan, Arto Valkonen, Kari Rissanen, *Eur. J. Org. Chem.*, 2015, 3235-3239.
3. "*Perfluoro-1,1'-biphenyl and perfluoronaphthalene and their derivatives as π-acceptors for anions*", **Hai Yi**, Markus Albrecht*, Arto Valkonen, Kari Rissanen, *New J. Chem.*, **2015**, *39*, 746.

Part 3 Acknowledgements

First of all, I am grateful for financial support from China Scholarship Council. Without this support, it is impossible for me to start my doctoral study abroad.

Then, my endless gratitude goes to Prof. Dr. Markus Albrecht, my honorific supervisor who provided me a research position in his group four years ago when I was in urgent need of a PhD student opportunity in Germany. Prof. Albrecht's kind invitation and strong support to me for the CSC scholarship application during that time must be memorable in my life. For my master's research subject is synthetic methodology which is obviously different from supramolecular chemistry on the research methods, I spent nearly 10 months to accommodate this new research subject and made many mistakes at the beginning of my doctoral study. Thanks for Prof. Albrecht's guidance to my study and patience to my mistakes for 4 years, I can be granted these research results and complete this doctoral dissertation.

All the time, I sincerely appreciate my two kindly academic supervisors: Prof. Dr. Markus Albrecht—my doctoral supervisor, and Prof. Dr. Li-ping Song—my master's supervisor. Without their powerful support, I cannot pursue scientific research so smoothly.

I greatly thank Prof. Dr. Dieter Enders and Prof. Dr. Wolfgang Stahl for examining this doctoral dissertation and attending my doctoral defense and sincerely thank Prof. Dr. Iris Oppel for organizing the doctoral defense.

I would like to express my gratitude to all my friends in Prof. Albrecht's group: Ms. Marita de Groot, Dr. Irene Latorre, Dr. Verena Gossen, Dr. Thomas Abel, Dr. Yuli Shang, "translator" Dr. Marcel Albrecht, "scientist" Dr. Michael Giese, "party" Dr. Elisabeth Isaak, "cola" Dr. Zhanhu Sun, "factory" Dr. Jan Stubenrauch, "neighbor" Ms. Tanja Königs, "Gurki juice" Mr. Sebastian Guski, "smoking＆drinking" Mr. Thomas Willms, "coffee＆beer" Mr. David Van Craen, "prodigy" Mr. Jan Hartmann and Ms. Xiying Zhang. Thank you for creating a beautiful life to me in Germany.

Many thanks to Prof. Kari Rissanen and Dr. Arto Valkonen, Dr. Fang-fang Pan, for their outstanding work on X-ray single crystal diffraction. Many thanks to Prof. Gerhard Raabe and Okan Köksal, for their computational chemistry work. Many thanks to all other faculties and staff in Institute of Organic Chemistry and to all the people who helped me ever before.

Without doubt, I must dedicate my deepest appreciation and huge sense of guilt to my parents and my extended family. They brought me up and provide me help and supporting whenever, but I have not been able to accompany with them at all time since 2004 when I entered into university.

At last, adoringly thank those pioneers and explores on natural science in history, for their scientific discovery making a better life for human; gratefully thank those readers who will clarify, improve or even overthrow the perspectives mentioned in this dissertation, for their investigation taking human mind much more approach to the natural truth.

Yi, Hai
06/29/2015, Aachen